

### REMARKS

Claims 7-12 have been cancelled as directed to a non-elected invention. Claim 5 has been cancelled and the subject matter of claim 5 has been incorporated into amended claim 1. Claim 1 has further been amended to recite the number of cells transplanted and to describe the characteristics of the transplanted cells. Claims 1, 2, and 6 have been amended to recite neural stem cells. Claims 3 and 4 have been amended to depend from claim 1. The amendments are supported by the claims as originally filed. The amendments to claims 1, 2, and 6 ("neural stem cells") are supported by disclosure throughout the specification, *e.g.* at page 4, line 5. The amendments to claim 1 are further supported by disclosure at page 6, lines 25-28, page 15, lines 16-17, and page 16, lines 5-9 of the specification. No new matter is added.

### *Information Disclosure Statement*

An information disclosure statement was filed July 24, 2001. The Examiner has indicated that although several copies of references were received, no PTO-1449 form was received. For the Examiner's convenience, and in order to fully comply with 37 CFR 1.98(a)(1), Applicant encloses herewith copies of the Information Disclosure Statement, the PTO-1449 form, each of the references cited, the transmittal letter, the stamped return postcard, and the stamped Express Mail Receipt, which were originally filed on July 24, 2001.

### *Claim Rejections under 35 U.S.C. § 112*

There is a sole rejection under 35 U.S.C. § 112, first paragraph for lack of enablement. According to the Examiner, "[t]he specification fails to provide an enabling disclosure for the methods of transplantation because the specification teaches that the only use for the method is to provide a therapeutic benefit to a subject and specification does not teach how to use the claimed methods to produce a therapeutic effect." (Office Action at page 3). Thus, the Examiner has argued that the specification fails to meet the "how to use" requirement of 35 U.S.C. § 112, first paragraph. This rejection should be withdrawn.

First, the rejection is improperly made under § 112, first paragraph. Where, as here, the Examiner has questioned the therapeutic efficacy or benefit, the rejection is properly the subject of a § 101 utility rejection (with a concurrent § 112, first paragraph rejection) on the basis that the claimed invention lacks a credible utility. *See* §§ 706.03(a)(1) and 2107 of the M.P.E.P. (and

particularly the discussion of the relationship between § 101 utility rejections and § 112, first paragraph rejections). Yet there is no § 101 rejection here. On this basis alone the rejection cannot stand.

Second, the “how to use” requirement of § 112, first paragraph is satisfied if “the specification contains within it a connotation of how to use, and/or the art recognizes that standard modes of administration are known and contemplated.” *See* § 2164.01(c) of the M.P.E.P. Applicant’s specification meets this requirement (discussed in detail below).

Third, a rejection under § 112, first paragraph is proper only if one reasonably skilled in the art could not make or use the invention from the disclosures in the patent coupled with information known in the art, without undue experimentation. *See United States v. Teletronics, Inc.*, 857 F.2d 778, 785 (Fed. Cir. 1988); *In re Wands*, 858 F.2d 731, 737 (Fed. Cir. 1988). Applicant’s specification meets this requirement (discussed in detail below).

***A. The Rejection under § 112, First Paragraph Does Not Conform To §706.03(a)(1) M.P.E.P.***

Claims 1-6 have been rejected under 35 U.S.C. § 112, first paragraph, for lack of enablement. The Examiner asserts that the specification does not teach how to use the claimed methods to produce a therapeutic effect in a host. According to the Examiner, the pending claims are not enabled because, although the claimed methods are drawn to methods of transplantation of progenitor cells to effect migration, integration, and differentiation into neurons, oligodendrocytes, or astrocytes, the only use contemplated in the specification for these methods is to provide a therapeutic benefit. Independent claim 1 does not require such a therapeutic benefit. Accordingly, Applicant contends that none of the pending claims needs to show such a therapeutic benefit.

Under the case law and its interpretation in the M.P.E.P, a rejection that questions the efficacy of a claimed invention is properly analyzed as a utility rejection that must conform to the Utility Guidelines set forth in §706.03(a)(1) of the M.P.E.P. However, there is no § 101 rejection here. Section 706.03(a)(1) of the M.P.E.P. makes clear that if the Examiner determines that the claimed invention has a credible utility, the rejection may not be applied. M.P.E.P. §706.03(a)(1).

In considering what constitutes a “credible utility,” the Guidelines provide that, to uphold

a utility-based § 112, first paragraph rejection, a case must represent one of those rare instances that meets the stringent criterion of being “totally incapable of achieving a useful result.” *See Brooktree Corp. v. Advanced Micro Devices, Inc.*, 977 F.2d 1555 (Fed. Cir. 1992), as discussed in the Legal Analysis accompanying the Utility Guidelines (M.P.E.P. § 2107). The only instances in which the Federal courts have found a lack of patentable utility were where, “based upon the factual record of the case, it was clear that the invention *could and did not work* as the inventor claimed it did” (M.P.E.P. § 2107, emphasis added). These rare cases have been ones in which the applicant either (a) failed to disclose any utility for the invention, or (b) asserted a utility that could be true only “if it violated a scientific principle, such as the second law of thermodynamics, or a law of nature, or was wholly inconsistent with contemporary knowledge in the art” (M.P.E.P. § 2107.01).

In conformance with the Guidelines, Applicant has asserted at least one utility for a method for transplantation of progenitor cells as claimed. The methods of the invention can be used in the treatment of various neurodegenerative diseases and disorders, wherein the transplanted cells will replace diseased, damaged or lost tissue in the host.

The Utility Guidelines state that “data generated using *in vitro* assays, or from testing in an animal model or a combination thereof almost invariably will be sufficient to establish therapeutic or pharmacological utility for a compound, composition, or process” (M.P.E.P. § 2107.02(a)).<sup>1/</sup> Applicant has provided disclosure in the specification establishing utility in an animal model. For example, human neural stem cells were transplanted into rat brain; behavioral changes associated with the grafted cells in lesioned animals were assessed; and histological analyses were used to examine graft viability, graft integration, and the phenotypic fate of the grafted cells. *See* Specification, Example 8 at page 25.

Thus, Applicant contends that, for this reason alone, the rejection should be withdrawn.

***B. The Specification Teaches One Skilled in the Art “How To Use” the Claimed Invention.***

The first paragraph of § 112 requires that, to enable a claimed invention, an application must describe “how to use” the invention. According to the Examiner, the specification does not

---

<sup>1/</sup> Consistent with this standard, in no case has a Federal court required an applicant to support an asserted utility with data from human clinical trials. M.P.E.P. § 2107.02(d).

teach how to use the claimed method for inducing *in vivo* migration of progenitor cells transplanted to the brain to produce a therapeutic effect.

Claim 1 has been amended to recite a method for transplanting neural stem cells wherein the cells are transplanted to a first locus of the brain, wherein, following infusion of a mitogenic growth factor, the cells migrate to a second locus of the brain, integrate into the parenchymal tissues, differentiate into neurons, oligodendrocytes, or astrocytes, and retain their responsiveness to the mitogenic growth factor. Methods for carrying out the claimed invention are described throughout the specification. *See, e.g.*, pages 14-16, 18-20, and 25-26 of the specification, and Examples 1, 2, 8, and 9, for detailed disclosure on obtaining, proliferating, and transplanting CNS neural stem cells to effect migration, integration, and differentiation of the cells following infusion of a mitogenic growth factor.

No additional enablement is needed. As stated by the Federal Circuit in Hybritech, Inc. v. Monoclonal Antibodies, Inc., 802 F.2d 1367, 231 U.S.P.Q. 81 (Fed. Cir. 1984): “A patent need not teach, and preferably omits, what is well known in the art.”

Thus, Applicant has provided an enabling description of “how to use” the claimed invention. Therefore, the “how to use” requirement of § 112 has been satisfied and this rejection should be withdrawn.

***C. One of Ordinary Skill in the Art Can Use (and Has Used) the Claimed Invention Without Undue Experimentation.***

Under 35 U.S.C. § 112, first paragraph, lack of enablement is found only if one reasonably skilled in the art could not make or use the invention from the disclosures in the patent coupled with information known in the art, without undue experimentation. *See United States v. Telectronics, Inc.*, 857 F.2d 778, 785 (Fed. Cir. 1988); *In re Wands*, 858 F.2d 731, 737 (Fed. Cir. 1988). Even if the experimentation required is complex, it is not necessarily undue if artisans skilled in the relevant art typically engage in such experimentation. *See In re Certain Limited-Charge Cell Culture Microcarriers*, 221 USPQ 1165, 1174 (Int’l Trade Comm. 1983).

The factors used to determine whether experimentation is undue include, but are not limited to the following: (1) the breadth of the claims; (2) the nature of the invention; (3) the amount of direction provided by the inventor; (4) the existence of working examples; (5) the level of predictability in the art; (6) the state of the prior art; (7) the level of one of ordinary skill



in the art; and (8) the quantity of experimentation needed to make or use the invention based on the content of the disclosure. *See In re Wands*, 858 F.2d at 737. No one of these factors is dispositive and the Examiner must consider the evidence as a whole. *Id.*; M.P.E.P. § 2104.01(a). Here, one of ordinary skill in the art would be able to routinely use the described methods to transplant CNS stem cells and to induce migration, integration and differentiation of these cells via infusion of a growth factor.

According to the Examiner, the instant specification does not disclose working examples that demonstrate a therapeutic effect in a diseased animal. In addition, the Examiner states that the instant specification fails to provide guidance relating to the amount of cells to inject, the site of injection, and the extent of cellular persistence required to provide any therapeutic benefit for any disorder. *See Office Action at page 3.* Applicants respectfully disagree.

The instant specification teaches that transplantation of cells to the brain of a subject is performed by stereotaxic surgery under anesthesia. The specification describes that the number of cells to be transplanted is 250,000 - 500,000 cells per deposit. The specification also teaches that the cells can be injected into multiple sites of the brain, including the striatum of the brain, parenchymal sites of the CNS, and intrathecal sites of the CNS. *See Specification at page 25, lines 20-23 and page 13, lines 17-18.* Furthermore, the specification teaches the placement of an infusion cannulae. For example, one such placement is in the lateral ventricle.

The specification also provides guidance as to the amount of growth factor to be infused. For example, the specification teaches that the total dose required to induce migration and proliferation of transplanted cells will vary from subject to subject, but may be, for example, about 400 ng/day of EGF infused. *See Specification at page 15, line 22, and Examples 8 and 9.* Moreover, Applicant has provided several working examples, including Examples 8, 9, and 15, which illustrate the transplantation of neural stem cells into rat brain and the induction of *in vivo* proliferation and migration of transplanted progenitor cells in the brain. *See Specification, pages 25 and 30-41.* Thus, Applicant asserts that, contrary to the Examiner's contention, the instant specification does provide numerous working examples that demonstrate how to use the claimed invention.

Additionally, the Examiner notes that the claims cover using any type of progenitor cell, but the teachings in the specification are limited to using neural stem cells. To expedite prosecution, Applicant has amended the claims to specify neural stem cells.

Moreover, according to the Examiner, the instant specification fails to provide an enabling disclosure because the methods of transplanting neural tissue are not routinely successful. To support this position, the Examiner cites Jackowski *et al.*, British J. of Neurosurgery 9:303-17 (1995). However, Jackowski *et al.* relates to the difficulties associated with the regeneration of adult mammalian CNS and PNS axons. Jackowski *et al.* does not address the transplantation of neural stem cells. In contrast, the methods of the claimed invention are directed to the transplantation of neural stem cells. As discussed previously, the specification fully enables the presently claimed methods. Thus, Applicant contends that those skilled in the art would be able to practice the claimed methods without undue experimentation.

Furthermore, numerous publications reflect the view of those skilled in the art that the claimed methods would provide a therapeutic benefit to the host.

For example, Qu *et al.*, Ageing, 12:1127-32 (2001) (courtesy copy attached as Ex. 1) report that, when human neural stem cells were transplanted into aged rats, the cells differentiated into neurons and astrocytes. Moreover, Qu *et al.* also report that both neurons and astrocytes migrated into the cortex and hippocampus in a well-defined and organized pattern, and that the rats demonstrated significantly improved cognitive function.

Akiyama *et al.*, Exp. Neurol., 167:27-39 (2001) (courtesy copy attached as Ex. 2) report that human neurosphere cultures transplanted into a demyelinated adult rat spinal cord produced extensive remyelination and that “the remyelinated axons conducted impulses at near normal conduction velocities”.

Kurimoto *et al.*, Neuroscience Letters, 306:57-60 (2001) (courtesy copy attached as Ex. 3) report that rat neural stem cell cultures transplanted into the eyes of adult rats that underwent ischemia-reperfusion injury invaded the retinal ganglion cell layer and the retinal inner nuclear layer, and integrated into the host retina where they expressed Map2ab, which indicated that the cells had differentiated into mature neurons. Likewise, Nishida *et al.*, Investigative Ophthalmology & Visual Science, 41:4268-74 (2000) (courtesy copy attached as Ex. 4) report that transplantation of neural stem cells into mechanically injured adult retina resulted in incorporation and subsequent differentiation of the grafted stem cells into neuronal and glial lineages.

Reubinoff *et al.*, Nature Biotech., 19:1134-40 (2001) (courtesy copy attached as Ex. 5) report that “[w]hen human neural progenitors were transplanted into the ventricles of newborn

mouse brains, they incorporated in large numbers into the host brain parenchyma, demonstrated widespread distribution, and differentiated into progeny of the three neural lineages.”

Mitome *et al.*, Brain, 124:2147-61 (2001) (courtesy copy attached as Ex. 6) report that epidermal growth factor-responsive neural precursor cells transplanted into wild-type and myelin-deficient shiverer (*shi*) mice engrafted robustly within the CNS and adopted glial phenotypes. Some of these transplanted cells functioned as oligodendrocytes, which produced myelin basic protein and morphologically normal internodal myelin sheaths.

Milward *et al.*, J. Neurosci. Res., 50:862-71 (1997) (courtesy copy attached as Ex. 7) show that canine CNS neural stem cells transplanted into a shaking (*sh*) pup myelin mutant dog (a model of human myelin diseases) and into the myelin-deficient (*md*) rat spinal cord resulted in the production of myelin by graft-derived cells. Similarly, Zhang *et al.*, Proc. Natl. Acad. Sci. USA, 96:4089-94 (1999) (courtesy copy attached as Ex. 8) report that when neural stem cell cultures generated from both juvenile and adult rats were transplanted into *md* rats, those cells produced “robust myelination”. Likewise, Brüstle *et al.*, Nature Biotechnol., 16:1040-44 (1998) (courtesy copy attached as Ex. 9) describe the implantation of fetal human CNS progenitor cells into mice that “acquire an oligodendroglial phenotype and participate in the myelination of host axons”. Yandava *et al.*, Proc. Natl. Acad. Sci. USA, 96:7029-34 (1999) (courtesy copy attached as Ex. 10) show that transplantation of CNS neural stem cells results in “global” cell replacement and therapeutically effective remyelination in the dysmyelinated shiverer (*shi*) mouse brain with repletion of myelin basic protein (MBP) and, in some cases, a decrease in symptomatic tremor.

Flax *et al.*, Nature Biotechnol., 16:1033-39 (1993) (courtesy copy attached as Ex. 11) show that human CNS neural stem cells transplanted into newborn meander tail (*mea*) mouse cerebella provided “replacement neurons” with the “definitive size, morphology, and location of cerebellar granule neurons”.

Fricke *et al.*, J. Neurosci., 19:5990-6005 (1999) (courtesy copy attached as Ex. 12) show that when CNS neural stem cells were transplanted into neurogenic regions in the adult rat brain, the *in vitro* propagated cells migrated specifically along the routes normally taken by endogenous neuronal precursors, exhibited substantial migration within the non-neurogenic region, and showed site-specific differentiation into both neuronal and glial phenotypes.

Aboody *et al.*, Proc. Natl. Acad. Sci. USA, 97:12846-51 (2000) (courtesy copy attached as Ex. 13) expressly state that neural stem cell cultures provide a transplantation “platform”

since, upon transplantation, those cells can both continue to express a foreign gene as well as migrate in a site specific fashion in host tissue for "dissemination of therapeutic genes".

Finally, Temple *et al.*, Nature, 414:112-17 (2001) (courtesy copy attached as Ex. 14) review the therapeutic potential of CNS neural stem cells. Specifically, Table 1 summarizes numerous CNS transplantation studies assessing stem and progenitor cell behavior and Box 1 describes a variety of therapeutic uses of transplanted stem cells to repair the nervous system, including for the treatment of Parkinson's disease, Huntington's disease, spinal cord injury, stroke, and multiple sclerosis.

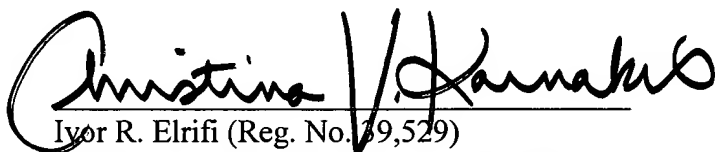
Thus, neural stem cells cultures have been shown by many researchers skilled in the art to be a useful tool for tissue-specific differentiation to provide a therapeutic benefit when transplanted into a host.

For all the foregoing reasons, the pending claims are enabled and this rejection should be withdrawn.

### CONCLUSION

On the basis of the foregoing, Applicants respectfully request that the rejection of the pending claims be withdrawn. If there are any questions regarding these remarks, the Examiner is encouraged to contact the undersigned at the telephone number provided below.

Respectfully submitted,

A handwritten signature in black ink, appearing to read "Christina V. Karnakis", is written over a horizontal line.

Ivor R. Elrifi (Reg. No. 39,529)  
Christina V. Karnakis (Reg. No. 45,899)  
Janine M. Susan (Reg. No. 46,119)  
Attorneys for Applicants  
c/o MINTZ, LEVIN, COHN, FERRIS,  
GLOVSKY AND POPEO, P.C.  
One Financial Center  
Boston, Massachusetts 02111  
Telephone: (617) 542-6000  
Telefax: (617) 542-2241

*Marked-up version showing changes made*

1. (Amended) A method for [inducing *in vivo* migration of progenitor] transplantation of at least about 500,000 mitogenic growth factor-responsive neural stem cells [transplanted to the brain, said method comprising the steps of :] capable of differentiating into neurons, oligodendrocytes, or astrocytes to the brain, wherein the cells

(a) [transplanting said progenitor cells to a first locus of the brain of a subject; and] are transplanted to a first locus of the brain of a living host subject;

(b) [inducing *in vivo* migration of said transplanted progenitor cells by infusing] migrate *in vivo* after implantation from the first locus to other anatomic sites for integration within the nervous system of the host subject following infusion of a mitogenic growth factor that does not induce differentiation of the neural stem cells at a second locus of the brain of said host subject;

(c) integrate *in situ* after implantation into the parenchymal tissues at a local anatomic site in the host subject; and

(d) differentiate *in situ* after integration into a cell selected from the group consisting of neurons, oligodendrocytes, and astrocytes

wherein the transplanted neural stem cells retain their *in vivo* responsiveness to the mitogenic growth factor.

2. (Amended) The method of claim 1, wherein said [progenitor] neural stem cells comprise mammalian embryonic progenitor cells.

3. (Amended) The method of claim [2] 1, wherein said first locus is in the striatum of the brain, and wherein said second locus is in the lateral ventricle of the brain.

4. (Amended) The method of claim [3] 1, wherein said *in vivo* migration of step (b) occurs towards said second locus.

5. Cancel

6. (Amended) The method of claim 1, wherein said [progenitor] neural stem cells are cultured in media comprising the mitogenic growth factor prior to transplantation.

-- 13. (New) The method of claim 6, wherein said culture is a suspension culture.

14. (New) The method of claim 6, wherein said culture is an adherent culture. --

# Human neural stem cells improve cognitive function of aged brain

T. Qu, C. L. Brannen, H. M. Kim and K. Sugaya<sup>CA</sup>

Department of Psychiatry, The Psychiatric Institute, The University of Illinois at Chicago, 1601 West Taylor Street, Chicago, IL 60612, USA

<sup>CA</sup>Corresponding Author

Received 9 January 2001; accepted 3 February 2001

The capability for *in vitro* expansion of human neural stem cells (HNSCs) provides a well characterized and unlimited source alternative to using primary fetal tissue for neuronal replacement therapies. The HNSCs, injected into the lateral ventricle of 24-month-old rats after *in vitro* expansion, displayed extensive and positional incorporation into the aged host brain with improvement of cognitive score assessed by the Morris

water maze after 4 weeks of the transplantation. Our results demonstrate that the aged brain is capable of providing the necessary environment for HNSCs to retain their pluripotent status and suggest the potential for neuroreplacement therapies in age-associated neurodegenerative disease. *NeuroReport* 12:1127-1132 © 2001 Lippincott Williams & Wilkins.

**Key words:** Aging; Differentiation; Engraftment; Memory; Migration; Progenitor; Transplantation

## INTRODUCTION

The discovery of multipotent neural stem cells (NSCs) in the adult brain [1,2] has wrought revolutionary changes in the theory on neurogenesis, a theory that now suggests that regeneration of neurons can occur throughout life. To further this revolution, we have recently shown that human neural stem cells (HNSCs) differentiated and survived >3 weeks in basal media without the addition of any supplements or exogenous factors [3]. This result suggests that HNSCs are capable of producing endogenous factors necessary for their own survival and neuronal differentiation. Together, these recent findings stimulated us to investigate the transplantation of HNSCs to determine whether or not the aged brain will provide the necessary environment needed for a successful HNSC transplantation. Here we show, for the first time to our knowledge, that not only did HNSCs expanded *in vitro* survive 30 days after xenotransplantation, retaining both multipotency and migratory capacity, but more remarkably, HNSC transplantation improved cognitive function in 24-month-old rats.

## MATERIALS AND METHODS

Detailed methods for the maintenance and proliferation of HNSCs have been described previously [4]. Briefly, the HNSCs were cultured in 20 ml serum-free supplemented growth medium consisting of HAMS-F12 (Gibco, BRL, Burlington, ON); antibiotic-antimycotic mixture (Gibco); B27 (Gibco); human recombinant FGF-2 and EGF (R and D Systems, Minneapolis, MN) and heparin (Sigma, St. Louis, MO). The cells were incubated at 37°C in a 5% CO<sub>2</sub> humidified incubation chamber (Fisher, Pittsburgh, PA).

To facilitate optimal growth conditions, HNP spheroids were sectioned into quarters every 2 weeks and fed by replacing 50% of the medium every 4-5 days.

Matured (6 months old) and aged (24 months old) male Fischer 344 rats were deeply anesthetized with sodium pentobarbital (50 mg/kg, i.p.). Using bregma as a reference point, about 10<sup>5</sup> cells were collected and slowly injected into the right lateral ventricle (AP -1.4; ML 1.8; DV 3.8 mm) of the brain using a stereotaxic apparatus (Devid Kopf). Immunosuppressant was not given to the animals. The memory score was tested before and after the injection of cells using the Morris water maze.

All animal experiments were conducted in strict accordance to guidelines of the university animal care committee. The Morris water maze was conducted as described before [5]. The water maze consisted of a large, circular tank (diameter 183 cm; wall height 58 cm) filled with water (27°C) opacified by the addition of powdered milk (0.9 kg). Beneath the water surface (1 cm), a clear escape platform (height, 34.5 cm) was positioned near the center of one of the four quadrants of the maze. The rats received three training trials per day for 7 consecutive days, using a 60 s inter-trial interval. A training trial consisted of placing the animal in the water for 90 s or until it successfully located the platform. If the rat failed to find the platform within the 90 s it was gently guided to the platform. For spatial learning assessment, the platform's location remained constant in one quadrant of the maze, but the starting position for each trial was varied. Every sixth trial was a probe trial, during which the platform was retracted to the bottom of the pool for 30 s and then raised and made available for escape. The training trials assess the acquisition and day-

to-day retention of the spatial task while the probe tests are used to assess the search strategy. At the completion of the spatial learning assessment, one session with six trials of cue training was performed. Rats were trained to escape to a visible black platform raised 2 cm above the surface of the water. The location of the platform was varied from trial to trial in order to assess sensorimotor and motivational functioning independent of spatial learning ability. Each rat was given 30 s to reach the platform and allowed to remain there briefly before the 30 s inter-trial interval. Accuracy of performance was assessed using a learning index score computed from the probe trials. The learning index is a derived measure from an average proximity (cumulative search error divided by the length of the probe trial) on the second, third, and fourth interpolated probe trials. Scores from these trials were weighted and summed to provide an overall measure of spatial learning ability. Lower scores on the index indicate a more accurate search in the vicinity of the target location; higher scores indicate a more random search and poor learning.

At 30 days post-transplantation, the rats were sacrificed by an overdose of sodium pentobarbital (70 mg/kg, i.p.) and perfused with phosphate buffered saline (PBS) followed by 4% paraformaldehyde. Brains were removed, placed into 4% paraformaldehyde fixative containing 20% sucrose and left overnight. The brains were sliced into 20  $\mu$ m coronal sections using a cryomicrotome. The sections were washed briefly in PBS and pretreated with 1 M HCl for 30 min at room temperature and neutralized with sodium borate (0.1 M, pH 8.0) for 30 min in order to increase the accessibility of the anti-bromodeoxyuridine (BrdU) antibody to the BrdU incorporated in the cell nuclei. After rinsing with PBS, sections were transferred to the solution containing 0.25% Triton X-100 in PBS (PBST) for 30 min. Then the sections were blocked in PBST containing 3% donkey normal serum for 1 h and incubated with sheep anti-BrdU (1:1000; Jackson IR Laboratories, Inc. West Grove, PA) or mouse anti-BrdU (1:200; DSHB, Iowa City, IA) diluted in PBST overnight at 4°C. After rinsing in PBS, donkey anti-mouse or donkey anti-sheep conjugated to rhodamine IgG (Jackson IR Laboratories, Inc.) was added at a 1:200 dilution in PBST for 2 h at room temperature in the dark. Then the sections were washed with PBS and incubated with mouse IgG2b monoclonal anti-human  $\beta$ III-tubulin, clone SDL3D10 (1:500, Sigma), goat anti-human glial filament protein (GFAP), N-terminal human affinity purified (1:200, Research Diagnostics Inc., Flanders, NJ) and Mouse IgG1 monoclonal anti-GFAP, clone G-A-5 (1:500, Sigma), respectively, overnight at 4°C in the dark. The corresponding secondary antibodies for them were donkey anti-mouse (1:200) and donkey anti-goat IgG (H+L; 1:200) conjugated to FITC (Jackson IR Laboratories, Inc.), respectively. Following a brief PBS washing, they were added into sections for 2 h incubation at room temperature in the dark. Sections were then washed thoroughly with PBS before mounting to glass slides. The mounted sections were covered with Vectashield with 4',6-diamidino-2-phenylindole.2HCl (DAPI, Vector Laboratories, Inc., Burlingame, CA) for fluorescent microscopic observation. Microscopic images were taken by using the Axiocam digital camera mounted on the Axioscope 2 with Axiovision software (Zeiss).

## RESULTS

The HNSCs were expanded without differentiation under the influence of mitogenic factors in supplemented serum-free media [3]. To differentiate between host and transplanted cells, the nuclei of the HNSCs were labeled by the incorporation of BrdU into the DNA. These labeled cells were subsequently injected unilaterally into the lateral ventricle of matured (6-month-old) and aged (24-month-old) rats. The cognitive function of these animals was assessed by the Morris water maze [5] before and 4 weeks after the transplantation of HNSCs. Before the HNSCs transplantation, some of the aged animals (aged memory unimpaired animals) had cognitive function in the range of the matured animals, while others (aged memory impaired animals) had cognitive function entirely out of the range of the matured animals (Fig. 1a). After the HNSC transplantation, most of the aged animals had cognitive function in the range of the matured animals. Strikingly, one of the aged memory impaired animals displayed behavior that was dramatically better than the level of the matured animals (Fig. 1a). Statistical analysis showed that cognitive function significantly improved in both matured ( $p < 0.001$ ,  $n = 8$ ) and aged memory impaired animals ( $p < 0.001$ ,  $n = 6$ ). In contrast, no improvement in cognitive function was observed in vehicle injected control animals ( $n = 6$ ), or aged memory unimpaired animals ( $n = 7$ ) after the HNSC transplantation (Fig. 1b). Three of the 13 aged animals showed deterioration of performance in the water maze after the HNSC transplantation. This fact needs to be further analyzed, but this may be due to the deterioration of the physical strength of these animals during the experimental period.

To investigate the morphology and population of differentiated HNSCs, we further analyzed brain sections taken after the second water maze task by immunohistochemistry with cell specific markers. The transplanted HNSCs, with BrdU-immunopositive nuclei, were stained for human  $\beta$ III-tubulin and human GFAP. Double immunolabeling with  $\beta$ III-tubulin and BrdU in 3 different planes from the same microscopic view clearly shows the co-localization of these two signals in the same cells (Fig. 2). According to the manufacturer's description, the anti- $\beta$ III-tubulin antibody may recognize the host (rat)  $\beta$ III-tubulin. Despite this, the specific co-localization of these  $\beta$ III-tubulin and BrdU at different planes indicates that the majority of  $\beta$ III-tubulin-immunopositive cells are indeed transplanted HNSCs. This may be due to the fact that  $\beta$ III-tubulin is mainly expressed in immature neurons, the majority of which are transplanted HNSCs in this study. The presence of these cell-specific antigens indicates that the transplanted HNSCs successfully differentiated into neurons and astrocytes, respectively. Immunohistochemical analysis of brain sections revealed cells intensely and extensively positive for human  $\beta$ III-tubulin staining. Specifically, these cells were located primarily in the bilateral cingulate and parietal cortices (layer II, IV and V; Fig. 3a,b) and hippocampus (CA1, dentate gyrus and CA2; Fig. 3c-e).

The transplanted HNSCs also differentiated into GFAP-immunopositive staining cells localized near the area where neuronal cells were found. Further analysis with double immunostaining revealed that donor-derived astrocytes co-localized with the neuronal fibers in the cortex



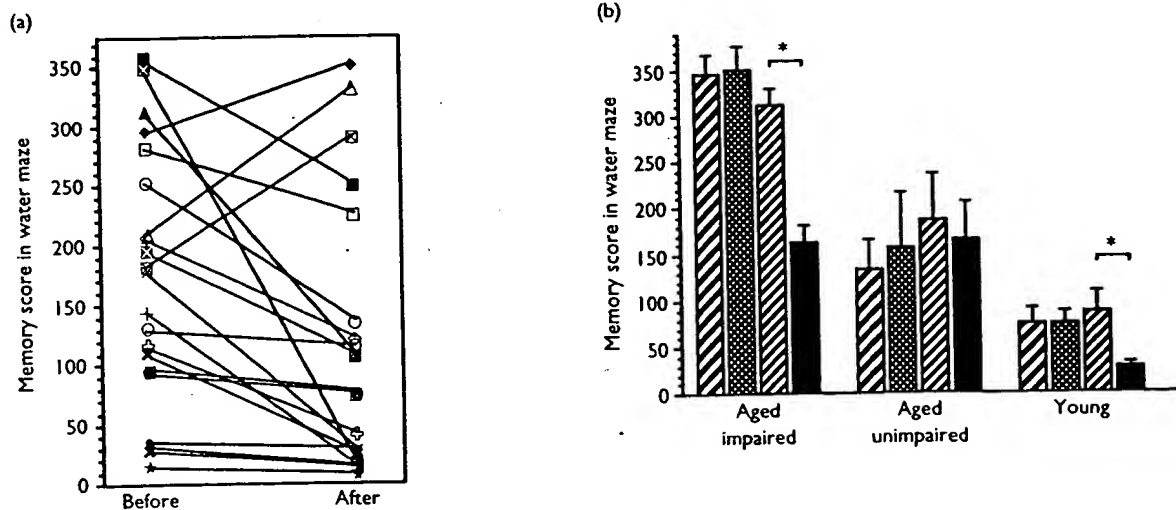


**Fig. 1.** Effect of HNSC transplantation on memory score in the water maze. (a) Individual memory score before and after the transplantation shows improvement in the majority of the animals. ■: Aged memory impaired animals, ▨: Aged memory unimpaired animals, ■: Matured animals. (b) Mean of memory score in each animal group before (▨) and after (▤) HNSC transplantation shows a significant improvement in aged memory impaired and young animals. The animals that received vehicle injection do not show significant difference in memory scores between before (▨) and after (■) the injection.

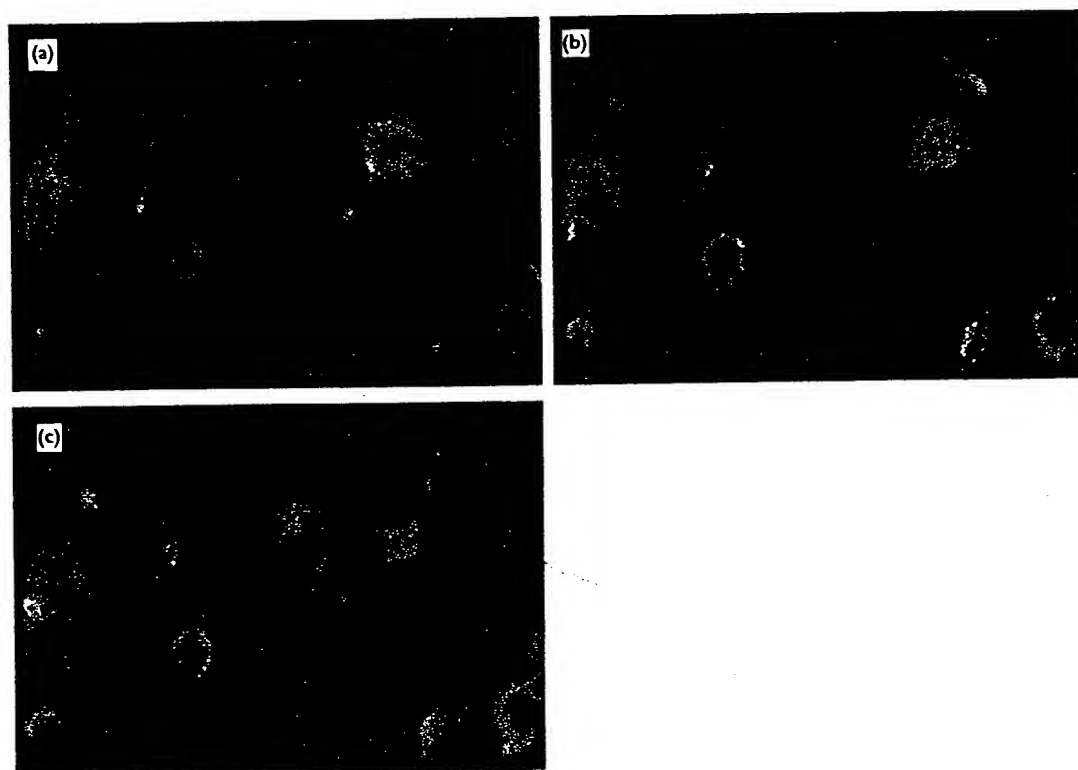


**Fig. 2.** Co-localization of  $\beta$ III-tubulin and BrdU immunoreactivity in the same cells. (a–c) Three different planes of the same microscopic view. The  $\beta$ III-tubulin-positive cells (green) show BrdU-positive nuclei (red) indicating that these cells are derived from transplanted HNSCs.

layer III (Fig. 3f) and CA2 region of hippocampus (Fig. 3e). These donor-derived astrocytes were large compared with host glia, having cell bodies 8–10  $\mu$ m in diameter with thick processes and BrdU-immunopositive nuclei (Fig. 3g).

We did not detect the above-mentioned morphologies and distribution of GFAP positive cells in the control rats that received no HNSC transplantation. When we stained with an anti-GFAP antibody that recognizes rat GFAP (Sigma,

clone G-A-5), the host astrocytes had small cell bodies with multiple delicate processes, which were distributed mainly in the white matter and around the edge of the brain (data not shown).

## DISCUSSION

There are two possible mechanisms to explain the beneficial effects of the HNSC transplantation on cognitive function of the host brain. One is replacement or augmentation of neuronal circuit by the HNSC-derived neurons and other is the neurotrophic action of factors released from the transplanted HNSCs. Although the following morphological study shows extensive incorporation of HNSCs and massive growth of neuronal fibers in the host brain area related to spatial memory task, HNSCs may still migrate toward the damaged neurons and rescue them by the production of neurotrophic factors. Therefore, a synergism between these two mechanisms may exist and allow for the successful transplantation.

Since the spatial memory of HNSC-transplanted animals as assessed by the Morris water maze improved, incorporation of HNSCs into the brain areas known to be related to spatial memory [5,6] allowed for an improvement in spatial memory. Although  $\beta$ III-tubulin is considered to be an early neuronal marker and physiological and electromicroscopic investigations will be required to determine the functional incorporation of these HNSC-derived neurons, the morphological observation indicates that functional association of these cells to the host brain occurred. Further histochemical analysis revealed that the  $\beta$ III-tubulin-positive donor-derived cells found in the cerebral cortex were characterized by having dendrites pointing to the edge of the cortex whereas in the hippocampus, donor-derived neurons exhibited morphologies with multiple processes and branches. These differential morphologies of the transplanted HNSCs in different brain regions indicate that site-specific differentiation of HNSCs occurs according to various factors expressed in each brain region.

We observed strong astrocyte staining in the frontal cortex layer 3 and CA2 region of hippocampus, areas where astrocytes are not normally present in the animal. The migration of HNSCs to the CA2 raises particular interest because CA2 pyramidal neurons highly express bFGF and the expression of bFGF is up-regulated by entorhinal cortex lesions [7-9]. The CA2 pyramidal neurons in the host brain may express bFGF as a response to a reduction of synaptic transmission, an event that may

occur during aging. Subsequently, this expressed bFGF can act as a signal for the transplanted HNSCs to respond, migrate and/or proliferate under the influence of bFGF produced in the host brain after the transplantation.

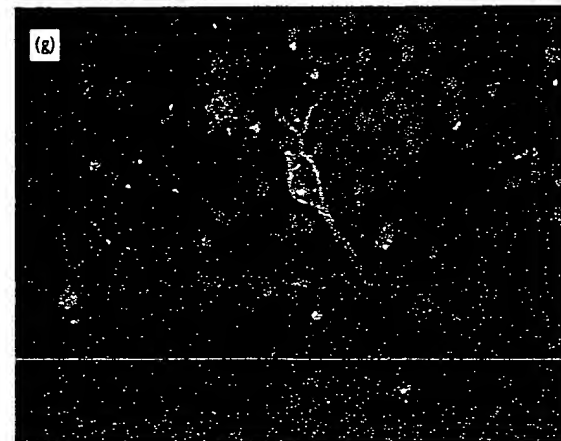
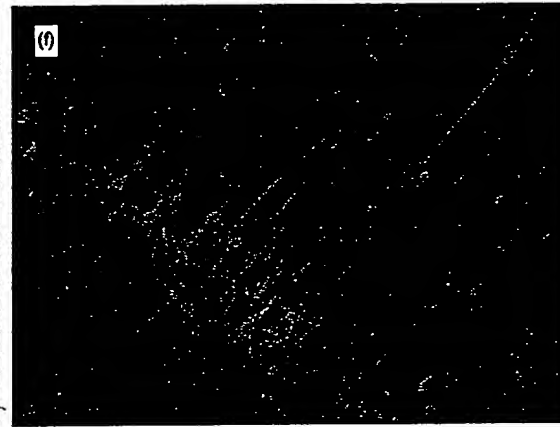
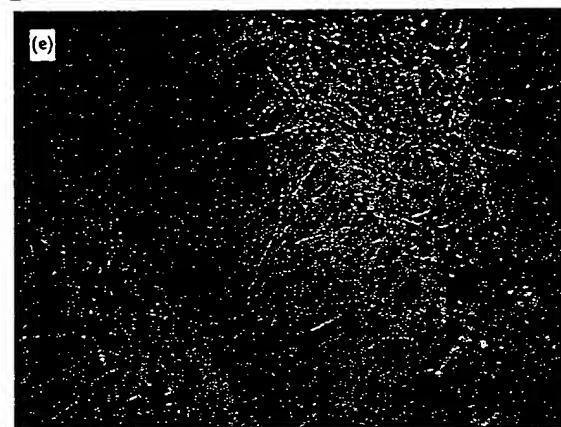
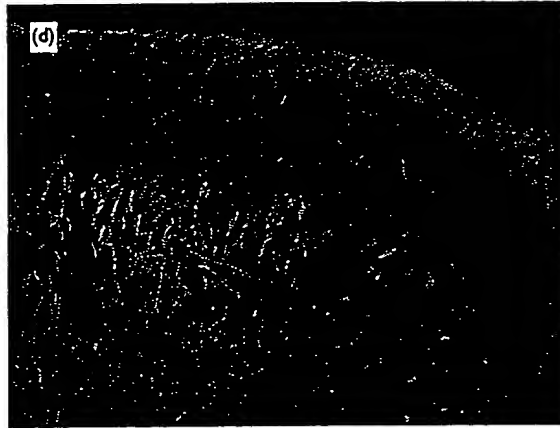
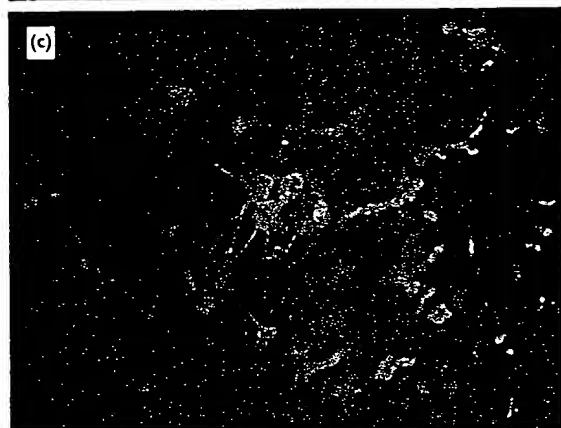
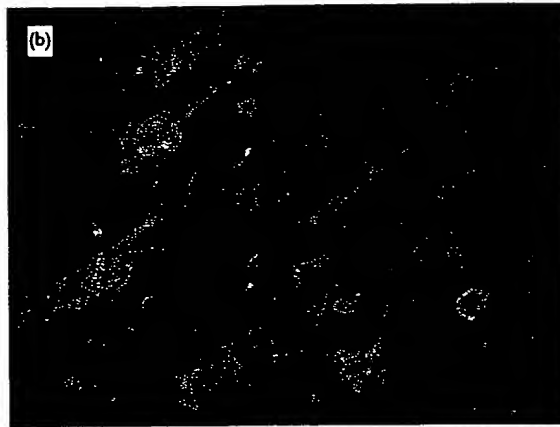
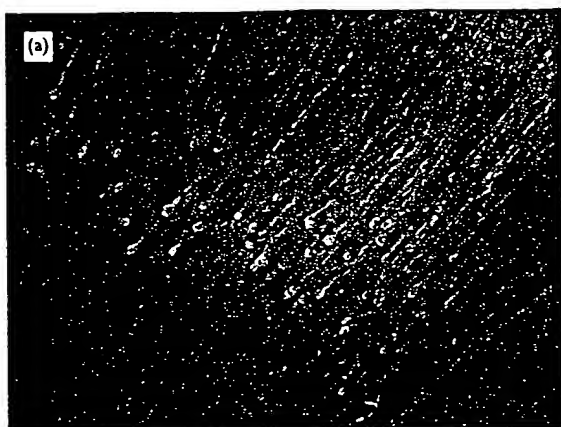
The regions rich in astrocyte staining are also the same regions where the extensively stained neuronal fibers were identified (Fig. 3a,c,e). During development glial cells have many complex functions, such as neuronal and axonal guidance, and production of trophic factors [10]. It has been suggested that following transplantation, migrating glial cells guide and support the growth and extension of neuronal fibers [11]. However, other studies have argued that glial cells may be detrimental by forming an extensive interface between the host and graft [12]. Although the mechanism(s) of glia-neuron interaction in the HNSC-transplanted host brain is not well understood, this overlapping distribution of glial and neuronal fibers strongly suggests that this interaction plays a pivotal role in the survival, migration, and differentiation of transplanted HNSCs.

The most significant difference in our experimental procedure is the lateral intraventricular transplantation of undifferentiated HNSCs in the form of neuro-spheroids. While many studies were done with intra-tissue injection of dissociated and partially differentiated NSCs [4,13-15], we employed spheroid injection because the dissociation of neuro-spheroids is known to cause immediate senescence of NSCs and increase the vulnerability of NSCs in culture [16]. Another added benefit of intraventricular injection is that since there is less tissue destruction, it may induce less recruitment of immune cells by the host. This is evidenced by the lack of increased host astrocyte staining without any immunosuppression. The mechanism behind transplanted cell migration into the brain through the ventricle is as yet still unknown. However, our results indicate that the mechanism may lie behind a direct integration into the host brain. Specifically, immunohistochemical analysis revealed that some of the BrdU cells were found to be situated along the lateral ventricular wall while a few appeared to have integrated directly into the cells lining the ventricle. Similar observations were reported in a variety of studies using neuronal transplantation to the lateral ventricle of animals. The intraventricular transplantation used in this study may provide an alternative route to the site-specific injection by which the grafted cells may gain access to various structures by the flow of CSF.

**Fig. 3.** Typical fluorescent immunohistochemical pictures in the aged rat brain 30 days after HNSC transplantation. We used  $\beta$ III-tubulin and GFAP immunoreactivity as markers for neuron and glia, respectively. (a) HNSCs migrated into the cortex and differentiated into neurons as indicated by the  $\beta$ III-tubulin-positive cells (green), which have morphologies typical of pyramidal cells in layer IV and V of the parietal cortex. Apical dendrites were pointed towards to the edge of the cortex. Since we labeled HNSC DNA with BrdU before the transplantation, the transplanted cells will have BrdU-positive nuclei (red). Contrarily, the host cell's nuclei are counterstained with DAPI (blue). (b) Higher magnification of the parietal cortex in cortex tubulin immunoreactivity in layer II and without  $\beta$ III-tubulin immunoreactivity in the layer III. (c) HNSCs migrated into the hippocampus and differentiated into neurons as indicated by the  $\beta$ III-tubulin-immunoreactive (green) positive cells show BrdU-positive nuclei (red) while many other host cell's nuclei are stained with only DAPI (blue). HNSCs tend to have larger nuclei than host cells. (d) HNSCs migrated into the hippocampus and differentiated into neurons as indicated by the  $\beta$ III-tubulin-immunoreactive (green) positive cells show BrdU-positive nuclei (red), having morphologies typical of pyramidal cells in CA1 pyramidal cell layer. These  $\beta$ III-tubulin-positive cells have BrdU-positive nuclei (red), indicating that these cells originated from transplanted cells. In contrast, host cell nuclei counterstained with DAPI (blue) are not  $\beta$ III-tubulin-positive. (e) Hippocampus CA2 shows a large number of GFAP-positive cells (red) and  $\beta$ III-tubulin-positive cells (green). (f) In the dentate gyrus as well as the  $\beta$ III-tubulin-positive cells (green) and GFAP-positive cells (red), many fibers were  $\beta$ III-tubulin positive. (g)  $\beta$ III-tubulin-positive cells (green) and GFAP-positive cells (red) were found in layer IV and layer III, respectively. We have not seen such a layer of astrocytes in normal rats without HNSC transplantation. (h) These GFAP-positive cells (green) show BrdU-positive nuclei (red), and have larger cell bodies and thicker processes than the host (rat) astrocytes.

in  
d,  
GF  
  
ne  
re  
ve  
al  
as  
ng  
of  
ed  
ve  
ne  
C-  
er-  
ly  
he  
ed  
  
al  
of  
ts.  
on  
5],  
on  
es-  
in  
ar  
ay  
is  
te  
m  
gh  
its  
ect  
to-  
lls  
all  
he  
re-  
ta-  
lar  
er-  
he  
he

AP  
the  
ere  
U-  
ill-  
tex  
with  
lin  
ve-  
ill-  
ste  
ells  
ats  
ses



Following immunohistochemistry, a symmetrical distribution of neurons and astrocytes at both sides of the host brain was observed, indicating that the progeny of these HNSCs have a great potential for migration. Although astrocytes have been shown to migrate over long distances following transplantation [17–19], there is experimental evidence showing that neurons do not migrate as widely as glial cells [20]. In our study, the neuronal precursors derived from the HNSCs seem to possess similar migratory ability as the astrocyte precursors. This may be due to the fact that we transplanted undifferentiated HNSCs and such an immature stage for both glia and neuron possesses the potential to migrate over long distances. The extensive incorporation of neuronal and glial cells found in the cortex and other sub-regions of the hippocampus may be interpreted as evidence for the significance of local cues or signals within these regions which enable these grafted NSCs to migrate. It remains to be demonstrated, however, to what extent these newly formed neurons can undergo complete maturation with physiologically functional connections to the host brain.

Many studies have discovered the existence of endogenous precursor cells in certain regions of the brain. These regions include the anterior subventricular zone (SVZ) and the hippocampal dentate gyrus, areas where neurogenesis continues into adulthood in mammalian species, including humans [21–23]. The presence of multipotent neural cells in the adult brain similar to the fetal neural stem cell in these brain regions indicates the importance of microenvironments to neural progenitors. Aging is characterized by increased levels of inflammation in the CNS [24,25]. Thus, it is reasonable to speculate that factors existing in the environment of the aged brain may direct the non-neuronal differentiation pathway. However, in our current study, the transplanted HNSCs successfully generated many morphologically functional neurons in the aged animals. In a previous study, we observed that initial glial differentiation of HNSCs was followed by neuronal differentiation in a serum-free culture media without any additional factor [3]. This finding suggests that glial differentiation caused by the serum deprivation produced factors that allowed neurons to differentiate. Since we observed an association of astrocytes and neurons derived from HNSCs in this study, we may have to consider the possibility that the donor astrocytes may direct the neuronal differentiation.

## CONCLUSION

In order to facilitate therapeutic HNSC application to the general adverse consequences of aging and neurodegenerative diseases, it is important to understand these environmental factors which direct the differentiation fate of these HNSCs to diverse lineages *in vivo*. While future studies are needed to elucidate these environmental factors, we have none the less demonstrated that HNSC transplantation into the brains of aged memory impaired rats significantly improved their cognitive function. Moreover, not only did the HNSCs successfully differentiate into neurons and astrocytes, but more importantly, both neurons and astrocytes migrated to the cortex and hippocampus in a well-defined and organized pattern in the adult brain.

## REFERENCES

1. Alvarez-Buylla A and Kim JR. *J Neurobiol* 33, 585–601 (1997).
2. Gould E, Reeves AJ, Graziano MS et al. *Science* 286, 548–552 (1999).
3. Brannen CL and Sugaya K. *Neuroreport* 11, 1123–1128 (2000).
4. Benninger Y, Marino S, Hardegger R et al. *Brain Pathol* 10, 330–341 (2000).
5. Sugaya K, Greene R, Personett D et al. *Neurobiol Aging* 19, 351–561 (1998).
6. Kesner RP. *Hippocampus* 10, 483–490 (2000).
7. Eckenstein FP, Kuzis K, Nishi R et al. *Biochem Pharmacol* 47, 103–110 (1994).
8. Gonzalez AM, Berry M, Maher PA et al. *Brain Res* 701, 201–226 (1995).
9. Williams TE, Meshul CK, Cherry NJ et al. *J Comp Neurol* 370, 147–158 (1996).
10. Pundt LL, Kondoh T and Low WC. *Brain Res* 695, 25–36 (1995).
11. Isacson O, Deacon TW, Pakzaban P et al. *Nature Med* 1, 1189–1194 (1995).
12. Zhou FC, Buchwald N, Hull C et al. *Neuroscience* 30, 19–31 (1989).
13. Blakemore WF and Franklin RJ. *Cell Transplant* 9, 289–294 (2000).
14. Rosser AE, Tyers P and Dunnett SB. *Eur J Neurosci* 12, 2405–2413 (2000).
15. Rubio FJ, Bueno C, Villa A et al. *Mol Cell Neurosci* 16, 1–13 (2000).
16. Svendsen CN, ter Borg MG, Armstrong RJ et al. *J Neurosci Methods* 85, 141–152 (1998).
17. Blakemore WF and Franklin RJ. *Trends Neurosci* 14, 323–327 (1991).
18. Hatton JD, Garcia R and UHS. *Glia* 5, 251–258 (1992).
19. Lundberg C, Horellou P, Mallet J et al. *Exp Neurol* 139, 39–53 (1996).
20. Fricker RA, Carpenter MK, Winkler C et al. *J Neurosci* 19, 5990–6005 (1999).
21. Gage FH. *Science* 287, 1433–1438 (2000).
22. Gould E, Reeves AJ, Fallah M et al. *Proc Natl Acad Sci USA* 96, 5263–5267 (1999).
23. Kornack DR and Rakic P. *Proc Natl Acad Sci USA* 96, 5768–5773 (1999).
24. Lee CK, Weindrich and Prolla TA. *Nature Genet* 25, 294–297 (2000).
25. Pedersen BK, Bruunsgaard H, Ostrowski K et al. *Int J Sports Med* 21(Suppl. 1), S4–9 (2000).

Acknowledgments: The authors would like to thank Andrew K. Sugaya for technical assistance.

## Transplantation of Clonal Neural Precursor Cells Derived from Adult Human Brain Establishes Functional Peripheral Myelin in the Rat Spinal Cord

Yukinori Akiyama,\* Osamu Honmou,\*†‡ Takaaki Kato,\* Teiji Uede,\*  
Kazuo Hashi,\* and Jeffery D. Kocsis†‡

\*Department of Neurosurgery, Sapporo Medical University School of Medicine, Sapporo, Hokkaido 060-8543, Japan; †Department of Neurology, Yale University School of Medicine, New Haven, Connecticut 06516; and ‡Neuroscience and Rehabilitation Research Centers, Department of Veterans Affairs Medical Center, West Haven, Connecticut 06516

Received December 22, 1999; accepted August 1, 2000

We examined the myelin repair potential of transplanted neural precursor cells derived from the adult human brain from tissue removed during surgery. Sections of removed brain indicated that nestin-positive cells were found predominately in the subventricular zone around the anterior horns of the lateral ventricle and in the dentate nucleus. Neurospheres were established and the nestin-positive cells were clonally expanded in EGF and bFGF. Upon mitogen withdrawal *in vitro*, the cells differentiated into neuron- and glia-like cells as distinguished by antigenic profiles; the majority of cells in culture showed neuronal and astrocytic properties with a small number of cells showing properties of oligodendrocytes and Schwann cells. When transplanted into the demyelinated adult rat spinal cord immediately upon mitogen withdrawal, the cells elicited extensive remyelination with a peripheral myelin pattern similar to Schwann cell myelination characterized by large cytoplasmic and nuclear regions, a basement membrane, and P0 immunoreactivity. The remyelinated axons conducted impulses at near normal conduction velocities. This suggests that a common neural progenitor cell for CNS and PNS previously described for embryonic neuroepithelial cells may be present in the adult human brain and that transplantation of these cells into the demyelinated spinal cord results in functional remyelination. © 2001 Academic Press

**Key Words:** neural precursor cells; axon; demyelination; glia; myelin; multiple sclerosis; Schwann cell.

### INTRODUCTION

Multipotent precursor or stem cells are present in the mammalian central nervous system (CNS) during development and in the adult brain (16, 26, 33, 38, 42, 48). A recent study has demonstrated that neurospheres can be developed from multipotent/progenitor

cells from neurogenic regions of the adult human brain (30). Neural precursor cells can be isolated and expanded in culture in the presence of mitogens such as epidermal growth factor (EGF) or basic fibroblast growth factor (bFGF) (8, 17, 20, 27, 53). After withdrawal of the mitogens and with appropriate growth factors or substrates these cells can differentiate into neurons or glia (44, 48). When transplanted into the embryonic or neonatal CNS both neurons (6, 50, 53) and oligodendrocytes (20, 37) have been generated. These cells appear to differentiate and integrate into the host CNS because they form functional synapses (neurons) and myelinate (oligodendrocytes) axons. However, when injected into the adult CNS, stem cells differentiate into primarily astrocytes (35). These results indicate that environmental signals may direct the specification of cell lineage.

Multipotential neural progenitor cells derived from the fetal human brain propagate and differentiate in culture and *in vivo* (10, 39, 52). Progenitor cells from adult animals have been cultured from the subependymal zone (SEZ) (25, 26, 38, 48), the subventricular zone (SVZ) (33, 38), the hippocampus (16, 42), and the spinal cord (27, 40, 46). A recent study suggested that ependymal cells may be a source of progenitor cells (25), but a GFAP-positive cell distinct from, but adjacent to, ependymal cells has been recently implicated as the primary neural progenitor cell type of the subventricular region (13).

While oligodendrocytes normally myelinate CNS axons, Schwann cells can remyelinate CNS axons after injury (14) and following transplantation into the demyelinated CNS (4, 22). Schwann cells can be derived from single cell clones of neural crest cells (31). Mujtaba *et al.* (40) have distinguished a common neural progenitor for the PNS and the CNS. They found that cultured neuroepithelial cells derived from embryonic rat spinal cords can differentiate into CNS precursors



TABLE 1

Tissue Derivation Sites for Cultures from Patients with Lobe Resections for Tumor Removal

Case	Age/sex	Diagnosis	Location	Culture
1	35/F	Glioma	Frontal lobe (SVZ/SEZ)	+
2	19/M	Glioblastoma	Frontal lobe (SVZ/SEZ)	+
3	64/F	Glioblastoma	Temporal cortex	-
4	62/F	Glioma (low grade)	Temporal lobe, hippocampus	+
5	44/F	Glioma (low grade)	Frontal cortex	-

*Note.* The patients ranged in age from 19 to 64 years old and all had a diagnosis of glioma or glioblastoma. Neural progenitor cells were cultured from frontal and temporal lobe tissue which included periventricular, subependymal, or subventricular zones. Cultures derived from frontal or temporal cortex did not yield neural progenitor cells in culture.

which can differentiate into CNS neurons and glia and PNS precursors which can differentiate into neural crest cells which give rise to peripheral neurons, Schwann cells, and smooth muscle. Recently, Keirstead *et al.* (28) demonstrated that immunoselected precursor cells from neonatal rat forebrain expressing the polysialylated (PSA) form of the neural cell adhesion molecule (NCAM), which mostly generate oligodendrocytes and astrocytes *in vitro*, can produce peripheral myelin *in vivo*.

To test the ability of neural precursor cells derived from the adult brain to differentiate into myelin-forming cells and repair the adult demyelinated CNS, we transplanted clonal neural progenitor cells derived from the adult human brain into an experimentally established glial-free zone in the dorsal columns of the rat spinal cord. Although these precursor cells differentiated upon mitogen withdrawal in culture into neurons and astrocytes and to a lesser extent oligodendrocytes, when transplanted into a demyelinated glial-free zone of the adult rat spinal cord, they extensively remyelinated the axons and restored near normal conduction velocity. The majority of the myelinated axons displayed a peripheral pattern of myelination which is characterized by P0 immunoreactivity, large nuclear and cytoplasmic regions of the myelin-forming cells surrounding the axons and a basement membrane. These data provide evidence that clonal neural precursor cells derived from the adult brain can give rise to Schwann-like cells which form functional myelin when transplanted into an axon-enriched glial-free environment of adult central white matter. Thus, these data suggest that a common neural progenitor cell for the CNS and the PNS described for embryonic neuroepithelial cells (40) may also be present in the adult human brain.

## METHODS

### *Derivation of Adult Human Tissue*

Brain tissue was obtained from five patients undergoing lobe resection for tumor (glioma) removal (Table

1). Either tissue was fixed and prepared for sectioning and immunohistochemistry or selective regions were dissociated for preparation of neurospheres. As our cells were derived from the adult human brain removed because of glioma, criteria were established to distinguish the neurospheres from the glioma cells. First, when cultured alone the glioma cells did not float but adhered to the bottom of the culture flasks. Moreover, they continued to propagate even when they became confluent; the neurosphere-derived cells stopped dividing upon becoming confluent. We also removed tissue from regions remote from the site of the glioma. The glioma cells continued to propagate with and without the presence of mitogens. The proliferative properties of the glioma cells, their adherence to the bottom of the flasks, and their inability to produce small floating cells that coalesce to form neurospheres indicate that these cells were likely not present in the neurosphere cultures utilized for this study.

### *Nestin Immunoreactivity in Brain Slices*

The whole human brain was obtained from a cadaver of a 24-year-old female. The cerebral cortex, subventricular zone, and hippocampus were fixed with 4% paraformaldehyde in 0.14 M Sorensen's phosphate buffer (pH 7.4) at 4°C for 24 h and dehydrated with 30% sucrose in 0.1 M phosphate-buffered saline (PBS) for overnight. The tissues were then placed in OCT compound (Miles Inc.) and frozen in liquid N<sub>2</sub>, and 10-μm sections were cut with a cryostat. Sections were dried onto silane-coated slides. Immunohistochemistry was carried out using an anti-nestin antibody (nestin; 1:5000 anti-monoclonal mouse anti-nestin, Chemicon). The primary antibody was visualized using Vectastain ABC-AP mouse IgG kit (Vector Laboratories) and alkaline phosphatase substrate kit 4 (BCIP/NBT; Vector Laboratories) according to the manufacturer's instruction. After immunostaining, slides were covered by coverglasses using Crystal/Mount (Biomedica Corp.). Photographs were taken on a Zeiss microscope (Axioskop FS).



### *Primary Culture of Adult Human Neural Precursor Cells*

Tissue samples were obtained from frontal cortex, temporal cortex, hippocampus, and the subventricular/subependymal zone of the frontal lobe in adult humans operated on to remove brain tumors (summarized in Table 1). The samples were dissected in L-15 medium; rinsed; enzymatically treated in L-15 containing 0.01% DNase I, 0.25% trypsin, and 0.1% collagenase at 37°C for 30 min; and mechanically dissociated by brief trituration with a fire-polished silicon-coated Pasteur pipette. The cells were collected by centrifugation, resuspended in serum-free medium (NPM, neural progenitor cell maintenance medium, Clonetics, San Diego, CA) supplemented with 10 ng/ml bFGF and 10 ng/ml EGF, and plated onto 100-mm<sup>2</sup> laminin-coated tissue culture plates at  $8 \times 10^5$  cells per plate. The next day, the cells were resuspended and then plated onto 100-mm<sup>2</sup> noncoated culture plates. Six hours later, the supernatant was collected and replated onto 100-mm<sup>2</sup> noncoated culture plates. Cells were maintained at 37°C in 5% CO<sub>2</sub>/95% O<sub>2</sub>. bFGF and EGF were added daily and culture medium was changed weekly. Spherical masses (i.e., neurospheres) became visible after 7–10 days in culture.

### *Clonal Expansion and Induced Differentiation of Adult Human Neural Precursor Cells*

A spherical mass of cells in the primary culture dish was collected under microscopy and was dissociated by incubation in HBSS containing 0.05% trypsin and 0.01% DNase I. The dissociated cells were cloned by limiting dilution in 96-well plates. After the single cell expansion, a spherical mass of cells in the secondary culture was collected and the same procedure was repeated for further subcloning. In all processes, cells which were not dissociated well were discarded to avoid contamination.

Differentiation of the clones was initiated by enzymatically and mechanically dissociating the cellular sphere (neurosphere) and culturing on polyethyleneimine-pretreated plates in the absence of mitogen.

### *Phenotypic Analysis in Vitro: Immunocytochemistry*

Cultured cells were rinsed in PBS and fixed for 15 min with a fixative solution containing 4% paraformaldehyde in 0.14 M Sorensen's phosphate buffer, pH 7.4, 4°C. Fixed cells were incubated for 15 min in a blocking solution containing 0.2% Triton X-100 and 5% normal goat serum before incubation with the primary antibody. The primary antibodies used were anti- $\alpha$ -microtubule-associated protein 2 (MAP-2; 1:10,000 monoclonal mouse anti-MAP-2, Upstate Biotechnology), anti- $\tau$  (1:1,000 monoclonal mouse anti- $\tau$ , Sigma), anti- $\beta$ -tubulin type III (TUBJ-1; 1:500 monoclonal mouse anti-

TUBJ-1, Babco), anti-neurofilament (NF; 1:1,000 monoclonal mouse anti-NF, Nitirei), anti-neuron-specific enolase (NSE; 1:1,000 polyclonal rabbit anti-NSE, Nitirei), anti-glial fibrillary acidic protein (GFAP; 1:200 polyclonal rabbit anti-GFAP, Nitirei), anti-O4 (O4; 1:100 monoclonal mouse anti-O4, Boehringer Mannheim), anti-galactocerebroside (GalC; 1:200 monoclonal mouse anti-GalC, Boehringer Mannheim), anti-nestin (nestin; 1:5,000 monoclonal mouse anti-nestin, Chemicon), anti-A2B5 (1:100 monoclonal mouse anti-A2B5, Boehringer Mannheim), anti-vimentin (Vim; 1:100 monoclonal mouse anti-Vim, Nitirei), anti-peripheral myelin protein (P0; 1:200 monoclonal rabbit anti-P0 antibody, kindly provided by Dr. D. Colman), and anti-S-100 protein (S-100; 1:1000 polyclonal rabbit anti-S-100, Nitirei). Triton-X was omitted in the reaction with A2B5, GalC, and O4 primary antibody. The primary antibody was visualized using goat anti-mouse and goat anti-rabbit IgG antibody with fluorescein (FITC) (1:100, Jackson ImmunoResearch Laboratories, Inc.) or alkaline phosphatase reaction (Zymed) according to the manufacturer's instructions. After immunostaining, coverslips were mounted cell side down on microscope slide using mounting medium (Dako). Photographs were taken on a Zeiss immunofluorescent microscope (Axioskop FS).

### *LacZ Transfection into the Clonal Adult Human Neural Precursors*

An expression vector for mammalian cells which contains the LacZ gene was used to transduce the bacterial  $\beta$ -galactosidase ( $\beta$ -gal) gene into clonally expanded neural precursors derived from the human brain. Clones of neural precursors were transfected by pcDNA3.1/His/LacZ (Invitrogen) constructed by cloning the  $\beta$ -gal gene into the pcDNA vector. The CMV provided the promoter for the  $\beta$ -gal gene. The simian virus 40 early promoter and the neomycin resistance gene, transmitting G418 resistance, are present downstream from the  $\beta$ -gal gene to permit selection of transfected colonies. Lipofectamine (20  $\mu$ g/ml; Gibco) was used to transfect the expression vector pcDNA3.1/His/LacZ (10  $\mu$ g/ml) to cultured precursors, which were rapidly proliferating under the influence of mitogen. Transfected precursors were then selected by incubation with the neomycin analogue G418 (400  $\mu$ g/ml). Five rats received transplants from neuroprecursors transfected with the LacZ gene.

### *Animal Preparation and Transplantation*

Experiments were performed on 12-week-old Wistar rats (8 unoperated controls, 10 demyelinated, and 15 demyelinated with transplants). The transplant experiments ( $n = 15$ ) were carried out in three groups of 5 rats for a repeat of three times. A focal demyelinated lesion was created in the dorsal column of the spinal

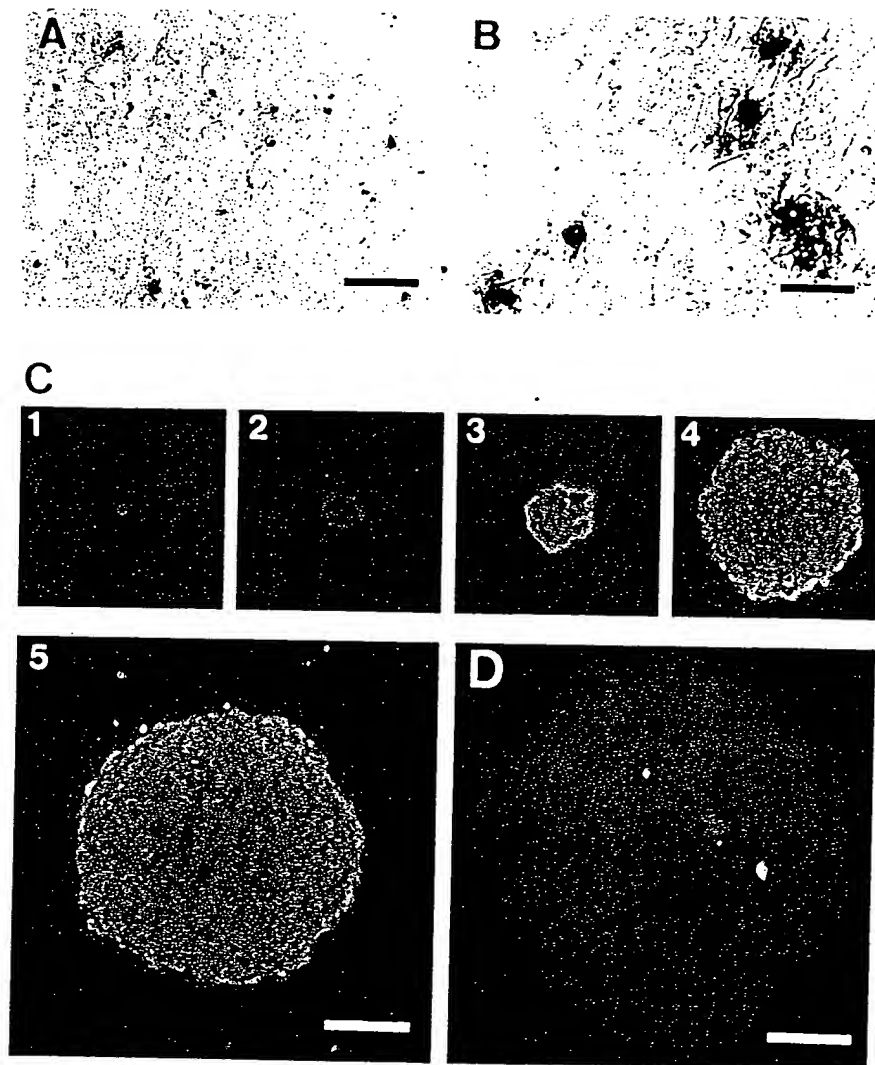


**FIG. 1.** The adult human brain harbors nestin-positive precursor cells. Immunohistochemical examination demonstrates scattered islands of the neural precursor cells in SVZ/SEZ (A and B). Nestin-positive cells are visualized by alkaline phosphatase reaction (A, lower magnification, bar 100  $\mu$ m; B, higher magnification, bar 25  $\mu$ m). (C) Clonal expansion of cells derived from adult human brain *in vitro*. High-power microscopic images in cultures. (C1) A single precursor cell in one well of a 96-well culture plate. (C2) In the presence of mitogen, a spherical cell mass begins to form after 4 days. The spherical appearance of adult human precursors after 1 week (C3), 2 weeks (C4), and 4 weeks (C5) *in vitro*. (D) Nestin-labeled neural aggregate derived from single cell expansion. Nestin positivity is visualized with fluorescein (FITC) (C1–C5, bar 100  $\mu$ m; D, bar 40  $\mu$ m).

cord using X-irradiation and ethidium bromide injection (EB-X) utilizing a method similar to that of Honmou *et al.* (22). Briefly, rats were anesthetized with ketamine (75 mg/kg) and xylazine (10 mg/kg) ip, and a 40-Gy surface dose of X-irradiation was delivered through a 2  $\times$  4-cm opening in a lead shield (4 mm thick) to the spinal cord caudal to the 10th thoracic level (T-10) using a Softex M-150 WZ radiotherapy machine (100 kV, 1.15 mA, SSD 20 cm, dose rate 200 cGy/min). Three days after irradiation, rats were anesthetized as above and, using sterile technique, a laminectomy was performed at T-11. The demyelinating lesion was induced by the direct injection of EB into the dorsal column via a drawn glass micropipette. Injections of 0.5  $\mu$ l of 0.3 mg/ml EB in saline were made at

depths of 0.7 and 0.4 mm near the midline of the dorsal columns at three longitudinal sites separated by 2 mm. A suspension of clonal progenitors ( $1 \times 10^4$  cells/ $\mu$ l) in 1  $\mu$ l medium was injected into the middle of the EB-X-induced lesion 3 days after the EB injection. Transplant-receiving rats were immunosuppressed with cyclosporin A (10 mg/kg/day, sc, kindly provided by Novartis Pharma AG, Basel, Switzerland).

#### Histological Examination

The rats were deeply anesthetized with sodium pentobarbital (50 mg/kg, ip) and perfused through the heart, first with PBS and then with a fixative solution containing 2% glutaraldehyde and 2% paraformalde-



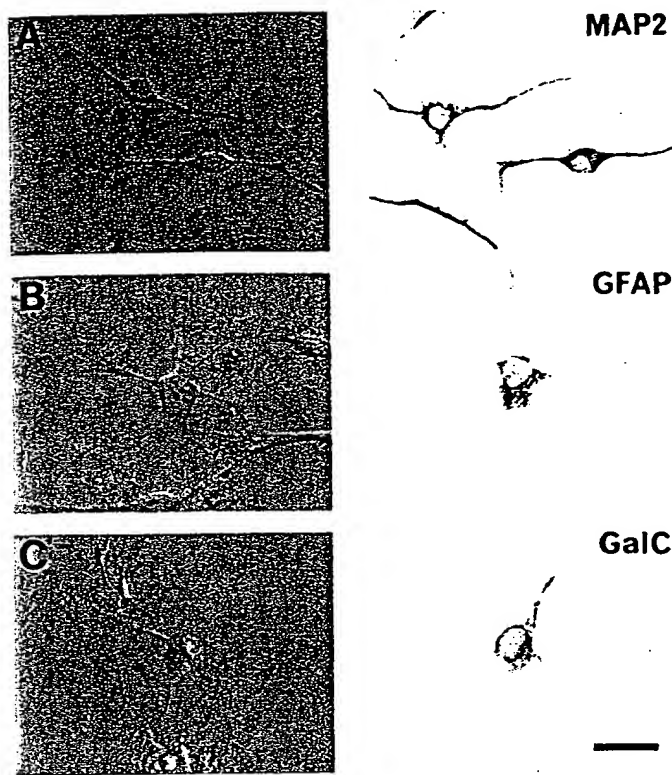


**FIG. 2.** Cell differentiation in culture after mitogen removal. Phase contrast photomicrographs showing a neuron-like cell (A, left), an astrocyte-like cell (B, left), and an oligodendrocyte-like cell (C, left). Immunolabeling of the cells with anti-MAP-2 (A, right), anti-GFAP (B, right), and anti-GalC (C, right) indicates neuronal, astrocytic, and oligodendrocytic phenotypes, respectively. The primary antibody was visualized using goat anti-mouse and goat anti-rabbit IgG antibody with alkaline phosphatase reaction. Bar, 25  $\mu$ m.

hyde in 0.14 M Sorensen's phosphate buffer, pH 7.4. Following *in situ* fixation for 10 min the spinal cord was carefully excised, cut into 1-mm segments, and placed into fresh fixative. The tissue was washed several times in Sorensen's buffer, postfixed with 1%  $\text{OsO}_4$  for 2 h at 25°C, dehydrated in graded ethanol solutions, passed through propylene oxide, and embedded in EPON. Thick sections (1  $\mu$ m) were cut, counterstained with 0.5% methylene blue, 0.5% azure II in 0.5% borax, and examined with a light microscope (Zeiss: Axioskop FS). Semithin sections were counterstained with uranyl and lead salts and examined with a JEOL JEM1200EX electron microscope operating at 60 kV.

#### Detection of $\beta$ -Galactosidase Reaction Products in Vitro and in Vivo

$\beta$ -Gal-expressing cells were detected *in vitro* by incubating the cultured neurospheres with X-Gal to form a blue color within the cell (data not shown). Neurospheres were fixed in 0.05% glutaraldehyde, washed with PBS, and then incubated with X-Gal to a final concentration of 1 mg/ml in X-Gal developer (35 mM

$\text{K}_3\text{Fe}(\text{CN})_6/35 \text{ mM } \text{K}_4\text{Fe}(\text{CN})_6 \cdot 3\text{H}_2\text{O}/2 \text{ mM } \text{MgCl}_2$  in phosphate-buffered saline). Cells were then incubated at 37°C overnight and examined by light microscopy for the presence of a blue reaction product.

Three weeks after transplantation,  $\beta$ -galactosidase-expressing Schwann-like cells were detected *in vivo*. Spinal cords were removed and fixed in 0.5% glutaraldehyde in phosphate buffer for 1 h. Sections (100  $\mu$ m) were cut with a vibratome and  $\beta$ -galactosidase-expressing Schwann-like cells were detected by incubating the sections at 37°C overnight with X-Gal to a final concentration of 1 mg/ml in X-Gal developer to form a blue color within the cell. The slices were then fixed in 10% paraformaldehyde in phosphate buffer overnight, dehydrated, and embedded in paraffin. Transverse sections (3  $\mu$ m) were cut and examined by light microscopy (Zeiss; Axioskop FS) for the presence of a blue reaction product ( $\beta$ -galactosidase reaction product).

#### Phenotypic Analysis in Vivo: Immunohistochemistry

Three weeks after transplantation, the peripheral myelin protein P0-expressing myelin-forming cells were detected *in vivo*. The rats were deeply anesthetized with sodium pentobarbital (50 mg/kg, ip) and perfused through the heart, first with PBS and then with a fixative solution containing 10% paraformaldehyde in 0.14 M Sorensen's phosphate buffer, pH 7.4. Spinal cords were removed, fixed in 10% paraformaldehyde in phosphate buffer for overnight, dehydrated, and embedded in paraffin. Transverse sections (3  $\mu$ m) were cut. Paraffin wax-embedded sections were dewaxed in xylene and treated with 1% hydrogen peroxide. Monoclonal rabbit anti-P0 antibody (1:200), polyclonal rabbit anti-NSE antibody (1:1000), and polyclonal rabbit anti-GFAP antibody (1:200) were applied. The primary antibody was visualized using goat anti-rabbit IgG antibody with peroxidase reaction. The nucleus was counterstained with hematoxylin. After dehydration with 70% alcohol, coverslips were mounted tissue side down on microscope slide using mounting medium (Dako). Photographs were taken on a Zeiss microscope (Axioskop FS).

#### Field Potential Recording

After induction of deep anesthesia (sodium pentobarbital 50 mg/kg, ip), the spinal cords of control ( $n = 5$ ), demyelinated ( $n = 5$ ), and transplanted rats ( $n = 5$ ) were quickly removed and maintained in an *in vitro* submersion-type recording chamber with a modified Krebs' solution (containing 124 mM NaCl, 26 mM  $\text{NaHCO}_3$ , 3 mM KCl, 1.3 mM  $\text{NaH}_2\text{PO}_4$ , 2 mM  $\text{MgCl}_2$ , 10 mM dextrose, 2 mM  $\text{CaCl}_2$ ; saturated with 95%  $\text{O}_2$  and 5%  $\text{CO}_2$ ) (Fig. 6A). Field potential recordings of compound action potentials were obtained with glass microelectrodes (1–5 M $\Omega$ ; 1 M NaCl) positioned in the dorsal columns, and signals were amplified with a

high-input impedance amplifier (Axoclamp 2A; Axon Inc.) and stored on a digitizer (Nicolet Pro 34). The axons were activated by electrical stimulation of the dorsal columns with bipolar Teflon-coated stainless-steel electrodes cut flush and placed lightly on the dorsal surface of the spinal cord. Constant current stimulation pulses were delivered through stimulus isolation units and the timing of the pulses was controlled by a digital timing device. The recorded field potentials were positive-negative-positive waves corresponding to source-sink-source currents associated with propagating axonal action potentials (22, 29); the negativity represents inward current associated with the depolarizing phase of the action potential.

All variances represent standard error ( $\pm$ SEM). Differences among groups were assessed by unpaired two-tailed *t* test to identify individual group differences. Differences were deemed statistically significant at  $P < 0.05$ .

## RESULTS

### *Regional Distribution of Nestin-Positive Cells in the Adult Human Brain*

Nestin immunoreactivity was studied in human brain sections obtained from the periventricular region of the frontal lobe, the hippocampal complex, and the frontal cortex. Islands of nestin-positive cells were found in each of these regions. The SEZ/SVZ regions located below the ependyma of the lateral margin of the anterior horn of the lateral ventricle contained a relatively high density of cells (Figs. 1A and 1B). The nestin-positive cells were either dispersed or localized in small groups. Within the hippocampal complex, the external surface of the dentate gyrus also contained a relatively high density of nestin-positive cells; Ammons horn (CA1-CA4) had a paucity of nestin-positive cells. Although frontal cortex had recognizable nestin-positive cells, they were scattered and much less dense and localized compared to the SEZ/SVZ and the dentate gyrus.

Brain tissue was removed from five patients (See Methods and Table 1) and divided from each patient for preparation of neurospheres in culture. We could prepare neurospheres from the SEZ/SVZ in two and from the temporal lobe/hippocampus in one patient (Table 1). We were unsuccessful in obtaining neurospheres from tissue in the temporal cortex and frontal cortex in two other patients. Neurospheres used in this study were prepared from the SEZ/SVZ from two patients.

### *Clonal Expansion of Nestin-Positive Cells*

Nestin-positive cells isolated from the adult human brains were expanded by daily addition of EGF and bFGF in serum-free medium (see Methods). These cells

grew as neurospheres and were expanded for a week or more in culture. A continuous supply of mitogens (EGF and bFGF) was important to repress differentiation and maintain a homogeneous population of self-renewing nestin-positive cells. As described below, upon mitogen withdrawal putative neuronal and glial lineages could be differentiated from these cells. In order to determine if the nestin-positive cells were generated by separate committed precursors or by a common multipotential precursor cell, a single cell clonal expansion method was used prior to mitogen withdrawal. Using the limiting dilution method (see Methods), individual dissociated cells (Fig. 1C1) from a sphere of nestin-positive cells were plated in a 96-well culture dish. An example of reestablishment of a neurosphere of nestin-positive cells from an individual cell is shown in Fig. 1C. Note the cellular proliferation in Figs. 1C1-1C5 over 4 weeks in culture. Figure 1D shows that these cells were indeed nestin positive after expansion. All expanded colonies displayed similar properties, thus indicating the clonal nature of the cells. Continued proliferation was observed for over 8 months *in vitro* in the presence of mitogen, and subclones could be established from these clonal cell lines allowing further expansion of the cells by repeating the limiting dilution method.

### *Characterization of the Human Precursor Cells Following Withdrawal of Mitogens in Culture*

While the purpose of this study was not to study in detail lineage of the precursor cells but to study their fate when transplanted into a demyelinated region *in vivo*, we carried out some phenotypic characterizations to define our precursor cell population. To examine the multipotentiality of clones, expanded spheres of the nestin-positive clonal cells were dissociated and plated on polyethyleneimine-coated coverslips and maintained in culture in the absence of mitogen. At least three morphologically distinct cell types were observed from a dissociated neurosphere of clonally expanded cells (Figs. 2A-2C). The antigenic and morphological features of these cells were similar to those of rat stem cell cultures described in detail elsewhere (26). The three most common morphologies of cells were relatively small fusiform cells typically with two or three neurites (Fig. 2A), a larger multipolar cell (Fig. 2B), and a small spherical multipolar cell (Fig. 2C). Cells showing these morphologies stained positively for MAP-2, GFAP, and GalC, respectively (Figs. 2A-2C, right panels; different cells from the left panels), thus suggesting neuron-, astrocyte-, and oligodendrocyte-like differentiation.

The relative distribution of these cell types with various markers for neurons and glia is shown in Fig. 3. Note that the largest proportions of cells stained with MAP-2, TUJ-1, NSE, GFAP, and Vim. A2B5-labeled

cells were very limited. A very small proportion of cells were labeled by GalC and S100; O4 and P0 staining was virtually absent. This pattern of staining was similar from clone to clone. In a limited number of experiments dual immunolabeling was carried out to directly show multiple cell lineage derived from a clonal cell (data not shown); i.e., some cells stained positive for MAP-2 and TUJ-1 suggesting neuronal elements while others in the field were negative for those markers but positive for GFAP. We are careful with this level of analysis not to define these cells as being fully committed to neurons or astrocytes, but rather that upon mitogen withdrawal in culture that they differentiate in a pattern consistent with these phenotypes. These results are in agreement with other studies showing a relatively large number of neuron-like and astrocyte-like cells differentiating from neural precursor cells in culture after mitogen withdrawal, and a paucity of oligodendrocytes and Schwann cells (26, 27).

#### *Transplantation of Neural Precursor Cells into a Glial-Free Spinal Cord Tract*

The dorsal columns of the lumbar spinal cords were X-irradiated and subsequently injected with a nuclear chelator, ethidium bromide, to kill glial cells and to inhibit mitosis of endogenous glial cells (EB-X model; see Methods). The lesion induced by this procedure is characterized by virtually complete loss of endogenous glial elements (astrocytes and oligodendrocytes) with preservation of axons, i.e., a demyelinated lesion with no glia. The lesion occupies the entire dorsoventral extent of the dorsal columns for 5–7 mm longitudinally (5, 22, 23). No endogenous invasion of Schwann cells, oligodendrocytes, or astrocytes occurs before 6 to 8 weeks at which time these cells begin to invade the lesion from its peripheral borders. Thus, a demyelinated and glial-free environment *in vivo* is present for at least 6 weeks.

Myelinated axons in the normal dorsal columns are shown in the photomicrograph in Fig. 4A. After induction of an EB-X lesion virtually all of the axons are demyelinated, and astrocytes and oligodendrocytes are killed providing an aglial environment with preserved demyelinated axons and macrophages with cellular debris (Fig. 4B). Three weeks after injection of clonal human neural precursor cells into the central region of the lesion in immunosuppressed rats (cyclosporin A; see Methods), there was extensive remyelination of the axons (Figs. 4C and 4D). Remyelination was observed across the entire coronal dimension of the dorsal columns and considerably throughout the anteroposterior extent of the lesion. While it is well established that no endogenous remyelination by oligodendrocytes or Schwann cells occurs in this lesion model for at least 6 weeks (5), some donor cells were transfected with the

reporter gene LacZ and X-Gal-positive cells were observed forming myelin (Fig. 4E).

The anatomical pattern of myelination was similar to that produced by Schwann cells, i.e., large cytoplasmic and nuclear regions surrounding the remyelinated axons (Fig. 4D, arrows). Immunoreactivity for the peripheral myelin-specific protein, P0, was observed in the myelin of the transplanted regions further indicating that Schwann cells were differentiated *in vivo* from the neural precursor cells (Fig. 4F). Electron microscopic examination of the remyelinated axons reveals ultrastructural features of peripheral myelin (Fig. 5A). The axons were ensheathed by relatively thick myelin surrounded by large cytoplasmic and nuclear regions characteristic of Schwann cell myelination (4, 22). Normal and demyelinated dorsal column axons are shown in Figs. 5B and 5C, respectively, for comparison. Moreover, a basement membrane, which is not observed around axons myelinated by oligodendrocytes, was observed around the myelin-forming cells after neural precursor cell transplantation (Fig. 5A, arrowheads). The morphological features and presence of P0 immunoreactivity indicate that the CNS-derived precursor cells differentiate *in vivo* into a cell with peripheral Schwann cell characteristics.

#### *Restoration of Normal Conduction Velocity in the Remyelinated Axons*

Spinal cords from control, demyelinated, and transplanted rats were removed and maintained in an *in vitro* recording chamber (see Methods). The dorsal columns were stimulated on the surface with bipolar electrodes and glass microelectrodes were used to record field potentials at various points through the lesion area (Fig. 6A). The recordings in Fig. 6B are superimposed traces of compound action potentials recorded 1

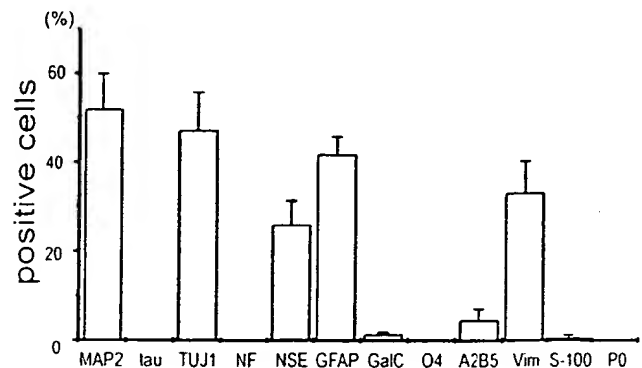
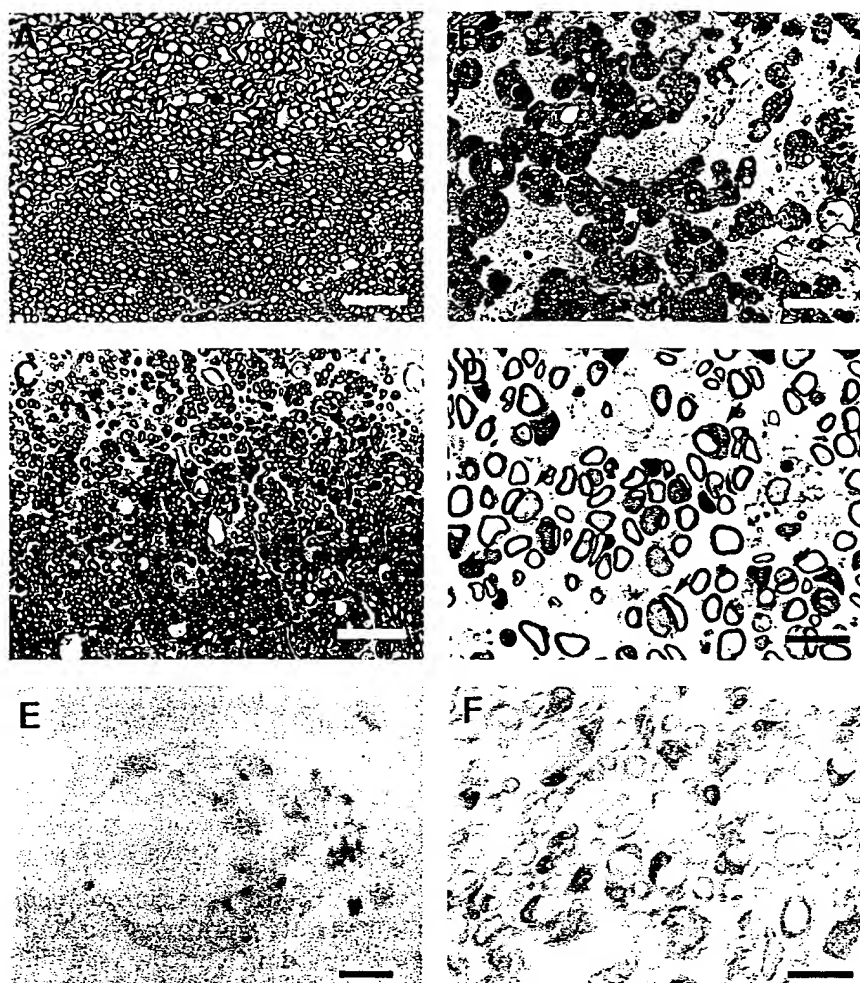


FIG. 3. Clones were differentiated in culture for 10 days in the absence of EGF and bFGF. Phenotypic analysis indicated a large proportion of cells expressing MAP-2, TUJ-1, NSE, GFAP, and Vim and a lesser proportion expressing GalC, A2B5, and S-100. Little expression of  $\tau$ , NF, O4, and P0 was observed. This suggests that these immature cells had characteristics of neuron and astrocytes and to a lesser extent immature oligodendrocytes and Schwann cells.



**FIG. 4.** Remyelination of the rat spinal cord following transplantation of adult human precursor cells. Normal (A), demyelinated (B), and remyelinated axons (C) of the dorsal column. (D) Remyelinated axons at higher magnification. The anatomical pattern of myelination was similar to that produced by Schwann cells (arrows). (E) The human cells in the rat EB-X lesions were visualized by  $\beta$ -galactosidase reaction products (blue). Note that the transplanted human cells are markedly labeled *in vivo* at the light microscopic level. (F) Antigenic phenotype of remyelinating cells in the lesions are P0 positive (peroxidase reaction, brown), and their nuclei are counterstained with hematoxylin (blue). P0 immunostaining demonstrates many Schwann-cell-like remyelination throughout the lesion (bar, A–C, 25  $\mu$ m; D, 10  $\mu$ m; E, 1  $\mu$ m; F, 7  $\mu$ m).

mm apart from control (Fig. 6B1), demyelinated (Fig. 6B2), and transplanted (Fig. 6B3) dorsal columns. The latencies of the responses in the demyelinated dorsal column (Fig. 6B2) are substantially delayed compared to controls (Fig. 6B1). However, following human neural precursor cell transplantation (Fig. 6B3) which led to extensive remyelination, the latencies are similar to controls. Conduction velocities were calculated for the three groups and are shown in Fig. 6C, indicating the restoration of conduction velocity in the transplanted group.

#### DISCUSSION

In this study we demonstrate that clonally expanded multipotential neural progenitor cells from the adult human brain can form functional Schwann cell-like myelin when transplanted into the demyelinated rat

spinal cord. These progenitor cells expressed nestin and were self-renewing in culture until induced to differentiate by removing mitogens from the culture. Antigenic analysis after mitogen removal in culture revealed the differentiation into both neuron- and glia-like cells. In general, neurons, astrocytes, and a low number of oligodendrocytes and Schwann cells were present in the mitogen-free cultures. Following transplantation into the demyelinated rat spinal cord, however, the vast majority of cells differentiated into a peripheral-type of myelin-forming cell which produced functional myelin.

#### *Clonal Expansion of Multipotential Adult Human Neural Precursor Cells*

Both proliferation and differentiation of the clonal multipotential neural precursors derived from the



**FIG. 5.** All demyelinated spinal cords that received adult human precursor cell injections showed clear evidence of remyelination (A) of the demyelinated axons in electron micrographs. Examination at higher magnification showed the presence of a basal lamina surrounding the fibers (arrowheads). The large cytoplasmic and nuclear regions of the cell and the presence of a basal lamina indicate a peripheral pattern of myelination. Normal (B) and demyelinated (C) axons in the dorsal columns at the electron microscopic level. Bar, 1  $\mu$ m.

adult brain could be controlled relatively efficiently. Several lines of evidence indicate that the cells in the clones are composed of a common multipotential cell rather than separate committed precursors. First, the proportion of neurons generated is independent of passage number, suggesting that the cellular properties are constant as the clones expand. This stability is supported by the unchanged differentiation capacity in clones of acutely dissociated cells and in subclones. Second, subcloning experiments demonstrate that multipotential secondary clones can be derived from a single primary clone, again showing the multipotentiality of single clonal cells. Asymmetric cell division

may still be an important mechanism for cell-type specification *in vivo* (11). However, a strict asymmetric model, in which only one of the daughter cells maintains multipotentiality, cannot account for the exponential increase in the neural precursor cells seen in our cultures.

#### *Differentiation of Neural Precursor Cells into Morphologically Defined Schwann-like Cells*

In the normal CNS axons with oligodendrocyte-associated myelination do not have large nuclear and cytoplasmic surrounds, nor do they have an associated basement membrane. Rather, the cell bodies of the oligodendrocyte are relatively small and remote from the site of axonal myelination. However, following transplantation of the clonal neural precursor cells into a demyelinated and aglial region of the spinal cord *in vivo*, extensive differentiation into myelin-forming cells with morphological and phenotypical characteristics of Schwann cells was observed. These cells exhibited the hallmark characteristics of peripheral myelin-forming cells, large nuclear and cytoplasmic regions surrounding the axons which in turn were covered by a basement membrane (3), and immunohistochemical analysis demonstrated that most of them were P0 positive. Keirstead *et al.* (28) recently demonstrated that neural precursor cells derived from the neonatal rat brain and immunoselected for glial commitment can produce P0-positive myelin-forming cells *in vivo*. We cannot rule out the possibility that some neuronal or glial differentiation occurred, because we observed a few NSE-positive or GFAP-positive cells in the EB-X lesion. Moreover, some of the myelinated profiles were more characteristic of oligodendrocyte myelination. Future quantitative immunohistochemical studies on these tissues will be important to more fully characterize the phenotypes of the myelin-forming cells after transplantation. However, the abundance of cells with distinct morphological and immunohistochemical features characteristic of peripheral myelin-forming cells (large nuclear and cytoplasmic regions around the axons surrounded by a basement membrane and their P0 positivity) clearly indicate that the transplanted precursor cells differentiated into a peripheral pattern of myelin-forming cells.

It is well established that peripherally derived Schwann cells can myelinate the spinal cord which is normally myelinated by oligodendrocytes (4, 14). Given that endogenous remyelination by Schwann cells can occur in the spinal cord in certain circumstances, it was important to ascertain that the myelin-forming cells were derived from the donor source and not from endogenous invasion of Schwann cells from the periphery. To address this issue we used a model system that prevents endogenous invasion of peripheral Schwann cells for 6 to 8 weeks; we studied the cells about 3



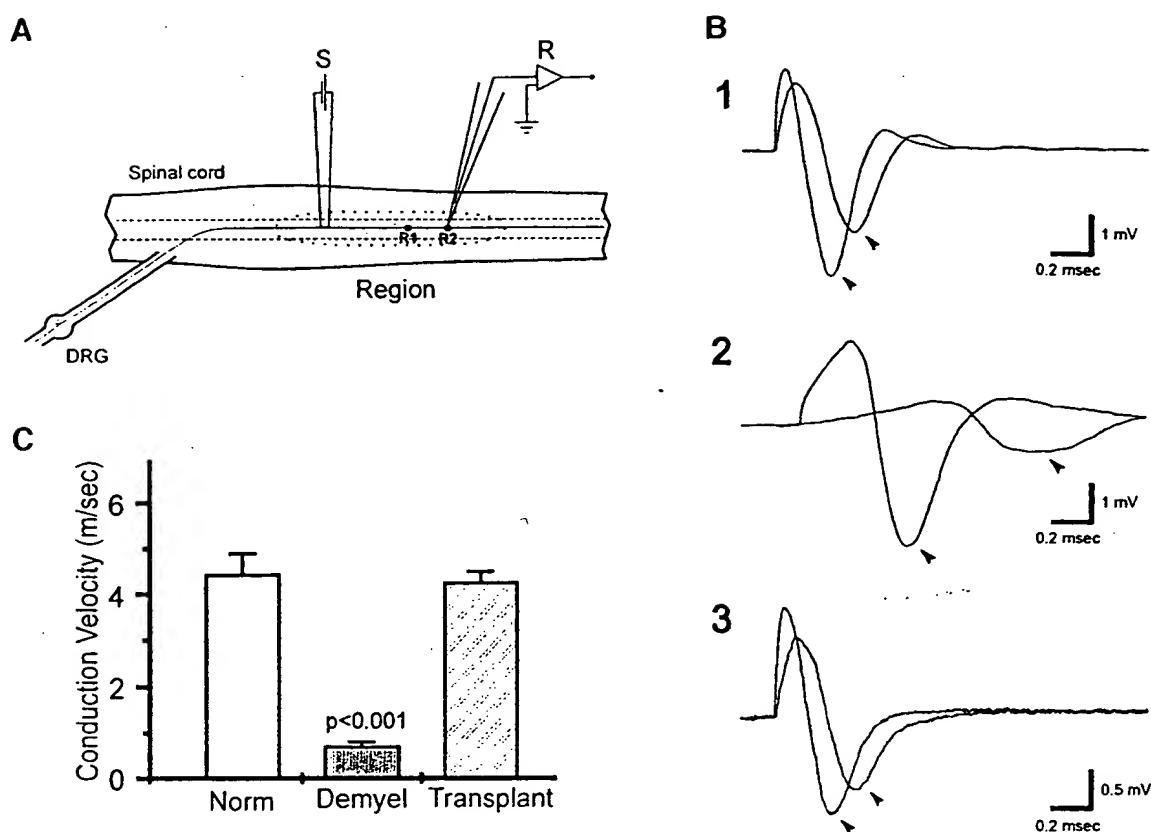


FIG. 6. (A) Schematic showing the dorsal surface of spinal cord with the positions of the stimulating (S) and recording (R) electrodes. Shaded region indicates the area of demyelination or remyelination. (B) Compound action potentials recorded at 1-mm increments along the dorsal columns in control (1), EB-X demyelinated (2), and transplant-induced remyelinated (3) axons. (C) Conduction velocity for the three groups ( $n = 5$ , each group) of axons recorded at 26°C. Bars, SEM.

weeks after transplantation which is well within the time window where no endogenous myelination occurs (4). The model utilizes X-irradiation to block host cell division followed by injections of ethidium bromide to chelate nucleic acids and kill the glial cells within the lesion zone. Moreover, in a limited number of experiments we transplanted LacZ-transfected donor progenitor cells and found X-Gal reactivity in cells exhibiting a peripheral myelination pattern. The extensive differentiation of neural precursor cells into Schwann cell-like cells in our studies is not likely the result of Schwann cell contamination in our cultures. The cells were derived from single cell clones showing homogeneous properties and the capacity to differentiate into either neurons or glia.

Kalyani *et al.* (27) suggest that appropriate manipulation of culture conditions (45, 51) could promote embryonic neuroepithelial cell differentiation into more restricted CNS and PNS neural precursor cells. Indeed, embryonic neuroepithelial cells derived from the spinal cord have been reported to give rise to PNS elements and to other cell types in the body including skin melanocytes (24, 31, 41). More recently, Mujtaba *et al.* (40) provide evidence for a common neural pro-

genitor cell derived from the embryonic spinal cord for the CNS and the PNS. Our results suggest that such a multipotential precursor may also be present in the adult human brain and that transplantation of these cells into the appropriate pathological environment of the adult CNS can allow Schwann cell differentiation and functional remyelination *in vivo*.

#### *Why Do Neural Precursor Cells Derived from Adult Brain Differentiate into Schwann-like Cells in CNS in Vivo?*

The Schwann cell differentiation *in vivo* may be the result of both the intrinsic capacity of the progenitor cells and the cellular and extracellular milieu of the transplant zone. In the EB-X lesion it is important to note that not only does this model lead to long-lasting demyelination, but all cellular elements inclusive of astrocytes and oligodendrocytes are killed within the lesion thus rendering the white matter tract aglionic and enriched in axons. The dominant cellular elements in the lesion are naked axons and macrophage-like scavenger cells in the glial-free environment. A large body of work indicates that axon-associated signals

may be important in aspects of Schwann cell differentiation (12, 43, 55). The development and maintenance of cell types are dependent upon and influenced by a number of intrinsic genetic factors as well as environmental signals (6, 47, 49, 54). Such signals may be provided by cell-to-cell contact, electrical stimulation, or the secretion of neurotransmitters and neurotrophic factors (9).

It should also be pointed out that interleukins released from macrophages have been implicated in Schwann cell differentiation following peripheral nerve injury (21, 32). It is conceivable that cytokines released from microglia or macrophages in the lesion site could contribute to the massive Schwann cell differentiation following neural precursor cell transplantation. It is possible then that the neural precursor cells derived from the adult human brain and transplanted into an axon-enriched environment *in vivo* in the absence of potential trophic influences from surrounding glia and neurons biases the differentiation of the neural precursor cells to a more restricted PNS lineage. It is important to note that EGF-responsive neural stem cells derived from fetal rodents formed an oligodendrocyte pattern of remyelination in myelin-deficient rats (20). This may result from differences in fetal and adult sources of the cells or a species difference. Another possibility is that the myelin-deficient rat, which has an abundance of astrocytes around the amyelinated axons, could provide a trophic influence for the differentiation of oligodendrocytes. It is not clear what the differences are between known totipotent stem cells derived from embryos and less defined progenitor cells derived from adult subependymal zone. It will be interesting to determine if embryonically derived stem cells form peripheral or central patterned myelin when transplanted into the adult demyelinated CNS.

#### *Potential of Neural Precursor Cells to Repair the Damaged CNS*

Neurons are not generated in large numbers in the adult mammalian CNS with the exception of the olfactory bulb (1, 34, 36) and the hippocampal formation (2, 7). Moreover, Gould *et al.* (18) have made the intriguing observation that learning can enhance neurogenesis in the adult hippocampus, possibly by differentiation of precursor cells. Cultured precursors derived from adult mice have been shown to differentiate into neurons and glia, but little is known about the mechanisms that regulate the differentiation of these cells (19). Both the clonal analysis and the response to growth factors reported here show that neural precursor cells derived from the adult human CNS have some properties that are similar to stem cells derived from embryonic neuroepithelium. Further delineation of similarities and differences between embryonic and

adult precursor cells is certainly important. While both share some similarities it is not clear that adult-derived cells are totipotent as are true stem cells derived from embryos, thus indicating the importance of investigations of both embryonic and adult brain-derived precursor cells.

While oligodendrocytes are the cells that normally myelinate CNS axons, peripheral myelin-forming cells such as Schwann cells (4, 22) and olfactory ensheathing cells (15, 23) can myelinate CNS axons *in vivo* and restore near normal conduction properties (22, 23). Peripheral myelin-forming cells may have the advantage if used as a cell therapy in multiple sclerosis (MS) patients of not having the antigenic properties of oligodendrocytes which elicit an immune response in MS patients (22). Harvesting sufficient numbers of Schwann cells from peripheral nerve biopsy and cell expansion is problematic. However, the development of human clonal neural precursor cells derived from either embryonic or adult CNS may allow for an abundant source of myelin-forming cells. Zhang *et al.* (56) have demonstrated that fetal neural stem cells can be treated to establish self-renewing pre-O2-A progenitors which form extensive oligodendrocyte myelination when transplanted into the myelin-deficient neonatal rat. Recently, Brustle *et al.* (6) have demonstrated that human embryonic stem-cell-derived glial precursors can be used as a source of myelinating transplants. Advances in the cell biology of progenitor cells derived from embryonic, fetal, or adult CNS open the prospect of developing cell lines as a potential source of a cell therapy for demyelinating diseases.

#### ACKNOWLEDGMENTS

We thank Dr. David Colman for the gift of anti-P0 antibody. This work was supported in part by grants from the Japanese Monbusyo (09671434 and 11770765), Japan Heart Foundation Research Grant, the National Multiple Sclerosis Society (U.S.A.), the National Institutes of Health (NS10174), and the Medical and Rehabilitation Development Services of the Department of Veterans Affairs.

#### REFERENCES

1. Altman, J. 1969. Autoradiographic and histological studies of postnatal neurogenesis. IV. Cell proliferation and migration in the anterior forebrain, with special reference to persisting neurogenesis in the olfactory bulb. *J. Comp. Neurol.* 137: 433-457.
2. Altman, J., and G. D. Das. 1965. Autoradiographic and histological evidence of postnatal hippocampal neurogenesis in rats. *J. Comp. Neurol.* 124: 319-335.
3. Berthold, C-H. 1978. Morphology of normal peripheral axons. In *Physiology and Pathobiology of Axons* (S. G. Waxman, Ed.), pp. 3-64. Raven Press, New York.
4. Blakemore, W. F., and A. J. Crang. 1985. The use of cultured autologous Schwann cells to remyelinate areas of persistent demyelination in the central nervous system. *J. Neurol. Sci.* 70: 207-223.

5. Blakemore, W. F., and R. C. Patterson. 1978. Suppression of remyelination in the CNS by X-irradiation. *Acta Neuropathol.* 42: 105-113.
6. Brustle, O., U. Maskos, and R. D. Mc Kay. 1995. Host-guided migration allows targeted introduction of neurons into the embryonic brain. *Neuron* 15: 1275-1285.
7. Cameron, H. A., C. S. Woolley, B. S. Mc Ewen, and E. Gould. 1993. Differentiation of newly born neurons and glia in the dentate gyrus of the adult rat. *Neuroscience* 56: 337-344.
8. Cattaneo, E., and R. Mc Kay. 1990. Proliferation and differentiation of neuronal stem cells regulated by nerve growth factor. *Nature* 347: 762-765.
9. Cepko, C. L., C. P. Austin, X. Yang, M. Alexiades, and D. Ezzeddine. 1996. Cell fate determination in the vertebrate retina. *Proc. Natl. Acad. Sci. USA* 93: 589-595.
10. Chalmers-Redman, R. M., T. Priestley, J. A. Kemp, and A. Fine. 1997. *In vitro* propagation and inducible differentiation of multipotential progenitor cells from human fetal brain. *Neuroscience* 76: 1121-1128.
11. Chenn, A., and S. K. Mc Connell. 1995. Cleavage orientation and the asymmetric inheritance of Notch1 immunoreactivity in mammalian neurogenesis. *Cell* 82: 631-641.
12. Devon, R., and R. Doucette. 1995. Olfactory ensheathing cells do not require L-ascorbic acid *in vitro* to assemble a basal lamina or to myelinate dorsal root ganglion neurites. *Brain Res.* 688: 223-229.
13. Doetsch, F., I. Caille, D. A. Lim, J. M. Garcia-Verdugo, and A. Alvarez-Buylla. 1999. Subventricular zone astrocytes are neural stem cells in the adult mammalian brain. *Cell* 97: 703-716.
14. Felts, P. A., and K. J. Smith. 1992. Conduction properties of central nerve fibers remyelinated by Schwann cells. *Brain Res.* 574: 178-192.
15. Franklin, R. J., J. M. Gilson, I. A. Franceschini, and S. C. Barnett. 1996. Schwann cell-like myelination following transplantation of an olfactory bulb-ensheathing cell line into areas of demyelination in the adult CNS. *Glia* 17: 217-224.
16. Gage, F. H., P. W. Coates, T. D. Palmer, H. G. Kuhn, L. J. Fisher, J. O. Suhonen, D. A. Peterson, S. T. Suhr, and J. Ray. 1995. Survival and differentiation of adult neuronal progenitor cells transplanted to the adult brain. *Proc. Natl. Acad. Sci. USA* 92: 11879-11883.
17. Gensburger, C., G. Labourdette, and M. Sensenbrenner. 1987. Brain basic fibroblast growth factor stimulates the proliferation of rat neuronal precursor cells *in vitro*. *FEBS Lett.* 217: 1-5.
18. Gould, E., A. Beylin, P. Tanapat, A. Reeves, and T. J. Shors. 1999. Learning enhances adult neurogenesis in the hippocampal formation. *Nature Neurosci.* 2: 260-265.
19. Gritti, A., E. A. Parati, L. Cova, P. Frolichsthal, R. Galli, E. Wanke, L. Faravelli, D. J. Morassutti, F. Roisen, D. D. Nickel, and A. L. Vescovi. 1996. Multipotential stem cells from the adult mouse brain proliferate and self-renew in response to basic fibroblast growth factor. *J. Neurosci.* 16: 1091-1100.
20. Hammang, J. P., D. R. Archer, and I. D. Duncan. 1997. Myelination following transplantation of EGF-responsive neural stem cells into a myelin-deficient environment. *Exp. Neurol.* 147: 84-95.
21. Heumann, R., D. Lindholm, C. Bandtlow, M. Meyer, M. J. Radeke, T. P. Misko, E. Shooter, and H. Thoenen. 1987. Differential regulation of mRNA encoding nerve growth factor and its receptor in rat sciatic nerve during development, degeneration, and regeneration: Role of macrophages. *Proc. Natl. Acad. Sci. USA* 84: 8735-8739.
22. Honmou, O., P. A. Felts, S. G. Waxman, and J. D. Kocsis. 1996. Restoration of normal conduction properties in demyelinated spinal cord axons in the adult rat by transplantation of exogenous Schwann cells. *J. Neurosci.* 16: 3199-3208.
23. Imaizumi, T., K. L. Lankford, S. G. Waxman, C. A. Greer, and J. D. Kocsis. 1998. Transplanted olfactory ensheathing cells remyelinate and enhance axonal conduction in the demyelinated dorsal columns of the rat spinal cord. *J. Neurosci.* 18: 6176-6185.
24. Jessen, K. R., A. Brennan, L. Morgan, R. Mirsky, A. Kent, Y. Hashimoto, and J. Gavrilovic. 1994. The Schwann cell precursor and its fate: A study of cell death and differentiation during gliogenesis in rat embryonic nerves. *Neuron* 12: 509-527.
25. Johansson, C. B., S. Momma, D. L. Clarke, M. Risling, U. Lendahl, and J. Frisen. 1999. Identification of a neural stem cell in the adult mammalian central nervous system. *Cell* 96: 25-34.
26. Johe, K. K., T. G. Hazel, T. Muller, M. M. Dugich-Djordjevic, and R. D. Mc Kay. 1996. Single factors direct the differentiation of stem cells from the fetal and adult central nervous system. *Genes Dev.* 10: 3129-3140.
27. Kalyani, A., K. Hobson, and M. S. Rao. 1997. Neuroepithelial stem cells from the embryonic spinal cord: Isolation, characterization, and clonal analysis. *Dev. Biol.* 186: 202-223.
28. Keirstead, H. S., T. Ben-Hur, B. Rogister, M. T. O'Leary, M. Dubois-Dalcq, and W. F. Blakemore. 1999. Polysialylated neural cell adhesion molecule-positive CNS precursors generate both oligodendrocytes and Schwann cells to remyelinate the CNS after transplantation. *J. Neurosci.* 19: 7529-7536.
29. Kocsis, J. D., and S. G. Waxman. 1980. Absence of potassium conductance in central myelinated axons. *Nature* 287: 348-349.
30. Kukekov, V. G., E. D. Laywell, O. Suslov, K. Davies, B. Schefler, L. B. Thomas, T. F. O'Brien, M. Kusakabe, and D. A. Steindler. 1999. Multipotent stem/progenitor cells with similar properties arise from two neurogenic regions of adult human brain. *Exp. Neurol.* 156: 333-344.
31. Le Douarin, N., C. Dulac, E. Dupin, and P. Cameron-Curry. 1991. Glial cell lineages in the neural crest. *Glia* 4: 175-184.
32. Lindholm, D., R. Heumann, M. Meyer, and H. Thoenen. 1987. Interleukin-1 regulates synthesis of nerve growth factor in non-neuronal cells of rat sciatic nerve. *Nature* 330: 658-659.
33. Lois, C., and A. Alvarez-Buylla. 1993. Proliferating subventricular zone cells in the adult mammalian forebrain can differentiate into neurons and glia. *Proc. Natl. Acad. Sci. USA* 90: 2074-2077.
34. Lois, C., and A. Alvarez-Buylla. 1994. Long-distance neuronal migration in the adult mammalian brain. *Science* 264: 1145-1148.
35. Lundberg, C., and A. Bjorklund. 1996. Host regulation of glial markers in intrastriatal grafts of conditionally immortalized neural stem cell lines. *NeuroReport* 7: 847-852.
36. Luskin, M. B. 1993. Restricted proliferation and migration of postnatally generated neurons derived from the forebrain subventricular zone. *Neuron* 173-189.
37. Milward, E. A., C. G. Lundberg, B. Ge, D. Lipsitz, M. Zhao, M. Hajhosseini, and I. D. Duncan. 1997. Isolation and transplantation of multipotential populations of epidermal growth factor-responsive neural progenitor cells from the canine brain. *J. Neurosci. Res.* 50: 862-871.
38. Morshead, C. M., B. A. Reynolds, C. G. Craig, M. W. Mc Burney, W. A. Staines, D. Morassutti, S. Weiss, and D. Van Der Kooy. 1994. Neural stem cells in the adult mammalian forebrain: A relatively quiescent subpopulation of subependymal cells. *Neuron* 13: 1071-1082.
39. Moyer, M. P., R. A. Johnson, E. A. Zompa, L. Cain, T. Morshed, and C. E. Hulsebosch. 1997. Culture, expansion, and transplan-



- tation of human fetal neural progenitor cells. *Transplant. Proc.* 29: 2040-2041.
40. Mujtaba, T., M. Mayer-Proschel, and M. S. Rao. 1998. A common neural progenitor for the CNS and PNS. *Dev. Biol.* 200: 1-15.
  41. Murphy, M., K. Reid, R. Dutton, G. Brooker, and P. F. Bartlett. 1997. Neural stem cells. *J. Invest. Dermatol. Symp. Proc.* 2: 8-13.
  42. Palmer, T. D., J. Takahashi, and F. H. Gage. 1997. The adult rat hippocampus contains primordial neural stem cells. *Mol. Cell. Neurosci.* 8: 389-404.
  43. Politis, M. J., K. Ederle, and P. S. Spencer. 1982. Tropism in nerve regeneration *in vivo*. Attraction of regenerating axons by diffusible factors derived from cells in distal nerve stumps of transected peripheral nerves. *Brain Res.* 253: 1-12.
  44. Qian, X., A. A. Davis, S. K. Goderie, and S. Temple. 1997. FGF2 concentration regulates the generation of neurons and glia from multipotent cortical stem cells. *Neuron* 18: 81-93.
  45. Rao, M. S., and D. J. Anderson. 1997. Immortalization and controlled *in vitro* differentiation of murine multipotent neural crest stem cells. *J. Neurobiol.* 32: 722-746.
  46. Rao, M. S., M. Noble, and M. Mayer-Proschel. 1998. A tripotential glial precursor cell is present in the developing spinal cord. *Proc. Natl. Acad. Sci. USA* 95: 3996-4001.
  47. Renfranz, P. J., M. G. Cunningham, and R. D. McKay. 1991. Region-specific differentiation of the hippocampal stem cell line HiB5 upon implantation into the developing mammalian brain. *Cell* 66: 713-729.
  48. Reynolds, B. A., and S. Weiss. 1992. Generation of neurons and astrocytes from isolated cells of the adult mammalian central nervous system. *Science* 255: 1707-1710.
  49. Shihabuddin, L. S., J. A. Hertz, V. R. Holets, and S. R. Whitemore. 1995. The adult CNS retains the potential to direct region-specific differentiation of a transplanted neuronal precursor cell line. *J. Neurosci.* 15: 6666-6678.
  50. Snyder, E. Y., C. H. Yoon, J. D. Flax, and J. D. Macklis. 1997. Multipotent neural progenitors can differentiate toward replacement of neurons undergoing targeted apoptotic degeneration in adult mouse neocortex. *Proc. Natl. Acad. Sci. USA* 94: 11663-11668.
  51. Stemple, D. L., and D. J. Anderson. 1992. Isolation of a stem cell for neurons and glia from the mammalian neural crest. *Cell* 71: 973-985.
  52. Svendsen, C. N., M. A. Caldwell, J. Shen, M. G. Ter Borg, A. E. Rosser, P. Tyers, S. Karmiol, and S. B. Dunnett. 1997. Long-term survival of human central nervous system progenitor cells transplanted into a rat model of Parkinson's disease. *Exp. Neurol.* 148: 135-146.
  53. Svendsen, C. N., D. J. Clarke, A. E. Rosser, and S. B. Dunnett. 1996. Survival and differentiation of rat and human epidermal growth factor-responsive precursor cells following grafting into the lesioned adult central nervous system. *Exp. Neurol.* 137: 376-388.
  54. Vicario-Abejon, C., M. G. Cunningham, and R. D. McKay. 1995. Cerebellar precursors transplanted to the neonatal dentate gyrus express features characteristic of hippocampal neurons. *J. Neurosci.* 15: 6351-6363.
  55. Voyvodic, J. T. 1989. Target size regulates calibre and myelination of sympathetic axons. *Nature* 342: 430-433.
  56. Zhang, S.-C., C. Lundberg, D. Lipsitz, L. T. O'Connor, and I. D. Duncan. 1998. Generation of oligodendroglial progenitors from neural stem cells. *J. Neurocytol.* 27: 475-489.



## Transplantation of adult rat hippocampus-derived neural stem cells into retina injured by transient ischemia

Yasuo Kurimoto<sup>a,\*</sup>, Hiroto Shibuki<sup>a</sup>, Yumi Kaneko<sup>a</sup>, Masaki Ichikawa<sup>a</sup>,  
Toru Kurokawa<sup>a</sup>, Masayo Takahashi<sup>b</sup>, Nagahisa Yoshimura<sup>a</sup>

<sup>a</sup>Department of Ophthalmology, Shinshu University School of Medicine, Matsumoto 390-8621, Japan

<sup>b</sup>Department of Ophthalmology and Visual Science, Kyoto University Graduate School of Medicine, Kyoto 606-8507, Japan

Received 19 March 2001; received in revised form 20 April 2001; accepted 20 April 2001

### Abstract

Neural stem cells are capable of differentiating along multiple central nervous system cell-type lineages, and their use as graft material has provided new strategies for the treatment of neuronal damage. We transplanted adult rat hippocampus-derived neural stem cells into eyes of adult rats that underwent ischemia-reperfusion injury. As control, the cells were also injected into normal rats eyes without ischemic insult. The rats were sacrificed at 1, 2, 4, and 8 weeks, and the eyes were examined histochemically. In eyes with the insult, the transplanted cells were well integrated into the host retinas and expressed Map2ab. In the control, none of the cells migrated into the retina. These results suggest that neural stem cells may be used as donor cells for transplantation to repair ischemic-injured retina. © 2001 Elsevier Science Ireland Ltd. All rights reserved.

**Keywords:** Retina; Neural stem cell; Ischemia-reperfusion; Transplantation; Rat; Animal model

Traditionally, retinal impairments by neuronal death or axonal severance have been considered incurable in humans and adult experimental mammals because the central nervous system (CNS) of adult mammals does not have a regenerative capacity. Although a number of attempts to repair damaged retinas using grafts of retinal tissue have been reported [3,5,6,11,14], they have encountered serious problems such as limited incorporation of grafted cells into the host retina and difficulty in supplying enough donor cells as has been already discussed [2,4,7,9,17,18,20]. Thus, the transplantation of retinal tissue is not promising as a therapeutic strategy for the treatment of retinal impairments from neuronal death at present.

The recent advances in the field of neural stem cells have brought great expectation that severe CNS damages can be repaired by using stem/progenitor cells [4,7,13,17]. It has been shown that transplanted neural progenitor cells, even heterotypical, can integrate with the host brain tissue and differentiate into appropriate neurons [15]. For the retina, an

earlier study demonstrated that transplanted adult rat hippocampus-derived neural stem cells (AHSCs) can be integrated into the host retina in normal neonatal rats [18]. Later studies showed that AHSCs were integrated into the host retina even in mature rats in genetically-degenerated retinas [20] and in mechanically-injured retinas [9]. These results have encouraged the development of novel therapies for treating retinal impairments using neural stem cells.

The *in vivo* retinal ischemia-reperfusion model is a standard experimental model that has been used to investigate the damage of the retina induced by transient ischemia. By inducing transient ischemia with high intraocular pressure, this model can avoid direct mechanical injury to the retina and optic nerve, and provide high reproducibility [1,12,19]. We transplanted AHSCs into eyes that had been damaged by ischemia-reperfusion. This report is the first study to perform neural stem cell transplantation into eyes with acquired retinal disease besides mechanical injury.

The preparation of AHSCs has been described in detail [10,18]. In brief, hippocampal progenitor cultures were prepared from the hippocampus of adult Fisher rats. The dissociated cells were cultured on polyornithine/laminin-coated dishes using a mixture of Dulbecco's modified Eagle's medium (DMEM)/Ham's F12 (1:1) supplemented with N2 (Gibco) and 20 ng/ml of recombinant human basic

\* Corresponding author. Schepens Eye Research Institute, Department of Ophthalmology, Harvard Medical School, 20 Staniford Street, Boston, MA, 02114 USA. Tel.: +1-617-912-7418; fax: +1-617-912-0101.  
E-mail address: kurina@vision.eri.harvard.edu (Y. Kurimoto).

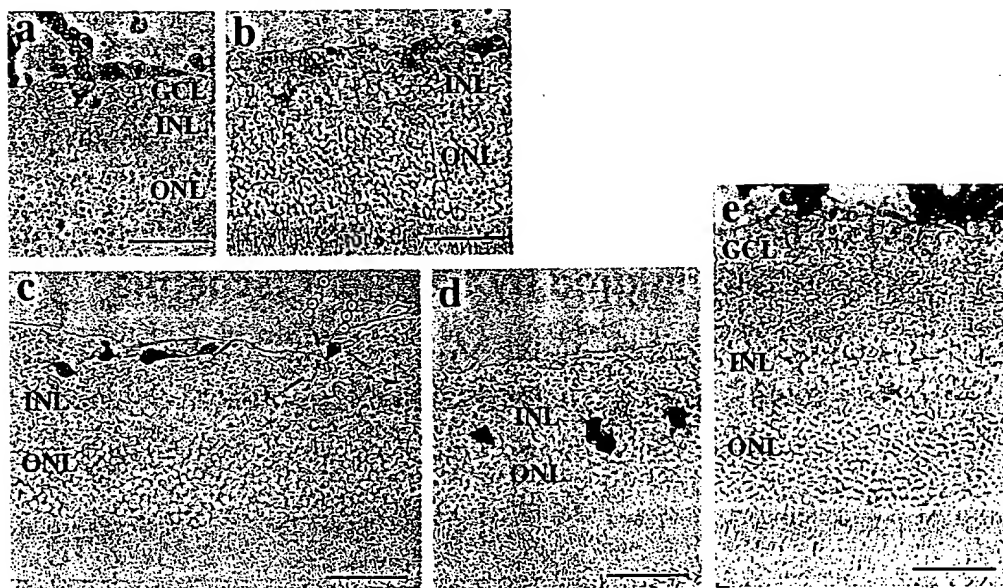


Fig. 1. Light microscopic photographs of host retinas demonstrating the transplanted AHSCs stained dark blue for  $\beta$ -Gal. In retinas with ischemia-reperfusion insult (a–d), prominent cell losses occurred primarily in the ganglion cell layers and inner nuclear layers as compared with the retina without the insult (e). (a) At 1 week after transplantation, the intravitreally injected AHSCs can be seen in the ganglion cell layer. (b) At 2 weeks after transplantation, the grafted AHSCs are seen in the inner nuclear layer. (c, d) At 8 weeks, the transplanted cells can be seen in various layers of the inner retina, and some of them seem to be process-bearing cells (c). (e) A control retina 2 weeks after transplantation with no ischemic insult. Intravitreally injected AHSCs are not present in the host retina. INL, inner nuclear layer. ONL, outer nuclear layer. Scale bars represent 50  $\mu$ m.

fibroblast growth factor (bFGF) (Genzyme). Isolated stem cells were genetically marked with  $\beta$ -galactosidase ( $\beta$ -Gal) and cloned. The PZ5 clone, previously characterized extensively [10], was used. The cultured and harvested cells were washed with DMEM/Ham's F12 and suspended at a density of 100,000 cells/ $\mu$ l in DMEM/Ham's F12 for transplantation.

Adult (8–12 week old) Fisher rats were anesthetized with an intraperitoneal injection of pentobarbital (60 mg/kg), and the pupils were dilated with topical 0.5% phenylephrine hydrochloride and 0.5% tropicamide in order to monitor the ocular fundi. Transient retinal ischemia was induced by raising the intraocular pressure to 110 mmHg for 60 min (see Ref. [12]). Immediately after beginning the reperfusion, the AHSCs were injected into the vitreous cavity of the treated eyes under trans-pupillary observation using a

binocular surgical microscope. The injection was made with a 10- $\mu$ l Hamilton microsyringe with a 30-gauge beveled needle. A total of 500 000 cells in 5  $\mu$ l of DMEM/Ham's F12 were injected. For control, the cells were also injected into eyes with no ischemic insult.

The rats were sacrificed 1, 2, 4, and 8 weeks after the transplantation ( $n = 4$  for the ischemic group and  $n = 3$  for the control group at each time point), and the eyes were processed for histochemical studies.

**In situ staining of grafted cells for  $\beta$ -Gal:** all of the enucleated eyes except the two described below were fixed in 2% paraformaldehyde, 0.1% glutaraldehyde, 0.02% NP-40, and 0.01% deoxycholate in PBS. After 1 h, the anterior segments were removed, and the  $\beta$ -Gal staining was done by placing the eye cups in a solution of 2.5 mM X-Gal, 5 mM potassium ferricyanate, 5 mM potassium ferro-

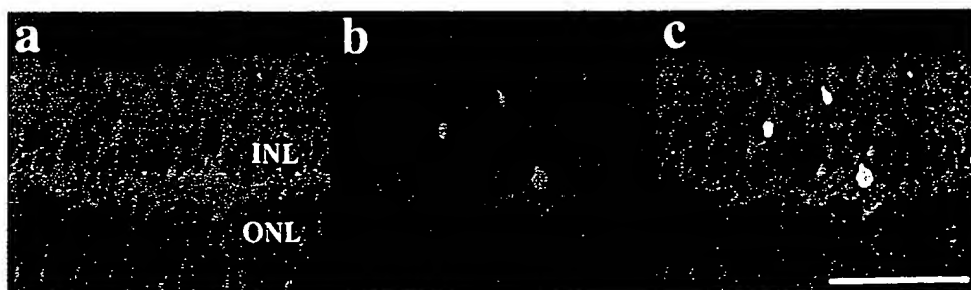


Fig. 2. Confocal images of the retina 4 weeks after AHSCs transplantation with ischemic insult. (a) Anti-Map2ab immunoreactivity. (b) Anti- $\beta$ -Gal immunoreactivity. (c) The merged image of anti-Map2ab and anti- $\beta$ -Gal immunoreactivity, showing the grafted AHSCs differentiate into mature neurons. INL, inner nuclear layer. ONL, outer nuclear layer. Scale bar represent 50  $\mu$ m.

cyanate, 2 mM MgCl<sub>2</sub> in PBS [16] at room temperature overnight. The stained tissue was washed with PBS and soaked in PBS containing 25% sucrose for cryoprotection. Ten-micrometer sections were cut on a cryostat and examined with a light microscope.

**Immunostaining:** two eyes of two animals sacrificed 4 weeks after ischemic insult were fixed in 4% paraformaldehyde, cryoprotected, and sectioned at 10  $\mu$ m on a cryostat. Double immunostaining was performed on these sections. The sections were processed for anti- $\beta$ -Gal (1:500, Promega) and anti-Map2ab (1:500, Sigma), and followed by reaction with FITC-conjugated secondary antibody (1:100, DAKO) to anti- $\beta$ -Gal and rhodamine-conjugated antibody (1:100, DAKO) to anti-Map2ab. Confocal microscopy was used to study these sections.

In every treated eye, transplanted cells were readily identified by the transgenic  $\beta$ -Gal marker. In the eyes that underwent ischemia-reperfusion insult, prominent cell loss were observed primarily in the ganglion cell layer and inner nuclear layer (Fig. 1). The changes were typical of the findings in ischemia-reperfusion insult described earlier [12].

In eyes with the ischemia insult, the intravitreally-injected AHSCs invaded the retinal ganglion cell layer by 1 week after the transplantation (Fig. 1a) and were identified in the retinal inner nuclear layer 2 weeks after the transplantation (Fig. 1b). At 4 weeks, the donor cells were integrated into the host retina and expressed Map2ab (Fig. 2) which indicated that the AHSCs had differentiated into mature neurons. At 8 weeks after the transplantation, the transplanted cells were integrated into the different layers of the inner retina (Fig. 1c,d) and appeared as process-bearing cells (Fig. 1c). A number of transplanted cells were detected within the vitreous cavity but the number decreased with increasing postinjection times (Fig. 1).

In the control animals without ischemic insult, AHSCs did not invade the host retina (Fig. 1e). Although many of the transplanted cells were observed to survive in the vitreous cavity at 2 weeks after transplantation, the numbers decreased at 4 weeks and were mostly gone at 8 weeks after the transplantation (data not shown).

These results demonstrated that intravitreally-injected AHSCs migrated and integrated into the host retinas of adult rats that had undergone ischemic insult while none of the cells migrated into the retina without ischemic insult. In the host retinas, many cells in the ganglion cell layer and inner nuclear layer were lost after the ischemic insult. The transplanted AHSCs migrated primarily into these layers and differentiated into mature neurons replacing some of the lost cells.

The observation that AHSCs did not enter the host retina in the control adult rats agrees with previous findings [18]. The question then arises as to why retinas damaged by ischemia will accept the migration and integration of transplanted neural stem cells while normal adult retinas will not. First, it is likely that some types of trophic factors or cytokines that promote survival, migration, and neuronal differ-

entiation of the transplanted stem cells are produced in the retina that had been injured by ischemia. It has already been reported that bFGF, which is known to be important for survival of AHSCs [10], is up-regulated in retinas after transient ischemic insult [8]. In addition to bFGF, other factors were probably up-regulated in the ischemic retina to stimulate migration and neural differentiation of the grafted cells.

Secondly, it is highly likely that serous components enter the retina because the blood–retina barrier is broken by the ischemic insult [19]. Such serous components, as well as intrinsically expressed factors, can promote survival, migration, and neuronal differentiation of the transplanted AHSCs. In the control animals, it is likely that the absence of such factors prevented the integration of the grafted cells into the host retina, and was probably the cause for the decrease of surviving AHSCs in the vitreous after the transplantation.

Another factor that might promote the migration of the transplanted cells is a disruption of the retinal internal limiting membrane. The retinal internal limiting membrane can be a barrier to cell invasion under normal conditions, but it could be interrupted by the ischemia. In the present study we suggest that disruptions of the retinal internal limiting membrane by ischemia allowed the AHSCs to enter the retina.

This experimental model of retinal injury by transient retinal ischemia induced by raising the intraocular pressure can be considered comparable to an acute glaucomatous attack, a central retinal artery occlusion, or an ischemic optic neuropathy. In these diseases, it has been generally believed that it is not possible to repopulate the lost retinal cells and repair the retinal injury. The present results have shown that intravitreally injected AHSCs can partly repopulate the lost host cells and differentiate into a neuronal lineage. However, it still is not known whether the transplanted cells can establish a functional network with host neural circuitry and acquire proper functions as retinal neurons. Nevertheless, our results suggest that neuronal stem cells are good candidates to reconstruct the neural circuitry of ischemic-injured retina, and show the potentiality of therapeutic transplantation using neuronal stem cells on retinal impairments that are generally regarded as incurable.

- [1] Anderson, D.R. and Davis, E.B., Sensitivities of ocular tissues to acute pressure-induced ischemia, *Arch. Ophthalmol.*, 93 (1975) 267–274.
- [2] Berson, E.L. and Jakobiec, F.A., Neural retinal cell transplantation: ideal versus reality, *Ophthalmology*, 106 (1999) 445–446.
- [3] del Cerro, M., Humayun, M.S., Sadda, S.R., Cao, J., Hayaishi, N., Green, W.R., del Cerro, C. and de Juan Jr., E., Histologic correlation of human neural retinal transplantation. *Invest. Ophthalmol. Vis. Sci.*, 41 (2000) 3142–3148.
- [4] Gage, F.H., Cell therapy, *Nature*, 392 (1998) 18–24.
- [5] Gouras, P., Du, J., Gelanze, M., Kwun, R., Kjeldbye, H. and Lopez, R., Transplantation of photoreceptors labeled with

- tritiated thymidine into RCS rats, *Invest. Ophthalmol. Vis. Sci.*, 32 (1991) 1704–1707.
- [6] Gouras, P., Du, J., Kjeldbye, H., Yamamoto, S. and Zack, D.J., Long-term photoreceptor transplants in dystrophic and normal mouse retina, *Invest. Ophthalmol. Vis. Sci.*, 35 (1994) 3145–3153.
- [7] McKay, R., Stem cells in the central nervous system, *Science*, 276 (1997) 66–71.
- [8] Miyashiro, M., Ogata, N., Takahashi, K., Matsushima, M., Yamamoto, C., Yamada, H. and Uyama, M., Expression of basic fibroblast growth factor and its receptor mRNA in retinal tissue following ischemic injury in the rat, *Graefes Arch. Clin. Exp. Ophthalmol.*, 236 (1998) 295–300.
- [9] Nishida, A., Takahashi, M., Tanihara, H., Nakano, I., Takahashi, J.B., Mizoguchi, A., Ide, C. and Honda, Y., Incorporation and differentiation of hippocampus-derived neural stem cells transplanted in injured adult rat retina, *Invest. Ophthalmol. Vis. Sci.*, 41 (2000) 4268–4274.
- [10] Palmer, T.D., Takahashi, J. and Gage, F.H., The adult rat hippocampus contains primordial neural stem cells, *Mol. Cell. Neurosci.*, 8 (1997) 389–404.
- [11] Seiler, M.J. and Aramant, R.B., Intact sheets of fetal retina transplanted to restore damaged rat retinas, *Invest. Ophthalmol. Vis. Sci.*, 39 (1998) 2121–2131.
- [12] Shibuki, H., Katai, N., Kuroiwa, S., Kurokawa, T., Yodoi, J. and Yoshimura, N., Protective effect of adult T-cell leukemia-derived factor on retinal ischemia-reperfusion injury in the rat, *Invest. Ophthalmol. Vis. Sci.*, 39 (1998) 1470–1477.
- [13] Shihabuddin, L.S., Ray, J. and Gage, F.H., Stem cell technology for basic science and clinical applications, *Arch. Neurol.*, 56 (1999) 29–32.
- [14] Silverman, M.S. and Hughes, S.E., Transplantation of photoreceptors to light-damaged retina, *Invest. Ophthalmol. Vis. Sci.*, 30 (1989) 1684–1690.
- [15] Suhonen, J.O., Peterson, D.A., Ray, J. and Gage, F.H., Differentiation of adult hippocampus-derived progenitors into olfactory neurons in vivo, *Nature*, 383 (1996) 624–627.
- [16] Sunayashiki-Kusuzaki, K., Kikuchi, T., Wawrousek, E.F. and Shinohara, T., Arrestin and phosducin are expressed in a small number of brain cells, *Brain Res. Mol. Brain Res.*, 52 (1997) 112–120.
- [17] Svendsen, C.N. and Smith, A.G., New prospects for human stem-cell therapy in the nervous system, *Trends Neurosci.*, 22 (1999) 357–364.
- [18] Takahashi, M., Palmer, T.D., Takahashi, J. and Gage, F.H., Widespread integration and survival of adult-derived neural progenitor cells in the developing optic retina, *Mol. Cell. Neurosci.*, 12 (1998) 340–348.
- [19] Wilson, C.A., Berkowitz, B.A., Funatsu, H., Metrikin, D.C., Harrison, D.W., Lam, M.K. and Sonkin, P.L., Blood-retinal barrier breakdown following experimental retinal ischemia and reperfusion, *Exp. Eye Res.*, 61 (1995) 547–557.
- [20] Young, M.J., Ray, J., Whiteley, S.J.O., Klassen, H. and Gage, F.H., Neuronal differentiation and morphological integration of hippocampal progenitor cells transplanted to the retina of immature and mature dystrophic rats, *Mol. Cell. Neurosci.*, 16 (2000) 197–205.

# Incorporation and Differentiation of Hippocampus-Derived Neural Stem Cells Transplanted in Injured Adult Rat Retina

Akihiro Nishida,<sup>1,2</sup> Masayo Takahashi,<sup>1</sup> Hidenobu Tanihara,<sup>1</sup> Ichiro Nakano,<sup>3</sup> Jun B. Takahashi,<sup>3</sup> Akira Mizoguchi,<sup>2</sup> Chizuka Ide,<sup>2</sup> and Yoshihito Honda<sup>1</sup>

**PURPOSE.** In a previous study it has been shown that adult rat hippocampus-derived neural stem cells can be successfully transplanted into neonatal retinas, where they differentiate into neurons and glia, but they cannot be transplanted into adult retinas. In the current study, the effect of mechanical injury to the adult retina on the survival and differentiation of the grafted hippocampal stem cells was determined.

**METHODS.** Mechanical injury was induced in the adult rat retina by a hooked needle. A cell suspension (containing 90,000 neural stem cells) was slowly injected into the vitreous space. The specimens were processed for immunohistochemical studies at 1, 2, and 4 weeks after the transplantation.

**RESULTS.** In the best case, incorporation of grafted stem cells was seen in 50% of the injured retinas. Most of these cells located from the ganglion cell layer through the inner nuclear layer close to the injury site. Immunohistochemically, at 1 week, more than half of the grafted cells expressed nestin. At 4 weeks, some grafted cells showed immunoreactivity for microtubule-associated protein (MAP) 2ab, MAP5, and glial fibrillary acidic protein (GFAP), suggesting progress in differentiation into cells of neuronal and astroglial lineages. However, they showed no immunoreactivity for HPC-1, calbindin, and rhodopsin, which suggests that they did not differentiate into mature retinal neurons. Immunoelectron microscopy revealed the formation of synapse-like structures between graft and host cells.

**CONCLUSIONS.** By the manipulation of mechanical injury, the incorporation and subsequent differentiation of the grafted stem cells into neuronal and glial lineage, including the formation of synapse-like structures, can be achieved, even in the adult rat retina. (*Invest Ophthalmol Vis Sci.* 2000;41:4268-4274)

Since the mid-1990s, it has been possible to isolate neural stem or progenitor cells from various parts of the central nervous system (CNS), such as the hippocampus, subventricular zone, spinal cord, and ependyma.<sup>1-4</sup> In general, these cells can expand in serum-free medium and proliferate in response to growth factors such as epidermal growth factor (EGF) or basic fibroblast growth factor (bFGF). From a clinical point of view, they have some potential advantages for retinal transplantation compared with embryonic or newborn retinal cells. First, they can be expanded through numerous passages

in vitro and frozen for storage. Second, they can be easily manipulated, such as by pretreatment with growth factors or gene transduction, before they are transplanted.

Adult rat hippocampus-derived neural stem cells, first isolated by Palmer et al.<sup>5</sup>, are one of the few cell lines that have been shown by clonal analysis to have multipotency and self-renewability. In a previous study of ours, we found that the hippocampal stem cells could be successfully transplanted and integrated into the neonatal rat retina but that when they were transplanted into adult eyes, they aggregated on the surface but never migrated into the retina.<sup>6</sup>

In this study, for the purpose of assessing the possibility and limitations of the use of brain-derived neural stem cells for retinal transplantation, we investigated whether these hippocampal stem cells could migrate and become incorporated into mechanically injured adult rat retinas.

## MATERIALS AND METHODS

### Preparation of Cells for Grafting

LacZ-labeled clonal adult rat hippocampus-derived neural stem cells (clone PZ5, kindly provided by Fred H. Gage, Salk Institute, La Jolla, CA) were used in this study. They were cultured on laminin/poly-L-ornithine-coated dishes containing Dulbec-

From the Departments of <sup>1</sup>Ophthalmology and Visual Sciences, <sup>2</sup>Anatomy and Neurobiology, and <sup>3</sup>Neurosurgery, Graduate School of Medicine, Kyoto University, Japan.

Supported in part by a Grant-in-Aid and Health Science Research Grants for Research on Brain Science from the Ministry of Health and Welfare of Japan, by grants from the Japan Society for the Promotion of Science and the Japan National Society for the Prevention of Blindness, and by Grants-in-Aid 090280101, 10897014, and 10044272 from the Ministry of Education, Science, Sports and Culture of Japan.

Submitted for publication May 22, 2000; revised July 5, 2000; accepted July 25, 2000.

Commercial relationships policy: N.

Corresponding author: Masayo Takahashi, Department of Ophthalmology and Visual Sciences, Graduate School of Medicine, Kyoto University, Sakyo-ku, Kawaharacho, Shogoin, Kyoto 606-8507, Japan. masataka@kuhp.kyoto-u.ac.jp



co's modified Eagles medium-Ham's F12 (DMEM-F12; Gibco, Rockville, MD) supplemented with N2 (Gibco) and 20 ng/ml bFGF (Genzyme, Cambridge, MA), and incubated at 37°C in a humidified atmosphere of 5% CO<sub>2</sub> in air. After having been subcultured for 2 weeks to 3 months, they were harvested for grafting with 0.05% trypsin in DMEM-F12, washed with 0.01% trypsin inhibitor (Wako, Osaka, Japan) in DMEM-F12, and suspended at a density of 30,000 cells/ $\mu$ l in high-glucose Dulbecco's phosphate-buffered saline (D-PBS, Gibco) containing 20 ng/ml bFGF.

### Animal Preparation and Grafting Procedure

Eight-week-old male Fischer rats ( $n = 30$ ) were obtained from Shimizu Laboratory Supplies (Kyoto, Japan). All experiments were conducted in accordance with the ARVO Statement for the Use of Animals in Ophthalmic and Vision Research. The animals were anesthetized with a mixture (1:1) of xylazine hydrochloride (4 mg/kg) and ketamine hydrochloride (10 mg/kg) administered intramuscularly. The pupils were dilated with 0.5% tropicamide and 2.5% phenylephrine eye drops. The corneas were anesthetized with drops of 0.4% oxybuprocaine hydrochloride. The eyeballs were perforated at the equator with a 27-gauge needle. A hooked 30-gauge needle was then inserted through the wound, and the retina was injured by scratching it parallel to the equator between the retinal vessels under direct observation with a surgical microscope equipped with a plano-concave contact lens for rats (Kyocon, Kyoto, Japan). Special care was taken to injure the whole layer of the retina, and success was affirmed by a small amount of subretinal bleeding. After the injury, 3  $\mu$ l of the cell suspension (containing 90,000 cells) was slowly injected into the intravitreal space with a microsyringe fitted with a 30-gauge blunt needle (15 rats, 30 eyes). As a control, 3  $\mu$ l of the cell suspension was injected into the intravitreal space of noninjured eyes (15 rats, 30 eyes). The results from five eyes of the control group were excluded due to complications of massive vitreous hemorrhage.

### Tissue Sectioning

The animals were anesthetized by inhalation of diethyl ether and fixed by transcardial perfusion with 4% paraformaldehyde (Merck, Darmstadt, Germany) in 0.1 M phosphate buffer (PB) 1, 2, and 4 weeks later. The eyes were enucleated to make eyecups. The eyecups were immersed in the same fixative for 2 hours at 4°C and then in 15%, 20%, and 25% sucrose-PBS for cryoprotection. They were embedded in optimal cutting temperature compound (OCT; Miles, Elkhart, IN) after adjustment of their horizontal planes parallel to the cutting plane, and 20- $\mu$ m frozen sections were made in a cryostat. Continuous sections including the injury site were cut for each eye.

### Immunocytochemistry

The specimens were washed with 0.1 M PB and then incubated with 20% skim milk (Dainihon-Seiyaku, Osaka, Japan) in 0.1 M PB containing 0.005% saponin (0.1 M PB-saponin; Merck) for 10 minutes to block nonspecific antibody binding. They were then incubated with primary antibodies diluted in 5% skim milk in 0.1 M PB-saponin for 24 hours at 4°C. Antibodies and concentrations used in this study were as follows: mouse monoclonal anti- $\beta$ -galactosidase ( $\beta$ -gal, 1:1000; Promega, Madison, WI), rabbit polyclonal anti- $\beta$ -gal (1:5000; Chemicon, Te-

mecula, CA), mouse monoclonal anti-nestin (1:1000; PharMingen, San Diego, CA), mouse monoclonal anti-microtubule associated protein (MAP) 2ab (1:100; Sigma, St. Louis, MO), mouse monoclonal anti-MAP5 (1:1000; Chemicon), rabbit polyclonal anti-glial fibrillary acidic protein (GFAP; 1:1000; Chemicon), rabbit anti-myelin basic protein (MBP; 1:500; UltraClone, Wellow, UK), mouse monoclonal anti-HPC-1 (1:1000; Sigma), mouse monoclonal anti-calbindin (1:500; Sigma), and rabbit anti-rhodopsin (1:1000; LSL, Tokyo, Japan).

After the reaction with primary antibodies, the specimens were washed with 0.1 M PB-saponin and incubated with secondary antibodies diluted in 5% skim milk in 0.1 M PB-saponin for 90 minutes. Antibodies and concentrations used in this study were as follows: fluorescein isothiocyanate (FITC)-conjugated sheep anti-mouse immunoglobulin (1:100; Amersham, Buckinghamshire, UK), FITC-conjugated donkey anti-rabbit immunoglobulin (1:100; Amersham), Cy5-conjugated goat anti-mouse IgG (1:200; Amersham), and Cy5-conjugated donkey anti-rabbit IgG (1:200; Amersham).

Sections were then washed with 0.1 M PB, mounted with glycerol-PBS (1:1) and observed with a laser-scanning confocal microscope (1024; Bio-Rad, Hercules, CA).

### Immunoelectron Microscopy

Immunoelectron microscopy using the silver-enhancement technique was done as described.<sup>7</sup> Briefly, after having been blocked with 20% skim milk in 0.1 M PB-saponin, the sections were incubated with the anti- $\beta$ -gal antibody (1:1000; Promega) and subsequently with an anti-mouse IgG antibody coupled with 1.4-nm gold particles (1:50; Nanoprobes, Stony Brook, NY). After the sections had been washed, they were fixed with 1% glutaraldehyde (Nacalai Tesque, Kyoto, Japan) in 0.1 M PB for 10 minutes, and the sample-bound gold particles were then silver-enhanced at 20°C for 12 minutes by use of an HQ-silver kit (Nanoprobes). They were again washed and postfixed with 0.5% osmium oxide (Nacalai Tesque) in 0.1 M PB at pH 7.3, dehydrated by passage through a graded series of ethanol (50%, 60%, 70%, 80%, 90%, 95%, and 100%), and embedded in epoxy resin. From these samples, ultrathin sections were cut, stained with uranyl acetate and lead citrate, and then observed with an electron microscope (JEM-1200EX; JEOL, Tokyo, Japan).

## RESULTS

### Incorporation and Distribution of Grafted Cells

In an attempt to elucidate the efficacy of transplantation of hippocampal stem cells into the adult rat retina, we injected them into the vitreous space. The stem cells were labeled with the *LacZ* gene retrovirally, so that we could identify  $\beta$ -gal-immunoreactive cells as the grafted cells. In our previous study, we confirmed that  $\beta$ -gal enzyme leaking from damaged or dead grafted cells was not taken up by host retinal cells.<sup>6</sup>

First, we compared the incidence of eyes with incorporated grafted cells between the injured group and the noninjured group. In the injured group, 1 week after transplantation,  $\beta$ -gal-immunoreactive cells were incorporated into the host retina in 10% of the experimental eyes (1 of 10). At 2 and 4 weeks, the percentage of eyes with incorporated cells increased to 50% (5 of 10) and 40% (4 of 10), respectively (Table 1). In the eyes with incorporated grafted cells, the grafted cells



TABLE 1. Incidence of Eyes with Incorporated Grafted Cells

	1 Week	2 Weeks	4 Weeks
Injured group	1/10	5/10*	4/10*
Noninjured group	0/5	0/10	0/10

Values are number of eyes with incorporated grafted cells/total surgically treated eyes. Five rats were used in each experiment. The results from five eyes of the noninjured group at 1 week were excluded because of complications of massive vitreous hemorrhage.

\* Incidence in the injured group was significantly higher than that in the noninjured group (Fisher's exact probability test,  $P < 0.05$ ).

were distributed around the site of injury, where GFAP immunoreactivity of the host retina was upregulated (Fig. 1A). In contrast, no eyes incorporated grafted cells in the noninjured group at any period after transplantation (Table 1). The grafted cells were found to have aggregated on the inner surface but never to have been incorporated into the host retina of the noninjured group (Fig. 1B). Statistical analysis by Fisher's exact probability test showed a significant difference ( $P < 0.05$ ) between the injured and noninjured groups in the incidence of successful incorporation of the grafted cells at both 2 and 4 weeks after transplantation.

The pattern of grafted cell distribution was almost the same at all times after the injection. The grafted cells were observed not only at the site of injury where normal retinal structure was destroyed, but also in the surrounding area where the normal retinal structure was retained. Most of them were situated in the inner nuclear layer (INL) with some in the ganglion cell layer (GCL), where they formed a layer-like structure. A few grafted cells were found on the inner surface of the retina and in the outer nuclear layer (ONL). The width of distribution of the incorporated grafted cells ranged between 790  $\mu\text{m}$  and 1200  $\mu\text{m}$  around the site of injury (data not shown). This width was much greater than that of the actual injury in all cases, which was less than 100  $\mu\text{m}$ .

The grafted cells adherent to the inner surface of the host retina in the injured group were round and had no processes, whereas most incorporated cells had elongated processes, and some of them showed morphologies reminiscent of amacrine and bipolar cells (Fig. 2).

## Immunohistochemistry on Sections after Transplantation

Immunohistochemical studies were performed on sections with incorporated grafted cells in the injured group. The sections were double immunostained with anti- $\beta$ -gal antibody and antibodies against specific cell-type markers. The cell-type markers used were nestin for immature or undifferentiated cells, MAPs for neuronal lineage cells, GFAP for astrocytes and Müller cells, MBP for oligodendrocytes, HPC-1 for amacrine cells, calbindin for horizontal and some amacrine cells, and rhodopsin for rod photoreceptor cells. The ratios of double-stained cells to  $\beta$ -gal-positive cells were calculated to estimate the characteristics of the grafted cells after transplantation.

Our preliminary studies showed the presence of nestin immunoreactivity in more than 96% of the cultured hippocampal stem cells; however, no immunoreactivity for other specific markers of differentiated cell types, including MAP2ab, MAP5, GFAP, MBP, HPC-1, calbindin, and rhodopsin, was detected (data not shown).

Among the grafted cells, nestin-positive cells were over 50% at the end of 1 and 2 weeks after transplantation; however, they decreased to 36% after 4 weeks (Table 2, Figs. 3A, 3B, 3C). MAP5-positive cells increased markedly from 1% to 22% between 1 and 2 weeks, whereas MAP2ab-positive cells gradually increased from 1 to 4 weeks (Table 2, Figs. 3D, 3E, 3F). As for the two glial markers, GFAP-positive grafted cells increased from 2% to 10% between 2 and 4 weeks, but MBP-positive cells were hardly observed from weeks 1 through 4 (Table 2, Figs. 3G, 3H, 3I). Immunoreactivity for retinal cell markers, HPC-1, calbindin, and rhodopsin was hardly detected in the grafted cells throughout the 4 weeks (Table 2, Figs. 3J, 3K, 3L).

The immunoreactivity for nestin and GFAP was also observed in the host Müller cells around the sites of injury, where the grafted cells were incorporated into the host retinas (Figs. 3A, 3B, 3C, 3G, 3H, 3I).

## Immunoelectron Microscopy on Sections at 4 Weeks after Transplantation

Immunoelectron microscopy was performed on sections of 4-week specimens. Grafted cells were identified by the presence of gold particles indicating immunoreactivity for  $\beta$ -gal. In

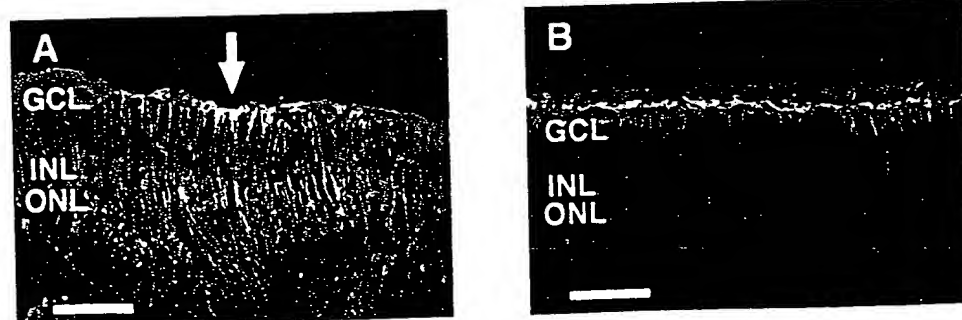
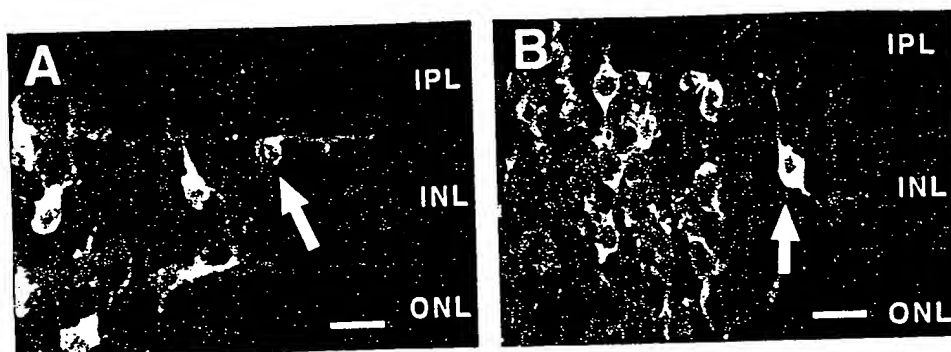


FIGURE 1. Double-label immunofluorescence study using antibodies against  $\beta$ -gal (green) and GFAP (red) in the injured group (A) and noninjured group (B) 2 weeks after the injection. (A)  $\beta$ -Gal-positive grafted cells were observed primarily in the GCL and INL in the host retina around the site of injury (arrow). Expression of GFAP in the host retina was upregulated. (B)  $\beta$ -Gal-positive cells were located on the inner surface of but not within the host retina. The expression of GFAP was localized in the astrocytes and the end feet of the Müller cells. Scale bar, 100  $\mu\text{m}$ .



FIGURE 2.  $\beta$ -Gal-immunoreactive grafted cells, which are similar to amacrine (A, arrow) and bipolar (B, arrow) cells, 1 and 4 weeks after transplantation, respectively. Scale bar, 20  $\mu$ m.



general, the grafted cells had heterochromatic nuclei and a large number of mitochondria (Figs. 4A, 4B).

In the inner plexiform layer (IPL) and at the innermost part of the INL, grafted cells were often found in a group (Fig. 4A). Some of them were irregular in shape and had pseudopodia that made contact with other grafted cells (Fig. 4A), which is a characteristic of actively migrating cells. Some other grafted cells had a relatively round shape and extended their processes to make close contact with host cells at the innermost part of the INL (Fig. 4B). At a higher magnification, symmetrical and asymmetrical membrane thickening, which represent puncta adherentia and synaptic junctions, respectively, were observed between graft and host cells (Figs. 4C, 4D) indicating that they formed close contacts with each other.

## DISCUSSION

Neural stem cells are expected to be useful clinically for replacing damaged neurons or for ex vivo gene therapy.<sup>8</sup> In the field of brain science, they have been tested on damaged brain models<sup>9,10</sup> as cell resources for replacement therapy. Also in the field of ophthalmology, it is reported that neural stem cells could be successfully transplanted into damaged retina.<sup>11-13</sup> Therefore, it is important to assess the application of neural stem cells for retinal transplantation therapy.

This study has shown the ability of hippocampus-derived neural stem cells to migrate and differentiate in the injured retina. However, the limitation of their differentiation into authentic retinal neurons was also recognized.

### Pattern of Incorporated Grafted Cells in the Host Retina

The incidence of the eyes with incorporated grafted cells increased between 1 and 2 weeks but did not change between 2 and 4 weeks. Some time may be required for the cells that have migrated onto the retinal surface to create graft-host contacts and to migrate into the host retina. This behavior of

the grafted cells is consistent with the results of our previous study.<sup>6</sup>

The grafted cells were located around the injured sites, where the expression of nestin and GFAP in the host Müller cells was upregulated. The width of the distribution of the grafted cells was much greater than that of the injury (less than 100  $\mu$ m) at any time point evaluated. We therefore speculate that the grafted cells migrated into the host retina not only from the injured site but also from the vitreous surface around the injured site where the host Müller cells were activated by the injury. This speculation was supported by our other experiments that hippocampal stem cells can also incorporate into chemically damaged retinas (data not shown). It has been reported that upregulation of the expression of nestin and GFAP in astrocytes or Müller cells occurred in the CNS including the retina after various types of damage.<sup>14-18</sup> It also has been shown that activated Müller cells express a number of cytokines such as bFGF, ciliary neurotrophic factor (CNTF), and transforming growth factor (TGF)- $\alpha$ .<sup>19-22</sup> It seems reasonable that the Müller cells that were activated by the mechanical injury may have played an important role in the migration and/or differentiation of the surviving grafted cells.

For the purpose of assessing the effect of retinal injury, we chose the vitreous cavity instead of the subretinal space for the site of injection of the neural stem cells. Subretinal injection itself causes retinal detachment and much damage to the retina.

### Differentiation and Integration of the Grafted Cells

The hippocampal stem cells used as the grafted cells were confirmed by immunocytochemistry to be immature cells. Before grafting, most of them expressed nestin. However, once they were grafted, the number of cells expressing nestin decreased. On the contrary, the cells expressing MAPs and GFAP increased with time, which suggests differentiation of the stem cells into cells of the neuronal and astroglial lineages. Among the MAPs, MAP2ab is thought to be a late marker of neuronal

TABLE 2. Differentiation Ratio of the Incorporated Grafted Cells in the Injured Group

	Nestin	MAP2ab	MAP5	GFAP	MBP	HPC-1	Calbindin	Rhodopsin
1 week	56.4	3.6	1.1	3.4	0.0	1.6	0.0	0.0
2 weeks	55.0 $\pm$ 3.2	5.1 $\pm$ 3.5	21.9 $\pm$ 7.6	2.3 $\pm$ 1.5	0.6 $\pm$ 0.5	1.0 $\pm$ 1.0	0.0 $\pm$ 0.0	0.2 $\pm$ 0.4
4 weeks	35.9 $\pm$ 19.0	9.7 $\pm$ 0.8	25.1 $\pm$ 10.7	9.9 $\pm$ 4.7	0.8 $\pm$ 1.3	0.3 $\pm$ 0.6	0.5 $\pm$ 0.9	0.0 $\pm$ 0.0

Values at 2 and 4 weeks are mean  $\pm$  SD and are the ratio of grafted cells double-stained with anti- $\beta$ -gal.

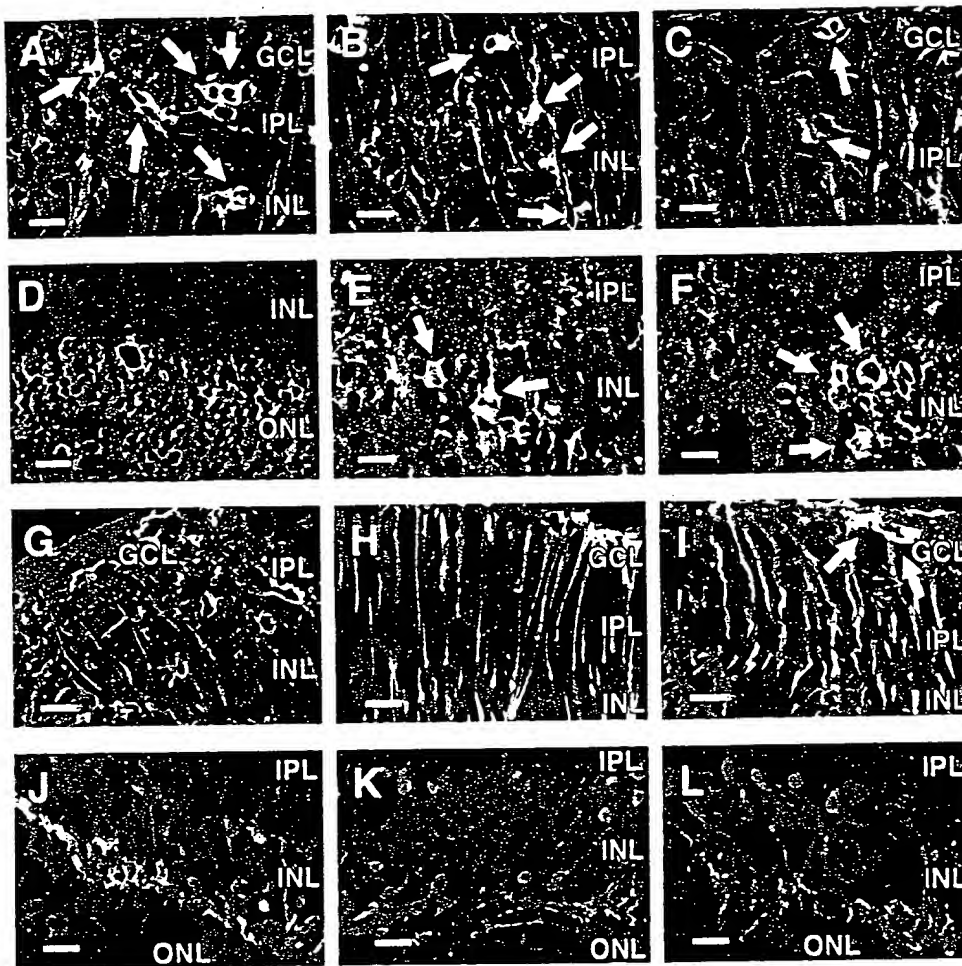


**FIGURE 3.** Double-label immunofluorescence at the end of 1 (A, D, G, and J), 2 (B, E, H, and K), and 4 (C, F, I, and L) weeks after cell transplantation. *Green:*  $\beta$ -Gal-immunoreactive cells; *red:* nestin- (A, B, and C), MAP5- (D, E, and F), GFAP- (G, H, and I), and calbindin- (J, K, and L) immunoreactive cells; *yellow:* double-stained cells (arrows). (A, B, and C) Nestin-positive grafted cells decreased in number from 1 to 4 weeks after transplantation. (D, E, and F) MAP5-positive grafted cells increased from 1 to 4 weeks after transplantation. (G, H, and I) Few GFAP-positive grafted cells are observed at 1 and 2 weeks after transplantation, but they begin to appear at 4 weeks. (J, K, and L) Calbindin-positive grafted cells are rarely observed at any time after the injection. Scale bar, 20  $\mu$ m.

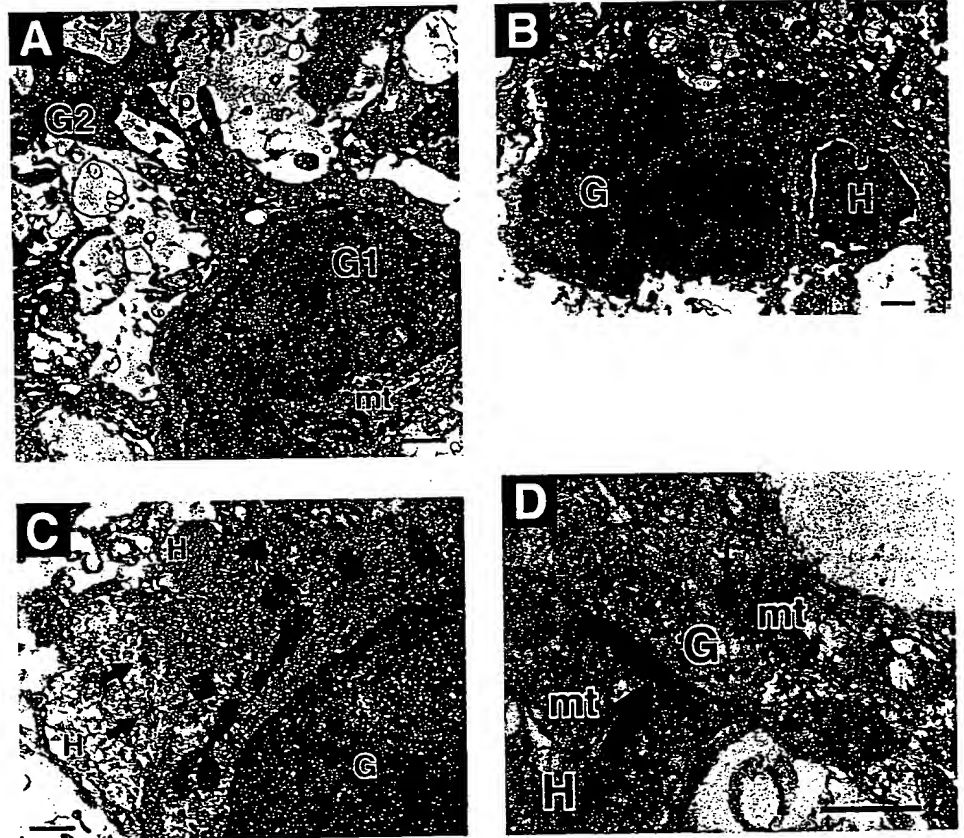
differentiation, because its expression increases as neuronal cells mature,<sup>23</sup> whereas the expression of MAP5 is generally abundant in neuronal cells at very early developmental stages.<sup>23</sup> These facts explain why the expression of MAP5 in the grafted cells increased earlier than that of MAP2ab. GFAP and MBP are markers for astrocytes and oligodendrocytes, respectively. The expression of MBP was hardly detected up to 4 weeks, whereas that of GFAP increased between 2 and 4 weeks after the grafting. This finding indicates that the hippocampal stem cells did not differentiate into oligodendrocytes but into astrocytes after the grafting, although they differentiated into both glial lineages *in vitro*.<sup>5</sup> It also suggests that the specific microenvironment in the retina, where no oligodendrocytes exist, may affect the fate of differentiation of the hippocampal stem cells. As for the retinal cell markers, HPC-1, calbindin, and rhodopsin, their expression in the grafted cells was hardly observed at any time after the grafting, indicating the failure of differentiation into retinal neurons even at the end of 4 weeks after the grafting. One possible reason for the failure is absence of unknown local cues in injured adult retina. There may be some unknown factors that are expressed only in earlier stages of retinal development and permit the hippocampal stem cells to differentiate into retinal neurons. Another possible explanation is limited plasticity of the hippocampus-derived neural stem cells. They may continue to possess the characteristics of cells in the hippocampus, from which they are derived, even after being transplanted into retinal tissue.

Immunoelectron microscopic study revealed the existence of graft-graft and graft-host contacts. The grafted cells formed puncta adherentia-like and asymmetrical synapse-like structures with the host cells. Not only mechanical contacts but also intercellular signaling could be formed between the graft and host cells. There are several reports describing graft-host synapse formation in the adult CNS in homotopic transplantation, such as retina to retina,<sup>24,25</sup> and also in heterotopic transplantation, such as retina to cerebellum.<sup>26</sup> It is still unknown whether these synapse-like structures actually function; however, the formation of such structures is significant evidence for integration of the grafted cells into the host retina.

### Deriving Retinal Neurons from Neural Stem Cells

Further studies are needed to establish the utility of neural stem cells for replacement and reconstruction of retinal neurons. One possibility is retina-derived neural progenitor cells. A recent study revealed that embryonic retina-derived neural progenitor cells can differentiate into photoreceptors *in vitro*.<sup>27</sup> If they maintain the characteristics of retinal cells through expansion *in vitro*, they may differentiate into retina-specific neurons after transplantation. Another possibility is modification of cellular characteristics of the hippocampus-derived neural stem cells for retina-specific differentiation by transfection of key molecules such as homeobox genes.<sup>28,29</sup> Also, pretreatment of the neural stem cells with growth factors is a possible means of controlling the cells' fate. In fact, in our

**FIGURE 4.** Immunoelectron microscopy on sections at 4 weeks after transplantation. (A) Grafted cells are identified by the presence of gold particles indicating immunoreactivity for  $\beta$ -gal. A gold-labeled grafted cell (G1) in the IPL extended its pseudopodia (p) and made contact with another grafted cell (G2). Note that the grafted cells contained a large number of mitochondria (mt). (B) A grafted cell (G) extended its process (arrow) and made close contact with a host cell (H) in the innermost part of the INL. (C) A grafted cell (G) in the INL formed contacts with host cells (H). Both symmetrical (arrows) and asymmetrical (arrow-head) membrane thickenings were observed. (D) An axon terminal of a grafted cell (G) labeled with gold particles (small arrows) in the IPL contained synaptic vesicles (arrow-heads) and formed a synapse-like structure with a host cell (H). Postsynaptic density (large arrow) was observed in the host cell. Scale bar: 1  $\mu$ m (A, B); 500 nm (C, D).



previous study, we found that some neurotrophins affect the differentiation of the hippocampal stem cells *in vitro*<sup>30</sup>; however, growth factors that can induce neural progenitor cells to produce retina-specific neurons have not yet been identified.

## CONCLUSIONS

In conclusion, this study has yielded basic and important information regarding the transplantation of adult rat hippocampus-derived neural stem cells into the adult retina. First, incorporation of the grafted neural stem cells was achieved in injured adult retinas. Second, some of the incorporated neural stem cells showed differentiation into neuronal lineage and formed graft-host contacts such as puncta adherentia- and synapse-like structures. Third, even after successful transplantation and differentiation into cells of the neuronal lineage, the neural stem cells failed to differentiate into retina-specific phenotypes as shown by expression of HPC-1, calbindin, and rhodopsin, possibly because of their basic inability or an absence of local cues essential for differentiation into retinal neurons.

## Acknowledgment

The authors thank Fred H. Gage at the Salk Institute for helpful comments.

## References

- Gage FH, Coates PW, Palmer TD, et al. Survival and differentiation of adult neuronal progenitor cells transplanted to the adult brain. *Proc Natl Acad Sci USA*. 1995;92:11879-11883.
- Weiss S, Dunne C, Hewson J, et al. Multipotent CNS stem cells are present in the adult mammalian spinal cord and ventricular neuroaxis. *J Neurosci*. 1996;16:7599-7609.
- Shihabuddin LS, Ray J, Gage FH. FGF-2 is sufficient to isolate progenitors found in the adult mammalian spinal cord. *Exp Neurol*. 1997;148:577-586.
- Johansson CB, Momma S, Clarke DL, et al. Identification of neural stem cell in the adult mammalian central nervous system. *Cell*. 1999;96:25-34.
- Palmer TD, Takahashi J, Gage FH. The adult rat hippocampus contains primordial neural stem cells. *Mol Cell Neurosci*. 1997;8:389-404.
- Takahashi M, Palmer TD, Takahashi J, Gage FH. Widespread integration and survival of adult-derived neural progenitor cells in the developing optic retina. *Mol Cell Neurosci*. 1998;12:340-348.
- Mizoguchi A, Yano Y, Hamaguchi H, et al. Localization of rabphilin-3A on the synaptic vesicle. *Biochem Biophys Res Commun*. 1994;202:1235-1243.
- Svendsen CN, Smith AG. New prospects for human stem-cell therapy in the nervous system. *Trends Neurosci*. 1999;22:357-364.
- Snyder EY, Macklis JD. Multipotent neural progenitor or stem-like cells may be uniquely suited for therapy for some neurodegenerative conditions. *Clin Neurosci*. 1995;3:310-316.
- Snyder EY, Yoon C, Flax JD, Macklis JD. Multipotent neural precursors can differentiate toward replacement of neurons undergoing targeted apoptotic degeneration in adult mouse neocortex. *Proc Natl Acad Sci USA*. 1997;94:11663-11668.
- Kurimoto Y, Shibuki H, Kaneko Y, et al. Transplantation of neural stem cells into the retina injured by transient ischemia [ARVO Abstract]. *Invest Ophthalmol Vis Sci*. 1999;40:S727. Abstract nr 3845.
- Whiteley SJO, Ray J, Klassen HJ, Young MJ, Gage FH. Survival and integration of neural progenitor cells transplanted to the dystrophic mouse retina [ARVO Abstract]. *Invest Ophthalmol Vis Sci*. 1999;40:S598. Abstract nr 3140.

13. Young MJ, Ray J, Whiteley SJO, Klassen HJ, Gage FH. Integration of the transplanted neural progenitor cells into the retina of the dystrophic rat [ARVO Abstract]. *Invest Ophthalmol Vis Sci.* 1999; 40:S728. Abstract nr 3846.
14. Frisén J, Johansson CB, Török C, Risling M, Lendahl U. Rapid, widespread, and longlasting induction of nestin contributes to the generation of glial scar tissue after CNS injury. *J Cell Biol.* 1995; 131:453-464.
15. Erickson PA, Fisher SK, Guerin CJ, Anderson DH, Kaska DD. Glial fibrillary acidic protein increases in Müller cells after retinal detachment. *Exp Eye Res.* 1987;44:37-48.
16. Lewis GP, Erickson PA, Guerin CJ, Anderson DH, Fisher SK. Changes in the expression of specific Müller cell proteins during long-term retinal detachment. *Exp Eye Res.* 1989;49:93-111.
17. Okada M, Matsumura M, Ogino N, Honda Y. Müller cells in detached human retina express glial fibrillary acidic protein and vimentin. *Graefes Arch Clin Exp Ophthalmol.* 1990;228:467-474.
18. Tanihara H, Hangai M, Sawaguchi S, et al. Up-regulation of glial fibrillary acidic protein in the retina of primate eyes with experimental glaucoma. *Arch Ophthalmol.* 1997;115:752-756.
19. Miyashiro M, Ogata N, Takahashi K, et al. Expression of basic fibroblast growth factor and its receptor mRNA in retinal tissue following ischemic injury in the rat. *Graefes Arch Clin Exp Ophthalmol.* 1998;236:295-300.
20. Cao W, Wen R, Li F, Lavail MM, Steinberg RH. Mechanical injury increases bFGF and CNTF mRNA expression in the mouse retina. *Exp Eye Res.* 1997;65:241-248.
21. Wen R, Song Y, Cheng T, et al. Injury-induced upregulation of bFGF and CNTF mRNAs in the rat retina. *J Neurosci.* 1995;15: 7377-7385.
22. Powers MR, Planck SR. Immunolocalization of transforming growth factor-alpha and its receptor in the normal and hyperoxia-exposed neonatal rat retina. *Curr Eye Res.* 1997;16:177-182.
23. Bates CA, Trinh N, Meyer RL. Distribution of microtubule-associated proteins (MAPs) in adult and embryonic mouse retinal explants: presence of the embryonic map, MAP5/1B, in regenerating adult retinal axons. *Dev Biol.* 1993;155:533-544.
24. Aramant RB, Seiler MJ. Fiber and synaptic connections between embryonic retinal transplants and host retina. *Exp Neurol.* 1995; 133:244-255.
25. Gouras P, Du J, Kjeldbye H, Yamamoto S, Zack DJ. Long-term photoreceptor transplants in dystrophic and normal mouse retina. *Invest Ophthalmol Vis Sci.* 1994;35:3145-3153.
26. Zwimpfer TJ, Aguayo AJ, Bray GM. Synapse formation and preferential distribution in the granule cell layer by regenerating retinal ganglion cell axons guided to the cerebellum of adult hamsters. *J Neurosci.* 1992;12:1144-1159.
27. Ahmad I, Dooley CM, Thoreson WB, Rogers JA, Afiat S. In vitro analysis of a mammalian retinal progenitor that gives rise to neurons and glia. *Brain Res.* 1999;831:1-10.
28. Furukawa T, Kozak CA, Cepko CL. Rax, a novel paired-type homeobox gene, shows expression in the anterior neural fold and developing retina. *Proc Natl Acad Sci USA.* 1997;94:3088-3093.
29. Mathers PH, Grinberg A, Mahon KA, Jamrich M. The Rx homeobox gene is essential for vertebrate eye development. *Nature.* 1997; 387:603-607.
30. Takahashi J, Palmer TD, Gage FH. Retinoic acid and neurotrophins collaborate to regulate neurogenesis in adult-derived neural stem cell cultures. *J Neurobiol.* 1999;38:65-81.

VOLUME 19 • NO 12 • DECEMBER 2001.

# nature biotechnology

<http://biotech.nature.com>

Univ. of Minn.  
Bio-Medical  
Library

**Neural progenitors from  
human ES cells**

**Plants disarm TNT**

**Gene delivery on steroids**

**Bone imaging**



© NOTICE: THIS MATERIAL MAY BE PROTECTED  
BY COPYRIGHT LAW (TITLE 17 U.S. CODE)

# Neural progenitors from human embryonic stem cells

Benjamin E. Reubinoff<sup>1,2,\*</sup>, Pavel Itsykson<sup>1</sup>, Tikva Turetsky<sup>1</sup>, Martin F. Pera<sup>4</sup>,  
Etti Reinhartz<sup>3</sup>, Anna Itzik<sup>3</sup>, and Tamir Ben-Hur<sup>3</sup>

The derivation of neural progenitor cells from human embryonic stem (ES) cells is of value both in the study of early human neurogenesis and in the creation of an unlimited source of donor cells for neural transplantation therapy. Here we report the generation of enriched and expandable preparations of proliferating neural progenitors from human ES cells. The neural progenitors could differentiate *in vitro* into the three neural lineages—astrocytes, oligodendrocytes, and mature neurons. When human neural progenitors were transplanted into the ventricles of newborn mouse brains, they incorporated in large numbers into the host brain parenchyma, demonstrated widespread distribution, and differentiated into progeny of the three neural lineages. The transplanted cells migrated along established brain migratory tracks in the host brain and differentiated in a region-specific manner, indicating that they could respond to local cues and participate in the processes of host brain development. Our observations set the stage for future developments that may allow the use of human ES cells for the treatment of neurological disorders.

ES cell lines are derived from the pluripotent cells of the early embryo<sup>1-3</sup>. ES cell lines can potentially maintain a normal karyotype infinitely on culture *in vitro* and can differentiate into any cell type<sup>4</sup>. ES cell lines have recently been derived from human blastocysts<sup>5,6</sup>, and their potential to differentiate into neural lineages has been demonstrated both *in vivo* in teratomas, and *in vitro*<sup>6-8</sup>. The differentiation of human ES cells into neural progeny may serve as an *in vitro* model for the study of early human neurogenesis. Furthermore, it may enable the development of *in vitro* models of human neurodegenerative disorders, the creation of high-throughput screens for the discovery of neuroprotective and neurotoxic agents, and the identification of novel genes, growth and differentiation factors that have a role in neurogenesis. The potential use of human ES cells as a renewable source of neural cells for transplantation and gene therapy<sup>9</sup> also attracts much public attention.

When ES cells are induced to differentiate *in vitro*, they give rise to a mixture of progeny from the three embryonic germ layers<sup>8,10</sup>. However, we require a means to control differentiation of ES cells into a purified neural progenitor cell population to realize many of their potential applications in neuroscience and regenerative medicine in the central nervous system (CNS). In the mouse ES cell system, strategies for the generation of enriched preparations of proliferating neural progenitors have been developed<sup>11,12</sup>. The *in vitro*-generated neural progenitors could differentiate *in vitro* into both glial cells and functional postmitotic neurons<sup>11</sup>. Transplantation experiments have demonstrated the potential of mouse ES cell-derived neural progenitors to participate in brain development<sup>13</sup>, to myelinate axons in host brain and spinal cord<sup>14,15</sup>, and to promote recovery after spinal cord injury<sup>16</sup>.

We have recently demonstrated that human ES cells can also give rise to neural progenitor cells *in vitro*, and have further demonstrated

that the progenitors can differentiate *in vitro* into mature neurons<sup>6</sup>. Here, we extend this work, demonstrating the derivation of highly enriched and expandable populations of proliferating neural progenitors from human ES cells. Furthermore, the neural progenitors could differentiate *in vitro* into mature neurons, astrocytes, and oligodendrocytes. When grafted into the brain ventricles of newborn mouse, the human neural progenitors migrated into the host brain and differentiated in a region-specific manner, according to normal developmental cues, into progeny from the three fundamental neural lineages.

## Results

**Derivation and propagation of progenitor cells from human ES cells.** To derive enriched preparations of neural progenitors, differentiation of human ES cells was induced by prolonged culture (three to four weeks) without replacing of the mouse embryonic fibroblast feeder layer<sup>6</sup>. One week after passage, changes in cell morphology could be identified mainly in the center of the colonies, indicating the initiation of early differentiation. At this time, the expression of transcripts of the neuroectodermal markers nestin and PAX-6 was demonstrated by RT-PCR (Fig. 1A). The expression of transcripts of neural markers could reflect either some constant background differentiation or the process of early neural differentiation.

During the next two weeks of culture, the process of differentiation was markedly accelerated, mainly in the center of the colonies, and cells with short processes that expressed the early neuroectodermal marker N-CAM (neural cell adhesion molecule) could be identified<sup>6</sup>. It appeared that the N-CAM<sup>+</sup> cells were growing out from adjacent but distinct areas that were composed of small, piled, tightly packed cells that did not react with the monoclonal antibody

<sup>1</sup>The Goldyne Savad Institute of Gene Therapy, <sup>2</sup>Department of Obstetrics and Gynecology, and <sup>3</sup>The Department of Neurology, The Agnes Ginges Center for Human Neurogenetics, Hadassah University Hospital, Jerusalem, Israel. <sup>4</sup>Monash Institute of Reproduction and Development, Monash University, Melbourne, Victoria, Australia. \*Corresponding author (reubinof@md2.huji.ac.il).

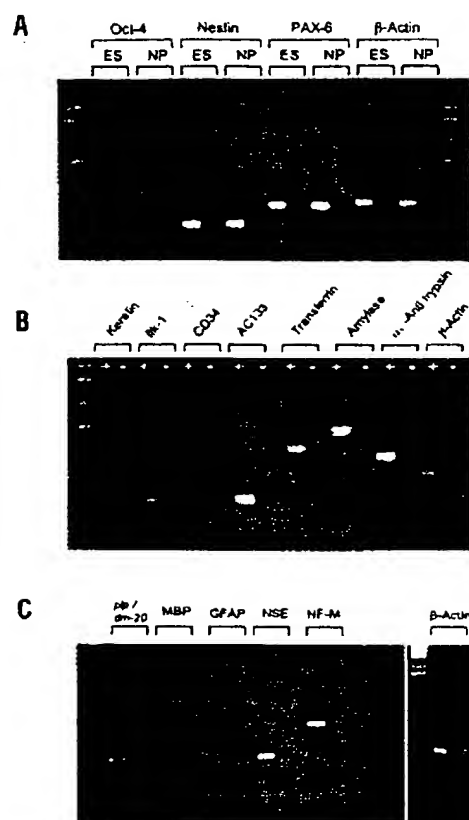


**Figure 1.** RT-PCR analysis of the expression of markers in human ES cell colonies, ES-derived spheres, and in differentiated cells originating from the spheres. (A) Oct-4, nestin, and PAX-6 in human ES cell colonies at one week after plating and in neural progenitor (NP) spheres. (B) The expression of non-neural marker genes in human ES cell-derived spheres. (C) Neuronal and glial markers in differentiated cells originating from human ES cell-derived neural progenitor spheres. All panels show 2% agarose gels stained with ethidium bromide. The symbols + and – indicate whether the PCR reaction was done with or without the addition of reverse transcriptase. A 1 kb plus DNA ladder was used in all panels. Oct-4 band is 320 bp, nestin 208 bp, PAX-6 274 bp, β-actin 291 bp, keratin 780 bp, β-tub 199 bp, CD34 200 bp, AC133 200 bp, transferrin 367 bp, amylase 490 bp, α1-antitrypsin 360 bp, p16 and dm-20 are 354 bp and 249 bp, respectively, MBP is 379 bp, GFAP is 383 bp, NSE is 254 bp, and NF-M is 430 bp.

GCTM-2, which identifies undifferentiated ES cells<sup>6</sup>, and did not express the early neuroectodermal marker N-CAM (data not shown). These distinct areas had a uniformly white-gray and opaque appearance under dark-field stereomicroscopy (Fig. 2A), and could be identified in 54% of the colonies (67/124). They were surrounded by cells with diverse morphologies expressing a large array of somatic and extraembryonic markers, including muscle actin and desmin<sup>6</sup>, α-fetoprotein, hepatocyte nuclear factor (HNF)-α, cardiac actin, and kallikrein (RT-PCR; not shown).

Assuming that the cells in the distinct areas gave rise to the adjacent N-CAM<sup>+</sup> cells, clumps of about 150 cells were mechanically isolated from these areas and replated in serum-free medium<sup>17</sup>. Under these culture conditions, the clumps formed free-floating spherical structures within 24 h.

Supplementing the medium with basic fibroblast growth factor (bFGF) and epidermal growth factor (EGF), a growth factor combination that is known to be effective for the propagation of human fetal- and adult-derived neuroepithelial progenitors<sup>17–26</sup>, facilitated

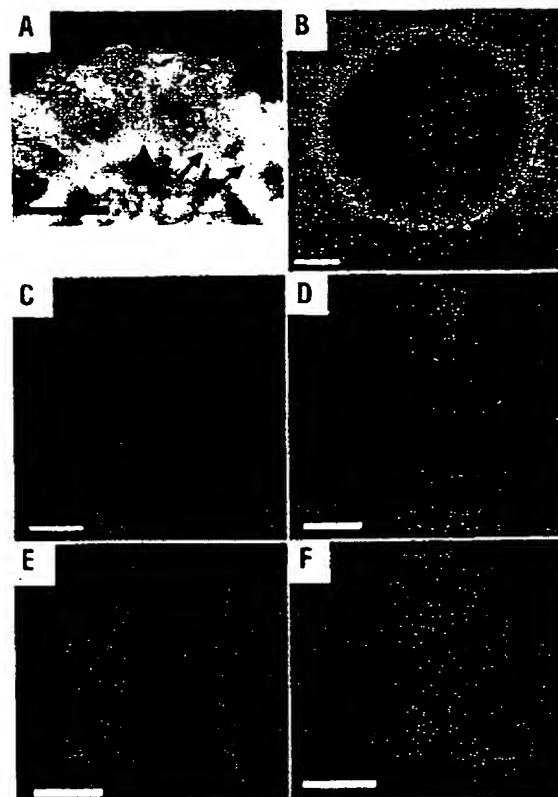


**Figure 2.** Analysis of morphology and marker expression in human ES-derived progenitor cells. (A) Dark-field stereomicroscopic photograph of a differentiating ES cell colony, four weeks after plating, with areas of cells (arrows) that are destined to give rise to neural progenitors. (B) Phase contrast micrograph of a sphere cultured in serum-free medium. (C–F) Indirect immunofluorescence staining of progenitor cells, 4–12 h after disaggregating of spheres and plating on adhesive substrate, for N-CAM, vimentin, nestin, and A2B5, respectively. Bars = 1.6 mm (A), 100 μm (B), 25 μm (C, E, F), 35 μm (D).

sequential propagation and expansion of the sphere cultures. During the first two weeks in culture, some cell death was observed and the spheres gradually acquired a uniform round morphology (Fig. 2B). A detailed analysis of marker expression and the growth and differentiation potential of the cells within the spheres was conducted in three preparations that were separately derived and propagated.

The level of proliferation of the cells within the spheres was monitored indirectly by measuring the increase in the volume of the spheres over time. Most of the cells within the spheres were viable as demonstrated by Trypan Blue staining ( $94 \pm 3.2\%$ ,  $n = 47$  spheres). A positive correlation between the volume of the spheres and the number of cells within the spheres (Fig. 3B) was documented at various passage levels (5–15 weeks after derivation), indicating that an increment in sphere volume could be used as an indirect indication of cell proliferation. The spheres grew over an 18- to 22-week period, after which time the volume of the spheres was stable or declined. A relatively rapid growth rate was observed during the first five to six weeks after derivation, with a population doubling time of ~4.7 days. It was followed by a 10- to 16-week period of slow and stable cell growth with a population doubling time of ~2.5 weeks. This proliferative capability could potentially allow a significant expansion of the progenitor cell cultures (Fig. 3A).

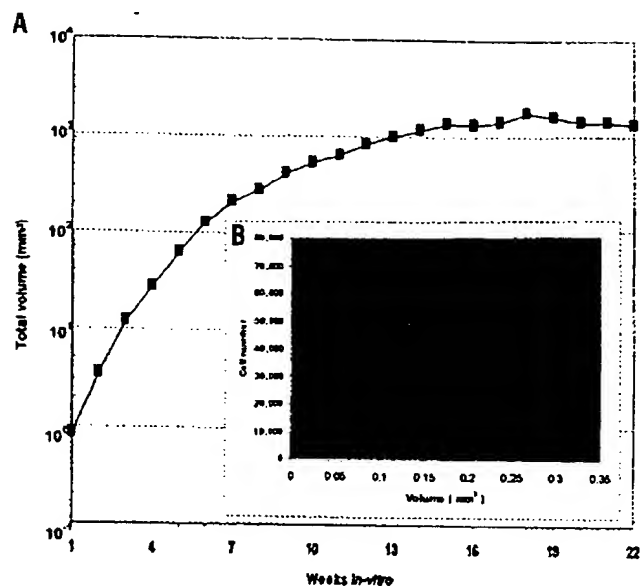


**Figure 3.** Cumulative growth curve for human ES-derived progenitor cells. (A) Continuous growth is evident during an 18- to 22-week period. The increment in the volume of the spheres was continuously monitored as an indirect measure of the increase in cell numbers. A linear positive correlation between the volume of the spheres and the number of cells within the spheres (B, insert) was maintained during cultivation.

**Characterization of the progenitor cells within the spheres.** Cells in the spheres expressed markers of neural progenitor cells, such as N-CAM (ref. 21; Fig. 2C), the intermediate-filament protein nestin<sup>22</sup> (immunostaining, Fig. 2E; RT-PCR, Fig. 1A), A2B5 (ref. 23; Fig. 2F), vimentin<sup>24</sup> (Fig. 2D), and the transcription factor PAX-6 (Fig. 1A). The expression of these markers was maintained with prolonged cultivation *in vitro* (18 weeks).

To evaluate the proportion of neural progenitors in the cultures, spheres were disaggregated into single cells that were plated, fixed, and analyzed for the expression of the early neural markers (Fig. 2C–F). A high proportion of the cells expressed N-CAM ( $99 \pm 1.6\%$ ,  $n = 11$  experiments), nestin ( $97 \pm 2.3\%$ ,  $n = 10$  experiments), and A2B5 ( $90.5 \pm 1.1\%$ ,  $n = 6$ ). A lower proportion of cells were immunoreactive to the vimentin-specific antibody ( $67 \pm 16.8\%$ ,  $n = 9$  experiments). These proportions were stable during cultivation of the spheres (up to 18 weeks).

Oct-4 is a member of the POU-domain transcription factor family whose expression is limited in the mouse to pluripotent cells and is downregulated upon differentiation<sup>25</sup>. We have previously demonstrated a similar pattern of expression in human ES cells<sup>6</sup>. Oct-4 was not expressed by cells in the neural progenitor spheres, indicating that undifferentiated human ES cells were not present within the spheres (Fig. 1A).

To determine whether cells that had acquired markers of other tissues or lineages were present within the spheres, the expression of markers representing derivatives of mesoderm, endoderm, and epidermis were examined. Cells within the spheres expressed transcripts of markers of hematopoietic/endothelial progenitors (CD34, AC-133, Flk-1), endoderm ( $\alpha$ 1-antitrypsin, transferring, and amylase) and epidermis (keratin), as demonstrated by RT-PCR (Fig. 1B). Markers of extraembryonic endoderm were not expressed by the progenitors ( $\alpha$ -fetoprotein and HNF- $\alpha$ , RT-PCR; not shown) or their differentiated progeny (low-molecular-weight cytokeratin and laminin immunostaining; not shown). The expres-

sion of transcripts of non-neural markers was evident after prolonged cultivation of the spheres. It could represent contamination by a small number of non-neural cells generated during the derivation of our cultures. Alternatively, it could represent plasticity of primitive neural progenitors that expressed markers, or gave rise to cells from other lineages<sup>26,27</sup>. Whatever the source, additional selection either on the basis of cell-surface markers<sup>18</sup> or on the expression of lineage-specific genes<sup>12</sup> may be needed to generate pure neural cultures.

***In vitro* neural differentiation.** The neural progenitors in the spheres could differentiate *in vitro* into derivatives of the three fundamental neural lineages. In general, differentiation was induced by plating whole spheres on an appropriate substrate in the absence of growth factors. Under these conditions the spheres attached rapidly, and cells migrated out to form a monolayer of differentiated cells (Fig. 4A).

For neuronal differentiation studies, spheres were plated on poly-D-lysine and laminin-coated dishes. After two to three weeks, cells that migrated out and formed a monolayer both displayed the morphology and also expressed the structural markers that are characteristic of immature neurons, such as  $\beta$ III-tubulin (Fig. 4B), the 70 kDa neurofilament proteins (Fig. 4C), and neuron-specific enolase (NSE; Fig. 1C). Moreover, the differentiated cells expressed markers of mature neurons such as the 160 kDa neurofilament proteins (NF-M, Fig. 4D; RT-PCR, Fig. 1C), MAP-2ab (Fig. 4E), and synaptophysin (Fig. 4F). Furthermore, the cultures contained cells that synthesized glutamate, expressed glutamic acid decarboxylase (GAD; the rate-limiting enzyme in GABA biosynthesis), synthesized GABA and serotonin, and expressed tyrosine hydroxylase (TH; Fig. 4G–K). Neurons that synthesized GABA and glutamate were relatively abundant, comprising 35% and 15% of the neuronal population, respectively. TH- and serotonin-producing cells were relatively rare (<1%).

For glial differentiation studies, spheres were plated on poly-D-lysine- and fibronectin-coated dishes and were cultured first in the presence of EGF, bFGF, and platelet-derived growth factor-AA (PDGF-AA), followed by culture in the presence of tri-iodothyronine (T3). The combination of bFGF and PDGF-AA is known to promote the proliferation of glial precursor cells<sup>14</sup>, whereas T3 has been shown to enhance differentiation of oligodendrocyte lineage cells from human embryonic neural spheres<sup>28</sup>.

Differentiation into astrocytes was demonstrated by the presence of cells that expressed glial fibrillary acidic protein (GFAP) (Fig. 4L; RT-PCR, Fig. 1C). Oligodendrocyte lineage cells were infrequent under our culture conditions and few cells were immunoreactive to O4, an antibody recognizing oligodendrocyte-specific glycolipids<sup>29</sup> (Fig. 4M). Differentiation to the oligodendrocyte lineage was further confirmed by demonstrating the expression of RNA transcripts of both myelin basic protein (MBP) and the *plp* gene (Fig. 1C). The *plp* gene encodes the proteolipid protein and its alternatively spliced product DM-20, which are major proteins of brain myelin<sup>21</sup>.

To evaluate the proportion of neurons versus glial cells following induction of differentiation, spheres that were propagated 10 weeks were disaggregated and plated on poly-D-lysine- and laminin-coated dishes and cultured in the absence of mitogens for five days. Fifty-seven percent of the cells were immunoreactive to anti- $\beta$ III-tubulin (a marker characteristic of immature neurons) and 26% to anti-GFAP. Therefore, at least 83% of the cells took on a neural fate. The potential of the neural progenitors to give rise to both neurons and glial cells *in vitro* was maintained for the duration of the 22 weeks of propagation.

**Integration and differentiation in host brain.** To explore the developmental potential of the human ES-derived neural progenitors *in vivo*, disaggregated bromodeoxyuridine (BrdU)-labeled



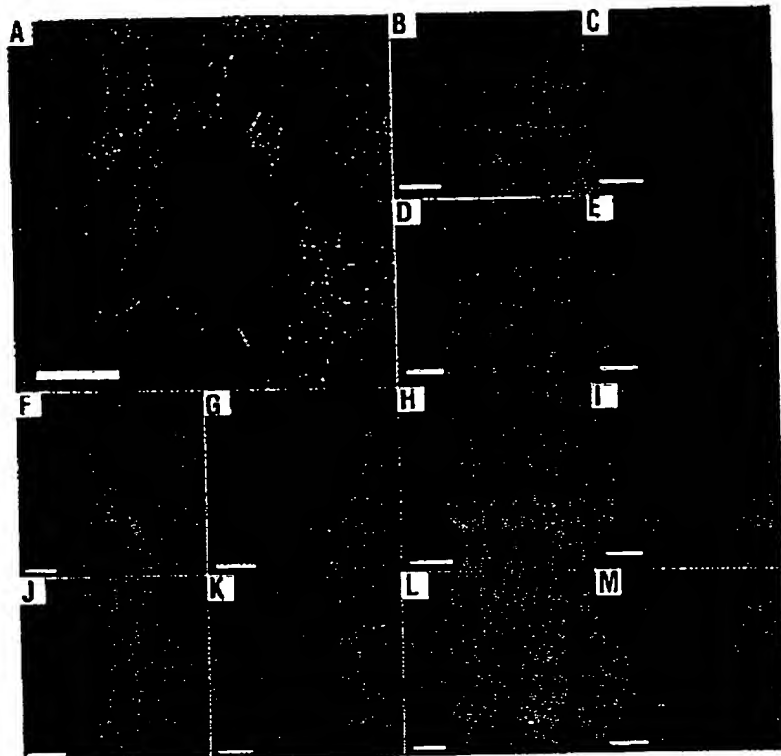


**Figure 4.** Phase contrast appearance and marker expression of differentiated cells originating from human ES-derived neural progenitor spheres. (A) Phase contrast micrograph of differentiated cells emanating from a sphere two weeks after plating onto an adhesive surface and culture in the absence of growth factors. (B–M) Indirect immunofluorescence microscopy of differentiated cells decorated with antibodies against the following neuronal and glial markers:  $\beta$ -tubulin (B), 70 kDa neurofilament proteins (C), 160 kDa neurofilament proteins (D), MAP2ab (E), synaptophysin (F), glutamic acid decarboxylase (G), GABA (H), glutamate (I), serotonin (J), tyrosine hydroxylase (K), GFAP (L), O4 (M). Bars = 200  $\mu$ m (A, D), 50  $\mu$ m (E), 20  $\mu$ m (B, C, F–M).

immunoreactive with anti-BrdU and with human-specific anti-mitochondrial antibody in various regions of host brain was similar.

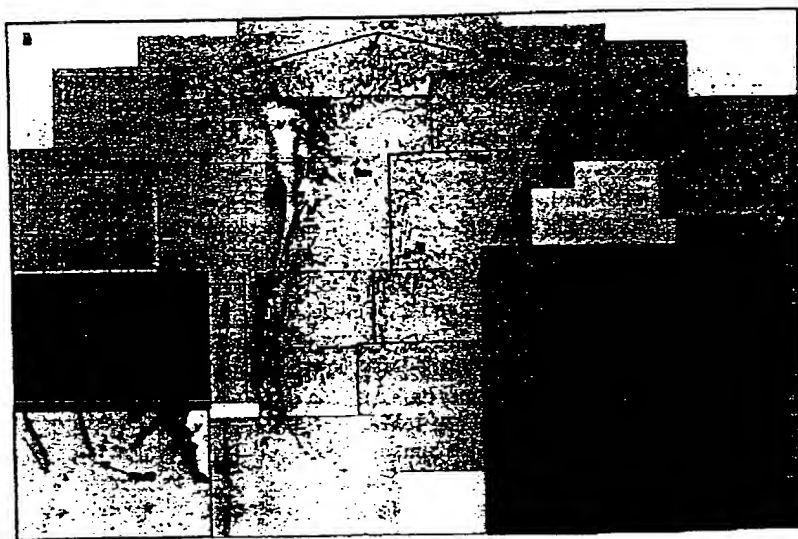
Brains that were examined a week after transplantation exhibited clusters of donor cells lining the ventricular wall (Fig. 5A). Four to six weeks following transplantation, human cells had left the ventricles and migrated in large numbers mainly as individual cells into the host brain parenchyma. The human cells demonstrated a widespread distribution in various regions of the host brain including periventricular areas, the entire length of the corpus callosum, fimbria, internal capsule, diencephalic tissue around the third ventricle, and dentate gyrus (Fig. 5B, E–H). Transplanted human cells also migrated anteriorly

from the subventricular zone along the rostral migratory stream (Fig. 5C) and populated the olfactory bulb, indicating their potential to respond to local cues and migrate along established host brain tracts.

Differentiation *in vivo* into the three fundamental neural lineages was demonstrated by immunochemical studies using anti-human cell type-specific antibodies or double-labeling experiments with both anti-BrdU or anti-human specific ribonuclear protein (RNP) and anti-neural cell type-specific antibodies. Glial differentiation of the transplanted cells was abundant in the periventricular areas that consist of white-matter tracks where glial differentiation in the post-natal period is predominant. *In vivo* differentiation into astrocytes was demonstrated by immunochemical staining with anti-human-

spheres were implanted into the lateral cerebral ventricles of newborn mice<sup>19</sup>. Transplantation was performed 9–15 weeks after derivation of the neural spheres. Histological and immunochemical evaluation of serial brain sections was performed 4–6 weeks after transplantation. Numerous BrdU<sup>+</sup> cells were found in 9 out of 14 recipient animals, and successful engraftment was documented with donor cells from the three neural progenitor populations (Fig. 5). Transplantation efficiency was highly variable. BrdU<sup>+</sup> cells were not observed in the brain parenchyma of control animals that received transplantation of killed, BrdU-labeled, neural progenitors (Fig. 5D). The human origin of the cells decorated with anti-BrdU was confirmed by double labeling with a combination of anti-BrdU and anti-human specific ribonucleoprotein antibodies (Fig. 6A–D). The identity of the transplanted human cells was also confirmed by immunofluorescent staining with human-specific anti-mitochondrial antibodies (Fig. 6E–G). The distribution of cells that were

**Figure 5.** Dissemination of transplanted BrdU<sup>+</sup> human ES-derived neural progenitor cells in the mouse host brain. (A) Two days after transplantation, most cells were found lining the ventricular wall. (B) After four to six weeks, most cells had left the ventricles (V) and populated the corpus callosum (CC), fimbria (fim), and internal capsule (ic). (C) Chains of BrdU<sup>+</sup> cells were found in the RMS. (D) In animals that were transplanted with dead BrdU-labeled cells, there was no BrdU staining in the brain parenchyma. (E) BrdU<sup>+</sup> cells in the periventricular white matter. (F) High magnification of BrdU<sup>+</sup> cells in the corpus callosum; in the cortical layer above the corpus callosum (\*) there were no BrdU<sup>+</sup> cells. (G) High-magnification image showing BrdU<sup>+</sup> cells populating the fimbria. (H) Low-magnification image showing BrdU<sup>+</sup> cells in the dentate gyrus. Str, striatum; hipp, hippocampus.



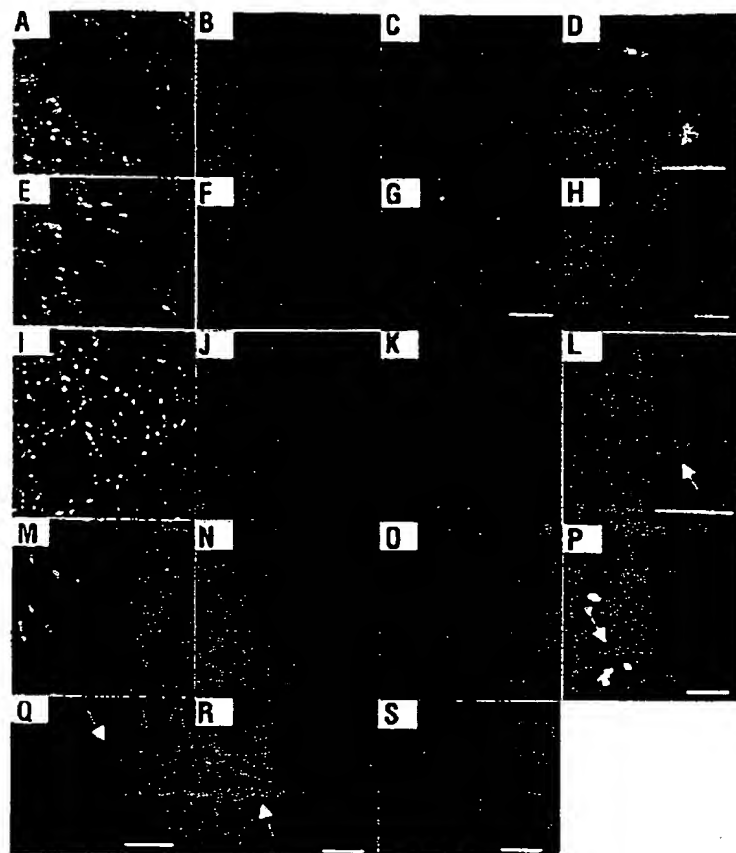


**Figure 6.** Identification of the transplanted cells in the brain by human and neural lineage-specific markers. (A–D) Nuclei (identified in Nomarski optics, panel A) were double labeled for BrdU (green fluorescence, panel B) and human-specific anti-RNP (red fluorescence, panel C). The nuclear co-localization (D) indicated that BrdU+ cells were indeed of human origin. (E–G) A typical chain of transplanted cells in the corpus callosum, stained with human-specific anti-mitochondrial antibody. The mitochondrial staining (green fluorescence, panel F) on Nomarsky background (blue; panel G, cell nuclei indicated by asterisks) shows typical perinuclear localization. (H) A periventricular transplant-derived astrocyte detected by a human-specific anti-GFAP antibody. (I–L) A transplant-derived astrocyte from the periventricular region. The nucleus (identified by Nomarski optics, panel I) is labeled with BrdU (J, green fluorescence), indicating its origin from the graft and surrounded by GFAP staining (K, L). (M–P) A human oligodendrocyte progenitor cell identified in the periventricular region. The cell membrane (M, arrows) and nucleus (M, arrow and asterisk) are identified by Nomarski optics. Co-labeling of nucleus by anti-BrdU (N) and cell membrane by anti-NG-2 (O) are demonstrated in image (P). (Q) A CNPase+ oligodendrocyte (green) in the corpus callosum, co-labeled with human-specific RNP (red). (R) A  $\beta$ -tubulin+ neuron (green fluorescence) in the olfactory bulb, co-labeled with human-specific RNP (red). (S) Neuronal processes in the fimbria, stained with a human-specific anti-70 kDa neurofilament. Bars = 10  $\mu$ m.

specific GFAP (Fig. 6H) and by double labeling for BrdU and GFAP (Fig. 6I–L). Transplanted cells that differentiated into the oligodendroglial lineage were demonstrated by double immunostaining with anti-BrdU and anti NG-2 (a marker of oligodendrocyte progenitors<sup>30</sup>) or anti-human RNP and anti-2',3'-cyclic nucleotide 3'-phosphodiesterase (CNPase; Fig. 6M–P and 6Q, respectively).

Neuronal differentiation of the human transplanted cells was specifically demonstrated in the olfactory bulb, a region where neurogenesis occurs after birth (Fig. 6R). Neuronal processes of transplanted cells were also detected by a human-specific anti-light chain neurofilament antibody in the fimbria (Fig. 6S).

There was no histological evidence of teratoma or non-neural tissue formation in any of the recipient animals.

## Discussion

Our findings show that a highly enriched population of proliferating neural progenitors may be derived from human ES cells. These neural progenitors are capable of extensive proliferation *in vitro* while retaining their potential to give rise to the three fundamental neural lineages and to participate in mammalian brain development. Derivation of proliferating, highly enriched tissue-specific progenitors from human ES cells, as exemplified here for the neural lineage, is expected to be highly valuable for the analysis of the stages of early development and for the development of a donor source for tissue reconstruction.

Our culture conditions promoted the undifferentiated proliferation of the human ES-derived neural progenitors for 20 weeks. Throughout cell propagation, expression of markers of early neuroectoderm was maintained, as was the progenitors' potential to differentiate into neurons and glial cells. The neural progenitors did not express markers of ES cells or the morphology and markers of differentiated neural cells. It should be noted that because the neural progenitors were not subjected to clonal analysis, it is not possible to determine whether our cultures contained multipotent human neural stem cells or a mixture of more restricted neural progenitors<sup>31</sup>. Nevertheless, our approach could distinguish among the early phases of human neurogenesis, including pluripotent ES stem cells, the proliferation of neural progenitors, and their differentiation into neurons and glial cells. This is the first step toward the development of more refined *in vitro* models that will distinguish between neural progenitors at various levels of commitment<sup>26</sup> and will allow the dissection of the cellular and molecular processes accompanying the various stages of development of the human nervous system.

Our data demonstrate that neural progenitors derived from human ES cells *in vitro* can respond appropriately to normal developmental cues *in vivo*. Following transplantation to the cerebral ventricles of newborn mice, the donor cells migrated in large numbers into the host brain parenchyma and became widely distributed. The engraftment efficiency was variable, and additional studies are required to determine to what extent, if at all, *in vivo* proliferation of transplanted cells contributed to the total number of human cells in host brains. Migration of the transplanted cells was not random, and the human progenitors followed established brain pathways, indicating that they respond to host's signals. The human ES cell-derived neural progenitors differentiated *in vivo* into neurons, astrocytes, and oligodendrocytes. Differentiation into neurons was demonstrated in the olfactory bulb where host differentiation into this lineage occurs in the postnatal period, whereas differentiation into astroglia and oligodendroglia was demonstrated in subcortical white-matter tracts where gliogenesis predominates and neurogenesis is complete<sup>32</sup>. These data demonstrate that cell fate was determined in a region-specific manner and according to the region's stage of development.

When ES cells, including those of human origin, are engrafted into various organs of young adult host mice, they may give rise to teratocarcinoma or teratomas<sup>3,4</sup>. We did not observe the formation of teratomas or non-neural tissues in any of the transplanted mice, and we also could not detect expression of the stem cell marker Oct-4 in the neural progenitor cultures. Thus, contamination by undifferentiated ES cells was probably eliminated by our selective derivation and propagation protocols. Nevertheless, given the expression of tran-

scripts of markers of non-neural lineages by the cells in our cultures, additional immunohistochemical and molecular studies are needed to determine whether non-neural human cells are generated in the host brain parenchyma. Thorough long-term studies are required to determine the safety of the transplantation of human ES cell-derived neural progeny, and to rule out potential hazards such as tumor formation or the development of cells from other lineages.

Data are accumulating rapidly regarding the signals and factors that govern the proliferation of neural progenitors and determine their fate during CNS development<sup>31</sup>. In this study we have used this knowledge to generate an enriched, expandable population of developmentally competent neural progenitors from human ES cells. This work serves as a platform for further manipulations with growth and differentiating factors that may eventually enable the derivation of specific neural cells<sup>33</sup>, and may facilitate the use of human ES cells as a useful tool in basic neuroscience research and regenerative medicine.

### Experimental protocol

**Derivation and culture of progenitor cells.** Human ES cells (HES-1 cell line<sup>6</sup>) with a stable normal (46XX) karyotype were cultured on mitomycin C mitotically inactivated mouse embryonic fibroblast feeder layer in gelatin-coated tissue culture dishes as described<sup>6</sup>. After three weeks of continuous culture, patches containing ~150 cells each were cut out from distinct areas within the differentiating ES colonies using the razor-sharp edge of a micro-glass pipette. Contamination by other cell types was avoided by paying careful attention to cut well within the distinct areas. The clusters of cells were transferred to plastic tissue culture dishes containing growth medium that consisted of Dulbecco's minimal essential medium (DMEM)/F12 (1:1), B27 supplementation (1:50), glutamine 2 mM, penicillin 50 units/ml, and streptomycin 50 µg/ml (Gibco, Gaithersburg, MD), and supplemented with 20 ng/ml human recombinant EGF and 20 ng/ml bFGF (R&D Systems, Inc., Minneapolis, MN). The clusters of cells developed into round spheres that were subcultured by dissection into quarters (by two no. 20 surgical blades; Swann-Morton, Sheffield, UK), every 7–21 days when their diameter exceeded 0.5 mm. Fifty percent of the medium was replaced every three to four days.

**Analysis of growth.** The increment in the volume of 24 spheres was monitored weekly starting from the first passage (one week after derivation). A stereomicroscope was used to measure the diameter of individual spheres, and their volume was calculated using the equation for the volume of a ball. The spheres were passaged every 7–21 days when the diameter of at least six spheres exceeded 0.5 mm. At each passage, six spheres (diameter >0.5 mm) were sectioned into quarters that were plated individually in a 24-well tissue culture dish. When growth was evaluated a week after passage, the sum of volumes of the daughter spheres was compared to the sum of volumes of the mother spheres.

**Immunohistochemistry studies.** Immunostaining of ES cell colonies to evaluate the expression of GCTM-2 and N-CAM was performed as described<sup>6</sup>. Standard protocols were used for the immunophenotyping of spheres, disaggregated progenitor cells, and differentiated cells. Fixation with 4% paraformaldehyde was used unless otherwise specified. Primary antibody localization was done by using swine anti-rabbit and goat anti-mouse immunoglobulins conjugated to fluorescein isothiocyanate (FITC 1:20; Dako, Carpinteria, CA), and goat anti-mouse IgM conjugated to Texas Red (1:50; Jackson Laboratories, West Grove, PA). Proper controls for primary and secondary antibodies revealed neither nonspecific staining nor antibody cross-reactivity.

To characterize the immunophenotype of cells within the aggregates, spheres that were cultivated 6–18 weeks were disaggregated and the single cells were plated on poly-D-lysine (30–70 kDa, 10 µg/ml; Sigma, St. Louis, MO) and laminin (4 µg/ml; Sigma), fixed after 4–12 h, and examined for the expression of N-CAM (acetone fixation, 1:10; Dako), nestin (rabbit antiserum, a gift of Dr. Ron McKay; 1:25), A2B5 (1:20; American Type Culture Collection, ATCC, Manassas, VA), and vimentin (methanol fixation, 1:20; Roche Diagnostics Australia, Castle Hill, NSW). Two hundred cells were scored within random fields (at 400x) for the expression of each of these markers, and the experiments were repeated at least three times.

For the study of the expression of extraembryonic endodermal markers,

whole spheres were plated on poly-D-lysine and fibronectin (5 µg/ml; Sigma), cultured four weeks in growth medium without growth factors, and examined for the expression of low-molecular-weight (LMW) cytokeratin (Beckton Dickinson, San Jose, CA) and laminin (1:500; Sigma).

Neuronal differentiation was induced by culturing the spheres on poly-D-lysine and laminin in growth medium without supplementation of growth factors for two to three weeks. In some of the experiments, starting from the sixth day after plating, the medium was supplemented with all-trans retinoic acid (10<sup>-4</sup> M; Sigma). Differentiated cells were analyzed for the expression of 160 kDa neurofilament protein (methanol fixation, 1:50; Chemicon, Temecula, CA), 70 kDa neurofilament protein (1:100; Chemicon), MAP2ab (1:100; Neomarkers, Union City, CA), glutamate (1:1,000; 1% (wt/vol) paraformaldehyde–1% (vol/vol) glutaraldehyde fixation; Sigma), synaptophysin (1:50; Dako), TH (Sigma), serotonin (1:1,000; Sigma), GAD (1:200; 1% (wt/vol) paraformaldehyde–1% (vol/vol) glutaraldehyde fixation; Chemicon; 1:200), GABA (1:1,000; Sigma), and β<sub>III</sub>-tubulin (1:150; Sigma). To determine the proportion of neurons that synthesized the various neurotransmitters, at least 100 cells were scored within random fields of the outgrowth from differentiating spheres (at 400x) for the expression of β<sub>III</sub>-tubulin and each of the neurotransmitters, and the experiments were repeated at least three times.

To enhance the differentiation toward the glial lineages, spheres were plated on poly-D-lysine and fibronectin, cultured two weeks in growth medium supplemented with recombinant human PDGF-AA (20 ng/ml), bFGF (20 ng/ml), and EGF (20 ng/ml), followed by two weeks in the presence of T3 (30 nM; Sigma) only. Differentiated cells were analyzed for the expression of GFAP (1:50; Dako) and O4 (1:10; Chemicon).

**Reverse transcription (RT)-PCR analysis.** Total RNA was collected from human ES cell colonies (one week after passage), from free-floating spheres, and from differentiated cells growing from spheres that were induced to differentiate to the neuronal or glial lineages as detailed above. Total RNA was isolated using RNA STAT-60 solution (TEL-TEST, Inc., Friendswood, TX) and was reverse-transcribed into complementary DNA (cDNA) with SuperScript First Strand Synthesis System (Gibco) using oligo (dT) as a primer according to the manufacturer's instructions. PCR was carried out using standard protocols with Taq DNA Polymerase (Gibco) or Tfi DNA Polymerase (Promega, Madison, WI). Primer sequences (forward and reverse) and the length of amplified products were as follows: Oct-4 (primers<sup>34</sup>); nestin, PAX-6, NSE, NF-M, *plp* (primers<sup>35</sup>); keratin, amylase, α1-antitrypsin (primers<sup>8</sup>); *flk-1*, CD34, AC133 (primers<sup>36</sup>); GFAP, MBP (primers<sup>30</sup>); *transferrin*: 5'-CTGACCTACCTGGGACAAT-3', 5'-CCATCAAGGCACAGC-3' (367 bp); α-fetoprotein: 5'-CCATGTACATGAGCACTGTTG-3', 5'-CTCCAATAACTCCTGGTATCC-3' (338 bp); HNF-α: 5'-GAGTTTACAGGCTTGTGGCA-3', 5'-GAGGGCAATTCCTGAGGATT-3' (390 bp). As a control for messenger RNA (mRNA) quality, β-actin transcripts were assayed using the same RT-PCR and the following primers: 5'-TACCACACAGGCCGAGCG-3', 5'-TCTCCTTCTGCATCCTGTCC-3' (291 bp). Amplification conditions were as follows: 94°C for 4 min followed by 40 cycles of 94°C for 15 s, 55°C for 30 s, 72°C for 45 s, and extension at 72°C for 7 min. Products were analyzed on a 2% agarose gel and visualized by ethidium bromide staining.

**Transplantation to the developing brain.** Spheres were cultured in the presence of BrdU (50 µM; Sigma) for 10 days. Fifty percent of the medium was replaced every three to four days with fresh medium containing fresh BrdU. The spheres were then disaggregated; 86% of the cells were viable as determined by Trypan Blue staining, and 40% were decorated by anti-BrdU. Approximately 50,000–100,000 cells (in 2 µl PBS) were injected into the lateral ventricles of newborn (P1) mice (Sabra mice; Harlan, Jerusalem, Israel) by using a glass micropipette (300 µm outer diameter) connected to a micro-injector (Narishige Inc., Tokyo, Japan). Transplantation of dead, BrdU-labeled, human ES cell-derived neural progenitors served as control experiments. The neural progenitors underwent three cycles of freezing by plunging into liquid nitrogen and thawing in room temperature just before transplantation. At one to six weeks of age, recipients were anesthetized and perfused with 4% paraformaldehyde in PBS.

**Detection and characterization of donor human neural progenitors in vivo.** Serial 7-µm frozen sections were examined by immunostaining after postfixation with acetone or with 4% paraformaldehyde. The transplanted cells were detected by immunostaining with antibodies for BrdU

## RESEARCH ARTICLE

(1:20; Dako), anti-human specific RNP antibody (1:20; Chemicon), and anti-human specific mitochondrial antibody (1:20; Chemicon). BrdU antibody was detected by using the peroxidase-conjugated Vectastain kit (Vector Laboratories, Burlingame, CA), developed with diaminobenzidine (DAB), or by using goat anti-mouse IgG conjugated to Alexa 488 (1:100; Jackson). Anti-RNP and mitochondrial antibodies were detected with goat anti-mouse IgM conjugated to Cy5 and goat anti-mouse IgG conjugated to Alexa488, respectively (1:100; Jackson). Transplanted astrocytes were identified by double staining for BrdU and GFAP (1:100; Dako) or by anti-human specific GFAP (1:100; Sternberger Monoclonals Inc., Lutherville, MD). Anti-CNase (1:100; Sigma) and anti NG2 (1:100; Chemicon) were used for the oligodendrocyte lineage. Neurons were detected by immunostaining with human-specific anti-neurofilament light chain (1:100; Chemicon) and anti- $\beta$ -tubulin (antibody as detailed above; 1:100). Goat anti-rabbit conjugated to Cy5 (1:100; Jackson) and goat anti-mouse IgG

conjugated to Alexa488 (1:100; Jackson) were used for detection of primary antibodies. Images were taken with a confocal microscope (Zeiss). The double-stain immunofluorescence signals were analyzed at multiple consecutive planes to ensure the co-localization of nuclear and cytoplasmic or membranal signals to the same cell.

## Acknowledgments

We gratefully acknowledge Eithan Galun for critically reviewing this manuscript, Neri Laufer for his generous support, and Orna Singer for assistance in cell culture. Many thanks to Mark Tarshish for his help in obtaining confocal images. The study was supported by a grant (No. 2005-1-99) from the Israeli Ministry of Science, a grant from Embryonic Stem Cells International (ESI) Pte Ltd., and by The Hilda Katz Blaustein Fund.

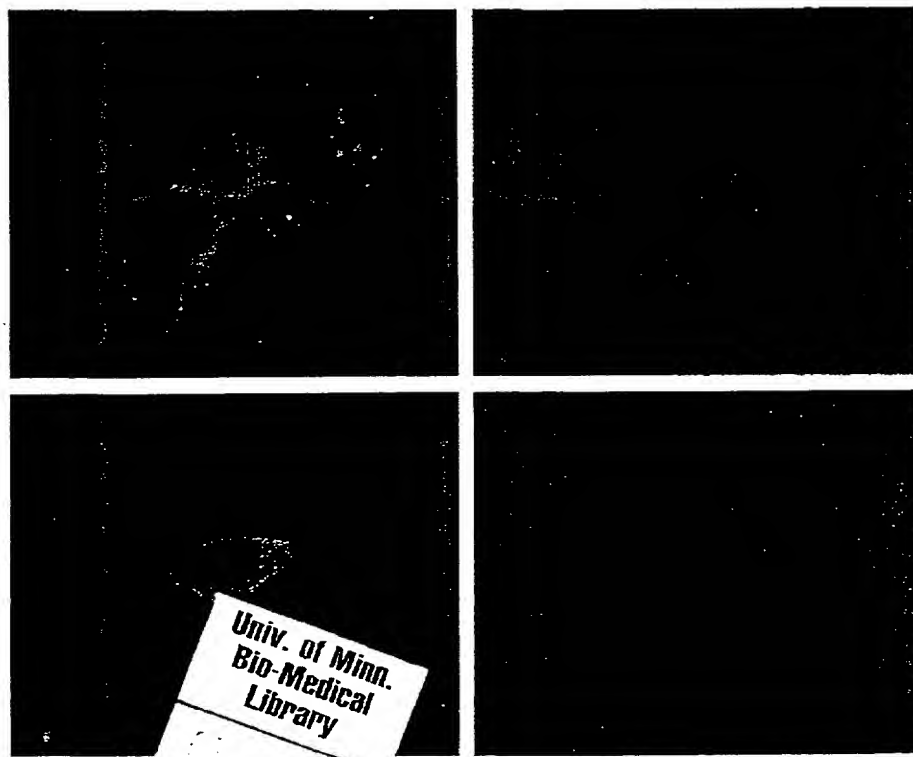
Received 31 July 2001; accepted 25 October 2001

- Martin, G.R. Isolation of a pluripotent cell line from early mouse embryos cultured in medium conditioned by teratocarcinoma stem cells. *Proc. Natl. Acad. Sci. USA* 78, 7634-7638 (1981).
- Evans, M.J. & Kaufman, M.H. Establishment in culture of pluripotential cells from mouse embryos. *Nature* 292, 154-156 (1981).
- Brook, F.A. & Gardner, R.L. The origin and efficient derivation of embryonic stem cells in the mouse. *Proc. Natl. Acad. Sci. USA* 94, 5709-5712 (1997).
- Robertson, E.J. Embryo derived stem cell lines. In *Teratocarcinomas and embryonic stem cells: a practical approach*. (ed. Robertson, E.J.) 71-112 (IRL Press, Oxford, UK; 1987).
- Thomson, J.A. *et al.* Embryonic stem cell lines derived from human blastocysts. *Science* 282, 1145-1147 (1998).
- Reubinoff, B.E., Pera, M.F., Fong, C.-Y., Trounstein, A. & Bongso, A. Embryonic stem cell lines from human blastocysts: somatic differentiation *in vitro*. *Nat. Biotechnol.* 18, 399-405 (2000).
- Itskovitz-Eldor, J. *et al.* Differentiation of human embryonic stem cells into embryoid bodies comprising the three embryonic germ layers. *Mol. Med.* 6, 88-95 (2000).
- Schuldiner, M., Yanuka, O., Itskovitz-Eldor, J., Melton, D.A. & Benvenisty, N. Effects of eight growth factors on the differentiation of cells derived from human embryonic stem cells. *Proc. Natl. Acad. Sci. USA* 97, 11307-11312 (2000).
- Svendsen, C.N. & Smith, A.G. New prospects for human stem-cell therapy in the nervous system. *Trends Neurosci.* 22, 357-364 (1999).
- Doetschman, T.C., Eistetter, H., Katz, M., Schmidt, W. & Kemler, R. The *in vitro* development of blastocyst-derived embryonic stem cell lines: formation of visceral yolk sac, blood islands, and myocardium. *J. Embryol. Exp. Morphol.* 87, 27-45 (1985).
- Okabe, S., Forsberg-Nilsson, K., Spiro, A.C., Segal, M. & McKay, R.D.G. Development of neuronal precursor cells and functional postmitotic neurons from embryonic stem cells *in vitro*. *Mech. Dev.* 59, 89-102 (1996).
- Li, M., Pevry, L., Lovell-Badge, R. & Smith, A. Generation of purified neural precursors from embryonic stem cells by lineage selection. *Curr. Biol.* 8, 971-974 (1998).
- Brustle, O. *et al.* *In vitro*-generated neural precursors participate in mammalian brain development. *Proc. Natl. Acad. Sci. USA* 94, 14809-14814 (1997).
- Brustle, O. *et al.* Embryonic stem cell-derived glial precursors: a source of myelinating transplants. *Science* 285, 754-756 (1999).
- Liu, S. *et al.* Embryonic stem cells differentiate into oligodendrocytes and myelinate in culture and after spinal cord transplantation. *Proc. Natl. Acad. Sci. USA* 97, 6126-6131 (2000).
- McDonald, J.W. *et al.* Transplanted embryonic stem cells survive, differentiate and promote recovery in injured rat spinal cord. *Nat. Med.* 5, 1410-1412 (1999).
- Svendsen, C.N. *et al.* A new method for the rapid and long term growth of human neural precursor cells. *J. Neurosci. Methods* 85, 141-152 (1998).
- Uchida, N. *et al.* Direct isolation of human central nervous system stem cells. *Proc. Natl. Acad. Sci. USA* 97, 14720-14725 (2000).
- Flax, J.D. *et al.* Engraftable human neural stem cells respond to developmental cues, replace neurons, and express foreign genes. *Nat. Biotechnol.* 18, 1033-1039 (1998).
- Vescovi, A.L. *et al.* Isolation and cloning of multipotential stem cells from the embryonic human CNS and establishment of transplantable human neural stem cell lines by epigenetic stimulation. *Exp. Neurol.* 156, 71-83 (1999).
- Volpert, L. *et al.* *Principles of development*. (Oxford University Press, New York; 1998).
- Lendhal, U., Zimmerman, L.B. & McKay, R.D.G. CNS stem cells express a new class of intermediate filament protein. *Cell* 60, 585-595 (1990).
- Mujtaba, T. *et al.* Lineage-restricted neural precursors can be isolated from both the mouse neural tube and cultured ES cells. *Dev. Biol.* 214, 113-127 (1999).
- Kilpatrick, T. & Bartlett, P.E. Cloning and growth of multipotential neural precursors: requirements for proliferation and differentiation. *Neuron* 10, 255-265 (1993).
- Niwa, H., Miyazaki, J. & Smith, A.G. Quantitative expression of Oct-3/4 defines differentiation, dedifferentiation or self-renewal of ES cells. *Nat. Genet.* 24, 372-376 (2000).
- Tropepe, V. *et al.* Direct neural fate specification from embryonic stem cells: a primitive mammalian neural stem cell stage acquired through a default mechanism. *Neuron* 30, 65-78 (2001).
- Clarke, D.L. *et al.* Generalized potential of adult neural stem cells. *Science* 288, 1660-1663 (2000).
- Murray, K. & Dubois-Dalq, M. Emergence of oligodendrocytes from human neural spheres. *J. Neurosci. Res.* 50, 146-156 (1997).
- Sommer, I. & Schachner, M. Monoclonal antibodies (O1-O4) to oligodendrocyte cell surface: an immunocytological study in the central nervous system. *Dev. Biol.* 83, 311-327 (1981).
- Dawson, M.R.I., Levine, J.M. & Reynolds, R. NG2 expressing cells in the central nervous system: are they oligodendroglial progenitors. *J. Neurosci. Res.* 61, 471-479 (2000).
- McKay, R. Stem cells in the central nervous system. *Science* 276, 66-70 (1997).
- Goldman, S.A. & Luskin, M.B. Strategies utilized by migrating neurons of the postnatal vertebrate forebrain. *Trends Neurosci.* 21, 107-114 (1998).
- Lee, S.H., Lumelsky, N., Studer, L., Auerbach, J.M. & McKay, R.D. Efficient generation of midbrain and hindbrain neurons from mouse embryonic stem cells. *Nat. Biotechnol.* 18, 675-679 (2000).
- van Eijk, M.J.T. *et al.* Molecular cloning, genetic mapping and developmental expression of bovine POU5F1. *Biol. Reprod.* 60, 1093-1103 (1999).
- Kukekov, V.G. *et al.* Multipotent stem/progenitor cells with similar properties arise from two neurogenic regions of adult human brain. *Exp. Neurol.* 156, 333-344 (1999).
- Shamblo, M.J. *et al.* Human embryonic germ cell derivatives express a broad range of developmentally distinct markers and proliferate extensively *in vitro*. *Proc. Natl. Acad. Sci. USA* 98, 113-118 (2001).

# BRAIN

*A journal of neurology*

Volume 124, Part 11, November 2001



OXFORD  
UNIVERSITY PRESS

BRAIN Online  
<http://www.brain.oupjournals.org>

# Towards the reconstruction of central nervous system white matter using neural precursor cells

Masato Mitome,<sup>1,\*</sup> Hoi Pang Low,<sup>1</sup> Anthony van den Pol,<sup>3</sup> John J. Nunnari,<sup>2</sup> Merrill K. Wolf,<sup>1,2</sup> Susan Billings-Gagliardi<sup>1,2</sup> and William J. Schwartz<sup>1</sup>

Departments of <sup>1</sup>Neurology and <sup>2</sup>Cell Biology, University of Massachusetts Medical School, Worcester and <sup>3</sup>Department of Neurosurgery, Yale University School of Medicine, New Haven, USA

Correspondence to: William J. Schwartz, Department of Neurology, University of Massachusetts Medical School, 55 Lake Avenue North, Worcester, MA 01655, USA  
E-mail: william.schwartz@umassmed.edu

\*Present address: Department of Oral Functional Science, Hokkaido University Graduate School of Dental Medicine, Sapporo, Hokkaido, Japan

## Summary

Epidermal growth factor-responsive neural precursor cells were used as donor cells for transplantation into wild-type and myelin-deficient shiverer (*shi*) mice. The cells engrafted robustly within the CNS following intracerebroventricular and cisternal transplantation in neonatal mice. The cells adopted glial phenotypes, and some functioned as oligodendrocytes, producing myelin

basic protein and morphologically normal internodal myelin sheaths. When individual *shi* mice received two transplants (on post-natal days 1 and 3), donor-derived cells disseminated widely and expressed myelin basic protein in central white matter tracts throughout the brain.

**Keywords:** demyelination; epidermal growth factor; myelin basic protein; oligodendrocyte; shiverer

**Abbreviations:**  $\beta$ -gal =  $\beta$ -galactosidase; BrdU = bromodeoxyuridine; DMEM/F-12 = Dulbecco's modified Eagle's medium and F-12 nutrient; EGF = epidermal growth factor; GFAP = glial fibrillary acidic protein; GFP = green fluorescent protein; P = post-natal day; MBP = myelin basic protein; *md* = myelin-deficient; *shi* = shiverer; PBS = phosphate-buffered saline; TBS = Tris-buffered saline, pH 7.6; CNPase = 2',3'-cyclic nucleotide 3'-phosphodiesterase

## Introduction

Oligodendrocytes are specialized cells in the CNS that synthesize myelin, the insulating sheath around axons that increases the speed and efficiency of impulse conduction. Disorders that injure or kill oligodendrocytes or affect myelination (multiple sclerosis, trauma and inherited leukodystrophies) lead to devastating neurological illness. An emerging therapeutic strategy for these conditions is to provide the CNS with new, healthy myelinating cells by transplantation, and studies in animal models suggest that myelin might be repaired using this approach (for reviews, see Blakemore and Franklin, 1991; Duncan *et al.*, 1997).

Initial work has suggested that transplanted cells survive, migrate and remyelinate more extensively if they are relatively less well differentiated than the mature oligodendroglial phenotype (Rosenbluth *et al.*, 1990; Gansmüller *et al.*, 1991; Warrington *et al.*, 1993; Archer *et al.*, 1997). Purified populations of bipotential glial progenitors have been expanded in culture and transplanted directly into the brains of shiverer (*shi*) mutant mice (Warrington *et al.*, 1992)

and the spinal cords of myelin-deficient (*md*) mutant and X-irradiated, ethidium bromide-lesioned rats (Groves *et al.*, 1993; Tontsch *et al.*, 1994; Franklin and Blakemore, 1995). Extensive myelination has been reported, but such cells may not have the capacity to survive or migrate through normal CNS tissue (Franklin *et al.*, 1996; Gensert and Goldman, 1997).

Recently, attention has turned to transplanting even less committed, primitive precursor ('stem') cells with increased mitotic and migratory capabilities (for reviews, see Alvarez-Buylla and Temple, 1998; Isacson, 1999; Armstrong and Svendsen, 2000). The potential for these cells to engraft and become functional oligodendrocytes has been demonstrated using a multipotent, immortalized stem-like cell line (Yandava *et al.*, 1999) and totipotent embryonic stem cells (Brüstle *et al.*, 1999; Liu *et al.*, 2000). However, the presence of viral oncogenes and the risk of intraventricular teratomas (Brüstle *et al.*, 1997) have stimulated the continued search for other transplantable cell types.

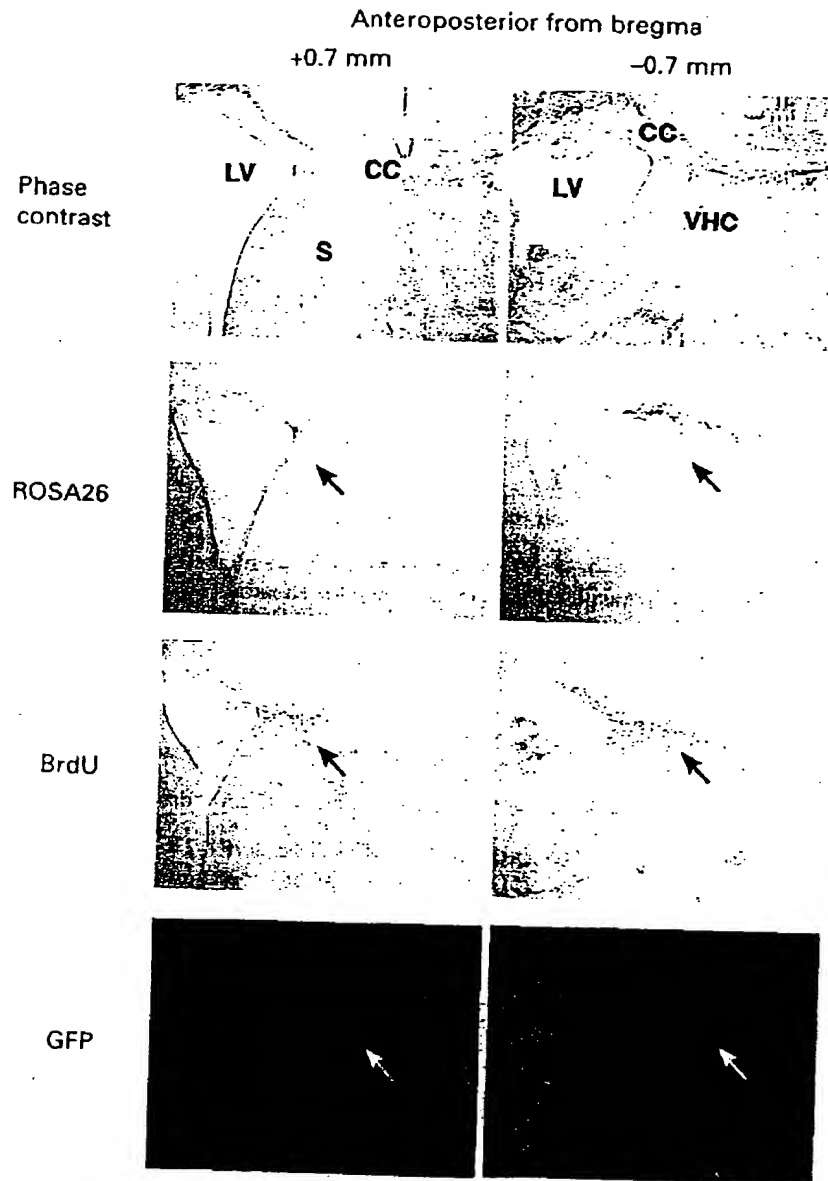


**Fig. 1** EGF-responsive neural precursors engraft in central white matter tracts. Coronal brain sections processed 2 weeks after injection of precursor cells into the lateral cerebral ventricle of neonatal mice. Cells were found in the corpus callosum and ventral hippocampal commissure, irrespective of their origin or labelling (ROSA26  $\beta$ -gal, ROSA26 pre-incubated with BrdU, or GFP). Arrows represent engrafted cells identified by X-gal histochemistry (blue, ROSA26), BrdU immunocytochemistry (brown, BrdU) or fluorescence (green, GFP). CC = corpus callosum; LV = lateral ventricle; S = lateral septum; VHC = ventral hippocampal commissure. Scale bar = 500  $\mu$ m.

An interesting candidate is the epigenetically propagated neural precursor cell derived from the striatal subventricular zone. When such cells are cultured in a chemically defined, serum-free medium with epidermal growth factor (EGF), they proliferate as cellular clusters floating in the medium ('neurospheres'). Clonal analyses indicate that such cells can

individually generate neurones, astrocytes and oligodendrocytes *in vitro* (Reynolds and Weiss, 1996; Gritti *et al.*, 1999). The subventricular zone is the source of endogenous precursors that can repair myelin damage *in vivo* (Gensert and Goldman, 1997; Nait-Oumesmar *et al.*, 1999). Donor-derived myelin has been observed after such cells are



propagated in culture with EGF and transplanted into the spinal cords of *md* rat and shaking pup, a myelin-deficient mutant dog (Hammang *et al.*, 1997; Milward *et al.*, 1997), and the retinas of young mice (Ader *et al.*, 2000); with basic fibroblast growth factor and transplanted into the spinal cords of X-irradiated ethidium bromide-lesioned rats (Keirstead *et al.*, 1999); and with neuroblastoma-conditioned medium and transplanted into the brains of *shi* mice (Avellana-Adalid *et al.*, 1996; Vitry *et al.*, 1999) and the embryonic telencephalic ventricles (Learish *et al.*, 1999) and post-natal spinal cords (Zhang *et al.*, 1998, 1999) of *md* rats. Human neural precursors can differentiate into oligodendrocytes after they are isolated, propagated and transplanted into the brains of mice and rats (Brüstle *et al.*, 1998; Flax *et al.*, 1998), raising the exciting possibility that such cells might eventually become an adaptable and potentially unlimited resource for clinical neurotransplantation.

Here we report the results of our studies using genetically marked, EGF-responsive neural precursors as donor cells for transplantation into wild-type and myelin-deficient *shi* mice. Since clinical disorders of myelination are multifocal and/or generalized, we injected our cells into the cerebral ventricles and/or cisternae to disseminate them as widely as possible; and since myelination occurs post-natally (for a review, see Lee *et al.*, 2000), we targeted our transplants to the brains of neonates. When individual *shi* mice received two such transplants [on post-natal days (P) 1 and 3], it was possible to demonstrate widely disseminated engraftment of cells that began to myelinate central white matter tracts throughout the brain.

## Methods

Methods for animal husbandry, surgery and sacrifice in our experiments were approved by the University of Massachusetts Institutional Animal Care and Use Committee.

## Animals

The *shi* mutation is maintained on a B6C3F1 hybrid-based stock, which at this time is >99.9% congenic at other loci. C57BL/6J females and C3H/H3J males (Jackson Laboratory, Bar Harbor, Me., USA) are intercrossed in our colony to generate B6C3F1 hybrids for breeding mutant mice. The *shi* colony is maintained by intercrossing *shi*/+ males and females, and recovering homozygous *shi* offspring. Twice a year, homozygous *shi* males are outcrossed to B6C3F1 wild-

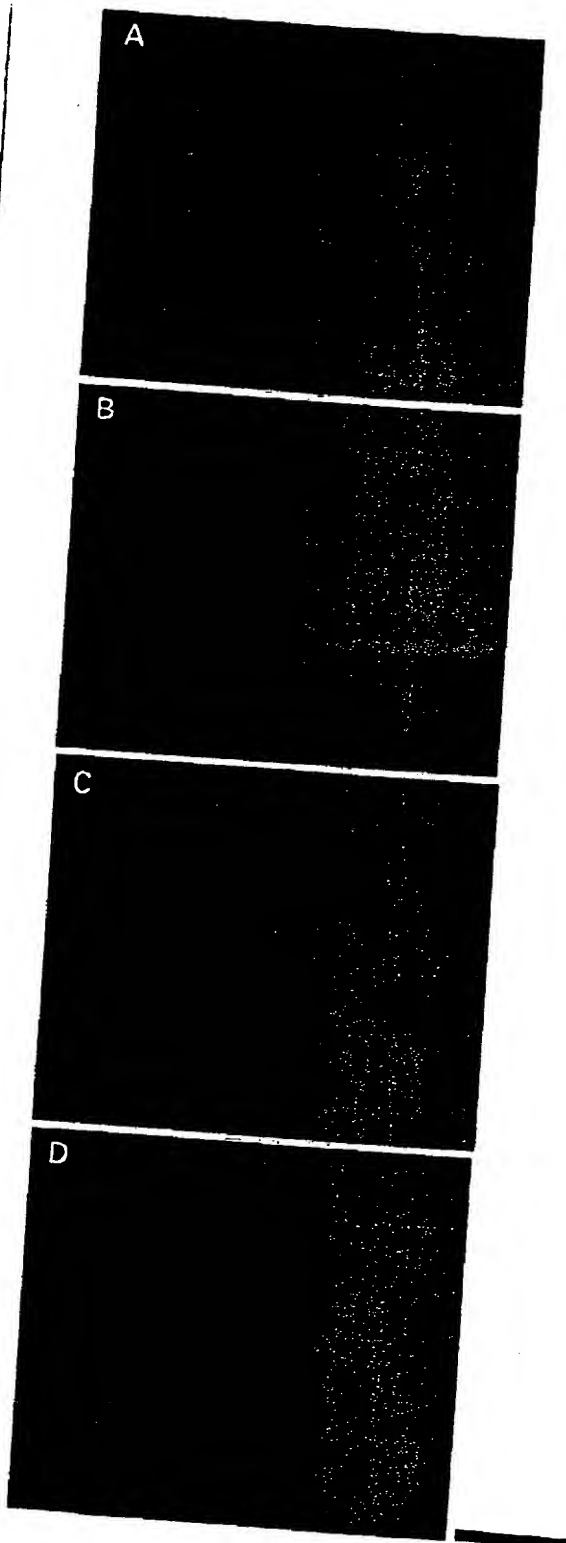


**Fig. 2** Engraftment persists long term. Coronal brain sections processed 8 weeks after injection of GFP-labelled precursor cells into the lateral cerebral ventricle of neonatal mice. Engrafted GFP<sup>+</sup> cells were found in corpus callosum (A), ventral hippocampal commissure (B), polymorph and molecular layers of the hippocampal dentate gyrus (C) and the subependymal layer of the olfactory bulb (D). Scale bar = 500  $\mu$ m.

2150 M. Mitome et al.

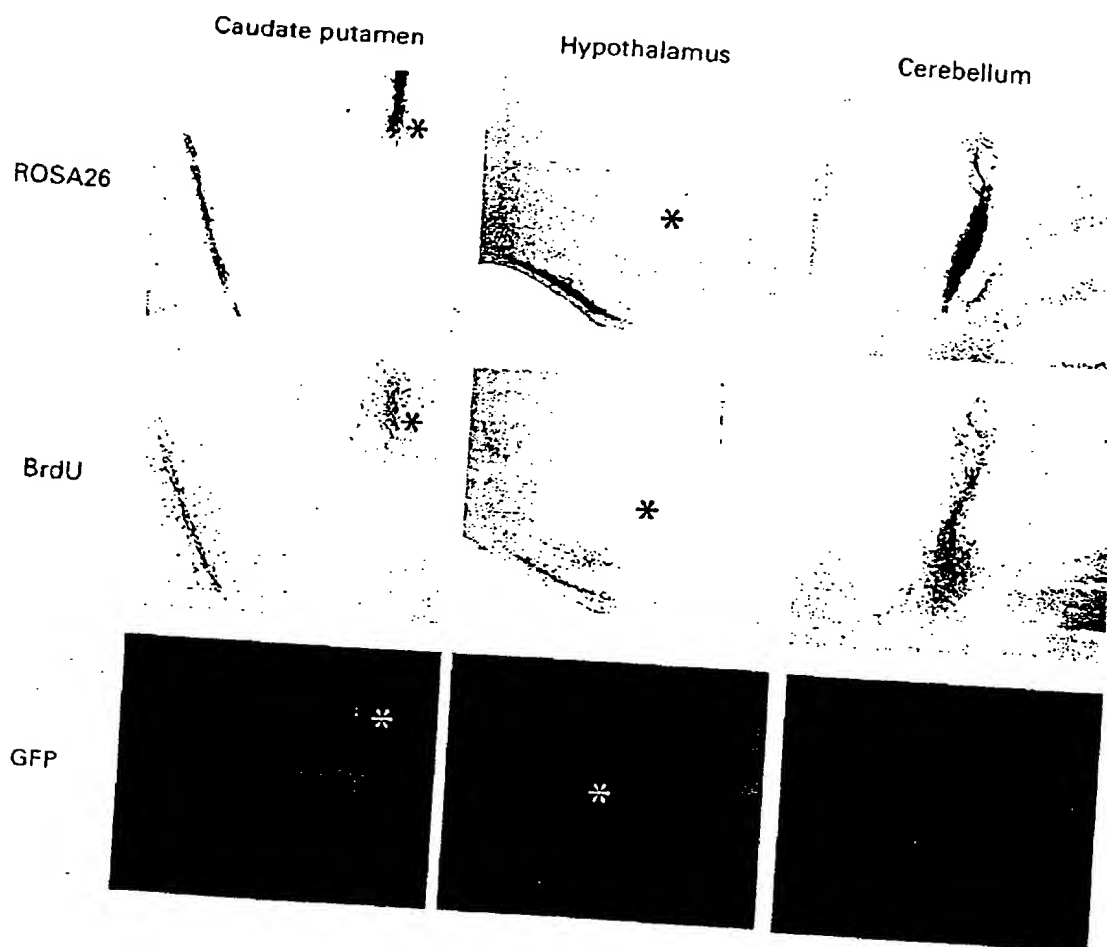


Fig. 3 EGF-responsive neural precursors engraft in regional white matter tracts. Coronal brain sections processed 2 weeks after injection of precursor cells into the caudate/putamen, anterior hypothalamus or cerebellar hemisphere of adult mice. Cells were found in neighbouring white matter tracts (lateral portion of corpus callosum, optic chiasm or cerebellar white matter, respectively) irrespective of their origin or labelling (ROSA26  $\beta$ -gal, ROSA26 pre-incubated with BrdU, or GFP). Asterisks represent injection site of engrafted cells labelled by X-gal histochemistry (blue, ROSA26), BrdU immunocytochemistry (brown, BrdU) or fluorescence (green, GFP). Scale bar = 500  $\mu$ m.

type females to produce the *shi*<sup>+</sup> breeders for the next generation. To produce homozygous *shi* mice, known homozygous *shi* males and females that have been identified by their pronounced tremor and ataxia are intercrossed. For transplant hosts, inbred male B6129F2/J and CD1 mice were obtained from Jackson Laboratory, and B6C3F1 wild-type and mutant mice were used from our colony.

### Cell culture

Donor cells were derived from E16 (where E1 = the day after overnight mating) striatum/subventricular zone tissue microdissected from embryonic B6.129-TgR(ROSA26)26S or transgenic mice (Jackson Laboratory) made by promoter trap insertion of a  $\beta$ -galactosidase ( $\beta$ -gal) reporter gene (Zambrowicz *et al.*, 1997) and transgenic mice expressing

an enhanced form of the jellyfish green fluorescent protein (GFP) under the control of the mouse prion promoter (Borchelt *et al.*, 1996; van den Pol and Ghosh, 2000) and a chicken  $\beta$ -actin-CMV (cytomegalovirus) immediate early enhancer (Niwa *et al.*, 1991; Ikawa *et al.*, 1995). Cells were isolated and propagated using a modification (Hulspas *et al.*, 1997) of the method developed by Reynolds, Weiss and associates (Reynolds and Weiss, 1992; Reynolds *et al.*, 1992). Tissue was placed in a 1 : 1 mixture of Dulbecco's modified Eagle's medium and F-12 nutrient (DMEM/F-12; Gibco-BRL, Gaithersburg, Md., USA) supplemented with 0.3% glucose, 23  $\mu$ g/ml insulin, 92  $\mu$ g/ml transferrin, 55  $\mu$ M putrescine, 27.5 nM sodium selenite, 50 U/ml penicillin-streptomycin, 20 nM progesterone and 20 ng/ml EGF (Becton Dickinson/Collaborative Biomedical Products, Bedford, Mass., USA). Tissue was triturated with a wet fire-

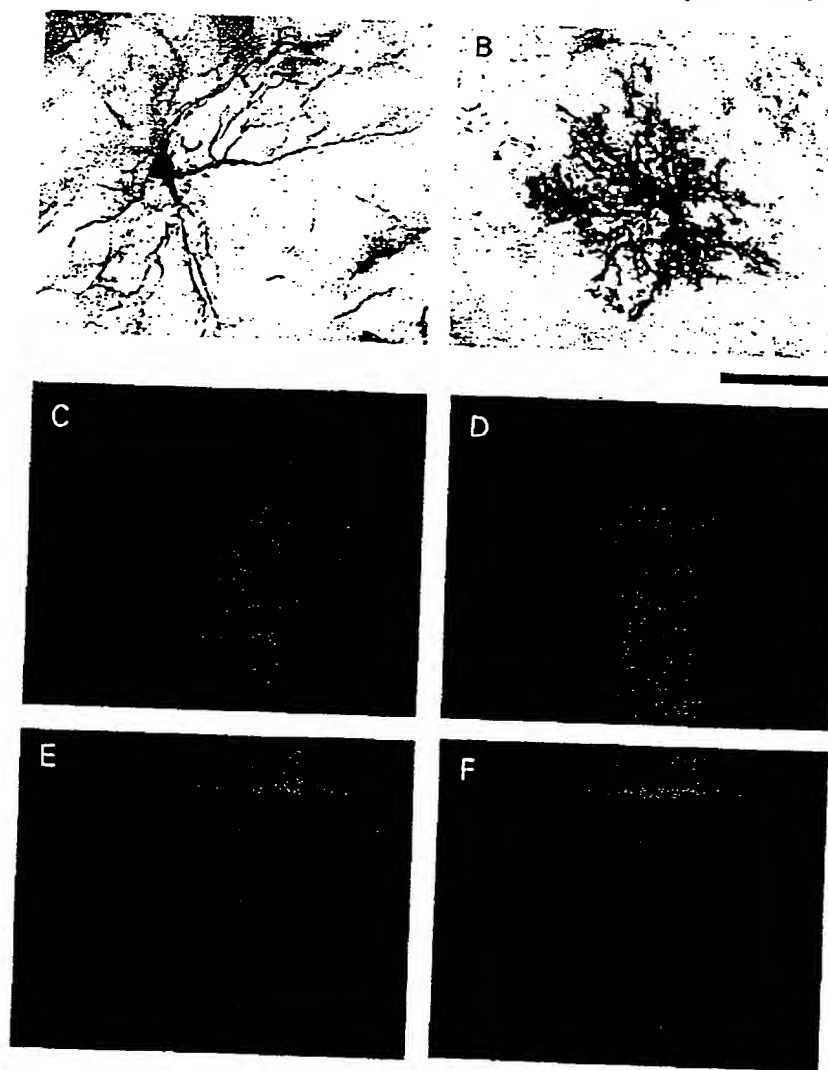


Fig. 4 Engrafted precursors give rise to astrocytes and oligodendrocytes. GFP immunocytochemistry revealed donor-derived cell morphologies characteristic of fibrillary (A) and protoplasmic (B) astrocytes. Confocal microscopy demonstrated engrafted GFP<sup>+</sup> cells (green in C and E) that were also immunopositive for either GFAP or CNPase (red in D and F, respectively). Scale bars = 30  $\mu$ m (A and B) and 20  $\mu$ m (C-F).

polished Pasteur pipette to obtain a 'single cell' suspension, and the cells were seeded at a density of  $1.5 \times 10^6$  viable cells/20 ml in 75-cm<sup>2</sup> flasks and maintained in a humidified incubator at 37°C and 95% atmospheric air/5% CO<sub>2</sub>. Cultures were fed with 5 ml of fresh medium every other day and passaged weekly. For transplantation, cells (passage number <5) were harvested, triturated to a 'single cell' suspension and the density adjusted to  $6 \times 10^4$  or  $1 \times 10^5$  viable cells/ $\mu$ l in 1 $\times$  DMEM/F-12. Some cells derived from ROSA26 mice were also treated with 1  $\mu$ M bromodeoxyuridine (BrdU) for 12 h before they were harvested for transplantation.

### Transplant surgery

Neonatal host mice ranging in age from post-natal day P1 to P3 (where P1 = the day of birth) were cryoanaesthetized and injected with 120 000 cells/2  $\mu$ l in either of the lateral cerebral ventricles or cisterna magna, or 60 000 cells/1  $\mu$ l into each lateral cerebral ventricle and 120 000 cells/2  $\mu$ l into the cisterna magna. The cellular suspension was expelled gently via a glass micropipette inserted transcutaneously into the desired location with the aid of a stereotaxic apparatus.

For transplants in older (>6-week-old) hosts, mice were anaesthetized with a solution of 25 mg/ml ketamine and 5 mg/ml xylazine (50  $\mu$ l/10 g i.p.) and fixed in a stereotaxic

2152 M. Mitome et al.

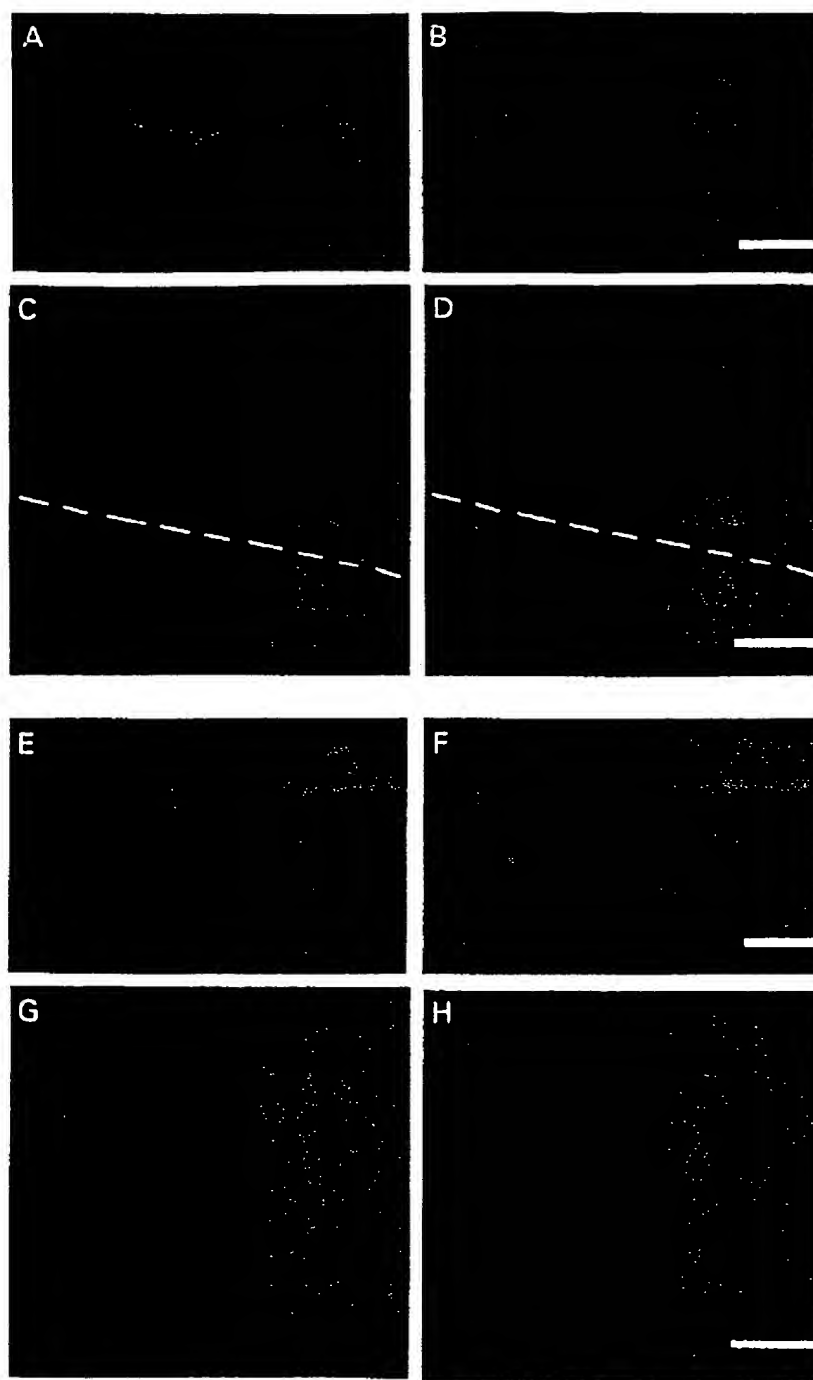


Fig. 5 Donor-derived oligodendrocytes express immunoreactive MBP in *shi* mutant mice. Coronal brain sections processed 8 weeks after injection of GFP-labelled precursor cells into the lateral cerebral ventricle of neonatal *shi* mutant mice. Confocal microscopy demonstrated engrafted GFP<sup>+</sup> cells in corpus callosum (green in A and C) and ventral hippocampal commissure (green in E and G) that also stained for immunoreactive MBP (red in B, D, F and H). The dotted white line (C and D) represents the inferior boundary of the corpus callosum; the green cells beyond the confines of the corpus callosum are not stained for MBP. Scale bars = 500  $\mu$ m (A, B, E and F) and 50  $\mu$ m (C, D, G and H).

apparatus. A 5-mm incision was made in the scalp to expose the dorsal aspect of the parietal bones, a hole was drilled with a dental burr and a suspension of 200 000 cells/2 µl was injected slowly over 5 min using a 10 µl Hamilton syringe according to the following coordinates: caudate/putamen [AP (anteroposterior) = 0.7, L (lateral) = 2.3, V (vertical) = -3.0], anterior hypothalamus (AP = 0.4, L = 0.3, V = -5.5) and cerebellum (AP = -6.0, L = 0.1, V = -1.5). Vertical coordinates were from dura, and all distances were in millimetres. The skin incision was apposed using Hemoclips.

### Light microscopy

Mice were deeply anaesthetized with sodium pentobarbital (10 mg i.p.) and perfused with ice-cold heparinized phosphate-buffered saline (PBS), followed by ice-cold 4% buffered paraformaldehyde fixative. Tissue was post-fixed for 2–5 h at 4°C, and 50 µm thick coronal sections were cut on a vibratome and stored at -20°C in cryoprotectant (30% sucrose, 30% ethylene glycol, 0.25 mM polyvinylpyrrolidone in PBS).

For X-gal histochemistry, free-floating sections were rinsed in PBS and incubated in a solution of 5 mM potassium ferricyanide, 5 mM potassium ferrocyanide, 2 mM magnesium chloride, 0.01% deoxycholic acid, 0.02% Nonidet P-40 and 1 mg/ml X-gal (Gold Biotechnology, St Louis, Mo., USA) overnight at 37°C. After rinsing in PBS and mounting on slides, the sections were counterstained with Nuclear Fast Red (Vector Laboratories, Burlingame, Calif., USA), rinsed in water, dehydrated, cleared and coverslipped in Permount.

For BrdU immunocytochemistry, free-floating sections were first washed in 0.05 M Tris-buffered saline (TBS), pH 7.6, followed by incubation in 0.5% hydrogen peroxide for 20 min and then 2 N hydrochloric acid for 20 min at 37°C. Sections were rinsed in TBS, transferred into blocking solution (5% bovine serum albumin, 0.1% Triton X-100 in TBS) for 30 min followed by anti-BrdU antibodies (0.2 µg/ml; Boehringer Mannheim, Indianapolis, Ind., USA) in 1% bovine serum albumin, 0.1% Triton X-100 in TBS overnight at room temperature. After rinsing in TBS, sections were incubated in horse anti-mouse biotinylated secondary antibodies (1 : 200 dilution in 1% bovine serum albumin, 0.1% Triton X-100 in TBS; Vector Laboratories) for 1–1.5 h at room temperature, followed by avidin-biotin-peroxidase complex (Vector Laboratories) with diaminobenzidine as the chromogen.

For co-localization studies with GFP, free-floating sections were rinsed and blocked with 10% normal goat serum and 0.4% Triton X-100 in TBS for 30 min to 1 h followed by incubation with the appropriate primary antibody for 1 h at room temperature. Primary antibodies were directed against GFP (rabbit, 1 : 500 = 0.2 µg/ml; Clontech, Palo Alto, Calif., USA), glial fibrillary acidic protein (GFAP) (rabbit, 1 : 500 = 25.6 µg/ml; Sigma), 2',3'-cyclic nucleotide 3'-

phosphodiesterase (CNPase) (mouse, 1 : 500; Sternberger Monoclonals, Lutherville, Md., USA) or myelin basic protein (MBP) (mouse, 1 : 1000 = 1 µg/ml; Sternberger Monoclonals). All antibody dilutions were made in 2% normal goat serum and 0.4% Triton X-100 in TBS. After washing, the sections were incubated in the appropriate Alexa Fluor 594 secondary antibodies (Molecular Probes, Eugene, Oreg., USA) for 1 h at room temperature in darkness and coverslipped in Prolong anti-fade reagent (Molecular Probes). Slides were examined using a Leica True Confocal Scanning Spectrophotometer microscope, with excitation wavelengths for GFP and Alexa Fluor 594 of 488 and 568 nm, respectively.

### Electron microscopy

Tissues from transplanted mutant and control mice were prepared for embedding following deep anaesthesia and intracardiac perfusion with 2% paraformaldehyde and 1% glutaraldehyde in 0.1 M phosphate buffer pH 7.4. Dissected blocks of brain and spinal cord were placed in a buffered solution containing 4% paraformaldehyde and 2% glutaraldehyde overnight. The tissue blocks and slices were post-fixed in 1% osmium tetroxide for 1–2 h, dehydrated in a graded series of ethanols, dissected further if needed, oriented appropriately and embedded in LX-112 resin. Sections 1–2 µm thick were stained with toluidine blue and examined by light microscopy in order to select regions for electron microscopic study.

### Results

Donor precursor cells for transplantation were derived from embryonic striatum/subventricular zone tissue that was dissociated and cultured in a serum-free medium with EGF. As the source of our foetal tissue, we used two strains of transgenic mice: one with a β-gal reporter that is expressed in all tissues at all stages of development and after birth (ROSA26), and the other with an enhanced form of GFP that is expressed strongly and stably in all neurones and glia of the CNS, labelling their cell bodies and processes to the terminals. Some of the ROSA26 cultures were also incubated with BrdU for 12 h prior to transplantation. Precursor cells were injected (120 000 cells/2 µl of medium without EGF) into the lateral cerebral ventricle of neonatal (P1–P3) mice, and tissue sections were examined for donor-derived cells using X-gal histochemistry, BrdU or GFP immunocytochemistry, or GFP fluorescence.

### EGF-responsive neural precursors engraft in central white matter tracts

When mice were killed 2 weeks after transplantation, labelled cells were observed as isolated clumps in the host brains. In all cases, small collections of cells were found within the corpus callosum, especially bordering the ventricular injection

2154 M. Mitome et al.

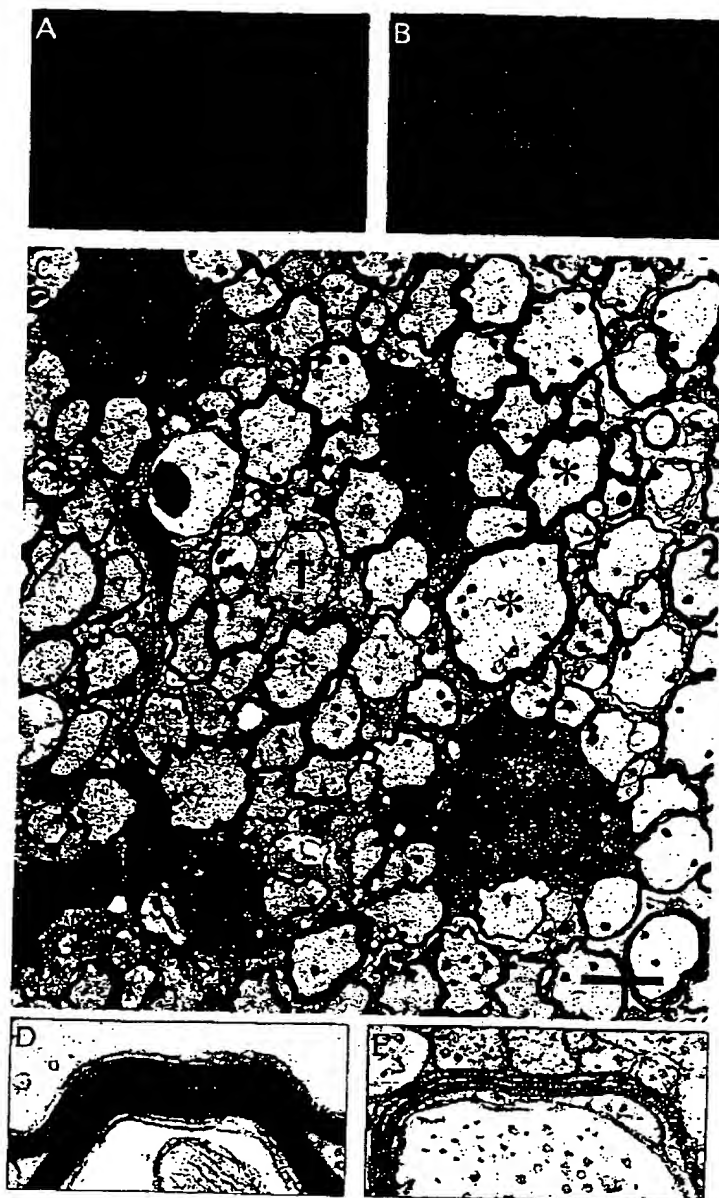


**Fig. 6** Donor-derived oligodendrocytes form normal myelin sheaths in *shi* mutant mice. Coronal spinal cord sections processed 12 weeks after injection of GFP-labelled precursor cells into the cisterna magna of neonatal *shi* mutant mice. Fluorescence microscopy demonstrated engrafted GFP<sup>+</sup> cells in the dorsal funiculus of the cervical spinal cord (green in A) that also stained for immunoreactive MBP (red in B). Ultrastructural analysis revealed some axons surrounded by abnormal myelin sheaths typical of age-matched non-transplanted *shi* (†, like E), but many more axons were completely enclosed by normally compacted myelin sheaths indistinguishable from wild-type (\*, like D). Scale bars = 500  $\mu$ m (A and B), 2  $\mu$ m (C) and 0.2  $\mu$ m (D and E).

site at the level of the lateral septum, but also more caudally within the corpus callosum at the levels of the ventral hippocampal commissure (also known as the commissure of the ventral fornix) and anterior hippocampus. Cells also engrafted reliably within the ventral hippocampal commissure itself, while they were variably observed lining the hippo-

campal alveus, fimbria and fissure. The distribution and number of implants were similar whether the donor cells were labelled for  $\beta$ -gal, BrdU or GFP (Fig. 1); and whether B6129F2/J, B6C3F1 or CD1 host strains were used. The overall transplant success rate for animals killed at 2 weeks was 78% (36 of 46 mice).

Eight weeks after transplantation, donor-derived cells were again located within the corpus callosum and ventral hippocampal commissure in all cases, but their numbers had clearly expanded to fill large, up to 1 mm long, segments of periventricular white matter (Fig. 2A and B). In some of the animals transplanted on P3, labelled cells were also seen in hippocampus (Fig. 2C), especially within the hilus and polymorph and molecular layers of the dentate gyrus. At least a few of these labelled hippocampal cells were found in 75% (15 out of 20) of mice examined at 8 weeks. Engraftment within the subependymal layer of the olfactory bulb was also observed in 8-week-old animals (Fig. 2D), but the overall success rate was only 35% (six out of 17 mice).

In a limited group of mice, 120 000 cells/2  $\mu$ l were injected into the cisterna magna rather than into the lateral cerebral ventricle. Eight weeks after transplantation, isolated groups of donor-derived cells were located in regions that included deep and hemispheric cerebellar white matter, lateral ascending sensory and pyramidal tracts of the brainstem, inferior colliculus and dorsal cervical spinal cord. The overall transplant success rate for posterior fossa structures in these animals was 45% (five out of 11 mice).

We also stereotactically implanted precursor cells (200 000 cells/2  $\mu$ l) directly into the unilateral caudate/putamen, anterior hypothalamus or cerebellar hemisphere of adult mice. Two weeks after transplantation, labelled cells in all three locations had survived preferentially within and/or migrated to neighbouring white matter tracts (Fig. 3). Transplant success rates were 78% (seven out of nine mice), 58% (seven out of 12 mice) and 88% (14 out of 16 mice) in caudate/putamen, hypothalamus and cerebellum, respectively.

No labelled cells were found in any of the brains of eight host mice transplanted with cells that had been killed in culture before their implantation, either by microwave fixation or by repeated cycles of freezing and thawing.

### *Engrafted precursors give rise to astrocytes and oligodendrocytes*

The distinctive localization of donor-derived cells around and within white matter tracts suggested that they might be assuming a glial phenotype, and immunocytochemical analysis was consistent with this cell type assignment. The morphology of GFP-labelled cells was revealed using fluorescence or with a polyclonal antibody directed against the protein; they included clear examples of fibrillary astrocytes within the corpus callosum and ventral hippocampal commissure (Fig. 4A) and protoplasmic astrocytes within adjacent grey matter (Fig. 4B). Individual GFP-labelled cells also co-expressed immunoreactive GFAP, an intermediate filament protein of astroglia (Fig. 4C and D). Other cells were identified as oligodendrocytes by labelling with a monoclonal antibody directed against CNPase, an enzymatic component of myelin membrane (Vogel and Thompson, 1988) (Fig. 4E and F).

We found no labelled cells in hippocampus or olfactory bulb that appeared to be clearly neuronal, and none co-expressed NeuN, a nuclear marker of terminally differentiated neurones within these regions (Mullen *et al.*, 1992).

### *Donor-derived oligodendrocytes produce MBP and form wild-type myelin sheaths around shi axons*

In order to determine if donor-derived oligodendrocytes were functionally active, we injected GFP-labelled precursor cells into the lateral cerebral ventricle of neonatal *shi* mutant hosts. The *shi* mutation is a large deletion in the MBP gene (Roach *et al.*, 1985), and homozygous mutants fail to produce the protein (a major structural component of the mature myelin sheath), leading to extensive dysmyelination with morphologically abnormal myelin sheaths (Privat *et al.*, 1979; Rosenbluth, 1980; Inoue *et al.*, 1981). These mice exhibit severe tremor, hindlimb ataxia, late-onset tonic seizures and a shortened lifespan. When such mice were killed 8 weeks after transplantation, the pattern of GFP-labelled cellular engraftment was similar to that seen in wild-type hosts, and the transplant success rate was 86% (six out of seven mice). Donor-derived, immunoreactive MBP was expressed in these transplanted mice. As shown for the corpus callosum (Fig. 5A and B) and ventral hippocampal commissure (Fig. 5E and F), the distribution of GFP fluorescence and MBP immunoreactivity was concordant. In some instances, MBP-positive processes were aligned as a bundle oriented parallel to the longitudinal axis of these commissures (Fig. 5G and H). No MBP labelling was present in tissue sections from which primary antibody was omitted, in non-transplanted *shi* mutants or in GFP-labelled cells lying just adjacent to myelinated white matter tracts (Fig. 5C and D).

To ascertain if donor-derived MBP expression was associated with normal myelin production, we stained plastic-embedded tissue sections from transplanted *shi* hosts with toluidine blue and chose heavily myelinated regions of the corpus callosum, pyramidal tracts (brainstem) and fasciculus gracilis/cuneatus (cervical spinal cord) for ultrastructural study. Most of the selected areas contained axons surrounded by abnormal myelin sheaths typical of age-matched non-transplanted *shi* (loosely wrapped or only partially compacted membranes), but also axons completely enclosed by normally compacted sheaths showing major dense lines throughout (morphologically indistinguishable from age-matched wild-type mice) (Fig. 6).

In several different samples, we counted areas (8650  $\mu$ m<sup>2</sup>) in which 75–80% of all myelinated axons had sheaths with unmistakably wild-type morphology, and in which virtually no larger calibre axons were unmyelinated. These myelin sheaths appeared generally thinner than in age-matched wild-type, and the usual relationship between axon diameter and sheath thickness was not strictly maintained. Axons enclosed by donor-derived and *shi* myelin sheaths were



2156 M. Mirome et al.

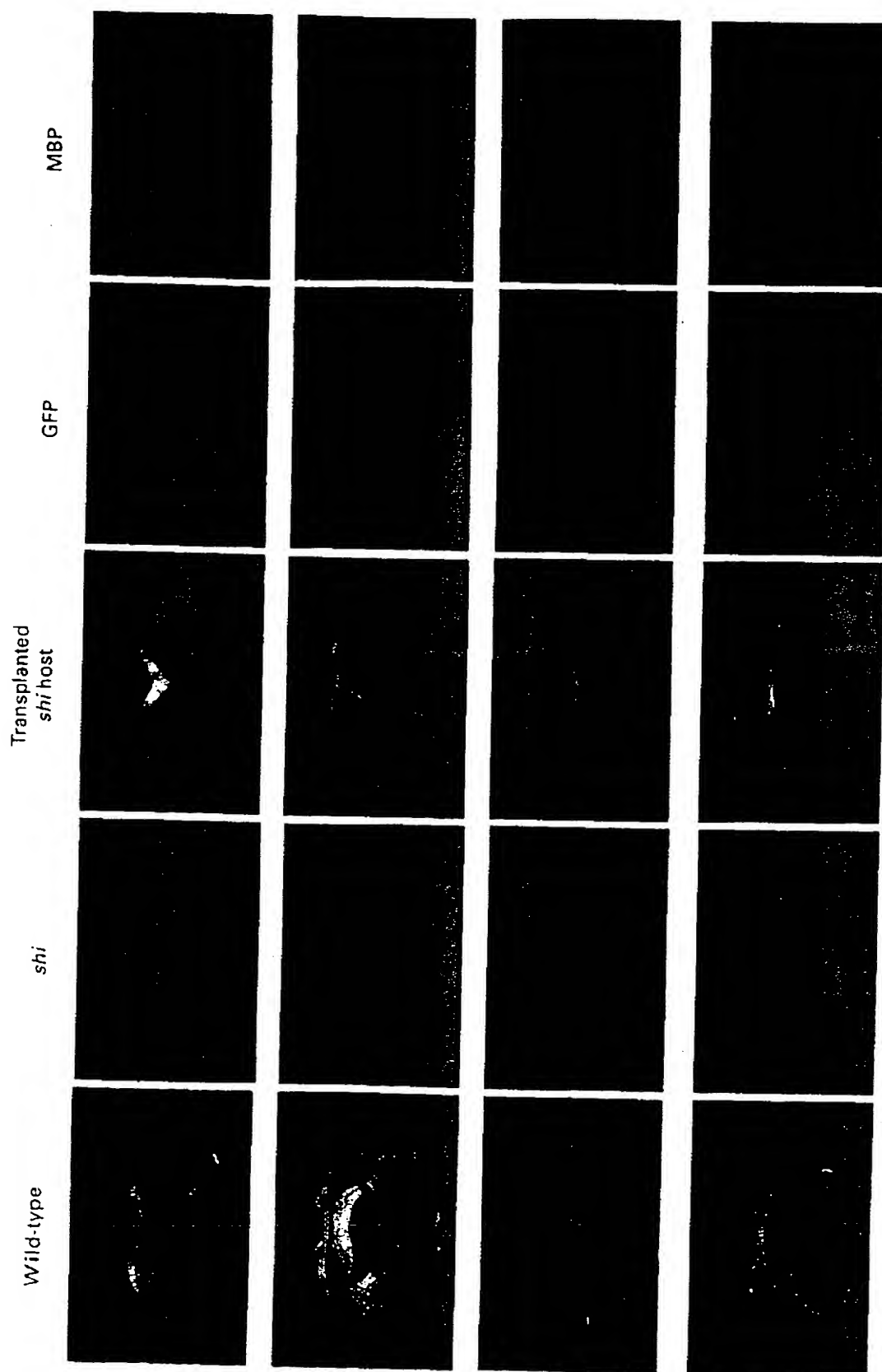


Fig. 7 Donor-derived cells begin to reconstitute central white matter in *shi* mutant mice. Coronal brain sections processed 12 weeks after two injections of GFP-labelled precursor cells into the lateral cerebral ventricle and cisterna magna of a neonatal *shi* mutant mouse. Transillumination of unstained cut tissue sections permits comparison of the distribution of central white matter in a wild-type and a non-transplanted *shi* mutant mouse with that in the transplanted *shi* mutant mouse. GFP<sup>+</sup> cells (green) and MBP immunoreactivity (red) mapped to these sites throughout the brain. Scale bar = 5 mm.

interspersed, and small bundles of microprocesses (characteristic of *shi* oligodendrocytes) often coursed near normal appearing sheaths, suggesting that donor-derived and host oligodendrocytes were intermingled within the white matter. Detailed examination of light and electron micrographs revealed no indications of myelin degeneration, inflammation or gliosis in white matter.

### ***Towards the reconstitution of CNS white matter tracts***

To increase the number and possible dispersion of transplanted cells in *shi* hosts, we designed a staged surgical protocol in which 60 000 cells/1  $\mu$ l were injected into each lateral cerebral ventricle and 120 000 cells/2  $\mu$ l were injected into the cisterna magna on P1, after which this procedure was repeated on P3. In some cases, a 5  $\mu$ l cell suspension was injected into the cisterna magna after a similar volume of CSF was removed from this compartment via a glass micropipette. When such mice were killed 8–12 weeks after transplantation, partially reconstituted white matter tracts were visible to the naked eye in unstained vibratome-cut tissue sections (Fig. 7). GFP-labelled cells and MBP immunoreactivity mapped to these tracts throughout the brain, forming morphologically normal myelin sheaths (Fig. 8). The success rate for such widely disseminated cellular engraftment with MBP production was 100% (10 out of 10 mice). As observed previously (see Fig. 5C and D), where donor-derived cells engrafted outside myelinated white matter tracts, they appeared to adopt an astrocytic phenotype without MBP labelling (Fig. 8).

### **Discussion**

Our data indicate that EGF-responsive neural precursor cells can engraft robustly within the CNS following intracerebroventricular and cisternal transplantation in neonatal mice. The cells adopted glial phenotypes, and some functioned as oligodendrocytes, producing MBP and morphologically normal internodal myelin sheaths. Donor-derived cells appeared to disseminate widely and expressed a predilection for central white matter tracts.

Robust transplant-derived myelination has been demonstrated previously in *shi* mutant mice, although not the widespread distribution seen in Fig. 7. Our particular results might be related to the cell type(s) transplanted as well as the route and timing of administration. In early reports employing *shi* mutants, transplants consisted of solid tissue fragments (Gumpel *et al.*, 1983; Gout *et al.*, 1988; Gansmüller *et al.*, 1991) or mature oligodendrocytes (Kohsaka *et al.*, 1986; Lubetzki *et al.*, 1988) deposited locally within brain or spinal cord; preferential migration of transplanted oligodendrocytes along white matter tracts has been observed after such injections (Lachapelle *et al.*, 1994). More recent studies using various precursor cell populations as donors

have also transplanted the cells as single focal tissue injections (Warrington *et al.*, 1992, 1993; Avellana-Adalid *et al.*, 1996; Vitry *et al.*, 1999; Liu *et al.*, 2000). We are aware of only two previous reports utilizing an intracerebroventricular approach in *shi* mutants. Friedman and colleagues transplanted embryonic cortical tissue fragments into the lateral ventricle of 1-month-old *shi* mice and showed that MBP staining often crossed to the contralateral hemisphere via the corpus callosum at the level of the implant (Friedman *et al.*, 1986). Yandava and colleagues transplanted a neural stem-like cell line into the cerebral ventricles of newborn *shi* mice; the donor cells engrafted extensively but non-selectively within both grey and white matter structures, expressing MBP and making normal-appearing myelin (Yandava *et al.*, 1999). Other workers have employed intracerebroventricular injections of precursor cells in *md* rats (Brüstle *et al.*, 1999; Learish *et al.*, 1999); but these injections were on embryonic day 17, before the expected peak of post-natal myelinogenesis, and there was no preferential migration of donor cells into white matter tracts. We are unaware of any previous reports that have tested more than one transplant injection per animal.

We do not yet understand the proclivity of EGF-responsive precursor cells for colonizing central white matter tracts. It is not known if the critical cells in these transplants are uncommitted stem cells that respond and differentiate according to local environmental cues or, alternatively, if they are lineage-restricted oligodendroglial progenitors that already exist in the cultures. In contrast to the multipotentiality of EGF-responsive 'neurosphere' cells *in vitro*, the *in vivo* differentiation of such cells after transplantation appears to be predominantly glial (Svendsen *et al.*, 1996, 1997; Carpenter *et al.*, 1997; Winkler *et al.*, 1998), even in an environment (e.g. foetal brain) that would be conducive to neurogenesis (Winkler *et al.*, 1998; Mitome *et al.*, 2001). This *in vivo* fate appears different from that of transplanted hippocampal precursor cells expanded *in vitro* with basic fibroblast growth factor, which can give rise to putative neurones in hippocampal dentate gyrus, olfactory bulb and retina (Gage *et al.*, 1995; Suhonen *et al.*, 1996; Takahashi *et al.*, 1998).

Our ultrastructural observations indicate that donor- and host-derived myelin were closely intermixed in transplanted brains. Abnormal *shi* oligodendrocytes were present even in areas with abundant donor myelin, as demonstrated by bundles of abnormal *shi* oligodendrocyte microprocesses and by the relatively consistent proportion (at least 10%) of axons surrounded by myelin with *shi* morphology. There always seemed to be some background level of host myelin, and we have not found areas in which all myelin sheaths were donor derived.

Notably, none of our transplanted *shi* mice showed any obvious qualitative improvement in their abnormal behavioural phenotype, although behavioural testing was not an aim of our study. The origin of the motor deficits in *shi* mice is not known for certain, although the absence of

2158 M. Mitome et al.



**Fig. 8** Donor-derived glia, immunoreactive MBP and normal myelin sheaths are found after multiple precursor cell injections in *shi* mutant mice. Sections of corpus callosum processed 10 weeks after multiple injections of GFP-labelled precursor cells into neonatal *shi* mutant mice. Fluorescence microscopy demonstrated engrafted GFP<sup>+</sup> cells (green in A) with MBP immunoreactivity (red in A) within the corpus callosum; electron microscopy (in B) demonstrated axons surrounded by normally compacted myelin sheaths like wild-type (boxed area in B shown at higher magnification in inset). Donor-derived cells that engrafted outside (ventral to) the corpus callosum (in A) adopted an astroglial-like phenotype and were not associated with immunoreactive MBP. Scale bars = 25  $\mu$ m (A), 0.5  $\mu$ m (B) and 0.1  $\mu$ m (inset).

measurable weakness suggests that disturbances involving the cerebellum and/or basal ganglia and their connections are more likely than defects of the pyramidal system. It may be that the restoration of one or several motor deficits (tremor, ataxia or seizures) depends on the myelination of specific regions, including grey matter, and not on a generalized increase in overall myelination of central white matter tracts. Furthermore, we do not yet know whether our donor-derived myelin reconstitutes all the structural specializations characteristic of wild-type myelin (e.g. around the nodes of Ranvier). It has been reported previously that transplantation of a neural stem-like cell line (Yandava *et al.*, 1999) or oligodendrocyte progenitors (Kuhn *et al.*, 1995) into *shi* mutants resulted in either diminished tremor or improved rotarod performance, respectively; but both of these studies relied primarily on single motor tests, and neither of them related improved motor function to the degree of myelination in specific individuals.

Importantly, the *shi* phenotype can be genetically rescued, at least partially, by expression of a wild-type *Mbp* transgene (Readhead *et al.*, 1987). *Shi* mice heterozygous for the *Mbp*<sup>+</sup> transgene have a generalized ~5–10% increase in myelination (Shine *et al.*, 1992), with improved rotarod performance but no change in tremor, ataxia or seizures (Kuhn *et al.*, 1995). In contrast, *shi* mice homozygous for the *Mbp*<sup>+</sup> transgene have overall levels of wild-type CNS myelin ~20–25% of normal and much diminished tremor, ataxia and few, if any, seizures. These data suggest that full restoration of wild-type myelin levels may not be necessary for significant neurological recovery.

Neural cell transplantation creates a kind of 'surgical' chimera, a myelin-deficient mutant with widespread incorporation of donor-derived oligodendrocytes producing apparently wild-type myelin. These mice provide a unique opportunity to test whether, and under what circumstances, such a transplant strategy can rescue the abnormal phenotype of dysmyelinated hosts at the morphological, physiological and behavioural levels.

## Acknowledgements

This research was supported by grants from the National Cancer Institute (CA 6842602), NASA (NAG8-1358), the National Institute of Neurological Disorders and Stroke (NS 10174, NS11425 and NS37788) and NSF. The contents of this publication are solely the responsibility of the authors and do not necessarily represent the official views of these awarding agencies.

## References

- Ader M, Meng J, Schachner M, Bartsch U. Formation of myelin after transplantation of neural precursor cells into the retina of young postnatal mice. *Glia* 2000; 30: 301–10.
- Alvarez-Buylla A, Temple S. Stem cells in the developing and adult nervous system. [Review]. *J Neurobiol* 1998; 36: 105–10.
- Archer DR, Cuddon PA, Lipsitz D, Duncan ID. Myelination of the canine central nervous system by glial cell transplantation: a model for repair of human myelin disease. *Nat Med* 1997; 3: 54–9.
- Armstrong RJ, Svendsen CN. Neural stem cells: from cell biology to cell replacement. [Review]. *Cell Transplant* 2000; 9: 139–52.
- Avellana-Adalid V, Nait-Oumesmar B, Lachapelle F, Baron-Van Evercooren A. Expansion of rat oligodendrocyte progenitors into proliferative 'oligospheres' that retain differentiation potential. *J Neurosci Res* 1996; 45: 558–70.
- Blakemore WF, Franklin RJ. Transplantation of glial cells into the CNS. [Review]. *Trends Neurosci* 1991; 14: 323–7.
- Borchelt DR, Davis J, Fischer M, Lee MK, Slunt HH, Ratovitsky T, et al. A vector for expressing foreign genes in the brains and hearts of transgenic mice. *Genet Anal* 1996; 13: 159–63.
- Brüstle O, Spiro AC, Karram K, Choudhary K, Okabe S, McKay RD. In vitro-generated neural precursors participate in mammalian brain development. *Proc Natl Acad Sci USA* 1997; 94: 14809–14.
- Brüstle O, Choudhary K, Karram K, Hüttner A, Murray K, Dubois-Dalcq M, et al. Chimeric brains generated by intraventricular transplantation of fetal human brain cells into embryonic rats. *Nat Biotechnol* 1998; 16: 1040–4.
- Brüstle O, Jones KN, Learish RD, Karram K, Choudhary K, Wiestler OD, et al. Embryonic stem cell-derived glial precursors: a source of myelinating transplants. *Science* 1999; 285: 754–6.
- Carpenter MK, Winkler C, Fricker R, Emerich DF, Wong SC, Greco C, et al. Generation and transplantation of EGF-responsive neural stem cells derived from GFAP-bNGF transgenic mice. *Exp Neurol* 1997; 148: 187–204.
- Duncan ID, Grever WE, Zhang S-C. Repair of myelin disease: strategies and progress in animal models. [Review]. *Mol Med Today* 1997; 3: 554–61.
- Flax JD, Aurora S, Yang C, Simonin C, Wills AM, Billingham LL, et al. Engraftable human neural stem cells respond to developmental cues, replace neurons, and express foreign genes. *Nat Biotechnol* 1998; 16: 1033–9.
- Franklin RJ, Blakemore WF. Glial-cell transplantation and plasticity in the O-2A lineage—implications for CNS repair. [Review]. *Trends Neurosci* 1995; 18: 151–6.
- Franklin RJ, Bayley SA, Blakemore WF. Transplanted CG4 cells (an oligodendrocyte progenitor cell line) survive, migrate, and contribute to repair of areas of demyelination in X-irradiated and damaged spinal cord but not in normal spinal cord. *Exp Neurol* 1996; 137: 263–76.
- Friedman E, Nilaver G, Carmel P, Perlow M, Spatz L, Latov N. Myelination by transplanted fetal and neonatal oligodendrocytes in a dysmyelinating mutant. *Brain Res* 1986; 378: 142–6.
- Gage FH, Coates PW, Palmer TD, Kuhn HG, Fisher LJ, Suhonen JO, et al. Survival and differentiation of adult neuronal progenitor cells transplanted to the adult brain. *Proc Natl Acad Sci USA* 1995; 92: 11879–83.

2160 M. Mitome et al.

- Gansmüller A, Clerin E, Krüger F, Gumpel M, Lachapelle F. Tracing transplanted oligodendrocytes during migration and maturation in the shiverer mouse brain. *Glia* 1991; 4: 580-90.
- Gensert JM, Goldman JE. Endogenous progenitors remyelinate demyelinated axons in the adult CNS. *Neuron* 1997; 19: 197-203.
- Gout O, Gansmüller A, Baumann N, Gumpel M. Remyelination by transplanted oligodendrocytes of a demyelinated lesion in the spinal cord of the adult shiverer mouse. *Neurosci Lett* 1988; 87: 195-9.
- Gritti A, Frölichsthal-Schoeller P, Galli R, Parati EA, Cova L, Pagano SF, et al. Epidermal and fibroblast growth factors behave as mitogenic regulators for a single multipotent stem cell-like population from the subventricular region of the adult mouse forebrain. *J Neurosci* 1999; 19: 3287-97.
- Groves AK, Barnett SC, Franklin RJ, Crang AJ, Mayer M, Blakemore WF, et al. Repair of demyelinated lesions by transplantation of purified O-2A progenitor cells. *Nature* 1993; 362: 453-5.
- Gumpel M, Baumann N, Raoul M, Jacque C. Survival and differentiation of oligodendrocytes from neural tissue transplanted into new-born mouse brain. *Neurosci Lett* 1983; 37: 307-11.
- Hammang JP, Archer DR, Duncan ID. Myelination following transplantation of EGF-responsive neural stem cells into a myelin-deficient environment. *Exp Neurol* 1997; 147: 84-95.
- Hulspar R, Tiarks C, Reilly J, Hsieh C-C, Recht L, Quesenberry PJ. In vitro cell density-dependent clonal growth of EGF-responsive murine neural progenitor cells under serum-free conditions. *Exp Neurol* 1997; 148: 147-56.
- Ikawa M, Kominami K, Yoshimura Y, Tanaka K, Nishimune Y, Okabe M. A rapid and non-invasive selection of transgenic embryos before implantation using green fluorescent protein (GFP). *FEBS Lett* 1995; 375: 125-8.
- Inoue Y, Nakamura R, Mikoshiba K, Tsukada Y. Fine structure of the central myelin sheath in the myelin deficient mutant shiverer mouse, with special reference to the pattern of myelin formation by oligodendroglia. *Brain Res* 1981; 219: 85-94.
- Isacson O. The neurobiology and neurogenetics of stem cells. [Review]. *Brain Pathol* 1999; 9: 495-8.
- Keirstead HS, Ben-Hur T, Rogister B, O'Leary MT, Dubois-Dalq M, Blakemore WF. Polysialylated neural cell adhesion molecule-positive CNS precursors generate both oligodendrocytes and Schwann cells to remyelinate the CNS after transplantation. *J Neurosci* 1999; 19: 7529-36.
- Kohsaka S, Yoshida K, Inoue Y, Shinozaki T, Takayama H, Inoue H, et al. Transplantation of bulk-separated oligodendrocytes into the brains of shiverer mutant mice: immunohistochemical and electron microscopic studies on the myelination. *Brain Res* 1986; 372: 137-42.
- Kuhn PL, Petroulakis E, Zazanis GA, McKinnon RD. Motor function analysis of myelin mutant mice using a rotarod. *Int J Dev Neurosci* 1995; 13: 715-22.
- Lachapelle F, Duhamel-Clerin E, Gansmüller A, Baron-Van Evercooren A, Villarroya H, Gumpel M. Transplanted transgenically marked oligodendrocytes survive, migrate and myelinate in the normal mouse brain as they do in the shiverer mouse brain. *Eur J Neurosci* 1994; 6: 814-24.
- Learish RD, Brüstle O, Zhang S-C, Duncan ID. Intraventricular transplantation of oligodendrocyte progenitors into a fetal myelin mutant results in widespread formation of myelin. *Ann Neurol* 1999; 46: 716-22.
- Lee JC, Mayer-Proschel M, Rao MS. Gliogenesis in the central nervous system. [Review]. *Glia* 2000; 30: 105-21.
- Liu S, Qu Y, Stewart TJ, Howard MJ, Chakraborty S, Holekamp TF, et al. Embryonic stem cells differentiate into oligodendrocytes and myelinate in culture and after spinal cord transplantation. *Proc Natl Acad Sci USA* 2000; 97: 6126-31.
- Lubetzki C, Gansmüller A, Lachapelle F, Lombail P, Gumpel M. Myelination by oligodendrocytes isolated from 4-6-week-old rat central nervous system and transplanted into newborn shiverer brain. *J Neurol Sci* 1988; 88: 161-75.
- Milward EA, Lundberg CG, Ge B, Lipsitz D, Zhao M, Duncan ID. Isolation and transplantation of multipotential populations of epidermal growth factor-responsive, neural progenitor cells from the canine brain. *J Neurosci Res* 1997; 50: 862-71.
- Mitome M, Low HP, de la Iglesia HO, Schwartz WJ. Constructing suprachiasmatic nucleus chimeras in vivo. *Biol Rhythm Res* 2001; 32: 221-32.
- Mullen RJ, Buck CR, Smith AM. NeuN, a neuronal specific nuclear protein in vertebrates. *Development* 1992; 116: 201-11.
- Nait-Oumesmar B, Decker L, Lachapelle F, Avellana-Adalid V, Bachelin C, Van Evercooren AB. Progenitor cells of the adult mouse subventricular zone proliferate, migrate and differentiate into oligodendrocytes after demyelination. *Eur J Neurosci* 1999; 11: 4357-66.
- Niwa H, Yamamura K, Miyazaki J. Efficient selection for high-expression transfectants with a novel eukaryotic vector. *Gene* 1991; 108: 193-9.
- Privat A, Jacque C, Bourre JM, Dupouey P, Baumann N. Absence of the major dense line in myelin of the mutant mouse 'shiverer'. *Neurosci Lett* 1979; 12: 107-12.
- Readhead C, Popko B, Takahashi N, Shine HD, Saavedra RA, Sidman RL, et al. Expression of a myelin basic protein gene in transgenic shiverer mice: correction of the dysmyelinating phenotype. *Cell* 1987; 48: 703-12.
- Reynolds BA, Weiss S. Generation of neurons and astrocytes from isolated cells of the adult mammalian central nervous system. *Science* 1992; 255: 1707-10.
- Reynolds BA, Weiss S. Clonal and population analyses demonstrate that an EGF-responsive mammalian embryonic CNS precursor is a stem cell. *Dev Biol* 1996; 175: 1-13.
- Reynolds BA, Tetzlaff W, Weiss S. A multipotent EGF-responsive striatal embryonic progenitor cell produces neurons and astrocytes. *J Neurosci* 1992; 12: 5465-74.
- Roach A, Takahashi N, Pravtcheva D, Ruddle F, Hood L. Chromosomal mapping of mouse myelin basic protein gene and structure and transcription of the partially deleted gene in shiverer mutant mice. *Cell* 1985; 42: 149-55.

- Rosenbluth J. Central myelin in the mouse mutant shiverer. *J Comp Neurol* 1980; 194: 639-48.
- Rosenbluth J, Hasegawa M, Shirasaki N, Rosen CL, Liu Z. Myelin formation following transplantation of normal fetal glia into myelin-deficient rat spinal cord. *J Neurocytol* 1990; 19: 718-30.
- Shine HD, Readhead C, Popko B, Hood L, Sidman RL. Morphometric analysis of normal, mutant, and transgenic CNS: correlation of myelin basic protein expression to myelinogenesis. *J Neurochem* 1992; 58: 342-9.
- Suhonen JO, Peterson DA, Ray J, Gage FH. Differentiation of adult hippocampus-derived progenitors into olfactory neurons in vivo. *Nature* 1996; 383: 624-7.
- Svendsen CN, Clarke DJ, Rosser AE, Dunnett SB. Survival and differentiation of rat and human epidermal growth factor-responsive precursor cells following grafting into the lesioned adult central nervous system. *Exp Neurol* 1996; 137: 376-88.
- Svendsen CN, Caldwell MA, Shen J, ter Borg MG, Rosser AE, Tyers P, et al. Long-term survival of human central nervous system progenitor cells transplanted into a rat model of Parkinson's disease. *Exp Neurol* 1997; 148: 135-46.
- Takahashi M, Palmer TD, Takahashi J, Gage FH. Widespread integration and survival of adult-derived neural progenitor cells in the developing optic retina. *Mol Cell Neurosci* 1998; 12: 340-8.
- Tontsch U, Archer DR, Dubois-Dalcq M, Duncan ID. Transplantation of an oligodendrocyte cell line leading to extensive myelination. *Proc Natl Acad Sci USA* 1994; 91: 11616-20.
- van den Pol AN, Ghosh PK. Prion promoter drives GFP expression in developing transgenic mice [abstract]. *Neurosci Soc Abstr* 2000; 26: 1855.
- Vitry S, Avellana-Adalid V, Hardy R, Lachapelle F, Baron-Van Evercooren A. Mouse oligospheres: from pre-progenitors to functional oligodendrocytes. *J Neurosci Res* 1999; 58: 735-51.
- Vogel US, Thompson RJ. Molecular structure, localization, and possible functions of the myelin-associated enzyme 2',3'-cyclic nucleotide 3'-phosphodiesterase. [Review]. *J Neurochem* 1988; 50: 1667-77.
- Warrington AE, Barbarese E, Pfeiffer SE. Stage specific, (O4<sup>+</sup>GalC<sup>-</sup>) isolated oligodendrocyte progenitors produce MBP<sup>+</sup> myelin in vivo. *Dev Neurosci* 1992; 14: 93-7.
- Warrington AE, Barbarese E, Pfeiffer SE. Differential myelinogenic capacity of specific developmental stages of the oligodendrocyte lineage upon transplantation into hypomyelinating hosts. *J Neurosci Res* 1993; 34: 1-13.
- Winkler C, Fricker RA, Gates MA, Olsson M, Hammang JP, Carpenter MK, et al. Incorporation and glial differentiation of mouse EGF-responsive neural progenitor cells after transplantation into the embryonic rat brain. *Mol Cell Neurosci* 1998; 11: 99-116.
- Yandava BD, Billingham LL, Snyder EY. 'Global' cell replacement is feasible via neural stem cell transplantation: evidence from the dysmyelinated shiverer mouse brain. *Proc Natl Acad Sci USA* 1999; 96: 7029-34.
- Zambrowicz BP, Imamoto A, Fiering S, Herzenberg LA, Kerr WG, Soriano P. Disruption of overlapping transcripts in the ROSA  $\beta$ geo 26 gene trap strain leads to widespread expression of  $\beta$ -galactosidase in mouse embryos and hematopoietic cells. *Proc Natl Acad Sci USA* 1997; 94: 3789-94.
- Zhang S-C, Lundberg C, Lipsitz D, O'Connor LT, Duncan ID. Generation of oligodendroglial progenitors from neural stem cells. *J Neurocytol* 1998; 27: 475-89.
- Zhang S-C, Ge B, Duncan ID. Adult brain retains the potential to generate oligodendroglial progenitors with extensive myelination capacity. *Proc Natl Acad Sci USA* 1999; 96: 4089-94.

Received February 19, 2001. Revised June 10, 2001.

Accepted June 25, 2001.

# Isolation and Transplantation of Multipotential Populations of Epidermal Growth Factor–Responsive, Neural Progenitor Cells From the Canine Brain

Elizabeth A. Milward, Cathryn G. Lundberg, Bin Ge, David Lipsitz, Ming Zhao, and Ian D. Duncan\*

Department of Medical Sciences, School of Veterinary Medicine, University of Wisconsin, Madison

Glial cell transplantation into myelin-deficient rodent models has resulted in myelination of axons and restoration of conduction velocity. The shaking (*sh*) pup canine myelin mutant is a useful model in which to test the ability to repair human myelin diseases, but as in humans, the canine donor supply for allografting is limited. A solution may be provided by self-renewing epidermal growth factor (EGF)–responsive multipotential neural progenitor cell populations (“neurospheres”). Nonadherent spherical clusters, similar in appearance to murine neurospheres, have been obtained from the brain of perinatal wildtype (*wt*) canine brain and expanded *in vitro* in the presence of EGF for at least 6 months. Most of the cells in these clusters express a nestin-related protein. Within 1–2 weeks after removal of EGF, cells from the clusters generate neurons, astrocytes, and both oligodendroglial progenitors and oligodendrocytes. Transplantation of lacZ-expressing *wt* neurospheres into the myelin-deficient (*md*) rat showed that a proportion of the cells differentiated into oligodendrocytes and produced myelin. In addition, cells from the neurosphere populations survived at least 6 weeks after grafting into a 14-day postnatal *sh* pup recipient and at least 2 weeks after grafting into an adult *sh* pup recipient. Thus, neurospheres provide a new source of allogeneic donor cells for transplantation studies in this mutant. *J. Neurosci. Res.* 50:862–871, 1997.

© 1997 Wiley-Liss, Inc.

**Key words:** epidermal growth factor; myelin deficient; neural progenitor cells; glial cell transplantation

## INTRODUCTION

Accumulating research in animal models raises hopes of using glial transplantation in therapy for human myelin diseases. Glia from a range of sources can myelinate axons in various recipient environments (reviewed in Duncan and Milward, 1995; Franklin and

Blakemore, 1995; Duncan, 1996). Most research uses rodent recipients with inherited myelin disorders (reviewed in Duncan and Milward, 1995; Duncan, 1996) or with chemically induced demyelinating lesions (Blakemore and Crang, 1983; Blakemore et al., 1995), but there are obvious limitations to extending such studies to humans. Myelin diseases such as multiple sclerosis may develop over years, whereas most rodent myelin mutants die before adulthood. Glial cells grafted into rodents can migrate substantial distances (1–2 cm) but may need to travel much farther to reach surgically inaccessible lesions in humans. Mechanisms of differentiation, myelination, or remyelination may also differ between species. Most studies on human glia have not found close resemblances to rat oligodendroglial growth factor responses, antigenic profiles, or adult progenitor cells, although some similarities do exist (Kennedy et al., 1980; Dickson et al., 1985; Yong et al., 1988; Aloisi et al., 1992; Armstrong et al., 1992; Yong and Antel, 1993; Gogate et al., 1994; Satoh and Kim, 1994; Scolding et al., 1995).

The canine shaking (*sh*) pup model may help bridge the gap between rodents and humans. Like some rodent models and certain forms of the human Pelizaeus-Merzbacher and X-linked spastic paraplegia diseases, it arises from an exonic point mutation in the protolipid protein gene (Nadon et al., 1990). The mutation arose spontaneously in Welsh springer spaniels and causes severe tremor from about 12 days of age after birth, followed by late onset convulsions (Griffiths et al., 1981; Duncan, 1995). The central nervous system (CNS) is

Contract grant sponsor: CytoTherapeutics.

Elizabeth Milward's present address is Centre for Education and Research on Ageing, University of Sydney and Concord Hospital, Concord, 2139, NWS, Australia.

\*Correspondence to: Dr. Ian D. Duncan, University of Wisconsin, School of Veterinary Medicine, 2015 Linden Drive West, Madison, WI 53706. E-mail: duncan@svm.vetmed.wisc.edu

Received 7 August 1997; Accepted 8 August 1997



severely hypomyelinated, with reduced numbers of mature oligodendrocytes (Duncan et al., 1983). Death normally occurs at about 3–4 months of age, but animals can live over 2 years with intensive rearing.

Xenografts of normal canine oligodendrocytes myelinate axons in myelin-deficient (*md*) rats (Archer et al., 1994), and allografting of canine glia into *sh* pup spinal cords shows that *sh* pup axons can be remyelinated (Archer et al., 1997). Allografting reduces immunologic complications but raises the problem of obtaining sufficient donor cells for transplantation, a common difficulty with species other than rodents. A solution may lie in the use of self-renewing, multipotential, growth factor-responsive neural progenitor cell populations, which grow in clusters dubbed “neurospheres” (Reynolds and Weiss, 1992, 1996; Reynolds et al., 1992). Cells in these populations generate neurons and astrocytes (Reynolds and Weiss, 1992, 1996; Reynolds et al., 1992) and oligodendroglial cells (Hammang et al., 1997; Reynolds and Weiss, 1996) in proportions that may be influenced by environmental manipulation. Murine neurospheres grafted into the *md* rat CNS generate cells that myelinate host axons (Hammang et al., 1994). Expandable multipotential populations of growth factor-responsive cells from the canine CNS could circumvent limitations of tissue availability for transplantation studies or in vitro analysis.

Although the presence of normal proteolipid protein or normal myelin production can distinguish normal from mutant oligodendrocytes after transplantation, both approaches are susceptible to technical or interpretational ambiguities. Recent glial transplantation has used *lacZ* expressing cells, obtained by stable transfection of rodent glial lines (Tontsch et al., 1994; Franklin et al., 1995, 1996) or from transgenic mice expressing *lacZ* under myelin protein promoters (Hammang et al., 1994; our unpublished data). Currently, no canine glial lines exist and neither approach can readily be applied in this species. Instead, we have tested the ability of the third generation PG13 retroviral vector system (Miller et al., 1991) to transduce *lacZ* expression in canine cells. Vector packaging in this system uses the Gibbon ape leukemia virus *env* protein, which includes both canine and human cells in its host range (Miller et al., 1991). A receptor, GLVR1, for this *env* protein is expressed abundantly in brain, with particularly high expression early in embryogenesis (Johann et al., 1992; Kavanaugh et al., 1994), making this system an ideal candidate for labeling canine neural progenitor cells.

We have obtained expandable multipotential populations of growth factor-responsive cells from the normal canine CNS and transduced these to express *lacZ* to provide labeled allogeneic donor cells for transplantation studies in *sh* pups or for xenografting into *md* rat recipients. We have also obtained similar populations

from mutant *sh* pup brain, which should enable further study of the effects of the *sh* mutation on CNS cells.

## MATERIALS AND METHODS

### Preparation of “Neurospheres” From *sh* and *wt* Littermate Pups

Wildtype (*wt*) and *sh* pups were obtained from a colony at the University of Wisconsin. Donors were aged from embryonic day 40 to postnatal day 8. After euthanasia with barbiturate solution, brains were placed in artificial high- $\text{Ca}^{2+}$ , low- $\text{Mg}^{2+}$  cerebrospinal fluid solution (2 mM  $\text{CaCl}_2$ , 1.3 mM  $\text{MgCl}_2$ , 124 mM NaCl, 5 mM KCl, 26 mM  $\text{NaHCO}_3$ , 10 mM D-glucose, pH 7.35) and the subventricular caudate nucleus, internal capsule, putamen/pallidum, and ventral mesencephalon separated and minced ( $<1 \text{ mm}^3$ ). Aliquots were dispersed mechanically by trituration or with enzymes (Reynolds and Weiss, 1992). All trituration was performed first with standard bore, then with fire-polished Pasteur pipettes, with the exception of trituration performed before transplant into *md* rats (see below), which used sequential passage through 20-, 23-, 25-, and 27-gauge needles. After filtration (35  $\mu\text{m}$  nylon mesh; Small Parts, Miami Lakes, FL), suspensions were centrifuged (5°C, 5 min, 400g), dispersed in EGF + medium, comprised of 20 ng/ml mouse submaxillary gland EGF (Collaborative Research, Bedford, MA) in Dulbecco's Modified Eagle's Medium/F12 (1:1) with additives as given elsewhere (Reynolds et al., 1992), and plated in uncoated tissue culture flasks. To obtain adherent differentiated populations, cells were collected by centrifugation (5°C, 5 min, 400g), resuspended in EGF- medium (the same base medium but with 1% fetal bovine serum replacing EGF) and plated on dishes coated with poly-L-ornithine (10  $\mu\text{g}/\text{ml}$ ).

### Immunofluorescence

Rabbit polyclonal antibodies were used to detect nestin (Rabbit 130 from Dr. R. McKay, National Institute of Neurological Disorders and Stroke, Bethesda, MD) and 68 kD neurofilament protein (from Dr. P. Gambetti, Institute of Pathology, Case Western Reserve University School of Medicine, Cleveland OH). Monoclonal antibodies were Rat 401 anti-nestin (Developmental Studies Hybridoma Bank, Iowa City, IA), O4 and O1 (from Dr. M. Schachner), and Ranscht anti-galactocerebroside (GC) (Boehringer Mannheim, Indianapolis, IN). All other antibodies, conjugates, and nonspecific immunoglobulins were from Jackson ImmunoResearch Laboratories (West Grove, PA). Negative controls were provided by omission of primary antibody or replacement with nonimmune rabbit serum or nonspecific mouse immunoglobulin. Secondary antibodies were the fluorescein-conjugates

goat anti-rabbit IgG and anti-mouse IgG, rhodamine-conjugated goat anti-mouse IgM, and biotin-SP-conjugated donkey anti-rabbit IgG and 7-amino-4-methylcoumarin-3-acetate-conjugated streptavidin. Cells were fixed with 4% paraformaldehyde (10 min, room temperature). Antibodies were diluted in 5% normal goat serum in phosphate buffered saline (with 0.1% Triton X-100 for antibodies to nestin). Aside from anti-GFAP (4°C, overnight), antibodies were incubated 1–2 hr at room temperature, followed by at least three buffer washes. After surface antigen labeling (O4, O1, Ranscht), samples were incubated in 5% glacial acetic acid:95% ethanol (v:v) for 10 min at –20°C and nestin, neurofilament, and glial fibrillary acidic protein (GFAP) antibodies used as above. Staining for combinations of O4, Ranscht and GFAP was as described elsewhere (Armstrong et al., 1992). Samples were mounted in CitiFluor (UKC Chemical Laboratory, Canterbury, UK) containing bisbenzimidazole H33342 fluorochrome (Calbiochem, La Jolla, CA).

#### Transduction of *lacZ* Expression in Canine Neurospheres

The PG13 retroviral packaging system, provided by Dr. M. Eiden, National Institute of Mental Health (Bethesda, MD), was maintained and used as previously described (Miller et al., 1991, 1993). Media conditioned for 6 days with packaged, defective, retroviral vector was harvested, filtered (0.45 µm), and used directly or stored at –70°C. Activity was confirmed using the Rat2 fibroblast line (Miller et al., 1991, 1993). Titers were in the order of 10<sup>5</sup> colony forming units per milliliter. Neurospheres were passaged (with trituration) into media consisting of EGF<sup>+</sup> medium:PG13-conditioned medium (1:1), with polybrene (4 µg/ml). After 20–24-hr incubation, cells were pelleted (5°C, 5 min, 400g), resuspended in EGF<sup>+</sup> medium, and collected 24–48 hr later by centrifugation (5°C, 5 min, 400g) for transplantation (below) or plating in EGF<sup>–</sup> medium on poly-L-ornithine coated dishes for immunocytochemistry as above or 5-bromo-4-chloro-3-indolyl β-D-galactosidase (X-gal) staining (Tontsch et al., 1994).

#### Transplantation of Canine Neurospheres

After centrifugation as above, cells were resuspended in EGF<sup>+</sup> medium and either pipette triturated, followed by removal of undissociated spheres by nylon mesh filtration (35 µm), or triturated with needles as above. After Trypan Blue viability assessment and counting, cells were pelleted as above, resuspended at 25,000–75,000 cells/µl in Ca/Mg-free Hank's buffered saline solution with 0.01% bovine serum albumin and placed on ice until transplantation into *sh* pups.

#### Transplantation of Canine Neurospheres Into *sh* Pup Recipients

Recipient pups (aged either 14 days or 7 months) were premedicated with analgesics and sedatives, induced with an ultra-short-acting barbiturate, then intubated and maintained with isoflurane and oxygen. Dorsal laminectomy was performed at thoracic and lumbar sites T13–L1, L1–L2, and L2–L3. Using a surgical microscope, a durotomy was carried out at each laminectomy site. A glass micropipette (30-µm bore) was inserted into the spinal cord and 2–4 µl of cell suspension slowly injected over a 1-minute period by using a micromanipulator and Hamilton syringe. Respiration was controlled with the neuromuscular blocking agent succinylcholine during the injection to minimize spine movement. Injection sites were marked with sterile charcoal, a fat graft placed in each laminectomy defect and muscle, subcutaneous tissue and skin reapposed. Two to six weeks after injection, pups were anesthetized, fixative-perfused, and stained for X-gal, then transverse slices were Epon embedded for 1-µm sectioning and staining with *p*-phenylenediamine (Tontsch et al., 1994).

#### Transplantation of Canine Neurospheres Into *md* Rat Recipients

Cells were exposed three times to retroviral vector-containing medium that had been stored at –70°C (one freeze-thaw cycle). This boosted the transduction efficiency obtained with stored media. Initial overnight vector exposure, centrifugation, and resuspension in EGF<sup>+</sup> medium were as described above; after 48 hr, cells were again passaged with trituration into EGF<sup>+</sup> medium:PG13-conditioned medium (1:1) with polybrene (4 µg/ml), incubated 4 hr, then centrifuged and resuspended as before. This was repeated 72 hr later. Cells were passaged with trituration 48 hr later, and after a further 24 hr, triturated as above, except that the last trituration used 25½- and 27-gauge needles sequentially, and placed on ice for transplantation. The *md* rat recipients were from a colony at the University of Wisconsin. Transplantation into *md* rat spinal cord consisted of either one or two injections, the latter 1 mm apart, each of 1 µl at 25–50,000 cells/µl at the thoracic–lumbar T13–L1 junction, using published protocols (Hammang et al., 1994). Recipients were treated daily with Cyclosporine A (10 mg/kg body weight). Conditions of final anesthesia, tissue fixation, processing for X-gal revelation, Epon embedding, 1-µm transverse sectioning, and *p*-phenylenediamine staining have been described (Hammang et al., 1994; Tontsch et al., 1994).

## RESULTS

### Preparation of Neurospheres From *sh* Pup and *w*<sup>t</sup> Littermate Pups

We tested various tissue dissociation techniques on several regions from embryonic or postnatal *w*<sup>t</sup> canine brains. Donors were aged between embryonic day 40 to postnatal day 2 (canine gestation is about 63 days). Cells from embryos multiply more rapidly and have been expanded *in vitro* at least 6 months.

Neurosphere-like clusters were derived from each of the subventricular caudate nucleus, internal capsule, putamen/pallidum, and ventral mesencephalon. For all protocols, the putamen/pallidum was consistently the poorest source, both in cluster yields and in long-term sustainability of cultures. Subventricular and ventral mesencephalon regions were the richest sources of neurospheres from embryonic and postnatal pups and the most amenable to sustained *in vitro* expansion, as is also the case in both embryonic and adult mice (Reynolds and Weiss, 1992; Reynolds et al., 1992; Hammang et al., 1994, 1997). Separate canine preparations were subsequently made from (1) ventral mesencephalon and (2) "striatum," comprised of pooled caudate nucleus and the adjacent portion of the inner capsule.

Rodent neurospheres are obtained from CNS by trituration alone or after enzyme treatment (Reynolds and Weiss, 1992; Reynolds et al., 1992). Trituration alone routinely generated neurospheres from canine CNS, but enzyme treatment failed to give useful yields from some pups and subsequently was not used. Moreover, compared with rodent neurospheres, even after isolation, canine neurospheres were harder to dissociate during subsequent passaging or for differentiation studies. Even forceful trituration failed to disperse all clusters and, gauged by Trypan Blue exclusion, damaged as many as 80% of cells (data not shown).

In the murine neurosphere system, when cells are first isolated from the CNS there is a period of cell death over the first 5 days *in vitro*, followed by progenitor division leading to sphere formation (Reynolds et al., 1992). This was not observed in the canine system. Instead, adherent spherical clusters of refractile cells of healthy appearance were first detectable at 4 hr postplating and were readily apparent by 12 hr in both striatal and ventral mesencephalic cultures. As preparations were filtered before plating, these clusters may arise from cell aggregation. Nonadherent spherical clusters containing four or more refractile cells were observed within 12–72 hr postplating in essentially all cultures (Fig. 1A.). Debris and unhealthy or dead-looking cells were typically present during the first 14 days, but apparently healthy spheres of increasing size continued to be observed

throughout this time. Dispersion of large clusters during passaging (see Methods and previous paragraph) yielded both small clusters and individual cells, with subsequent sphere growth allowing expansion at a split ratio of 1:2 every 2–4 weeks for at least 6 months.

After expansion by passaging between two to nine times in the presence of EGF, adherent differentiated populations were obtained by partially dissociating neurospheres by trituration and plating onto poly-L-ornithine substrata in EGF medium. (As noted above, spheres could not be completely dissociated without excessive cell destruction.) Cells were fixed 1 hr to 28 days later. By 1 hr postplating, spheres had attached to the substratum. By 24 hr, emergent cells began to form monolayer "halos" around spheres.

Rat401 monoclonal and rabbit polyclonal 130 antibodies were used to reveal expression of nestin, a neural progenitor marker, in striatal or ventral mesencephalon-derived neurospheres. At 1, 4, and 24 hr postplating, fluorescence was above background levels in most cells (Fig. 1B), although labeling intensity with either antibody was low compared with staining seen with Rat401 in murine systems (Hammang et al., 1994; our unpublished observations), suggesting epitopic differences between canine and rodent nestin species. Both cells in clusters and some cells in the monolayer expressed nestin, but by 24 hr postplating many cells in the monolayer were apparently unlabeled (Fig. 1B) and no nestin staining was detectable after 10 days *in vitro* (not shown). Patterns of nestin staining were similar in cells originally derived from different CNS regions.

Monoclonal antibody to the 68 kD NF protein detected cells with morphologies resembling neurons or immature neuronal cells at 25 days postplating in both striatal and ventral mesencephalon-derived cultures (Fig. 1C). As revealed by this antibody, many of these cells had long, very fine processes. No cells expressing the 68-kD NF protein were detected at earlier times. Cells expressing GFAP, some with stellate morphology, were detected at all times examined from 7 days postplating onward in both striatal and ventral mesencephalon-derived cultures (Fig. 1D).

Markers used with or without concomitant GFAP staining to identify oligodendrocyte-type 2 astrocyte lineage cells were the O4 and Ranscht antigens (Sommer and Schachner, 1981; Ranscht et al., 1982). Process-bearing cells expressing O4 were detected within and surrounding spheres at all times examined from 7 days postplating onward in both striatal and ventral mesencephalon-derived cultures (Fig. 1E). Some, but not all, of these O4+ cells also expressed GFAP. Neither cells of stellate morphology nor process-bearing cells with morphologies typical of O4+ cells were observed in freshly

866 Milward et al.

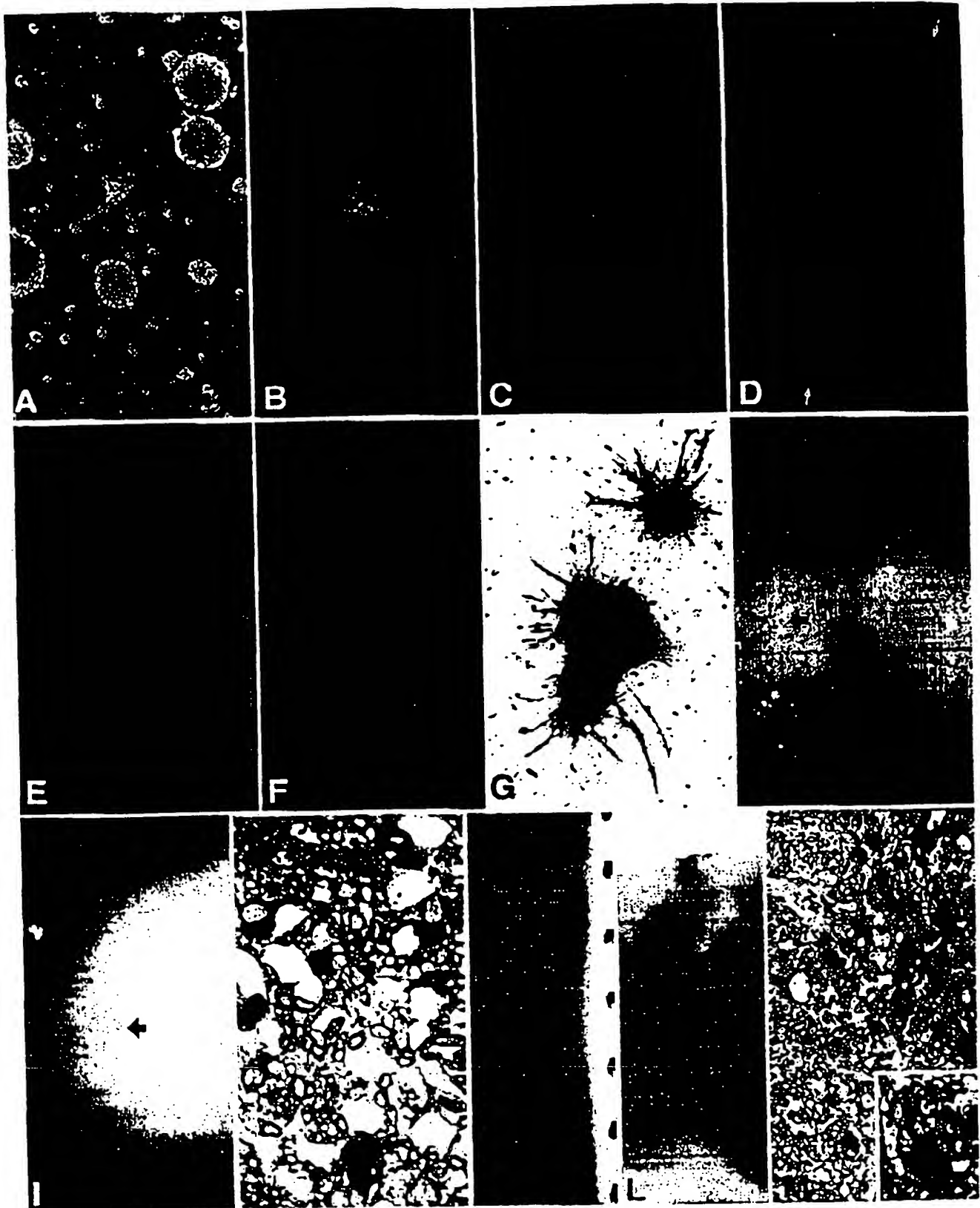


Figure 1.

plated neurosphere cultures nor in the surrounding halos of cells migrating out of the neurospheres in the first 24 hours after plating. Ranscht antigen expression was not detected at either 7 or 10 days postplating in any cultures but was observed at 12 days postplating in all cultures in a very small percentage of O4<sup>+</sup> cells (estimated to be <1%). These typically had morphologies classically associated with oligodendrocytes, with many highly branched processes (Fig. 1F). Such morphologies were not observed in freshly plated neurosphere cultures nor in

the surrounding halos of cells migrating out of the neurospheres in the first 24 hr after plating from either earlier or later passages. These morphologic observations and patterns of marker expression, in particular the delayed and separate appearances of the Ranscht antigen and the 68-kD NF protein, provide direct evidence that differentiation along CNS lineages is occurring in this system.

The PG13 packaging system uses the Gibbon ape leukemia virus *env* protein (Miller et al., 1991). The retroviral vector we used in this system is based on the plasmid pLXSN and contains *lacZ* under the SV40 promoter (Miller et al., 1993). This vector/packaging combination transduced *lacZ* expression in a substantial proportion of cells in the canine neurosphere preparations generated from perinatal pups (Fig. 1G). We first used allografting into *sh* pups to address the issue of whether neurosphere-derived cells can survive in the adult *sh* pup CNS environment. Adult *sh* pups are extremely rare, and although the lifespan of *sh* pups can be increased to more than 2 years with intensive rearing, individual adults may nonetheless die at any time after 3–4 months even without the added risks arising from surgery. For these reasons, in this initial study, survival in an adult animal was examined in the short term, and a postnatal animal was used to examine survival in the longer term. Fixation and processing conditions for combined *lacZ* and myelin detection have been refined in numerous rat studies and are not optimal with respect to tissue preservation in the larger canine system, where animal rarity restricts optimization. Thus, the myelinating capacity of neurosphere populations was examined by xenografting into *md* rats, which also provides more stringent environmental conditions than allografting. Aliquots of populations destined for allografts or xenografts were plated under differentiating conditions, as above and in Methods, for parallel examination of *in vitro* differentiation and *lacZ* expression. The appearance of differentiation markers in these cultures followed the same time course as was described above.

Populations of proliferative canine neurospheres, originally derived from striatum of embryonic day 40–50 normal pups, were transduced to express *lacZ* and transplanted into the spinal cords of a postnatal 14 day and an adult (7 months) *sh* pup. (Donor cells had undergone three and nine passages *in vitro*, respectively, before transplant.) The postnatal pup was killed at 6 weeks and the adult pup at 2 weeks posttransplant. After X-gal staining, transverse sections of the spinal cord in the regions of the thoracic and lumbar injection sites (T13–L1, L1–L2, and L2–L3) revealed distinct clusters of blue patches in each of the postnatal and adult animals not only at the site of implantation in the dorsal column but also in the lateral or ventral columns and gray matter (Fig. 1H, I), suggesting that migration of implanted cells

Fig. 1. Generation and transplantation of EGF-responsive canine neural progenitor populations. A: Preparation from the striatum of a normal E45–50 pup at 48 hr after isolation from the CNS, showing spherical clusters resembling neurospheres containing refractile cells of healthy appearance. B: Nestin immunoreactivity (green) occurs in cells within and around spheres in normal E50 canine striatal neurosphere preparations 24 hr after plating in EGF medium. Some surrounding cells, visualized by nuclear labeling with Hoechst bisbenzimidazole H33342 (blue), do not express nestin. C: Cells from normal E50 canine striatal neurospheres 25 days after plating in EGF medium, labeled for the 68-kD neurofilament protein (green) and Hoechst bisbenzimidazole H33342 (blue). D: Cells from normal E50 canine striatal neurospheres with stellate and other morphologies expressing GFAP (blue) 7 days after plating in EGF medium. Nuclei are also labeled blue with Hoechst 33342, which does not label cell processes, allowing GFAP-negative cells to be visualized (arrows). E: Expression of O4 antigen (red) in cells from normal E50 canine ventral mesencephalon neurospheres 12 days after plating in EGF medium. F: Occasional O4-positive cells also react with the Ranscht anti-galactocerebroside antibody at this time. G: Expression of *lacZ* in normal canine neurospheres after transduction using the PG13 retroviral vector system. H: Transverse section of the spinal cord of a 2-month *sh* pup, 6 weeks after transplantation of *lacZ*-labeled *wt* canine neurospheres at 14 days after birth. Blue clusters are visible in several regions of the cord (arrows). I: Transverse section of the spinal cord of a 7–8-month *sh* pup, 2 weeks after transplantation of *lacZ*-labeled *wt* canine neurospheres. A blue cluster is visible in the lateral column of the spinal cord (arrow). J: Microscopy of transverse sections shows graft cells apparently integrated normally into the adult *sh* pup cytoarchitecture (arrows). Vacuolation in this section is due to the method of fixation and not the transplanted cells. The section is counterstained with paraphenylenediamine. K: Blue clusters are visible for several millimeters along the dorsal midline of the spinal cord of an *md* rat that received *lacZ*-labeled canine neurospheres 1 week after birth (1-mm markers on right). L: The same spinal cord shown in K, showing blue labeling throughout the dorsal column at the site of injection. M: In a 1- $\mu$ m section from the spinal cord shown in L, scattered myelinated fibers (more than seen in nontransplanted *md* rats) are present. Details of a normal oligodendrocyte with a long cytoplasmic process extending to a myelinated axon (arrow) are shown in the inset. Such cells are not normally seen in areas outside of the transplant.

may have occurred. Our previous studies have shown that there is an acute passive dispersion of cells only along the dorsal column, up to 8 mm from the site of transplantation (Lipsitz et al., 1995). Similar studies with Hoechst labeled cells have also shown a localization of transplanted cells immediately after transplant to the dorsal columns (Zhang and Duncan, unpublished data). The fixation used failed to preserve structures optimally in the adult mutant, but nonetheless light microscopy of tissue sections clearly demonstrated *lacZ*-expressing cells in association with areas containing myelin (Fig. 1J). These cells appeared to have integrated into the surrounding cytoarchitecture, with no evidence of rejection.

Xenografts into *md* rat recipients were used to obtain further evidence for the ability of neurosphere-derived cells to myelinate host axons in a myelin-deficient environment. To facilitate routine studies in these rats, a triple exposure protocol was used for successful transduction of *lacZ* expression by using media conditioned with packaged, defective, retroviral vector that had been stored frozen before use (Methods). Canine neurospheres were transduced to express *lacZ* and implanted into the dorsal columns of spinal cords of 7-day postnatal *md* rats at the thoracic-lumbar (T13-L1) junction (Methods). At 11 days posttransplant, low-power light microscopy revealed blue X-gal reaction product spread up to 6 mm along the dorsal midline of at least three transplant recipients in each of two separate experiments (Fig. 1K). This typically appeared as clusters of small blue patches or dots, rather than the more homogeneously distributed streak of blue-labeled cells often seen after glial cell transplantation (Tontsch et al., 1994). Transverse sections (1  $\mu$ m) of recipient spinal cords revealed grafted cells in the dorsal columns in areas containing myelinated axons (Fig. 1L) and, strikingly, a grafted cell with a long cytoplasmic process in contact with a myelinated axon (Fig. 1M). By electron microscopy (EM), the myelin was found to have a normal intraperiod line that is lacking in host myelin.

## DISCUSSION

We have obtained cell populations from *wr* canine perinatal striatum and ventral mesencephalon that closely resemble murine EGF-responsive multipotential neural progenitor cell populations (neurospheres). The clusters of canine cells are similar in appearance to murine spheres and can be expanded with passaging for at least 6 months in vitro in the presence of EGF. On removal of EGF, cells within the clusters generate neurons, astrocytes, and oligodendroglia. Cells from these cultures can survive at least 6 weeks in postnatal and at least 2 weeks in adult *sh* pup recipients. This is the first time neurosphere transplant survival has been demonstrated in the

adult CNS. Neurospheres thus provide a new source of allogeneic donor cells for transplantation studies in this mutant. Moreover, grafting of *wr* neurospheres into *md* recipient spinal cords resulted in the production of apparently normal myelin by graft-derived cells, showing that these cells are able to myelinate a myelin-deficient host. The ability of neurosphere-derived cells to myelinate under xenograft conditions is encouraging for future studies involving human neurospheres, which must first be tested by xenografting. In addition, the PG13 retroviral vector packaging system, based on the Gibbon ape leukemia virus *env* protein, provides a new means of labeling donor cells. With a host range also including humans and rodents, this system is likely to be useful for transplantation studies in various species.

Our observations of neurospheres within a few hours of the initial preparation of cultures from the CNS suggest rapid extensive reaggregation of cells. Early "spheres" are unlikely to arise from proliferation of single progenitors as canine neurospheres grow slowly compared with murine neurospheres maintained in identical media (our unpublished observations). Human fetal neurosphere preparations also grow very slowly compared with murine preparations and may require different combinations of factors for optimal growth (B. Reynolds, personal communication). Faster growth apparently occurred in preparations obtained from embryonic, as opposed to postnatal, canine CNS. Because initial yields from postnatal pups were in general lower than those obtained from embryos, the relative success of the latter may reflect either or both developmental differences in the proliferative capacities of progenitors or growth-enhancing autocrine effects, which may occur in higher density cultures.

Removal of EGF resulted in the sequential appearance, over a period of 3–4 weeks, of cells with distinctive differentiated morphologies expressing markers of mature astrocytes, oligodendrocytes, and neurons, which were not detected in freshly plated neurosphere preparations. Thus canine neurosphere-derived cells differentiate along at least two lineages, although we could not verify that these neurospheres do, in fact, contain multipotential cells rather than subpopulations of lineage-committed, unipotent progenitor cells, because the slow growth rate of these cells has prevented clonal analysis to date. Clonal analysis has confirmed the existence of self-replicating neural stem cells in analogous EGF-responsive murine neural progenitor populations (Reynolds and Weiss, 1996), and the long-term expandability of canine populations is indirect evidence that such cells may be present. However, whether or not stem cells are present, as the first expandable differentiating system established from canine brain, neurospheres provide a means to study at least three of the major CNS cell species, which has not



previously been available in the dog and which should facilitate studies both of normal canine and also of *sh* pup CNS.

Although secondary to the aims of the present study, we have had preliminary success in generating neurospheres from *sh* pup mutant embryos (data not shown), providing a new *in vitro* system for characterizing the effects of the mutation. The developmentally regulated alternative splicing pattern of the myelin proteolipid protein gene is altered in the *sh* mutant, suggesting delayed mutant oligodendrocyte maturation (Nadon et al., 1990). Proteolipid protein gene expression may also have functions in CNS development before myelinogenesis. The ability to generate neurospheres that are similar in many respects to those derived from *wt* brain should facilitate studies on differentiation of *sh* pup oligodendrocytes. Such *sh* pup neurospheres could also be used as a target in gene transfer studies. In addition, our success in expanding neurospheres from the *sh* pup mutant suggests that this approach could extend the range of models amenable to study and may be applicable to very rare mutants, in which limited availability of affected animals has restricted characterization to date.

Although expansion of the canine populations is slow compared with the murine case, the scarcity of source tissue in the canine system makes these cells a valuable alternative to primary culture. Analysis of growth factor effects in the canine system may permit faster expansion of these cells *in vitro*. Basic fibroblast growth factor (bFGF) stimulates proliferation of some rodent neural progenitor populations (Lillien and Cepko, 1992; Richards et al., 1992; Ray and Gage, 1994; Kilpatrick and Bartlett, 1995; Vescovi et al., 1993) and has been implicated in oligodendroglial proliferations and inhibition of differentiation or population reversion to more immature phenotypes in both rat (Bogler et al., 1990; McKinnon et al., 1990) and human models (Armstrong et al., 1992; Gogate et al., 1994). It could well have similar effects in the canine system, in which bFGF (5–100 ng/ml) may increase proliferation in canine oligodendroglial-enriched cultures (Hoffman and Duncan, 1995). Sequential growth factor mixtures could enhance first proliferation then differentiation of canine neural progenitor cells.

Myelin deficiency may activate compensatory mechanisms. Even when these are insufficient to override effects of endogenous myelin gene mutations, the environment may nonetheless express factors favoring oligodendrogenesis and myelinogenesis by transplanted cells. Neurospheres generated myelinogenic oligodendrocytes when transplanted into the *md* rat, and furthermore, grafted neurosphere-derived cells survived not only in the neonatal but also in the adult *sh* pup. Thus the adult

canine environment is able to support the survival of perinatal neural progenitor cells, at least in the short term. This is consistent with the existence of neural progenitor cells in adult rodent CNS (Reynolds and Weiss, 1992; Richards et al., 1992). The number of myelinated axons observed after xenografting of canine neurospheres into the *md* rat was considerably more than is seen in nontransplanted *md* rats, although less has been seen with allografts of murine neurospheres, which myelinate large areas of the *md* cord (Hammang et al., in press). In view of the *in vitro* differences in expansion rates discussed above, canine neurospheres may also take longer to expand and mature *in vivo* than murine neurospheres, even though the presence of apparently myelinating transplant-derived oligodendrocytes after only 11 days *in vivo* suggest canine oligodendrocytes differentiate more rapidly *in vivo* than *in vitro*. This system should be valuable for future study of survival, growth, and myelinating ability of grafted cells, particularly in adult recipients, with ultimate applications in humans.

Unlike some more differentiated CNS cell species, neural progenitor cells may not express both classic histocompatibility molecules and may thus, at least initially, provoke a less intense host immune reaction (Bartlett et al., 1990). Although null mutant studies suggest peripheral transplant rejection can occur in the absence of both class I and II molecules, as far as we are aware this has yet to be established for the CNS, which is relatively immunologically privileged. Neurospheres also offer the prospect of generating mixed populations of neural cell species in a controllable manner. Because both astrocytes (Raff et al., 1985; Richardson et al., 1988) and neurons (Barres and Raff, 1993; Hardy and Reynolds, 1993) have been implicated in oligodendroglial migration and differentiation and may also influence myelination, this could benefit transplant-derived remyelination. As well as advantages of manipulability and *in vitro* expandability, these cells provide a multipotential, proliferation-competent pool from which differentiated populations may arise in response to environmental cues. Implantation of small donor populations could ultimately assist in maintaining lifelong reservoirs from which CNS cell populations may be renewed through endogenous or externally manipulated environmental signals.

## ACKNOWLEDGMENTS

We are grateful to Drs. M. Dubois-Dalcq, M. Carpenter, and S. Zhang for reading the manuscript and Drs. C. Johe and T. Mueller for assistance and discussions. This study was supported by a grant from Cyto-Therapeutics.



## REFERENCES

- Aloisi F, Giampalao A, Russo G, Paschle C, Levi G (1992): Developmental appearance, antigenic profile, and proliferation of glial cells of the human embryonic spinal cord: an immunocytochemical study using dissociated cultured cells. *Glia* 5:171-181.
- Archer DR, Leven S, Duncan ID (1994): Myelination by cryopreserved xenografts and allografts in the myelin-deficient rat. *Exp Neurol* 125:268-277.
- Archer DR, Cuddon PA, Lipsitz D, Duncan ID (1997): Myelination of the canine central nervous system by glial cell transplantation: a model for repair of human myelin disease. *Nat Med* 3:54-59.
- Armstrong R, Dorn HL, Kufia CV, Friedman E, Dubois-Dalq ME (1992): Pre-oligodendrocytes from adult human CNS. *J Neurosci* 12:1538-1547.
- Barras BA, Raff MC (1993): Proliferation of oligodendrocyte precursor cells depends on electrical activity in axons. *Nature* 361:258-260.
- Bartcu PF, Rosenfeld J, Bailey KA, Cheesman H, Harvey AR, Kerr RSC (1990): Allograft rejection overcome by immunoselection of neuronal precursor cells. *Prog Brain Res* 82:153-160.
- Blakemore WF, Crang AJ (1983): The effect of chemical injury on oligodendrocytes. In Cuzner ML, Kelly RE (eds): "Viruses and Demyelinating Diseases." London: Academic Press, pp 167-190.
- Blakemore WF, Crang AJ, Franklin RJM (1995): Transplantation of glial cells. In Ransom BR, Kettenmann H (eds): "Neuroglial Cells." New York: Oxford University Press, pp 869-882.
- Bogler O, Wren D, Burnett SC, Land H, Noble M (1990): Cooperation between two growth factors promotes extended self-renewal and inhibits differentiation of oligodendrocyte-type-2 astrocyte (O-2A) progenitor cells. *Proc Natl Acad Sci USA* 87:6368-6372.
- Dickson JG, Kesselring J, Walsh FS, Davison AN (1985): Cellular distribution of O4 antigen and galactocerebroside in primary cultures of human fetal spinal cord. *Acta Neuropathol (Berl)* 68:340-344.
- Duncan ID (1995): Inherited disorders of myelination of the central nervous system. In Ransom BR, Kettenmann H (eds): "Neuroglial Cells." New York: Oxford University Press, pp 990-1009.
- Duncan ID (1996): Glial cell transplantation and remyelination of the CNS. *Neuropathol App Neurobiol* 22:87-100.
- Duncan ID, Milward FA (1995): Glial cell transplants: experimental therapies of myelin diseases. *Brain Pathol* 5:301-310.
- Duncan ID, Griffiths IR, Munz M (1983): Shaking pups: a disorder of central myelination in the spaniel dog. III. Quantitative aspects of glia and myelin in the spinal cord and optic nerve. *Neuropathol App Neurobiol* 9:355-368.
- Franklin RJM, Blakemore WF (1995): Glial-cell transplantation and plasticity in the O-2A lineage—implications for CNS repair. *Trends Neurosci* 18:151-156.
- Franklin RJM, Bayley SA, Milner R, French-Constant C, Blakemore WF (1995): Differentiation of the O-2A progenitor cell line CG-4 into oligodendrocytes and astrocytes following transplantation into glia-deficient areas of CNS white matter. *Glia* 13:39-44.
- Franklin RJM, Bayley SA, Blakemore WF (1996): Transplanted CG-4 cells (on oligodendrocyte progenitor cell line) survive, migrate and contribute to the repair of areas of demyelination in X-irradiated and damaged spinal cord but not in normal spinal cord. *Exp Neurol* 137:263-276.
- Gogate N, Verma L, Zhou J-M, Milward E, Rusten R, O'Connor M, Kufia C, Kim J, Hudson L, Dubois-Dalq M (1994): Plasticity in the adult human oligodendrocyte lineage. *J Neurosci* 14:4571-4587.
- Griffiths IR, Duncan ID, McCulloch M, Harvey MJA (1981): Shaking pups: a disorder of central myelination in the spaniel dog. I. Clinical, genetic and light microscopical observations. *J Neurol Sci* 50:423-433.
- Hammang JP, Reynolds BA, Weiss S, Messing A, Duncan ID (1994): Transplantation of epidermal growth factor-responsive neural stem cell progeny into murine central nervous system. *Methods Neurosci* 21:281-293.
- Hammang JP, Archer DR, Duncan ID (1997): Myelination following transplantation of EGF-responsive neural stem cells into a myelin-deficient environment. *Exp Neurol* 141:502-508.
- Hardy R, Reynolds R (1993): Rat cerebral cortical neurons in primary culture release a mitogen specific for early (G13+/U4-) oligodendroglial progenitors. *J Neurosci Res* 34:589-600.
- Hoffman KL, Duncan ID (1995): Canine oligodendrocytes undergo morphological changes in response to basic fibroblast growth factor (bFGF) in vitro. *Glia* 14:33-42.
- Johann SV, Gibbons JJ, O'Hara B (1992): GLVR1, a receptor for gibbon ape leukemia virus, is homologous to a phosphate permease of *Neurospora crassa* and is expressed at high levels in the brain and thymus. *J Virol* 66:1635-1640.
- Kavanagh MP, Miller DG, Zhang W, Law W, Kovak SL, Kahar D, Miller AD (1994): Cell-surface receptors for gibbon ape leukemia virus and amphotropic murine retrovirus are inducible sodium-dependent phosphate symporters. *Proc Natl Acad Sci USA* 91:7071-7075.
- Kennedy PGE, Lisak RP, Raff MC (1980): Cell type-specific markers for human glial and neuronal cells in culture. *Lab Invest* 43:342-351.
- Kilpatrick TJ, Bartlett PF (1995): Cloned multipotential precursors from the mouse cerebellum require FGF-2, whereas glial restricted precursors are stimulated with either FGF-2 or EGF. *J Neurosci* 15:3653-3661.
- Lillien L, Cepko C (1992): Control of proliferation in the retina: temporal changes in responsiveness to FGF and TGF $\alpha$ . *Development* 115:253-266.
- Lipsitz D, Archer DR, Duncan ID (1995): Acute dispersion of glial cells following transplantation into the myelin-deficient rat spinal cord. *Glia* 14:237-242.
- McKinnon RD, Matsui T, Dubois-Dalq M, Aaronson SA (1990): FGF modulates the PDGF-driven pathway of oligodendrocyte development. *Neuron* 5:603-614.
- Miller AD, Garcia JV, von Suhr N, Lynch CM, Wilson C, Eiden MV (1991): Construction and properties of retrovirus packaging cells based on gibbon ape leukemia virus. *J Virol* 65:2220-2224.
- Miller AD, Miller DG, Garcia VJ, Lynch CM (1993): Use of retroviral vectors for gene transfer and expression. *Methods Enzymol* 217:581-599.
- Nadon NL, Duncan ID, Hudson LD (1990): A point mutation in the proteolipid protein gene of the "shaking pup" interrupts oligodendrocyte development. *Development* 110:529-537.
- Raff MC, Abney ER, Fok-Seang J (1985): Reconstitution of a developmental clock in vitro: a critical role for astrocytes in the timing of oligodendrocyte differentiation. *Cell* 42:61-69.
- Ranscht B, Clapham PA, Price J, Noble M, Seifert W (1982): *Proc Natl Acad Sci USA* 79:2709-2713.
- Ray J, Gage FH (1994): Spinal cord neuroblasts proliferate in response to basic fibroblast growth factor. *J Neurosci* 14:3548-3564.

- Reynolds BA, Weiss S (1992): Generation of neurons and astrocytes from isolated cells of the adult mammalian central nervous system. *Science* 255:1707-1710.
- Reynolds BA, Weiss S (1996): Clonal and population analyses demonstrate that an EGF-responsive mammalian embryonic CNS precursor is a stem cell. *Dev Biol* 175:1-13.
- Reynolds BA, Tetzlaff W, Weiss S (1992): A multipotent EGF-responsive striatal embryonic progenitor cell produces neurons and astrocytes. *J Neurosci* 12:4565-4574.
- Richards LJ, Kilpatrick TJ, Bartlett PF (1992): De novo generation of neuronal cells from the adult mouse brain. *Proc Natl Acad Sci USA* 89:8591-8595.
- Richardson WD, Pringle N, Mosley MJ, Westmark B, Dubois-Dalcq M (1988): A role for platelet-derived growth factor in normal gliogenesis in the central nervous system. *Cell* 53:309-319.
- Sato J, Kim SU (1994): Proliferation and differentiation of fetal human oligodendrocytes in culture. *J Neurosci Res* 39:260-272.
- Scolding NJ, Ruyner PJ, Sussman J, Shaw C, Compston DAS (1995): A

## EGF Responsive Canine Neural Progenitors 871

- proliferative adult human oligodendrocyte progenitor. *NeuroReport* 6:441-445.
- Sommer I, Schachner M (1981): Monoclonal antibodies (O1-O4) to oligodendrocyte cell surfaces: an immunological study in the central nervous system. *Dev Biol* 83:311-327.
- Tontsch U, Archer DR, Dubois-Dalcq M, Duncan ID (1994): Transplantation of an oligodendrocyte cell line leading to extensive myelination. *Proc Natl Acad Sci* 91:11616-11620.
- Vescovi AL, Reynolds BA, Fraser DD, Weiss S (1993): Basic fibroblast growth factor regulates the proliferative fate of both unipotent (neuronal) and bipotent (neuronal/astroglial) epidermal growth factor-generated progenitor cells. *Neuron* 11:951-966.
- Yong VW, Antel JP (1993): Culture of glial cells from human brain biopsies. In Fedoroff S, Richardson A (eds): "Protocols for Neural Cell Culture." New York: The Humana Press Inc., pp 81-95.
- Yong VW, Kim SU, Kim MW, Shin DH (1988): Growth factors for human glial cells in culture. *Glia* 1:113-123.

## Adult brain retains the potential to generate oligodendroglial progenitors with extensive myelination capacity

SU-CHUN ZHANG\*, BIN GE, AND IAN D. DUNCAN

Department of Medical Sciences, School of Veterinary Medicine, University of Wisconsin, 2015 Linden Drive West, Madison, WI 53706

Communicated by William F. Dove, University of Wisconsin, Madison, WI, February 4, 1999 (received for review August 27, 1998)

**ABSTRACT** Remyelination of focal areas of the central nervous system (CNS) in animals can be achieved by transplantation of glial cells, yet the source of these cells in humans to similarly treat myelin disorders is limited at present to fetal tissue. Multipotent precursor cells are present in the CNS of adult as well as embryonic and neonatal animals and can differentiate into lineage-restricted progenitors such as oligodendroglial progenitors (OPs). The OPs present in adults have a different phenotype from those seen in earlier life, and their potential role in CNS repair remains unknown. To gain insights into the potential to manipulate the myelinating capacity of these precursor and/or progenitor cells, we generated a homogenous culture of OPs from neural precursor cells isolated from adult rat subependymal tissues. Phenotypic characterization indicated that these OPs resembled neonatal rather than adult OPs and produced robust myelin after transplantation. The ability to generate such cells from the adult brain therefore opens an avenue to explore the potential of these cells for repairing myelin disorders in adulthood.

Remyelination of the central nervous system (CNS) in patients where host remyelination fails or where the endogenous myelinating cells are genetically impaired may be achieved, at least focally, by glial cell transplantation. It has been assumed that human fetal brain will be the only viable source of myelinating cells for human transplantation, because oligodendroglial progenitors (OPs) derived from embryonic animals have a greater capacity for myelination than mature cells after transplantation (1, 2). However, the availability of human fetal tissues remains a practical and ethical concern, and it would be preferable if the neonatal or adult human brain could be used as a source of myelinating cells. It has been established that OPs are present in adult human brain (3). Such cells have also been described in patients with multiple sclerosis (4) and in rodents with chronic experimental allergic encephalomyelitis (5). Despite their presence in chronic multiple sclerosis lesions, remyelination may be inadequate (6, 7), and either exogenous myelinating cells must be targeted to lesions or host cells must be recruited to aid in repair.

Two types of OP [also designated *in vitro* as oligodendrocyte type-2 astrocyte (O2A) progenitor] exist in the CNS; the neonatal OP (O2A<sup>perinatal</sup>) that appears in the rat postnatally and disappears about 6 weeks after birth, and the adult OP (O2A<sup>adult</sup>) (8, 9). The O2A<sup>adult</sup>, which is identified by the mAb O4 *in situ* and *in vitro*, has a phenotype that distinguishes it from its neonatal counterpart. The most thoroughly characterized O2A<sup>adult</sup> cells are those isolated from adult rat optic nerves, although similar cells are found in other parts of the CNS such as the spinal cord (10). Unlike the O2A<sup>perinatal</sup>, the O2A<sup>adult</sup> does not express the intermediate filament vimentin or a ganglioside recognized by the mAb A2B5. The O2A<sup>adult</sup> cells also have a longer cell cycle time ( $65 \pm 18$  h) and are less

motile ( $4 \pm 1 \mu\text{m/h}$ ) than O2A<sup>perinatal</sup> (9). These characteristics suggest that they would only have a limited capacity to remyelinate demyelinated areas of the brain. In fact, it is not yet known whether these cells produce myelin *in vivo*, for example, after transplantation.

The OPs are generally thought to be derived from multipotent neural precursor cells or early progenitor cells in the CNS. Neural stem cells, which can give rise to both neurons and glia, have been found in the CNS of both embryonic and mature animals (11, 12). Clonal analyses suggest that the stem cells from adult CNS are similar to those of embryonic origin (11). At least, these adult stem cells can differentiate into neurons, astrocytes, and oligodendrocytes *in vitro*. It is not yet known whether adult stem cells differentiate into O2A<sup>adult</sup> directly.

We have been studying the transition from multipotent precursor cells to lineage-restricted OPs and have shown that it is possible to generate a large number of self-renewing OPs from neural precursor cells derived from embryonic and neonatal brain (13, 14). Because multipotent stem cells exist in adult CNS, we sought to explore whether the OPs derived from adult neural stem or precursor cells have the capacity for extensive myelination. If this were proven in the rodents, a similar approach could provide cells for transplantation or suggest means for the induction of endogenous progenitors to enhance host repair in humans.

### MATERIALS AND METHODS

**Cell Culture.** The neural precursor cells in suspension culture ("neurospheres") were prepared from subependymal striata of Wistar rats aged 3 and 16 months according to a protocol detailed previously (13, 15). The culture medium was DMEM/F-12 (1:1) supplemented with insulin (25  $\mu\text{g/ml}$ ), transferrin (100  $\mu\text{g/ml}$ ), progesterone (20 nM), putrescine (60  $\mu\text{M}$ ), and sodium selenite (30 nM). The above medium, referred to as "neurosphere medium," was supplemented with 20 ng/ml human recombinant epidermal growth factor (EGF) or EGF plus 20 ng/ml of basic fibroblast growth factor (bFGF) (Collaborative Biomedical Products, Bedford, MA). In the initial week of culture, B27 (GIBCO) was added to the above medium. The cultures were incubated in a humidified atmosphere of 5% CO<sub>2</sub>/95% air with a partial medium change every other day.

The B104 neuroblastoma cells were cultured according to Louis *et al.* (16), and the conditioned medium (B104CM) was collected and filtered after 3 days of conditioning the B104 cells with serum-free "neurosphere medium."

**BrdUrd Incorporation Assay.** The coverslip cultures were incubated in 10  $\mu\text{M}$  BrdUrd (Sigma) for various periods (see

**Results**), fixed in acidic ethanol, and immunostained with anti-BrdUrd antibody (Amersham Pharmacia) at a dilution of 1:10, followed by fluorescein-labeled secondary antibody. For cell cycle time estimation, the cultures were exposed to BrdUrd for a period of 0.5, 1, 3, 5 and up to 16–24 h. The BrdUrd-labeled cells and the total cells stained with Hoechst were counted under a fluorescent microscope. The percentage of the labeled cells was plotted against the time the cells were pulsed, and the cell cycle time was estimated according to the graphic method of Sasaki *et al.* (17).

**Assay of Cell Migration.** A single sphere was plated onto ornithine-coated 35-mm dishes in a drop of medium. After the sphere attached (10–15 min), 1.5 ml of medium was added gently. Only the samples with successfully attached sphere and without floating cells were followed at 4, 8, and 24 h postplating. The outgrowth of the sphere was examined under the phase-contrast microscope, and the images were photographed and stored in a computer. The longest distance from the edge of a sphere to the cell body in each quarter of the outgrowth was measured and the average distance of cells moved out of a single sphere at specific time points was calculated (13). At least 8 spheres were followed throughout the period of each individual experiment, and the experiment was repeated twice.

**Immunocytochemistry.** Free-floating spheres or coverslip cultures were immunolabeled with fluorescein-tagged secondary antibodies (Jackson ImmunoResearch) according to the procedure detailed previously (13). The following primary antibodies were used. Monoclonal antibody anti-nestin (IgG) was a supernatant of mouse hybridoma rat401 (diluted 1:5), provided by Developmental Studies Hybridoma Bank (The Johns Hopkins University, Baltimore). A2B5 was a culture medium of mouse hybridoma clone 105 (American Type Culture Collection, CRL-1520, used at 1:100 dilution). O4 and O1 (both were IgM) were provided by M. Schachner. Anti-myelin basic protein (MBP, mouse IgG, 1:100) was from Boehringer Mannheim. Anti-vimentin (mouse IgG) and anti- $\beta$ III-tubulin (rabbit IgG) were purchased from Sigma (1:100). Polyclonal antibodies anti-glial fibrillary acidic protein (GFAP, 1:200) was purchased from Dako, and anti-platelet-derived growth factor receptor  $\alpha$  (PDGFR $\alpha$ , 1:100) was from Santa Cruz Biotechnology.

**Transplantation of Oligosphere Cells.** The oligospheres were triturated into single cells and were then concentrated to 50,000 cells per microliter. One microliter of cell suspension was transplanted into the spinal cord of postnatal day 6–8 myelin-deficient (*md*) rats according to the procedure described (13, 18). The injection site was marked with sterile charcoal before the incision was sutured.

Twelve to fourteen days after transplantation, the recipient rats were anesthetized with pentobarbital (i.p.) and perfused with 4% formaldehyde. The spinal cord was dissected and the white streak representing myelin made by the transplanted cells was measured. The spinal cords were then trimmed for immunostaining with anti-proteolipid protein (PLP, a gift from I. R. Griffiths, University of Glasgow) or for resin-embedding as described (13, 14).

## RESULTS

**Establishment of OP Cultures from Adult Rats.** The OPs were generated from neural precursors by using the approach described (13, 14). In the present study, cultures of neurospheres were initiated from subependymal striata of adult Wistar rats (aged 3 and 16 months). When cultured in the presence of EGF and absence of substrate, scattered phase-bright cells were found among debris at 4–7 days *in vitro* (DIV). These few cells grew into spheres in the subsequent 2–3 weeks. These spheres were triturated into single cells and expanded in the presence of EGF alone or EGF plus bFGF.

Expanded neurosphere cells were immunopositive for nestin (Fig. 1 *a* and *b*), an intermediate filament protein mainly expressed by stem or precursor cells (19). When plated on poly(ornithine)-coated coverslips in the presence of 1% FBS but the absence of EGF or bFGF, the neurosphere cells migrated out and differentiated into a mixture of mainly astroglia (GFAP+) with flattened cell bodies and thick processes and some oligodendroglia (O4+). Some spheres also contained neurons that were  $\beta$ III-tubulin+ (data not shown). The neurospheres were triturated into single cells and passaged in neurosphere medium with the presence of EGF and bFGF. These observations suggest that neurosphere cells are undifferentiated neural precursor cells, similar to those isolated from embryonic and neonatal striatum (13, 14).

To generate OPs from neurospheres, we gradually changed the EGF-containing medium to B104CM-containing medium by replacing one-fourth of the former medium with the latter medium every other day. During the transition period (1–2 weeks), the number and size of spheres did not increase. This is similar to the phenomenon observed in the neurosphere cultures from neonatal rat (13). By week two, the size and number of spheres began to increase. Three to four weeks later, the cultures were passaged in medium containing B104CM (30%) but no EGF or bFGF by plating  $1 \times 10^6$  cells into a 75-cm<sup>2</sup> flask. New spheres with various sizes formed in

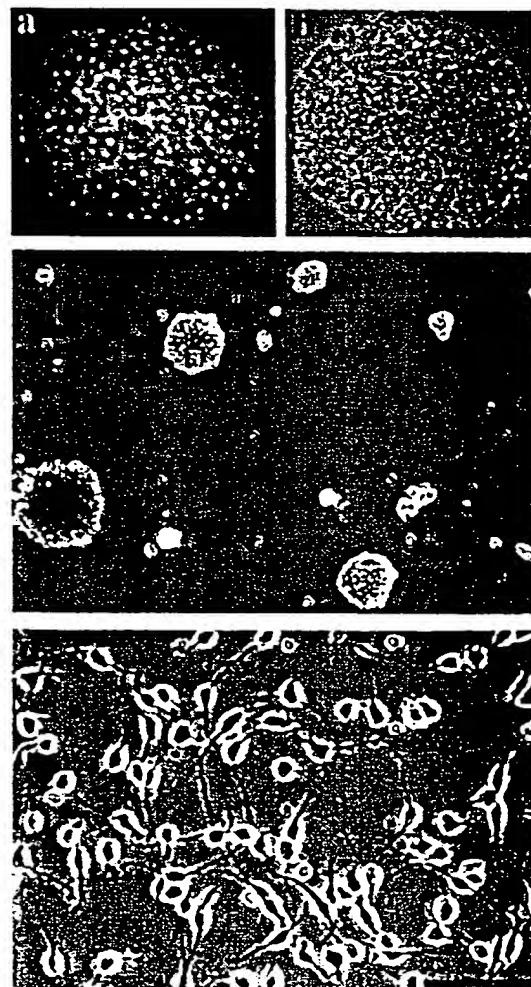


FIG. 1. A neurosphere (from 16-month-old rat) grown in the presence of EGF immunostained with nestin indicated that all cells were nestin+ (*a*). *b* shows the phase-contrast image of *a*. (*c*) New spheres were generated from disaggregated oligosphere cells. (*d*) Disaggregated oligosphere cells displayed bipolar or tripolar morphology in the presence of B104CM. (Bar = 100  $\mu$ m.)

1 week (Fig. 1c). When the spheres were triturated into single cells and plated onto ornithine-coated coverslips, all cells displayed bipolar or tripolar morphology, typical of O2A progenitors (Fig. 1d). Therefore, the spheres were now referred to as "oligospheres," a term that was first used by Evercooren and colleagues (24). Similar results were obtained when generating oligospheres from neurospheres that were derived from both 3-month- and 16-month-old rat brains by using the same protocol.

**Antigenic Expression of Oligosphere Cells.** The O2A<sup>perinatal</sup> displays a bipolar morphology and is positive for A2B5, whereas the O2A<sup>adult</sup> is unipolar and O4+ (9). In contrast to the O2A<sup>adult</sup> previously derived from the adult optic nerve, all oligosphere cells exhibited bi- or tripolar morphology and expressed vimentin, A2B5, and PDGFR $\alpha$  (Fig. 2a–c) when the oligospheres were disaggregated and cultured on ornithine-coated coverslips at a density of  $1 \times 10^5$  per coverslip in the presence of B104CM. These cells were negative for O4 (Fig.

2d). Within a week, the cultures were confluent. Similar results were obtained when the cells were cultured in the presence of both PDGF (10 ng/ml) and bFGF (20 ng/ml) except that they did not reach confluency until about 10 DIV. When the cells were cultured in the presence of PDGF alone with addition of PDGF every other day for 7 DIV, many cells were still bipolar or tripolar (Fig. 2e) and the majority were positive for A2B5 ( $90.9 \pm 2.4\%$ ;  $n = 5$ ), vimentin, and PDGFR $\alpha$ . A small number of cells ( $5.2 \pm 3.0\%$ ;  $n = 5$ ), however, became multiprocess-bearing and O4+. In addition, some cells were round without processes. These round cells were positive for A2B5 and vimentin but negative for O4, similar to those seen in the presence of B104CM.

**Differentiation of Oligosphere Cells.** The O2A<sup>adult</sup> cells differentiate more slowly than their neonatal counterparts (9). To assess the potential and speed of differentiation, oligosphere cells were cultured in the medium consisting of DMEM and 0.5% FBS. The cultures were immunostained with O4, O1,

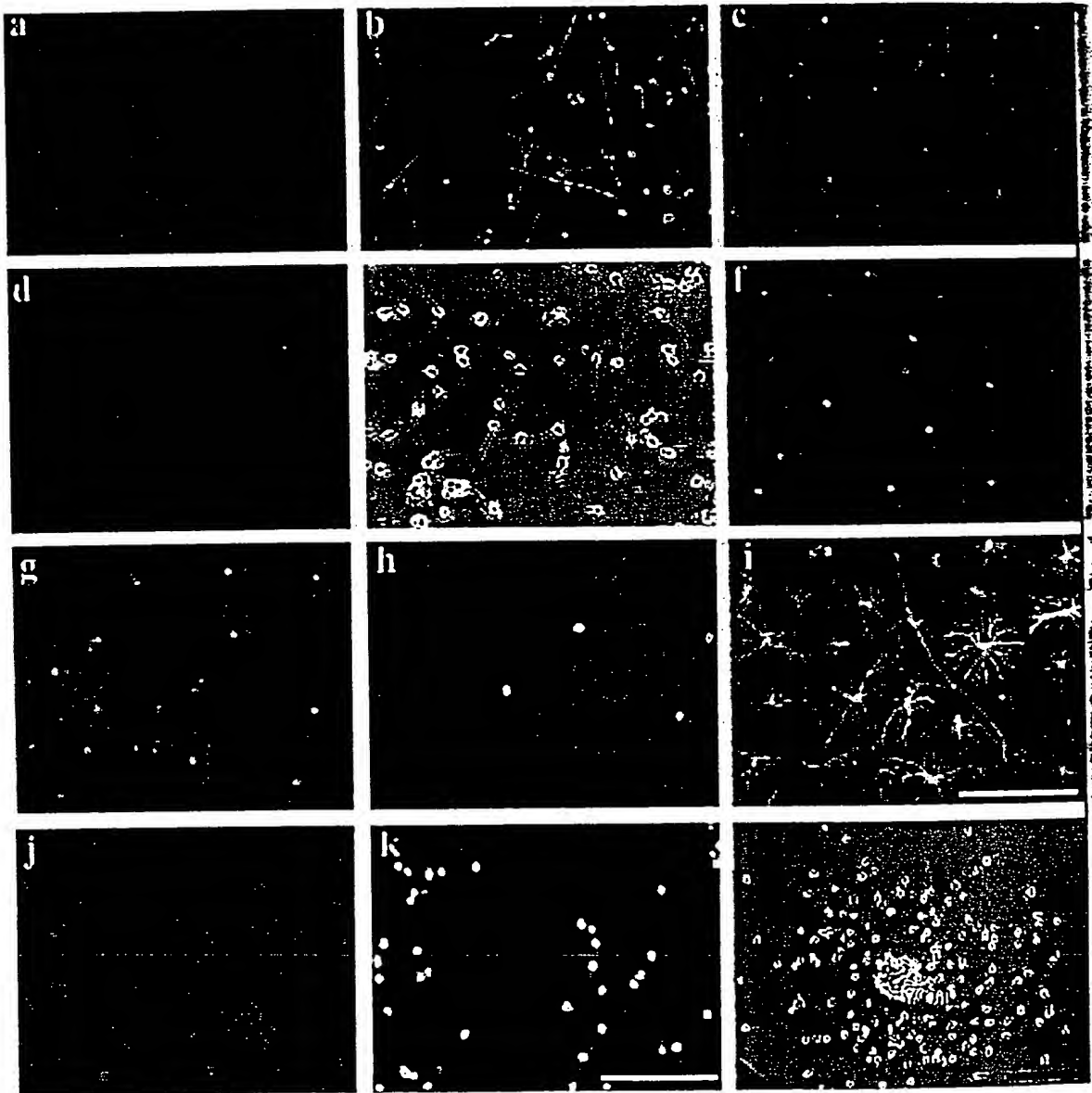


FIG. 2. The oligosphere cells cultured on ornithine-coated coverslips in the presence of B104CM were positive for vimentin (a), A2B5 (b), and PDGFR $\alpha$  (c) but negative for O4 (d). In the presence of PDGF alone for 7 DIV, the oligosphere cells were largely bipolar or tripolar. There were also round cells (arrowheads) and a few multiprocess-bearing cells (arrows) (e). In the presence of 0.5% FBS for 2 DIV, all cells were O4+ (f) and many cells were O1+ (g). At 7 DIV, cells were MBP+ (h). In the presence of 10% FBS, almost all cells were positive for GFAP (i) and A2B5+ (j). Incubation of the culture with BrdUrd for 20 h indicated that the majority of cells were labeled in the nuclei (yellow in k). All cells were A2B5+ (red in k). (l) A single sphere plated on ornithine-coated dish in the presence of B104CM for 24 h shows that bipolar cells migrated out of the sphere. The nuclei of cells in (f–h) were stained with 4',6-diamidino-2-phenylindole (DAPI). (Bar = 100  $\mu$ m.)

and anti-MBP antibodies, which recognize progressively later developmental stages of oligodendroglial lineage. At 2 DIV, virtually all of the cells were O4+ (Fig. 2f). At the same time,  $57.5 \pm 4.4\%$  ( $n = 6$ ) of the cells were already O1+, although the staining was mainly in the cell bodies and main processes (Fig. 2g). At 3 DIV, the majority of cells were O1+. At 5–7 DIV, most cells were positive for MBP, displaying membrane-like structures (Fig. 2h). In the presence of high concentrations of FBS (5–10%), the majority of cells were flattened, with star-shaped processes, and expressed both GFAP (Fig. 2i) and A2B5 (Fig. 2j). Similar results were obtained when oligosphere cells of passage 4 or 12 from both ages were examined.

**Proliferation Potential.** When  $1 \times 10^6$  oligosphere cells were plated in the presence of 30% B104CM,  $(8.8 \pm 1.2) \times 10^6$  ( $n = 3$ ) cells were obtained in 7 DIV. A similar number of cells were generated when oligospheres from passage 2–12 were examined. The oligospheres could also be expanded in the presence of PDGF plus bFGF, although the yield was lower.

The cell cycle time for oligosphere cells in the presence of B104CM was estimated by using the graphic method described by Sasaki (17). The phase of DNA synthesis was deduced as 6.8–8.4 h from the linear regression of BrdUrd incorporation over incubation time (based on three independent experiments). The total cell cycle time was estimated to be about 20 hours. Incubation of the cells with BrdUrd for 20 h led to  $\approx 92\%$  of the cells labeled with anti-BrdUrd (Fig. 2k).

To assess the proliferation potential of oligosphere cells in response to growth factors, oligospheres (passage 4 and 10) were triturated and cultured for 3 days on coated coverslips in the presence of B104CM (30% vol/vol), bFGF (20 ng/ml), PDGF (10 ng/ml), and PDGF plus bFGF. The cultures were then exposed to BrdUrd for 4 h, and the incorporation of BrdUrd into nuclei was assessed. Without the presence of B104CM or above growth factors, cells differentiated into oligodendrocytes (O1+) and did not incorporate BrdUrd. In the presence of B104CM or growth factors, cells incorporated BrdUrd into their nuclei. The highest percentage of cells incorporating BrdUrd were the cells treated with B104CM (46%), followed by bFGF plus PDGF, bFGF, and PDGF (Table 1). This pattern of growth response of oligosphere cells is similar to that of O2A<sup>perinatal</sup> cells in response to growth factors (20, 21).

To examine whether a single cell can renew itself and regenerate an oligosphere, a single sphere cell was plated in each well of a 96-well plate containing 200  $\mu$ l of B104CM (30%)-containing neurosphere medium (13). After 7 days, the plates were reexamined, and the wells containing sphere(s) were marked. The percentage of the cells able to generate new sphere(s) was  $\approx 29\%$  (32/111). The clonally expanded cells retained the same potential to differentiate into oligodendroglia or type-2 astroglia *in vitro* (see above). Similar results were obtained when a single cell was plated into ornithine-coated 96-well plate except that the generated cells did not form a sphere (data not shown).

**Migration of Oligosphere Cells.** After the oligosphere attached, individual cells migrated out of the sphere within 1 h. At 4 h post-plating, cells were found surrounding the whole sphere. The migration velocity was calculated based on the average distance of cells moving away from the sphere at 4, 8, 12, and 24 hours post-plating. Migration velocity was  $25 \pm 5.4$   $\mu$ m/h ( $n = 10$ ) in the presence of B104CM and  $13.5 \pm 1.7$

$\mu$ m/h ( $n = 8$ ) in the presence of PDGF (10 ng/ml) for oligospheres (passage 8) derived from the 3-month-old rat. Cells migrating out of the sphere were bipolar (Fig. 2l). Unlike the oligosphere cells derived from neonatal rat, the pattern of migration was not always radially oriented. Similar results were obtained when spheres from the 16-month-old rat (passage 6) were examined.

**Myelination Potential by Oligosphere Cells.** Oligosphere cells of passage 8 from a 16-month-old rat and passage 4 and 12 derived from a 3-month-old rat were transplanted into the spinal cords of 24 *md* rats. Twelve to fourteen days after transplantation, a white streak, of average 4 mm (3.0–6.5 mm) in length, was present in the dorsal column of the spinal cord of the *md* rat, which is otherwise semitranslucent because of the lack of myelin (Fig. 3a). A white streak of  $3.9 \pm 1.25$  mm ( $n = 7$ ) formed by cells of passage 4 and  $3.8 \pm 1.5$  mm ( $n = 8$ ) formed by cells of passage 12 that were both derived from the 3-month-old rat. When cells (passage 8) from the 16-month-old rat were transplanted, a white streak of  $4.2 \pm 1.0$  mm ( $n = 9$ ) formed. There was no difference in the degree of longitudinal spread of transplanted cells and myelination by cells from both ages or cells from passage 4 and 12. A cross section of the spinal cord indicated that the white patch occupied most of the dorsal funiculus. Immunostaining of the spinal cord sections indicated that the myelin sheaths formed by the transplanted cells were positive for PLP (Fig. 3b) as well as for MBP (data not shown). The host spinal cord lacks PLP-positive myelin because of a mutation in the PLP gene (22), although PLP+ oligodendrocytes were detected in freshly prepared tissues (Fig. 3b). Toluidine blue-stained semithin sections (1  $\mu$ m) confirmed that the majority of axons in the dorsal funiculus were myelinated (Fig. 3c). There was no obvious difference between the samples with cells from different ages in terms of the amount of myelin that are present in the transverse section.

## DISCUSSION

The major finding of this study is that the adult brain can be used as a source of OPs with the O2A<sup>perinatal</sup> phenotype and that these cells can be propagated extensively to generate a large number of progenies that maintain their myelinating potential. If similar approaches were feasible in humans, it would be possible to generate large numbers of cells by *ex vivo* manipulation with growth factors, before transplantation. Similarly, it raises the possibility that such cells might be induced to expand by *in vivo* growth factor application and be recruited to target areas of demyelination in the human brain.

**Oligosphere Cells Derived from Adult Brain Resemble O2A<sup>perinatal</sup> Cells.** O2A<sup>perinatal</sup> cells can be isolated and expanded from neonatal rodents by using growth factors or conditioned media when the cells are in peak proliferation (23–25). We have explored alternative means of deriving such cells from multipotential neural precursor cells isolated from neonatal (13) or embryonic rat brains (S.-C.Z., unpublished data) by analogy to the hematopoietic cell lineage development (26). Because multipotential precursor cells exist in the CNS of adult (11, 15) as well as in embryonic stage (12), it is possible that OPs may be generated from adult CNS precursor cells as well. Therefore, the establishment of a homogeneous population of OPs from adult neural precursors was not unexpected. However, that all of the cells were positive for vimentin and A2B5 but negative for O4 contrasts with the antigenic phenotype of the O2A<sup>adult</sup> as isolated directly from adult rat optic nerves (9). More importantly, the oligosphere cells proliferate much more vigorously and differentiate and migrate faster than the O2A<sup>adult</sup> progenitors detailed in a series of studies performed by Noble and colleagues (9, 28–30). Therefore, the OPs from adult neural precursor cells resemble neonatal rather than adult O2As isolated directly

Table 1. BrdUrd incorporation by oligosphere cells

	PDGF	bFGF	PDGF/bFGF	B104CM
BrdUrd+, %	$29.5 \pm 2.84$	$34.2 \pm 2.27$	$36.9 \pm 3.25$	$46 \pm 4.13$

BrdUrd+ cells and total cells were counted in four optic fields of each coverslip. Each group consisted of at least four coverslips. Total cell counts in each group were 3,300–3,965. The data were from the experiment with passage 4 cells derived from a 3-month-old rat.



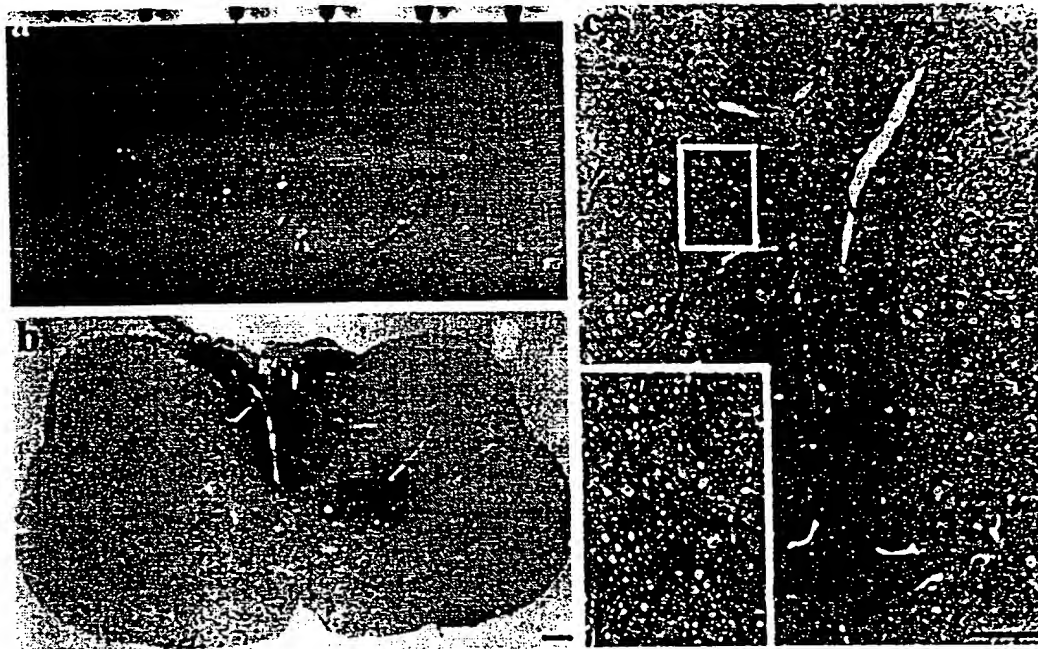


FIG. 3. Transplantation of oligosphere cells from a 16-month-old rat into *md* rats. Twelve to fourteen days later, a white streak of myelin was seen along the dorsal surface of the cord (*a*). The black dots are sterile charcoal marking the injection site. The space bar on top represents 1 mm. (*b*) Immunostaining of the transplanted cord showed PLP+ myelin in the dorsal funiculus with some myelin also appeared in the gray matter. Other areas of the spinal cord showed no PLP+ myelin except the PLP+ cell bodies. (*c*) Semithin sections stained with toluidine blue demonstrated that the dorsal funiculus was occupied by a large number of myelin sheaths. Inset is the enlargement of the boxed area in *c*. (Bar = 100  $\mu$ m.)

from rat optic nerves. This conclusion is further supported by the antigenic expression and proliferation potential of oligosphere cells when they were cultured in the presence of PDGF instead of B104CM, a culture condition similar to that under which O2A<sup>adult</sup> cells were characterized (9, 27). It should be noted that the population expansion does not parallel the cell cycle time of oligosphere cells. This is mainly due to cell death after mechanical disaggregation and death within spheres. The slower migration in the presence of PDGF alone is potentially accounted for by the techniques used and the growth factors present. Small *et al.* (27) measured the distance a cell moved (in all directions) directly by time-lapse cinematography. We could only measure the linear distance away from the sphere. In the presence of B104CM, the adult oligosphere cells migrated in a similar velocity as neonatal oligosphere cells (13). This result suggests that adult oligosphere cells are similarly motile to neonatal oligosphere cells and that factors other than PDGF also contribute to the migration of OPs. This is further supported by the similar extent of myelination by transplanted adult oligosphere cells as by neonatal oligosphere cells (13) or by the CG4 oligodendroglial progenitor cell line (18).

**Oligosphere Cells Are Derived from Neural Precursor Cells.** The O2A<sup>adult</sup> are derived from their neonatal counterparts (29, 31) and may regain the neonatal phenotype temporarily under certain circumstances, such as in the presence of both bFGF and PDGF (30, 32). Is the generation of neonatal-type OPs in the present study attributable to B104CM converting the adult OPs into neonatal progenitors? Our finding does not support this possibility, because the source cells (neurospheres) are nestin+ and the replacement of B104CM with PDGF in oligosphere cell cultures does not lead to the expression of the O2A<sup>adult</sup> phenotype. We have attempted to generate oligospheres directly from (mechanically and enzymatically) dissociated adult (5-month-old) rat brain and optic nerves by using B104CM. The resultant culture contained floating cells that survived for up to 2 weeks in suspension but did not proliferate (data not shown). A recent observation also indicated that B104CM did not enhance the proliferation of purified O2A<sup>adult</sup> progenitors (31) or convert the O2A<sup>adult</sup> to O2A<sup>perinatal</sup> (B. A.

Barres, personal communication). B104CM is a potent mixture in selecting and propagating O2A<sup>perinatal</sup> in culture (23–25). It may be speculated that some O2A<sup>perinatal</sup> are selectively expanded by B104CM in the present study. The presence of O2A<sup>perinatal</sup> in the adult CNS was reported based on their bipolar morphology and A2B5 positivity in a mixed culture (33). However, when the mixed glial cultures were irradiated, no O2A<sup>perinatal</sup> developed (34), implying that in that study, O2A<sup>perinatal</sup> cells were being generated *de novo* from A2B5-negative progenitor cells that were also present in the cultures. In a purified culture system, the O2A cells from adult (2-month-old) rat optic nerve displayed bipolar morphology and were immunoreactive to A2B5 (31), similar to those reported by French-Constant and Raff (33). Yet they had a very slow turnover rate (cell cycle time around 3 days), characteristic of O2A<sup>adult</sup> cells. In our preparation of neurosphere cultures, these rare O2A<sup>perinatal</sup> (if they are present) would be unlikely to survive in the condition without substrate and survival factors such as PDGF for a long time (>4 weeks). Our previous study (13) indicated that EGF is not a survival factor for OPs in suspension cultures. Our failure to generate oligospheres directly from dissociated adult brain and optic nerves suggests that either there are no O2A<sup>perinatal</sup> present or such cells do not survive the procedure and culture condition. Therefore, the cells used for generating OPs are unlikely to contain cells that are already in the oligodendroglial lineage. Thus, the present study extends our previous argument that factors in B104CM may induce neural precursor cells to commit to oligodendroglial lineage while at the same time maintain the OPs in a state of self-renewal (13).

**Multipotent Neural Precursor Cells as a Source for Remyelination.** The generation and extensive propagation of the neonatal type of OPs from the adult rat brain has an important impact on the design of strategies for promoting remyelination *in vivo*. In the first instance, as we show here, it may be possible to similarly derive progenitor cells of the neonatal phenotype from the adult human brain for transplantation. Extensive animal studies suggest that transplantation of myelinating cells, especially their progenitor cells, may be an effective



approach (1, 2, 36, 37). In clinical human trials, however, cell availability becomes a problem if the cells are to be obtained from a source other than the patient. At present, human fetal tissues are the only source of immature neural cells. However, there are long-term practical and ethical concerns on the availability of such tissue, including stringent safety concerns. Here we show that it is possible to generate a large number of OPs from a small source of tissue in the rodent brain. A similar approach may be possible by biopsy from the human brain with *ex vivo* conversion of neural precursors to OPs with subsequent expansion. Such transplantation would therefore be autologous and obviate the need for immunosuppression.

The alternative approach is to recruit endogenous OPs to instigate repair. Cells that are responsible for remyelination in adults are mainly dividing "progenitor cells" (38, 39). The O4<sup>+</sup> multiprocess-bearing cells that are regarded as the O2A<sup>adult</sup> *in vivo* have been found in the CNS of normal and (myelin) diseased animals and humans (4, 5, 40). The apparent lack or limit of remyelination in terms of the universal existence of O4<sup>+</sup> O2A<sup>adult</sup> suggests that either the environment or the cells' intrinsic properties (or both) is responsible. In the presence of (lyssolecithin-induced) demyelination, retrovirus-labeled proliferating progenitors failed to migrate even a short distance (<500  $\mu$ m) over a period of 4 weeks to perform remyelination (38). Such a poor migration behavior may be intrinsic to the multiprocess-bearing O2A<sup>adult</sup> rather than due to the nonpermissive environment, because transplanted neonatal OPs migrate a long distance and myelinate axons in dysmyelinated adult CNS (1, 36). Neuronal progenitors can also migrate a long distance from subependymal area to olfactory bulb in adult environment (41). In a separate study by Keirstead *et al.* (39), O2A<sup>adult</sup> (identified by NG2 labeling) adjacent to focally demyelinated lesions decreased in number with time and were not mitotic, and they suggested therefore that the O2A<sup>adult</sup> are inherently incapable of regeneration (39). Therefore, strategies designed to simply increase the number of O2A<sup>adult</sup>, such as by delivering PDGF into the CNS (35), may not be effective. An alternative avenue to this strategy, therefore, is to promote the *in vivo* regeneration of the O2A<sup>perinatal</sup> from host neural precursors or stem cells, in a similar fashion as suggested by the present study. Such cells are present in subependymal areas of the adult CNS and can differentiate into neurons and glia (11), therefore close to commonly affected areas in multiple sclerosis (6). The motility of O2A<sup>perinatal</sup> might also indicate their ability to migrate to other parenchymal sites. The key to the application of these strategies in humans will be the identification of growth factors that have the biological effects both *in vitro* and *in vivo* on these precursor cells.

This work is supported by National Institutes of Health Grant NS33710.

- Archer, D. R., Cuddon, P. A., Lipsitz, D. & Duncan, I. D. (1997) *Nat. Med.* 3, 54–59.
- Warrington, A. E., Barbarese, E. & Pfeiffer, S. E. (1993) *J. Neurosci. Res.* 34, 1–13.
- Armstrong, R., Dorn, H. H., Kufta, C. V., Friedman, E. & Dubois-Dalcq, M. (1992) *J. Neurosci.* 12, 1538–1547.
- Wolswijk, G. (1998) *J. Neurosci.* 18, 601–609.
- Nishiyama, A., Yu, M., Drazba, J. A. & Tuohy, V. K. (1997) *J. Neurosci. Res.* 48, 299–312.
- Prineas, J. W. & McDonald, W. I. (1997) in *Greenfield's Neuropathology*, eds. Graham, D. I. & Lantos, P. L. (Arnold, London), 6th Ed., pp. 813–881.
- Raine, C. S. (1997) *J. Neuroimmunol.* 77, 135–152.
- Raff, M. C., Miller, R. H. & Noble, M. (1983) *Nature (London)* 303, 390–396.
- Wolswijk, G. & Noble, M. (1989) *Development (Cambridge, U.K.)* 109, 691–698.
- Engel, U. & Wolswijk, G. (1996) *Glia* 16, 16–26.
- Weiss, S., Dunne, C., Hewson, J., Wohl, C., Wheatley, M., Peterson, A. C. & Reynolds, B. A. (1996) *J. Neurosci.* 16, 7599–7609.
- Reynolds, B. A. & Weiss, S. (1996) *Dev. Biol.* 175, 1–13.
- Zhang, S. C., Lundberg, C., Lipsitz, D., O'Connor, L. T. & Duncan, I. D. (1998) *J. Neurocytol.* 27, 475–489.
- Zhang, S. C., Lipsitz, D. & Duncan, I. D. (1998) *J. Neurosci. Res.* 54, 181–190.
- Reynolds, B. A. & Weiss, S. (1992) *Science* 255, 1707–1710.
- Louis, J. C., Magal, E., Muir, D., Manthorpe, M. & Varon, S. (1992) *J. Neurosci. Res.* 31, 193–204.
- Sasaki, K., Murakami, T. & Takahashi, M. (1987) *Cytometry* 8, 526–528.
- Tontsch, U., Archer, D. R., Dubois-Dalcq, M. & Duncan, I. D. (1994) *Proc. Natl. Acad. Sci. USA* 91, 11616–11620.
- Lendahl, U., Zimmerman, L. & McKay, R. D. G. (1990) *Cell* 60, 585–595.
- McKinnon, R. D., Matsui, T., Dubois-Dalcq, M. & Aaronson, S. A. (1990) *Neuron* 5, 603–614.
- McKinnon, R. D., Smith, C., Behar, T., Smith, T. & Dubois-Dalcq, M. (1993) *Glia* 7, 245–254.
- Duncan, I. D. (1995) in *Neuroglia*, eds. Ransom, B. R. & Kettenmann, H. R. (Oxford Univ. Press, Oxford), pp. 990–1009.
- Hunter, S. F. & Bottenstein, J. E. (1990) *Dev. Brain Res.* 54, 235–248.
- Avellana-Adalid, V., Nait-Oumesmar, B., Lachapelle, F. & Evercooren, A. B. (1996) *J. Neurosci. Res.* 45, 558–570.
- Juurlink, B. H. J., Thorburne, S. K. & Devon, R. M. (1996) in *Protocols for Neural Cell Culture*, eds. Fedoroff, S. & Richardson, A. (Humana, Totowa, NJ), 2nd Ed., pp. 143–156.
- Morrison, S. J., Uchida, N. & Weissman, I. L. (1995) *Annu. Rev. Cell Dev. Biol.* 11, 35–71.
- Small, R., Riddle, P. & Noble, M. (1987) *Nature (London)* 328, 155–157.
- Wolswijk, G., Riddle, P. N. & Noble, M. (1991) *Glia* 4, 495–503.
- Wren, D., Wolswijk, G. & Noble, M. (1992) *J. Cell Biol.* 116, 167–176.
- Wolswijk, G. & Noble, M. (1992) *J. Cell Biol.* 118, 889–900.
- Shi, J., Marinovich, A. & Barres, B. A. (1998) *J. Neurosci.* 18, 4627–4636.
- Hunter, S. F. & Bottenstein, J. E. (1991) *J. Neurosci. Res.* 28, 574–582.
- Ffrench-Constant, C. & Raff, M. C. (1986) *Nature (London)* 319, 499–502.
- Noble, M. & Murray, K. (1984) *EMBO J.* 3, 2243–2247.
- Ijichi, A., Noel, F., Sakuma, S., Weil, M. M. & Tofilon, P. J. (1996) *Gene Ther.* 3, 389–395.
- Duncan, I. D., Grever, W. E. & Zhang, S. C. (1997) *Mol. Med. Today* 3, 554–561.
- Blakemore, W. F., Franklin, R. J. M. & Noble, M. (1996) in *Glial Cell Development: Basic Principles and Clinical Relevance*, eds. Jessen, K. R. & Richardson, W. D. (Oxford Univ. Press, Oxford), pp. 209–220.
- Gensert, J. M. & Goldman, J. E. (1997) *Neuron* 19, 197–203.
- Keirstead, H. S., Levine, J. M. & Blakemore, W. F. (1998) *Glia* 22, 161–170.
- Reynolds, R. & Hardy, R. (1997) *J. Neurosci. Res.* 47, 455–477.
- Goldman, S. A. & Luskin, M. B. (1998) *Trends Neurosci.* 21, 107–114.

# Chimeric brains generated by intraventricular transplantation of fetal human brain cells into embryonic rats

Oliver Brüstle<sup>1,2\*</sup>, Khalid Choudhary<sup>1</sup>, Khalad Karram<sup>1,2†</sup>, Anita Hüttner<sup>1</sup>, Kerren Murray<sup>2</sup>, Monique Dubois-Dalcq<sup>3</sup>, and Ronald D.G. McKay<sup>1</sup>

<sup>1</sup>Laboratory of Molecular Biology, National Institute of Neurological Disorders and Stroke, National Institutes of Health, Bethesda, MD 20892-4092. <sup>2</sup>Department of Neuropathology, University of Bonn Medical Center, 53105 Bonn, Germany. <sup>3</sup>Unité de Neurovirologie et Régénération du Système Nerveux, Institut Pasteur, 75724 Paris cedex 15, France. \*These two authors contributed equally to this work. \*Corresponding author (e-mail: brustle@uni-bonn.de).

Received 6 July 1998; accepted 29 September 1998

Limited experimental access to the central nervous system (CNS) is a key problem in the study of human neural development, disease, and regeneration. We have addressed this problem by generating neural chimeras composed of human and rodent cells. Fetal human brain cells implanted into the cerebral ventricles of embryonic rats incorporate individually into all major compartments of the brain, generating widespread CNS chimerism. The human cells differentiate into neurons, astrocytes, and oligodendrocytes, which populate the host fore-, mid-, and hindbrain. These chimeras provide a unique model to study human neural cell migration and differentiation in a functional nervous system.

Keywords: stem cell, neural progenitor cell, cell therapy

Detailed knowledge of the molecular signals controlling human precursor cell migration and differentiation is a prerequisite for the understanding of human central nervous system (CNS) development. While individual aspects of cell migration and differentiation are accessible *in vitro*, the molecular interactions governing these events in a complex system such as the developing CNS can be studied only *in vivo*. Data on neural migration and differentiation in an intact nervous system are particularly important for the design of cell replacement strategies for the treatment of human CNS disorders. An experimental model that permits the analysis of normal and disease-derived human neurons and glia in an unperturbed nervous system would greatly facilitate the study of human CNS development, disease, and repair.

Self-renewing multipotential neural stem cells can be isolated from both the embryonic and adult rodent brain and generate all three major cell types of the CNS<sup>1,2</sup>. Similarly, human neural precursors can be cultured in the presence of basic fibroblast growth factor (FGF2) and, upon growth factor withdrawal, differentiate into neurons, astrocytes, and oligodendrocytes<sup>3,4</sup>. To analyze the properties of human neural precursors *in vivo*, we have developed a transplant paradigm in which human cells are individually incorporated into a xenogeneic host brain without eliciting traumatic or immunological reactions. Human donor cells were not implanted into the brain tissue but merely deposited in the cerebral ventricles of embryonic rats, allowing them free access to large areas of the neuroepithelium<sup>5,6</sup>. The human donor cells left the ventricle and migrated in large numbers into the rat brain where they differentiated along with the endogenous cells into neurons and glia. We propose that this new approach can be used for the *in vivo* study of the biological properties of primary and disease-derived human neural precursors as a prelude to the design of therapeutic strategies for neurodegenerative diseases.

## Results

Widespread incorporation of transplanted human precursors.

Human neural precursors isolated from fetal brain fragments recovered 53–74 days postconception were transplanted immediately or after culture in defined medium containing FGF2 and/or epidermal growth factor (EGF), which promote growth of multipotent rodent neural precursors *in vitro*<sup>3,4</sup>. Cells were either grown as monolayer cultures or propagated in uncoated tissue culture dishes to form floating spheres<sup>7,8</sup>. In both types of cultures, differentiation into neurons, astrocytes, and oligodendrocytes could be readily induced by growth factor withdrawal<sup>3</sup>.

Using intrauterine surgery, human donor cells were grafted into the telencephalic vesicle of embryonic day (E)17–E18 rats<sup>9</sup>. The transplanted cells were traced by DNA *in situ* hybridization with a human-specific probe to the *alu* repeat element<sup>10</sup> and immunohistochemistry with a human-specific antibody to glutathione-S-transferase (GST $\pi$ ). One to eight weeks after transplantation, recipients of acutely dissociated ( $n=12$ ) and growth factor-treated preparations ( $n=32$ ) showed incorporated human cells in a variety of gray matter regions, including olfactory bulb, cortex (Fig. 1A), hippocampus, striatum (Fig. 1B and 2), septum (Fig. 3C), tectum (Figs. 1C and 3F), thalamus (Fig. 3D), hypothalamus (Figs. 4D–F), and brain stem. Human cells were symmetrically distributed in recipient brains grafted with single cell suspensions (Fig. 3C). Animals examined during the first postnatal week also exhibited small clusters of residual donor cells attached to the ventricle walls (Fig. 3A). Transplanted spheres were entrapped in periventricular locations and gave rise to a halo of cells that migrated long distances into the host brain (Fig. 3D). Seven to eight weeks after transplantation, sphere-derived cells were found distributed over large areas of the recipient brain (Fig. 1D–E, 3F, 4A–H, 5B). Both freshly dissociated and cultured human neural precursor cells were incorporated into the host white matter. Recipient animals killed between 1 and 7 weeks of age showed abundant GST $\pi$ -positive cells in the major fiber tracts such as the internal capsule (Fig. 1D), corpus callosum (Fig. 1D, inset), anterior and posterior commissures, stria medullaris, fornix, fimbria, as well as fiber tracts in pons and brain stem (Fig. 4G–H). In addition, several recip-

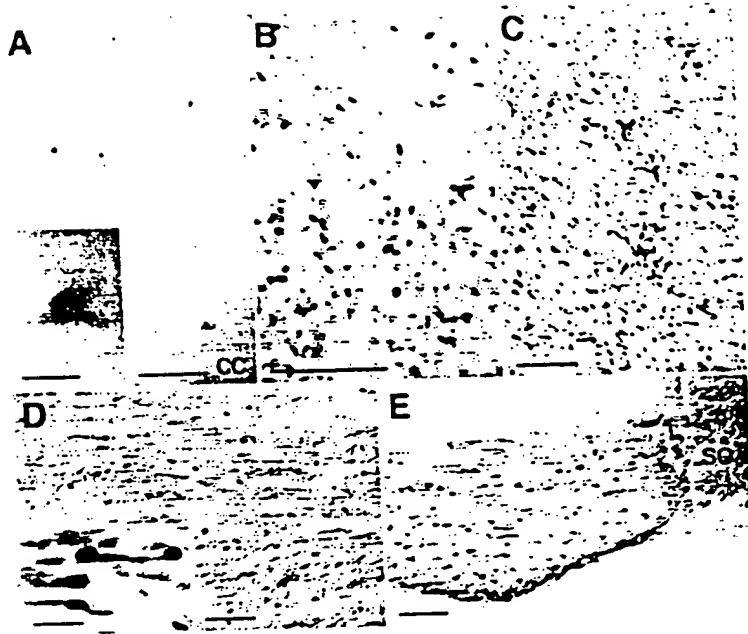


Figure 1. Incorporation of human neural precursor cells into the developing rat brain, visualized by human-specific DNA in situ hybridization (dark nuclear labeling). (A–C) Freshly dissociated cells and (D, E) cells derived from 7-week-old EGF-generated spheres. (A) cortex (postnatal day [P] 30; inset: hybridized nucleus); (B) striatum (P16); (C) inferior colliculus (P16); (D) internal capsule (P45) and corpus callosum (inset); (E) optic nerve (P45). (B), (C), and the inset in (D) are counterstained with hematoxylin to visualize host nuclei. cc: corpus callosum; so: supraoptic nucleus. Bars = 100  $\mu$ m (insets: 20  $\mu$ m).

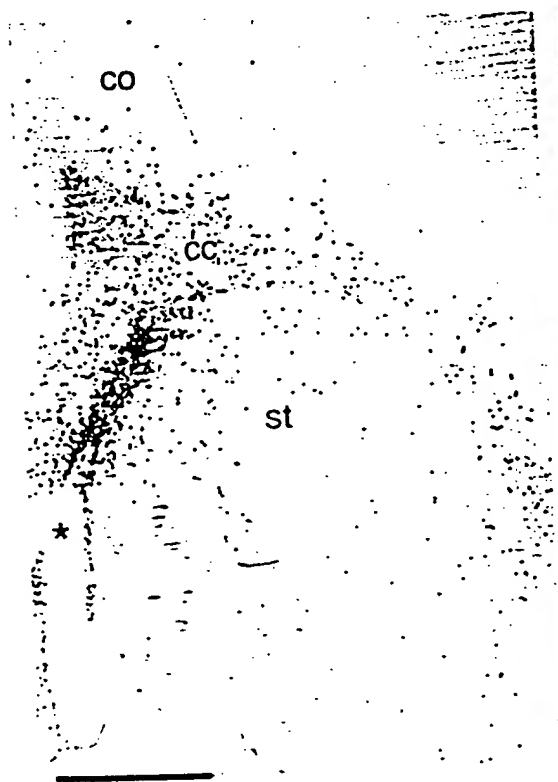


Figure 2. Human neural precursors grown for 6 weeks as monolayers in EGF- and FGF-containing media incorporated into the subventricular zone of the lateral ventricle and migrating into corpus callosum (cc), striatum (st), and cortex (co). Shown is a 50  $\mu$ m vibratome section through a 7-week-old rat brain. Cells hybridized with the human *alu* probe are labeled with red dots. \*lateral ventricle. Bar = 1 mm.

ients exhibited prominent accumulations of human cells in the optic nerve (Fig. 1E). In some animals, the transplanted cells replaced large parts of the subventricular zone (SVZ) of the lateral ventricles. Two months after transplantation, these cells appeared to have migrated from the SVZ into the corpus callosum and adjacent cortical and striatal regions (Fig. 2). Numerous donor-derived cells were also found in white matter and cortex of the cerebellum (Fig. 3E). In some instances, the transplanted cells accumulated around host blood vessels or formed long chain-like structures extending into host gray and white matter (data not shown). Thus, human cells, like rodent cells<sup>1,2,4,5</sup>, can engraft at various levels of the neuraxis following transplantation into the ventricle of embryonic hosts.

In vivo differentiation of human neural precursors. During the first 2 postnatal weeks, human donor cells detected with the GST $\pi$  antibody frequently exhibited uni- or bipolar morphologies characteristic of a migratory phenotype with a leading process and a trailing cell body (Fig. 3B). Human cells incorporated into the molecular layer of the cerebellum maintained immature phenotypes with radially oriented processes for more than 7 weeks (Fig. 3E). At this stage, many of the GST $\pi$ -labeled human cells in other brain regions had acquired multipolar oligodendroglial morphologies (Fig. 3F) and displayed immunoreactivity to an antibody recognizing oligodendrocyte-specific glycolipids (Fig. 4A–C). In addition, these cells expressed myelin basic protein (MBP) in both the cell body and within processes extending to myelin internodes, suggesting active myelination<sup>10</sup> (Figs. 4D–F). These data are compatible with studies showing

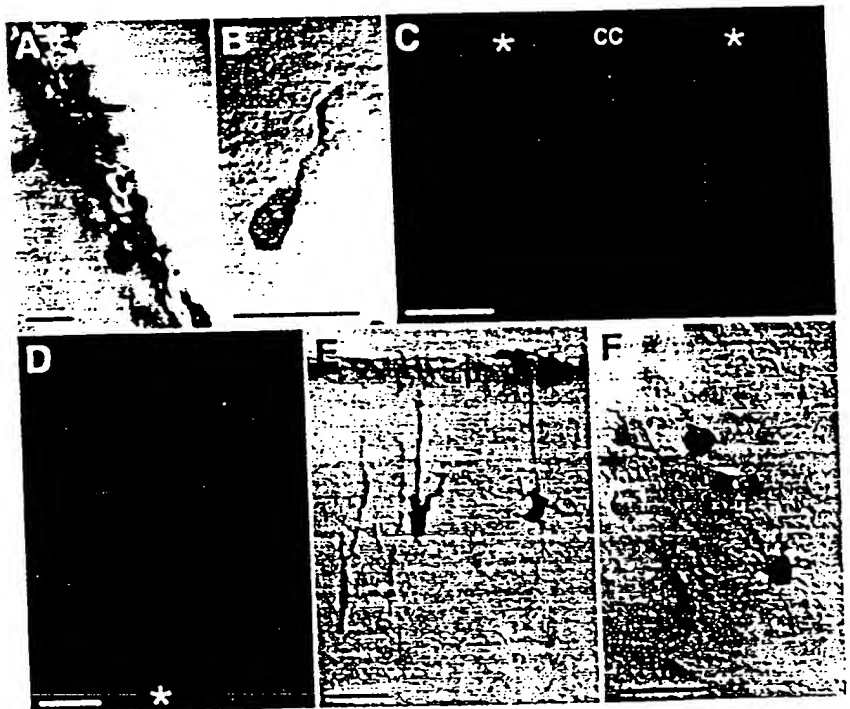


Figure 3. Morphological features of human neural precursors transplanted into the embryonic rat brain, visualized with a human-specific antibody to GST $\pi$ . (A) Residual donor cells attached to the ventricle wall of a 3-day-old recipient animal. (B) Donor cell migrating through the striatal subventricular zone of a neonatal host. (C) Incorporation of freshly dissociated human donor cells in the septum of a 2-week-old host. (D) A human neural sphere grown for 6 weeks in EGF- and FGF-containing media incorporated into the thalamus of a 7-week-old host. (E) GST $\pi$ -positive cells with immature radial phenotypes in the cerebellar molecular layer of a P45 animal. (F) Donor cells with multipolar oligodendroglial morphologies in the tectum, 8 weeks after transplantation of EGF-generated spheres. \*ventricles; cc: corpus callosum; p: pial surface. (A, B, E, and F) immunoperoxidase; (C–D) immunofluorescence. Bars = 20  $\mu$ m (A, B, E, and F), 1 mm (C), 200  $\mu$ m (D).

## RESEARCH

strong GST $\pi$  expression in rodent oligodendrocytes". The presence of human oligodendrocytes was confirmed by immunohistochemical detection of the myelin protein 2',3'-cyclic nucleotide 3'-phosphodiesterase (CNP) in cells hybridized with the *alu* probe (Figs. 4G and H). Some of the donor cells appeared to form CNP-positive sheaths around host axons (Fig. 4H). Although there are presently no antibodies that would distinguish human from rat CNS myelin,

these patterns of MBP and CNP expression suggest that the transplanted human oligodendrocytes myelinate host axons.

Human astrocytes incorporated into the rat brain were identified by double labeling of hybridized cells with an antibody to glial fibrillary acidic protein (GFAP; Fig. 5A and B). These cells were also immunoreactive to an antibody to human adrenoleukodystrophy protein (ALDP), a peroxisomal protein strongly expressed in

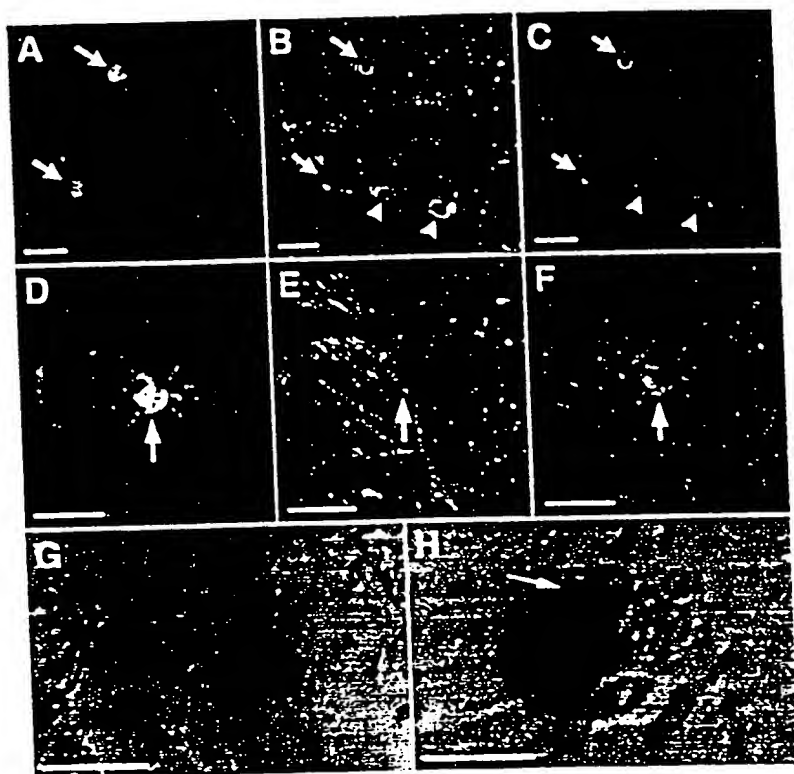


Figure 4. Human oligodendrocytes derived from transplanted (A-C, G-H) EGF- and (D-F) EGF/FGF2-generated spheres incorporated into the brain of 7-week-old rats. (A-C) Donor (arrows) and host (arrowheads) oligodendrocytes in the cortex, double labeled with antibodies to GST $\pi$  (A and C: green) and O4 (B and C: red). (D-F) Human oligodendrocyte incorporated in the host hypothalamus, coexpressing GST $\pi$  (D and F: green) and MBP (E and F: red). (G-H) Human oligodendrocytes in fiber tracts of the ventral brain stem, hybridized with the human *alu* probe (black) and double labeled with an antibody to CNP, which is also staining several myelin internodes (G, brown). Arrow in (H) indicates CNP staining around putative adjacent axons. (A-F) immunofluorescence confocal laser microscopy; (G-H) immunoperoxidase. Bars = 20  $\mu$ m (A-F), 10  $\mu$ m (G and H).

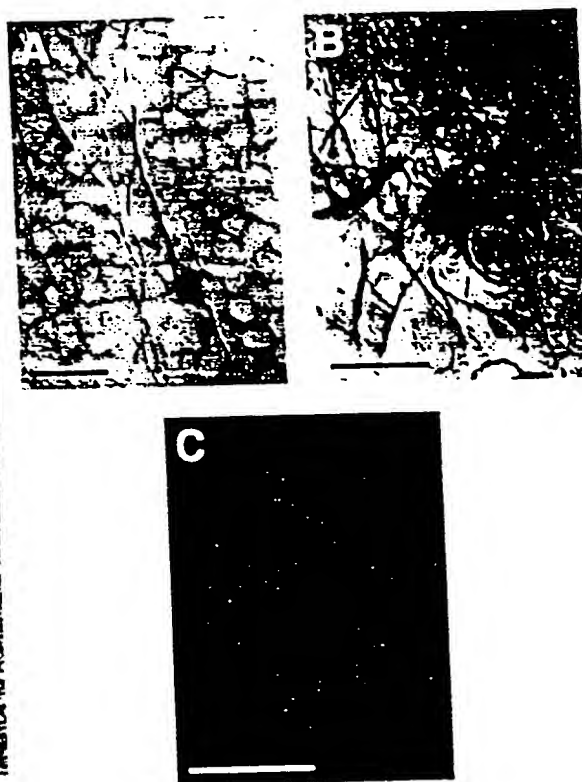


Figure 5. Astrocytic differentiation of the transplanted cells. (A) Hybridized human cell exhibiting radial GFAP-positive processes in the tectum of a 3-day-old recipient. (B) Human astrocyte with a stellate morphology in the tectum of a 7-week-old host, double labeled by in situ hybridization and an antibody to GFAP. Cells are derived from (A) FGF2- and (B) EGF-generated spheres. (C) ALDP expression in a human astrocyte in the ventral telencephalon, 18 days after transplantation of an FGF2-expanded monolayer culture into the ventricle of an E18 rat. Bars = 20  $\mu$ m.

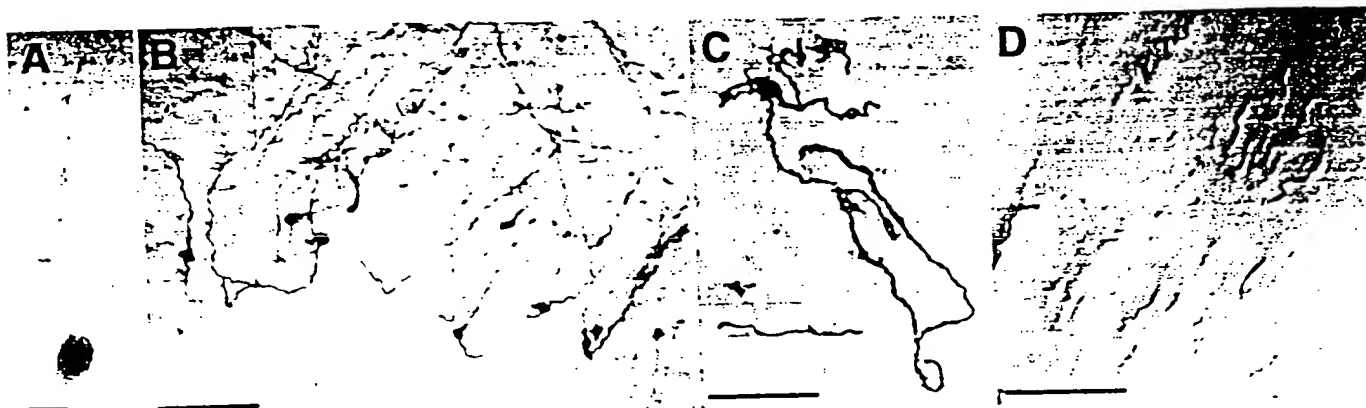


Figure 6. Human neurons incorporated into the rat brain. (A) An individual neuron, hybridized with the *alu* probe (black) and double labeled with a human-specific antibody to neurofilament (hNF-M; brown) in the cortex of a 30-day-old host grafted with freshly dissociated human precursor cells at E17. (B-C) Immunohistochemical detection of  $\beta$ -galactosidase-positive human cells in (B) tectum and (C) hypothalamus of 2-week-old recipients. Donor cells grown for 4 weeks in defined medium containing 10 ng/ml FGF2 were transduced with an adenovirus carrying the *lacZ* gene and transplanted into E17 recipients. (D) hNF-M-positive human axons at the transition of corpus callosum and cortex, 51 days after intraventricular transplantation of 7-week-old EGF-generated neural spheres. Bars = 10  $\mu$ m (A), 100  $\mu$ m (B), 50  $\mu$ m (C), and 20  $\mu$ m (D).

human astrocytes and microglia (Fig. 5C). Astrocytes with stellate morphologies were found in gray and white matter of forebrain, midbrain, and cerebellum. In neonatal animals, some of the donor-derived astrocytes exhibited conspicuous radially oriented processes (Fig. 5A).

A human-specific antibody to medium-sized neurofilament (hNF-M)<sup>27</sup> was used to visualize transplanted neurons (Fig. 6). Seven to eight weeks after transplantation, numerous immunopositive axonal profiles were detected in the host gray and white matter (Fig. 6D). Donor-derived axons were particularly abundant in cortex and within large fiber tracts such as the corpus callosum and the anterior commissure. As the human hNF-M antibody labeled mostly axons, it only occasionally allowed the identification of neuronal cell bodies (Fig. 6A). In contrast, both neuronal cell bodies and processes could be identified after transplantation of cultured cells infected with an adenovirus harboring the *lacZ* gene, an experiment done to explore the feasibility of gene transfer into transplanted human cells. Immunohistochemical detection of  $\beta$ -galactosidase showed neurons with polar morphologies and long axons incorporated into the host tissue (Figs. 6B and C).  $\beta$ -galactosidase expression was also found in cells with glial morphologies in both gray and white matter, although double immunofluorescent analyses will be required to identify the different types of human cells expressing the transgene.

## Discussion

Human neural precursor cells implanted into the cerebral ventricle of embryonic rats incorporate efficiently into the host brain, generating widespread CNS chimerism. Donor cells transplanted as single cell suspensions or spheres migrate into a variety of telencephalic, diencephalic, and mesencephalic regions and differentiate into oligodendrocytes, astrocytes, and neurons. As in mouse-rat neural chimeras<sup>28</sup>, no signs of rejection were observed up until at least 2 months after transplantation, indicating immunological tolerance of the transplanted xenogeneic cells by the embryonic rat brain. The ability to incorporate into a xenogeneic recipient brain is maintained after prolonged proliferation of the donor cells in defined, growth factor-containing medium. Moreover, donor cells transduced *in vitro* with an adenoviral vector continue to express the transgene after incorporation into the host brain.

Previous studies have shown that human neural precursors transplanted directly into the brain tissue of adult immunosuppressed rodents form cell clusters with limited spread of the transplanted cells into the adjacent host brain<sup>10,29</sup>. In contrast, intraventricular transplantation into embryonic hosts permits widespread delivery of human cells to many brain regions. The widespread distribution of the transplanted human cells is similar to the incorporation pattern observed after intrauterine transplantation of rodent cells<sup>30,31</sup>. In both cases, the transplanted cells appear to follow endogenous migratory routes. For example, human precursors leaving the ventricle migrated into the optic nerve, where they acquired oligodendroglial morphologies. This observation is reminiscent of the migration of oligodendrocyte precursors from the third ventricle into the optic nerve<sup>32</sup>. Donor cells in the SVZ of the lateral ventricle migrated into the corpus callosum and adjacent cortical and striatal regions (Fig. 2), similar to the migration of glial cells generated postnatally in the rat subventricular zone<sup>33</sup>. These similarities suggest that donor cell migration is not primarily determined by cell-autonomous properties but by guidance cues within the host brain. Responsiveness of human donor cells to migration cues within a rodent brain implies remarkable conservation of these signals across species.

The SVZ serves as an endogenous source of multipotential neural precursors that give rise to neurons and glia throughout life<sup>34</sup>. The ability to introduce human neural precursors into the rat

SVZ offers an interesting perspective for the study of cell replacement in the nervous system. Future cell replacement strategies may no longer depend on cell transplantation but focus on the external modulation of endogenous neuro- and gliogenesis by gene transfer and growth factor delivery<sup>35,36</sup>. Incorporation of human cells into a rodent SVZ provides a unique opportunity to explore the efficacy of these strategies *in vivo*.

Our data suggest that many of the human cells leaving the SVZ populate the white matter and acquire oligodendroglial phenotypes (Fig. 2). Following migration, differentiated human oligodendrocytes express the myelin proteins MBP and CNP and form CNP-positive sheaths around host axons, suggesting myelin formation (Fig. 4H). Transplants into myelin-deficient mutants will determine the exact amount and distribution of human myelin within the host brain<sup>37,38</sup>. Thus, the model described might be used and adapted in various ways to study the mechanisms of myelin repair in human demyelinating diseases<sup>39</sup>. As these diseases affect large areas of the CNS, repair of myelin by transplantation would require widespread delivery of oligodendrocytes to the host brain. So far, oligodendrocyte transplants have been generally performed as intraparenchymal grafts, resulting in successful yet spatially restricted remyelination in a variety of animal models<sup>40,41</sup>. The strategy presented here can be exploited to optimize widespread remyelination in demyelinating diseases. Initially, this approach will be particularly relevant to the question of myelin repair in human leukodystrophies occurring in the perinatal period<sup>42</sup>.

Combined with gene transfer into the human donor cells, this chimera model will permit the study of molecular mechanisms regulating human neural migration and differentiation in a functional brain. Alternatively, human donor cells can be introduced into embryos of transgenic mice overexpressing factors known to promote precursor cell migration and differentiation. Such a strategy can be used to assay the effect of trophic factors on human neural cells in a live nervous system. These studies should be particularly useful for the design of cell replacement strategies as well as for probing the efficacy of gene transfer protocols in the human CNS. The lack of traumatic and reactive alterations in the chimeric brains could make this approach a useful tool for the *in vivo* analysis of neural cells obtained from patients with neurological diseases. Incorporation of affected cells into an unperturbed nervous system may provide new insights into the cellular pathogenesis of these diseases and serve as a model to assay the effects of pharmaceutical agents on human neurons and glia *in vivo*.

## Experimental protocol

**Dissociation of human donor cells.** Human fetal brain specimens were obtained with consent of the mothers from the Birth Defect Research Laboratory, University of Washington, Seattle (supported by NIH/NICHD grant HD 00836, IRB number 26-0769-A). Cerebral fragments cleaned in sterile conditions and shipped overnight in hibernation buffer<sup>43</sup> typically yielded cell preparations with a viability of 80–95%. Eleven specimens, obtained between 53 and 74 days postconception, were used for this study. Tissue fragments were washed five times in calcium- and magnesium-free Hanks' buffered salt solution (CMF-HBSS) and mechanically triturated to single cell suspensions in the presence of 0.1% trypsin and 0.1% DNase (Worthington, Freehold, NJ).

**Cell culture.** Human neural precursor cells were grown in defined medium containing DMEM/F12 (Life Technologies, Rockville, MD), glucose, glutamine, sodium bicarbonate, 25  $\mu$ M insulin (Intergen, New York), 100  $\mu$ M human apo-transferrin (Intergen), 20 nM progesterone (Sigma St. Louis, MO), 100  $\mu$ M putrescine (Sigma), 30 nM sodium selenite (Sigma), penicillin/streptomycin, 10–20 ng/ml FGF2 and/or 20 ng/ml EGF (R&D Systems, Minneapolis, MN). Monolayer cultures were propagated for 1–4 weeks in tissue culture plates coated with fibronectin (Life Technologies; 1  $\mu$ g/ml) or polyornithin (Sigma; 1.5  $\mu$ g/ml). Cells were passaged mechanically using a cell scraper. Immediately prior to transplantation, cells were triturated in the presence of 0.1% DNase. Neural spheres were generated by growing



## RESEARCH

dissociated cells up to 7 weeks in uncoated tissue culture plates as described. Both types of cultures yielded abundant proliferating cells that expressed nestin, an intermediate filament typically found in neural precursors. Upon growth factor withdrawal, monolayer cultures and plated spheres differentiated into neurons, astrocytes, and oligodendrocytes expressing the cell type-specific antigens  $\beta$ -III tubulin, GFAP, and O4, respectively (A.H. unpublished observations). Growth factor treatment was continued until the day before transplantation. Selected monolayer cultures growing in 10 ng/ml FGF2 were infected with an adenoviral vector carrying the *lacZ* gene under control of the cytomegalovirus immediate-early promoter. Starting 24 h before transplantation, subconfluent 10 cm plates were incubated in 5 ml medium containing  $1.5 \times 10^6$  pfu of concentrated viral supernatant. Immediately prior to transplantation, cells were washed three times in CMF-HBSS and harvested by incubation in 0.05% trypsin. Following incubation in soybean trypsin inhibitor (Life Technologies), cells were briefly triturated in the presence of 0.1% DNase.

**Intrauterine transplantation.** Timed pregnant Sprague-Dawley rats (E17-E18) were anesthetized with ketamine-HCl (80 mg/kg) and xylazine (10 mg/kg), and  $0.25-4 \times 10^6$  cells (suspended in 1–5  $\mu$ l CMF-HBSS) were injected into the telencephalic vesicle of each embryo as described. Spheres were sedimented at 150 G for 3 min, washed several times in CMF-HBSS, and implanted using a glass capillary with a 200  $\mu$ m orifice (20–50 spheres per recipient brain). Larger spheres were mechanically fragmented prior to transplantation. In contrast to recipient animals grafted with mouse cells, human-rat neural chimeras showed a high rate of mortality within the first 2 postnatal days (30–40%). Incorporated cells were found in 31 of 44 analyzed recipient brains transplanted with acutely dissociated cells ( $n = 12$ ; eight positive), monolayer ( $n = 13$ ; 11 positive), or sphere cultures ( $n = 19$ ; 12 positive).

**Immunohistochemistry.** Zero to seven weeks after spontaneous birth, recipients were anesthetized and perfused with 4% paraformaldehyde in phosphate-buffered saline (neonatal animals were fixed by immersion). Serial 50  $\mu$ m vibratome sections were characterized with antibodies to GFAP (1:100; ICN Biomedicals, Costa Mesa, CA, and 1:500; Sternberger Monoclonals, Baltimore, MD), human glutathione-S-transferase (1:200; Biotrin, Dublin), human ALDP (1:400), phosphorylated medium molecular weight human neurofilament (clone HO14, 1:50), CNP (1:200; Sigma), O4 (1:5; Boehringer Mannheim, Indianapolis, IN), MBP (1:200; Boehringer), and  $\beta$ -galactosidase (1:500; 5Prime3Prime, Boulder, CO). Antigens were visualized using appropriate fluorophore or peroxidase-conjugated secondary antibodies. Specimens were examined on Zeiss Axioplan, Axiovert, and Laser Scan microscopes.

**In situ hybridization.** Donor cells were identified using a digoxigenin end-labeled oligonucleotide probe to the human *anu* repeat element. DNA-DNA in situ hybridization was performed as described. Briefly, sections were treated with 25  $\mu$ g/ml pronase in 2 $\times$  SSC, 5 mM EDTA for 15 min at 37°C, dehydrated, and denatured in 70% formamide, 2 $\times$  SSC for 12 min at 85°C. After dehydration in cold ethanol, sections were hybridized overnight at 37°C in 65% formamide, 2 $\times$  SSC, 250  $\mu$ g/ml salmon sperm DNA. Washes were 50% formamide, 2 $\times$  SSC (20 min, 37°C), and 0.5 $\times$ SSC (15 min, 37°C). Hybridized probe was detected using an alkaline phosphatase-conjugated antibody to digoxigenin (Boehringer).

## Acknowledgments

We thank Y. Maeda for providing the adenoviral vector and J. Trojanowski and P. Aubourg for the HO14 and ALDP antibodies, respectively. We would also like to thank John Rajan and his group for coordinating the tissue transfer and the Myelin Project for support to M.D.-D. and K.M. Roberto Bruzzone, Kimberly Jones, and Bernard Register critically read the manuscript.

- Weiss, S., Reynolds, B.A., Vescovi, A.L., Morshead, C., Craig, C.G., and van der Kooy, D. 1996. Is there a neural stem cell in the mammalian forebrain? *Trends Neurosci.* 19:387–393.
- McKay, R.D.G. 1997. Stem cells in the central nervous system. *Science* 276:66–71.
- Sabate, C., Horellou, P., Vigne, E., Colin, P., Perricaudet, M., Buc-Caron, M.H., et al. 1995. Transplantation to the rat brain of human neural progenitors that were genetically modified using adenoviruses. *Nat. Genet.* 9:256–260.
- Buc-Caron, M.H. 1995. Neuroepithelial progenitor cells explanted from human fetal brain proliferate and differentiate in vitro. *Neurobiol. Dis.* 2:37–47.
- Murray, K., and Dubois-Daico, M. 1997. Emergence of oligodendrocytes from human neural spheres. *J. Neurosci. Res.* 50:146–156.
- Brüstle, O., Maskos, U., and McKay, R.D.G. 1995. Host-guided migration allows targeted introduction of neurons into the embryonic brain. *Neuron* 15:1275–1285.
- Campbell, K., Olsson, M., and Björklund, A. 1995. Regional incorporation and site-specific differentiation of striatal precursors transplanted to the embryonic forebrain ventricle. *Neuron* 15:1259–1273.
- Brüstle, O., Spiro, C.A., Karim, K., Choudhary, K., Okabe, S., and McKay, R.D.G. 1997. In vitro-generated neural precursors participate in mammalian brain development. *Proc. Natl. Acad. Sci. USA* 94:14809–14814.
- Olsson, M., Bierregaard, K., Winkler, C., Gates, M., Björklund, A., and Campbell, K. 1998. Incorporation of mouse neural progenitors transplanted into the rat: embryonic forebrain is developmentally regulated and dependent on regional and adhesive properties. *Eur. J. Neurosci.* 10:71–85.
- Reynolds, B.A., and Weiss, S. 1992. Generation of neurons and astrocytes from isolated cells of the adult mammalian central nervous system. *Science* 255:1707–1710.
- Brüstle, O., Cunningham, M., Tabar, V., and Studer, L. 1997. Experimental transplantation in the embryonic, neonatal, and adult mammalian brain, pp. 3.10.11–13.10.28 in *Current protocols in neuroscience*. Crawley, J., Gerfen, C., McKay, R.D.G., Rogawski, M., Sibley, D., and Skolnick, P. (eds.). John Wiley, New York.
- Rubin, C.M., Houck, C.M., Deminger, P.L., Friedmann, T., and Schmid, C.W. 1980. Partial nucleotide sequence of the 300-nucleotide interspersed repeated human DNA sequences. *Nature* 284:372–374.
- Fishell, G. 1995. Striatal precursors adopt cortical identities in response to local cues. *Development* 121:803–812.
- Lim, D.A., Fishell, G.J., and Alvarez-Buylla, A. 1997. Postnatal mouse subventricular zone neuronal precursors can migrate and differentiate within multiple levels of the developing neuraxis. *Proc. Natl. Acad. Sci. USA* 94:14832–14836.
- Brophy, P.J., Boccaccio, G.L., and Colman, D.R. 1993. The distribution of myelin basic protein mRNAs within myelinating oligodendrocytes. *Trends Neurosci.* 16:515–521.
- Cammer, W., and Zhang, H. 1992. Localization of Pi class glutathione-S-transferase in the forebrains of neonatal and young rats: evidence for separation of astrocytic and oligodendrocytic lineages. *J. Comp. Neurol.* 321:40–45.
- Fouquet, F., Zhou, J.M., Ralston, E., Murray, K., Troalen, F., Magal, E., et al. 1997. Expression of the adrenoleukodystrophy protein in the human and mouse central nervous system. *Neurobiol. Dis.* 3:271–285.
- Trojanowski, J.O., Mantione, J.R., Lee, J.H., Seid, D.P., You, T., Inge, L.J., et al. 1993. Neurons derived from a human teratocarcinoma cell line establish molecular and structural polarity following transplantation into the rodent brain. *Exp. Neurol.* 122:283–294.
- Wictorn, K., Brundin, P., Gustavii, B., Lindvall, O., and Björklund, A. 1990. Reformation of long axon pathways in adult rat central nervous system by human forebrain neuroblasts. *Nature* 347:556–558.
- Wictorn, K., Brundin, P., Sauer, H., Undvall, O., and Björklund, A. 1992. Long distance oriented axonal growth from human dopaminergic mesencephalic neuroblasts implanted along the nigrostriatal pathway in 6-hydroxydopamine lesioned adult rats. *J. Comp. Neurol.* 323:475–494.
- Svensson, C.N., Caldwell, M.A., Shen, J., ter Borg, M.G., Rosser, A.E., Tyers, P., et al. 1997. Long-term survival of human central nervous system progenitor cells transplanted into a rat model of Parkinson's disease. *Exp. Neurol.* 148:135–146.
- Ono, K., Yasui, Y., Rutishauser, U., and Miller, R.H. 1997. Focal ventricular origin and migration of oligodendrocyte precursors into the chick optic nerve. *Neuron* 19:283–292.
- Levison, S.W., Chuang, C., Abramson, B.J., and Goldman, J.E. 1993. The migrational patterns and developmental fates of glial precursors in the rat subventricular zone are temporally regulated. *Development* 119:611–622.
- Alvarez-Buylla, A., and Lois, C. 1995. Neuronal stem cells in the brain of adult vertebrates. *Stem Cells* 13:263–272.
- Craig, C.G., Tropea, V., Morshead, C.M., Reynolds, B.A., Weiss, S., and van der Kooy, D. 1996. In vivo growth factor expansion of endogenous subependymal neural precursor cell populations in the adult mouse brain. *J. Neurosci.* 16:2649–2658.
- Kuhn, H.G., Winkler, J., Kempermann, G., Thal, L.J., and Gage, F.H. 1997. Epidermal growth factor and fibroblast growth factor-2 have different effects on neural progenitors in the adult rat brain. *J. Neurosci.* 17:5820–5829.
- Gumpel, M., Lachapelle, F., Gansmuller, A., Baulac, M., Baron van Evercooren, A., and Baumann, N. 1987. Transplantation of human embryonic oligodendrocytes into shiverer brain. *Ann. NY Acad. Sci.* 495:71–85.
- Seitman, D., Gansmuller, A., Baron-Van Evercooren, A., Gumpel, M., and Lachapelle, F. 1996. Myelination by transplanted human and mouse central nervous system tissue after long-term cryopreservation. *Acta Neuropathol.* 91:82–88.
- Duncan, I.D., Grever, W.E., and Zhang, S.C. 1997. Repair of myelin disease: strategies and progress in animal models. *Mol. Med. Today* 3:554–561.
- Groves, A.K., Barnett, S.C., Franklin, R.J.M., Crang, A.J., Mayer, M., Blakemore, W.F., et al. 1993. Repair of demyelinated lesions by transplantation of purified O-2A progenitor cells. *Nature* 362:453–455.
- Tontsch, U., Archer, D.R., Dubois-Daico, M., and Duncan, I.D. 1994. Transplantation of an oligodendrocyte cell line leading to extensive myelination. *Proc. Natl. Acad. Sci. USA* 91:11616–11620.
- Blakemore, W.F., Olby, N.J., and Franklin, R.J.M. 1995. The use of transplanted glial cells to reconstruct glial environments in the CNS. *Brain Pathol.* 5:443–450.
- Lachapelle, F. 1995. Glial transplants: an in vivo analysis of extrinsic and intrinsic determinants of dysmyelination in genetic variants. *Brain Pathol.* 5:289–299.
- Duncan, I.D., and Milward, E.A. 1995. Glial cell transplants: experimental therapies of myelin diseases. *Brain Pathol.* 5:301–310.
- Nave, K.A., and Boeslup-Tanguy, O. 1996. X-linked developmental defects of myelination: from mouse mutants to human genetic diseases. *The Neuroscientist* 2:33–43.
- Dunnett, S.B., and Björklund, A. 1992. *Neural transplantation: a practical approach*. Oxford University Press, New York.
- Lendahl, U., Zimmermann, L.B., and McKay, R.D.G. 1990. CNS stem cells express a new class of intermediate filament protein. *Cell* 60:585–595.

VOLUME 16 NUMBER 11 • NOVEMBER 1998

# Nature Biotechnology

<http://biotech.nature.com>

**Human neural stem cells**

Univ. of Minn.  
Bio-Medical  
Library

**Transgenic fowl will fly**

**A-rad-idopsis for tracking Chernobyl**

**Multigene transformation of rice**



# “Global” cell replacement is feasible via neural stem cell transplantation: Evidence from the dysmyelinated *shiverer* mouse brain

(myelination/mutants/oligodendroglia/regeneration)

BOOMA D. YANDAVA, LORI L. BILLINGHURST, AND EVAN Y. SNYDER\*

Departments of Neurology, Pediatrics, and Neurosurgery, Harvard Medical School and Children's Hospital, Boston, MA 02115

Communicated by Richard L. Sidman, Harvard Medical School, Southborough, MA, April 6, 1999 (received for review February 23, 1999)

**ABSTRACT** Many diseases of the central nervous system (CNS), particularly those of genetic, metabolic, or infectious/inflammatory etiology, are characterized by “global” neural degeneration or dysfunction. Therapy might require widespread neural cell replacement, a challenge not regarded conventionally as amenable to neural transplantation. Mouse mutants characterized by CNS-wide white matter disease provide ideal models for testing the hypothesis that neural stem cell transplantation might compensate for defective neural cell types in neuropathologies requiring cell replacement throughout the brain. The oligodendrocytes of the dysmyelinated *shiverer* (*shi*) mouse are “globally” dysfunctional because they lack myelin basic protein (MBP) essential for effective myelination. Therapy, therefore, requires widespread replacement with MBP-expressing oligodendrocytes. Clonal neural stem cells transplanted at birth—using a simple intracerebroventricular implantation technique—resulted in widespread engraftment throughout the *shi* brain with repletion of MBP. Accordingly, of the many donor cells that differentiated into oligodendroglia—there appeared to be a shift in the fate of these multipotent cells toward an oligodendroglial fate—a subgroup myelinated up to 52% (mean = ~40%) of host neuronal processes with better compacted myelin of a thickness and periodicity more closely approximating normal. A number of recipient animals evinced decrement in their symptomatic tremor. Therefore, “global” neural cell replacement seems feasible for some CNS pathologies if cells with stem-like features are used.

Many diseases of the central nervous system (CNS) are characterized not by discrete, focal neuropathology but, rather, by extensive, multifocal, or even “global” neural degeneration or dysfunction. Such conditions may require widespread replacement not only of therapeutic molecules, such as enzymes, but of neural cells, as well. “Global” cellular replacement has been regarded as beyond the capabilities of neural transplantation, which previously has been used in situations in which grafts are placed in single, relatively circumscribed, anatomic locations (e.g., the striatum in Parkinsonism). However, we previously demonstrated that neural stem cells (NSCs) can disseminate therapeutic gene products throughout the CNS (1, 2). We hypothesized that transplantation of NSCs also might work in situations requiring “global” replacement of degenerated or dysfunctional neural cells.

An NSC is an immature, uncommitted cell that exists in the developing and even adult nervous system and gives rise to the array of more specialized cells of the CNS (3–15). It is defined by its ability to self-renew, to differentiate into cells of most (if not all) neuronal and glial lineages, and to populate developing or

degenerating CNS regions. The recognition that NSCs, propagated in culture, could be reimplanted into mammalian brain, where they could reintegrate appropriately and stably express foreign genes (1–9), provided hope that their use might make feasible a variety of novel therapeutic strategies. When exogenous NSCs are transplanted into germinal zones, they circumvent the blood–brain barrier, migrate to distant CNS regions, and participate in the normal development of multiple regions throughout the brain and at multiple stages (from fetus to adult), integrating seamlessly within the parenchyma, differentiating appropriately into diverse neuronal and glial cell types. Thus, their use as graft material can be considered almost analogous to hematopoietic stem cell-mediated reconstitution of bone marrow. In one of their earliest uses as a therapeutic tool, NSCs were implanted at birth, using a simple, rapid, intracerebroventricular injection technique. They delivered a missing gene product ( $\beta$ -glucuronidase) throughout the brain of a mouse in which the gene was mutated in all cells (the MPS VII mutant, a model of the neurodegenerative lysosomal storage disease mucopolysaccharidosis type VII), cross-correcting the widespread neuropathology of host neurons and glia by creating virtually chimeric brain regions (1). We hypothesized that a similar method might accomplish “global” replacement of degenerated or dysfunctional neural cells.

Mutant mice characterized by CNS-wide white matter disease because of oligodendrocyte dysfunction provide ideal models for testing this hypothesis. The *shiverer* (*shi*) mouse suffers from extensive dysmyelination because of an autosomal recessive defect that renders its oligodendrocytes dysfunctional in homozygous animals: a deletion of five of seven exons comprising the gene encoding myelin basic protein (MBP) makes the cells incapable of producing this oligodendroglial component that is essential for effective compact myelination (16–20). Severe tremors develop by 2–3 weeks of age. Therapy for this cell-autonomous defect would require extensive replacement with functional MBP-producing oligodendrocytes. (In a sense, replacement of both an abnormal neural cell type and a dysfunctional gene is entailed.) It is known that the *shi* cellular and behavioral phenotypes can be rescued by introducing the wild-type MBP gene into the germ line (17). However, this approach is not applicable to clinical therapies. The *shi* phenotype has been treated in discrete regions by injecting a fragment of primary CNS tissue containing normal, mature, MBP-expressing oligodendrocytes (19) in much the same way as other relatively focal, demyelinated lesions have been addressed by cells from various stages within the oligodendrocyte lineage (21, 22). However, this does not correct the global abnormality of *shi* CNS myelin. The most differentiated oligodendrocytes migrate minimally from the injection site, whereas cells that migrate more broadly are less

The publication costs of this article were defrayed in part by page charge payment. This article must therefore be hereby marked “advertisement” in accordance with 18 U.S.C. §1734 solely to indicate this fact.

PNAS is available online at [www.pnas.org](http://www.pnas.org).

Abbreviations: CNS, central nervous system; NSC, neural stem cell; X-gal, 5-bromo-4-chloro-3-indolyl  $\beta$ -D-galactoside;  $\beta$ -gal,  $\beta$ -galactosidase; LM, light microscopy; EM, electron microscopy.

\*To whom reprint requests should be addressed at: Harvard Medical School, Children's Hospital, 300 Longwood Avenue, 248 Enders Building, Boston, MA 02115. e-mail: [Snyder@A1.TCH.Harvard.Edu](mailto:Snyder@A1.TCH.Harvard.Edu).

likely to differentiate into mature myelinating cells (23). In contrast to resident oligodendrocytes and more differentiated precursors, multipotent, migratory NSCs tend not to differentiate until instructed by regional cues. This property might circumvent these problems. Therefore, NSCs were transplanted at birth into the brains of *shi* mutants, using the same intracerebroventricular implantation technique devised for diffuse engraftment of enzyme-expressing NSCs to treat global metabolic lesions (1, 2).

## MATERIALS AND METHODS

**Animals.** *Shi* breeders were obtained initially from The Jackson Laboratory, and a colony was maintained thereafter in our facility. With careful husbandry, homozygous *shi* males and females (2–5 months of age) can mate with each other: a *shi/shi* genotype was ensured by using the progeny of such homozygous matings.

**Transplantation.** On the day of birth, *shi/shi* pups (and unaffected controls) received bilateral intracerebroventricular injections of a suspension of NSCs (clone C17.2) as described (1, 2). C17.2 is a stable, prototypical NSC clone originally derived from neonatal mouse cerebellum but capable of participating in the development of most other regions upon implantation into germinal zones throughout the brain (1, 2, 6, 24–26). The NSCs differentiate into neurons in regions undergoing neurogenesis or into glia, where gliogenesis is ongoing (6, 24, 25). Therefore, they emulate endogenous NSCs as well as NSC clones propagated by a variety of techniques from other structures (3–15). After 0–2 mitoses in the first 48 hr posttransplant, they become quiescent and intermingle nondisruptively with endogenous progenitors. The total cell number per region (host plus donor) is not increased. The clone constitutively and stably expresses *lacZ* [encoding  $\beta$ -galactosidase ( $\beta$ -gal), detectable by the 5-bromo-4-chloro-3-indolyl  $\beta$ -D-galactoside (X-gal) histochemical reaction]. Undifferentiated NSCs, maintained in culture and prepared for transplantation as detailed elsewhere (1, 2, 24–26), were resuspended in PBS at  $4 \times 10^4$  cells/ $\mu$ l. The lateral ventricles of cryoanesthetized pups were visualized by transillumination of the head (1, 2); 2  $\mu$ l of the cellular suspension was expelled gently via a glass micropipette inserted transcutaneously into each ventricle (gaining access to the subventricular zone). Pups were returned to maternal care until weaning. Six homozygous litters of eight offspring each were transplanted.

**Analysis of Engrafted Brains.** At various intervals between 2 and 8 weeks after transplantation, serial coronal sections of recipient brains were processed with X-gal histochemistry and/or an anti- $\beta$ -gal antibody (Cappel, 1:1,000) to detect *lacZ*-expressing donor-derived cells as detailed previously (25, 27). The phenotypes of those cells were assessed by light microscopy (LM), immunocytochemistry, and electron microscopy (EM) by using predesignated, standard criteria detailed elsewhere (24–30). Although donor NSCs give rise to a range of neurons and glia *in vivo* [as in our previous reports (1, 2, 24–27)], this study was confined to an assessment of donor-derived oligodendroglia and their potential replacement; therefore, for the purposes of this study, all cells, both donor and host, were classified as either “oligodendrocytes” or “not oligodendrocytes.” Because multiple modes of analysis could be performed on the same tissue, multiple parameters could be correlated in the same animal.

Morphologic analysis first was performed at the LM level by using bright-field, differential interference contrast (DIC) and/or immunofluorescence microscopy. Engrafted cells then were assessed by using ultrastructural criteria by EM for the direct visualization and quantitative morphometrics of cell type-specific components, including myelin (24–30). X-gal-processed tissue was prepared for EM as detailed previously (24–26). The X-gal reaction product forms a crystalline blue precipitate that is nondiffusible and electron dense, permitting donor-derived *lacZ*-expressing cells to be identified and distinguished unequivocally

from unlabeled endogenous cells at both LM and EM levels (24–30) (see Figs. 4D and 5A). The precipitate typically is localized to the nuclear membrane, forming a nuclear ring within donor-derived cells (often overlying the nucleus), endoplasmic reticulum (ER), and other cytoplasmic organelles, and it frequently extends into cellular processes. Despite the presence of accepted LM features and immunocytochemistry markers, CNS cell types, and, particularly, functional oligodendrocytes, have been most extensively and reliably characterized ultrastructurally. Established criteria for cell-type assignment [detailed elsewhere (16–30)] were used. We also have validated independently these criteria by correlating ultrastructural, histologic, and antigenic profiles of individual donor-derived and host cells as detailed previously (24–30). Briefly, a cell was scored as an “oligodendrocyte” if it possessed the following ultrastructural criteria: was a small (5- to 8- $\mu$ m diameter), round or oval cell with a smooth, regular perikaryon and a distinctively dark nucleus and cytoplasm (an appearance created by numerous fine granules); possessed a large, prominent nucleus (occupying more than one-half of the area of the cell) with dense heterochromatin margined against the nuclear membrane and/or clumped centrally; possessed a thin rim of cytoplasm that, though not voluminous, could appear as a mass at the cellular poles when the nucleus lay eccentrically; and possessed a moderate number of short, round mitochondria and often long, meandering, distended ER (16–24, 28–30). Association with myelinated fibers, if visible in the same plane of section, helped confirm an oligodendroglial phenotype. Cells not meeting these criteria were scored as “nonoligodendrocytes.”

Morphometric analysis of myelin on electron micrographs entailed assessment of the degree of compaction, including noting the presence of major dense lines (MDLs) (the oligodendroglial cytoplasmic membrane appositions that constitute the wraps of myelin) and quantifying both periodicity (a measure of interlamellar distance between myelin wraps as represented by the distance between intraperiod lines and/or MDLs) and width of the total myelin wrap. Measurements in engrafted regions of *shi* cerebrum were compared with those in unengrafted areas of the same mouse (internal control) and with those in analogous, homotopic regions of the cerebrum of age-matched affected and unaffected, unengrafted control mice. Cell counts and morphometrics were performed under EM on randomly, systematically selected representative fields and EM grids from multiple noncontiguous sections spanning the cerebrum of experimental and control mice. Cell-type assignments were confirmed independently by three observers blinded to the experiment.

The presence of MBP *in vivo* classically has been used in grafting studies into *shi* (31) to distinguish normal donor from mutant oligodendrocytes. For immunocytochemistry analysis of brain tissue, 20- $\mu$ m-thick, 4% paraformaldehyde-fixed cryosections or 10- $\mu$ m-thick, paraffin-embedded sections were reacted with a polyclonal antibody raised in rabbit against MBP (gift of D. Colman, Mt. Sinai; 1:200) by using standard immunoperoxidase (Vectastain, Vector Laboratories) or immunofluorescence procedures as detailed previously (2, 24, 25, 27). For analysis of cultured cells, a cellular monolayer was processed by using standard immunoperoxidase techniques. NSC-derived cells expressed MBP in culture after prolonged periods *in vitro* (>2 weeks) and/or after supplementation with conditioned medium from primary cultures of dissociated mouse cerebrum, a conclusion that appears to emulate the stably engrafted state.

**Western Blot Analysis.** Western blot analysis, using standard techniques and the above-referenced anti-MBP antibody, was performed on myelin-enriched membrane fractions (32) of whole-brain lysates prepared from semiserial coronal sections of transplanted *shi/shi* mice at 4–5 weeks of age, as well as age-matched, untransplanted *shi/shi* and unaffected controls.

**Behavioral Assessment.** Functional improvement in representative recipient animals was assayed by quantifying the amount of tremor by (i) scoring recorded cage behavior and (ii) measuring



FIG. 1. NSCs can express MBP. Two engraftable NSC clones, known to give rise to oligodendrocytes *in vivo* after transplantation, are reacted with an antibody to MBP *in vitro* by using immunoperoxidase methodology. (A) A subpopulation of NSC clone C17.2 (arrows) differentiates into MBP-expressing cells after exposure to conditioned medium from a primary culture of newborn mouse forebrain. (B) Cells from clone C27.3 that spontaneously differentiated toward MBP expression. The present experiments were performed by using clone C17.2 because of prior experience with these cells in CNS-wide gene therapy engraftment paradigms.

the amplitude of tail tremor, a readily accessible, reliable, and reproducible measure of whole-body tremor.

Cage behavior of both transplanted ( $n = 10$ ) and untransplanted ( $n = 3$ ) affected mice as well as unaffected controls ( $n = 3$ ) was videotaped and graded independently by three investigators blinded to the experiment. A four-point neurologic scoring scale was used, where a score of "1" corresponded to completely abnormal behavior and a score of "4" denoted a completely normal neurologic exam. Animals were rated according to their (i) exploring/grooming behavior, (ii) voluntary movement, (iii) tail movement and degree of tremor, and (iv) proprioception, coordination, and posture. Unaffected control mice, on this blinded assessment, achieved a mean score of  $3.91 \pm 0.14$ , which was significantly different from the mean score of  $2.09 \pm 0.08$  received by untransplanted *shi* mutant controls ( $P < 0.00001$ ), suggesting the sensitivity and validity of this assay with minimal interobserver variability. Each experimental animal similarly was graded blindly. At the completion of the study, upon breaking of the animals' identity codes, each score was calculated for a statistically significant difference from unaffected and affected/untransplanted animals. Mean scores of the groups also were compared.

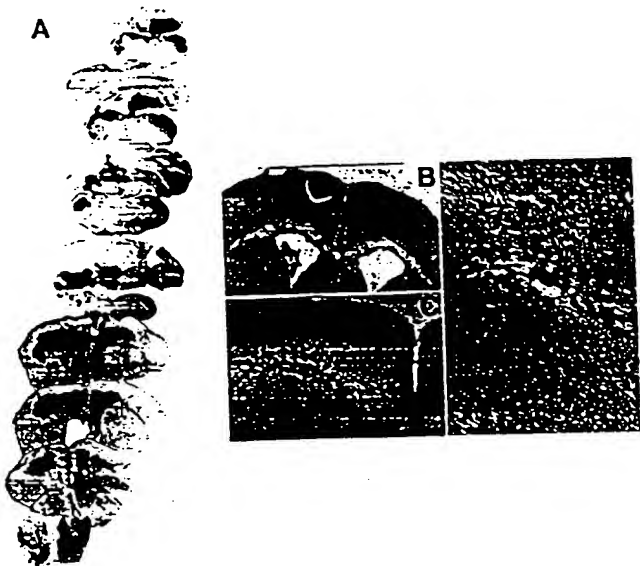


FIG. 2. NSCs engraft extensively throughout the *shi* dysmyelinated brain, including within white tracts. *LacZ*-expressing NSCs were transplanted into newborn *shi* mutants and analyzed systematically at intervals between 2 and 8 weeks after engraftment. (A) Semiserial coronal sections through the *shi* brain at adulthood demonstrate widely disseminated integration of blue X-gal donor-derived cells throughout the neuraxis. (B-D) Progressively higher magnification of donor-derived cell integration in white tracts (arrows) at 2 weeks of age.

Because tremor is the most prominent feature of the *shi* behavioral phenotype, it was quantified directly by measuring the degree of tail displacement perpendicularly from a straight line drawn in the direction of the animal's forward movement (tail amplitude) (see Fig. 6 C and D). Measurements were made by coating an animal's tail in India ink and then permitting the mouse to move freely in one direction on a sheet of graph paper. The tail of an unaffected nontremulous animal draws a line with virtually no perpendicular displacement from the direction of movement (i.e., the long axis of the body); e.g., amplitude = 0 cm. The tail of a "shivering" animal demarcates a broad region of movement (tremor) about the line (i.e., displacement perpendicular to that axis; e.g., amplitude = 4 cm).

## RESULTS AND DISCUSSION

The use of NSCs to address the widespread oligodendroglial pathology of the *shi* CNS was predicated on three observations: (i) our previous determination that NSC clones are capable of differentiating into morphologically, immunocytochemically, and ultrastructurally proven oligodendrocytes *in vitro* and *in vivo* after transplantation into wild-type mouse brain (2, 6, 24, 25, 27); (ii) our confirmation at the outset of these experiments that they are capable of producing MBP (Fig. 1); and (iii) our prior experience that the implantation and integration of exogenous NSC clones into germinal zones of fetuses and newborns (1, 2, 26, 27) could ensure their dissemination throughout a recipient's brain, with normal development of the virtually chimeric regions to which they contribute.

Therefore, clonal NSCs were transplanted at birth into the brains of *shi* mice (as well as unaffected controls), using the same intracerebroventricular implantation technique devised previously for the widespread engraftment of enzyme-expressing NSCs to treat global metabolic lesions (1, 2). Within 24 hr after implantation, consistent with our prior observations (1, 2, 27),

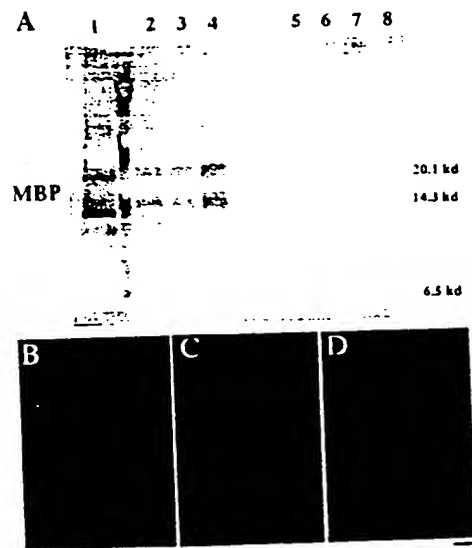


FIG. 3. MBP expression in mature transplanted and control brains. (A) Western analysis for MBP in whole-brain lysates. The brains of three representative transplanted *shi* mutants (lanes 2-4) express MBP at levels close to that of an age-matched, unaffected mouse (lane 1, positive control) and significantly greater than the amounts seen in untransplanted (lanes 7 and 8, negative control) or unengrafted (lanes 5 and 6, negative control), age-matched *shi* mutants. (Identical total protein amounts were loaded in each lane.) (B-D) Immunocytochemical analysis for MBP. (B) The brain of a mature unaffected mouse is immunoreactive to an antibody to MBP (revealed with a Texas Red-conjugated secondary antibody). (C and D) Age-matched engrafted brains from *shi* mice similarly show immunoreactivity. Untransplanted *shi* brains lack MBP. Therefore, MBP immunoreactivity also classically has been a marker for normal, donor-derived oligodendrocytes (C and D) in transplant paradigms (31).

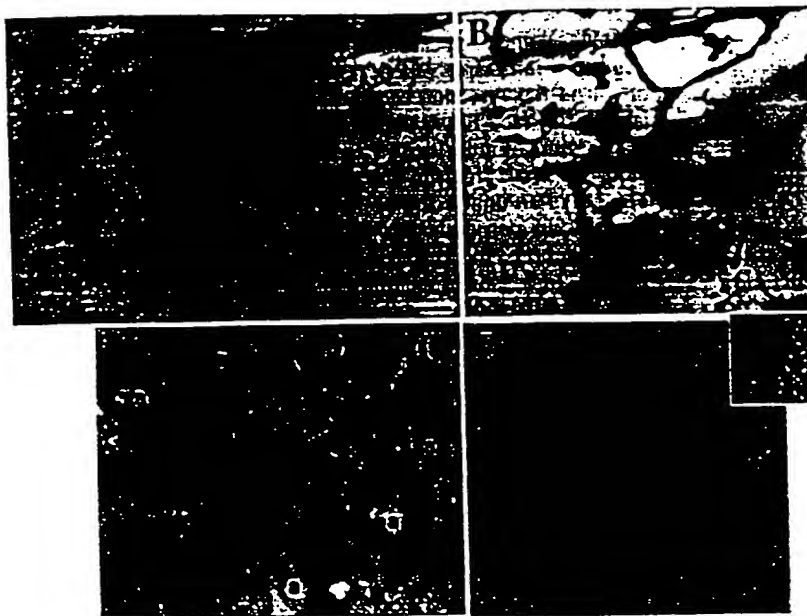


FIG. 4. Engrafted NSCs in recipient *shi* mutants differentiate into oligodendrocytes. (A and B) Donor-derived X-gal<sup>+</sup> cells in representative sections through the corpus callosum possess characteristic oligodendroglial features (small, round or polygonal cell bodies with multiple fine processes oriented in the direction of the neural fiber tracts). (C) Close-up of a representative donor-derived anti- $\beta$ -gal immunoreactive oligodendrocyte (arrow) extending multiple processes toward and beginning to wrap large, adjacent axonal bundles ("a") viewed on end in a section through the corpus callosum. That cells such as those in A–C (and in Fig. 3 C and D) are oligodendroglia is confirmed by the representative electron micrograph in D (and in Fig. 5A), demonstrating the defining ultrastructural features detailed in *Materials and Methods*. A donor-derived X-gal-labeled oligodendrocyte ("LO") can be distinguished by the electron-dense X-gal precipitate that typically is localized to the nuclear membrane (arrow), endoplasmic reticulum (arrowhead), and other cytoplasmic organelles. The area indicated by the arrowhead is magnified in the *Inset* to demonstrate the unique crystalline nature of individual precipitate particles.

NSCs integrated within the subventricular zone throughout the length of the ventricular system and, by 1–2 weeks posttransplant, had migrated into and engrafted extensively within the *shi* brain parenchyma (Fig. 2). At maturity, *lacZ*<sup>+</sup> donor-derived cells were integrated seamlessly throughout the *shi* neuraxis (Fig. 2A), including within white tracts (Fig. 2B–D). The brains of transplanted *shi* mutants, as assessed by Western analysis of whole-brain lysates (Fig. 3A), now expressed readily detectable levels of MBP (lanes 2–4) that contrasted markedly with the absence of MBP in unengrafted, age-matched *shi* brains (lanes 5–8) and compared favorably with that present in unaffected brains (lane 1). Immunocytochemistry analysis using an antibody to MBP

(Fig. 3B–D) (31) confirmed expression of MBP at the cellular level in engrafted *shi* brains (Fig. 3C and D) with an immunoreactivity comparable to that in nonmutant brains (Fig. 3B). Therefore, transplantation of NSCs into the MBP-deficient *shi* brain resulted in widespread engraftment with repletion of significant amounts of whole-brain MBP.

This observation lent support to the expectation that, had donor NSCs indeed differentiated into mature, normal oligodendrocytes, then they would effectively enwrap host axons and dendrites with better-compacted myelin. The phenotype of transplanted NSCs, therefore, was confirmed by LM and EM.

Under bright field, such donor-derived, *lacZ*<sup>+</sup> cells, particularly within white tracts, indeed possessed a morphology classic fo-

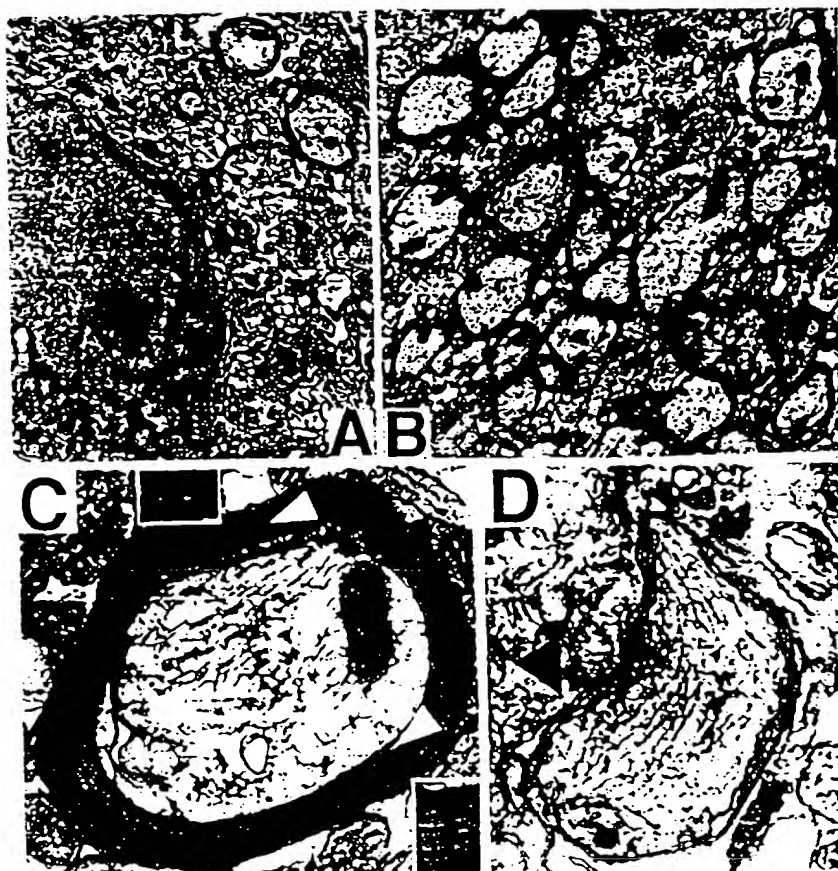


FIG. 5. NSC-derived "replacement" oligodendrocytes appear functional as demonstrated by ultrastructural evidence of myelination of *shi* axons. In regions of MBP-expressing NSC engraftment, *shi* neuronal processes become enwrapped by thick, better-compacted myelin. (A) At 2 weeks posttransplant, a representative donor-derived, labeled oligodendrocyte ("LO") [recognized by extensive X-gal precipitate ("p") in the nuclear membrane, cytoplasmic organelles, and processes] is extending processes (a representative one is delineated by arrowheads) to host neurites and is beginning to ensheath them with myelin ("m"). (B) If engrafted *shi* regions, such as that in A, are followed over time (e.g., to 4 weeks of age as pictured here), the myelin begins to appear healthier, thicker, and better compacted (examples indicated by arrows) than that in age-matched, untransplanted control mutants. (C) By 6 weeks posttransplant, these mature into even thicker wraps: ~40% of host axons are ensheathed by myelin (a higher-power view of a representative axon is illustrated in C) that is dramatically thicker and better compacted than that of *shi* myelin [an example of which is shown in D (black arrowhead) from an unengrafted region of an otherwise successfully engrafted *shi* brain]. In C, open arrowheads indicate representative regions of myelin that are magnified in the adjacent respective *Insets*; major dense lines are evident.

Table 1. Morphometric and behavioral analysis

Parameter	Normal	Shiverer	
		Unengrafted	Engrafted
Neuronal processes with myelin and MDLs, %	96.7	0	37.8
Periodicity of myelin, <sup>†</sup> nm	4.5 ± 0.2	24.4 ± 5.8	10.5 ± 0.7
Width of myelin wrap, nm	138 ± 5	59.5 ± 1.5	135 ± 20
Degree of tremor (as tail displacement), <sup>‡</sup> cm	0	4	1.2 ± 1.6
Behavioral score <sup>§</sup> (scale = 1–4)	3.91 ± 0.14	2.09 ± 0.08	3.72 ± 0.20

\*MDLs, major dense lines, an indication of compacted myelin; the data represent the mean percentage of axons and dendrites with MDLs in representative specimens examined.

<sup>†</sup>See *Materials and Methods* for definition. The shorter the distance, the better compacted and, hence, more normal the myelin.

<sup>‡</sup>See "Behavioral Assessment" in *Materials and Methods* as well as Fig. 6 C and D for a description. Zero centimeter of tail displacement suggests minimal to no tremor; 4 cm of displacement reflects extensive tremor. Of the 10 transplanted *shi* mice examined, 6 actually showed zero displacement.

<sup>§</sup>See "Behavioral Assessment" in *Materials and Methods* as well as Fig. 6 A and B for a description of the scoring system. Unengrafted *shi* mutants scored significantly worse than normal mice ( $P < 0.0001$ ); the scores for successfully engrafted *shi* mice examined in this fashion, however, ( $n = 6$ ) were statistically indistinguishable from those of normal mice ( $P = 0.20$ ) and significantly better than unengrafted *shi* mice ( $P < 0.0001$ ). Unsuccessfully transplanted *shi* mice ( $n = 4$ ; mean score =  $1.97 \pm 0.29$ ) were indistinguishable from untransplanted *shi* [i.e., significantly different from scores in the "normal" column ( $P < 0.0003$ ), not statistically different from scores in the "unengrafted *shi*" column].

oligodendrocytes (Fig. 4 A–C), typically extending processes toward large axonal bundles (Fig. 4C). The crystalline X-gal precipitate is electron-dense, ensuring unambiguous designation and characterization of donor-derived cells even at the EM level (8, 24–30). EM analysis of x-gal+ donor-derived cells confirmed that they met the defining ultrastructural criteria of oligodendrocytes (e.g., Figs. 4D and 5A) (detailed in *Materials and Methods*).

Therefore, donor NSCs could differentiate into ultrastructurally confirmed oligodendrocytes in the engrafted *shi* brain. Of interest was the additional observation that, although these multipotent donor cells were able to differentiate into multiple neural cell types in the engrafted *shi* brains, a significantly greater percentage of engrafted NSCs differentiated toward an oligodendroglial phenotype in the *shi* brain (28%) than in normal controls (16%;  $\chi^2 = 0.015$ ), suggesting that NSCs actually may be compensating somewhat specifically for oligodendrocyte dysfunction in *shi*. Of note, a similar shift in the fate of this same clone of multipotent NSCs toward a neuronal phenotype was detected in developing (26) and adult (25) mouse brain when that neural cell type was deficient or defective and required compensation. Taken together these observations suggest that NSCs might possess a mechanism whereby their differentiation is directed to replenish deficient or inadequate cell types. Such behavior may reflect a fundamental developmental strategy with therapeutic utility.

The successful repletion of MBP in the *shi* brain suggested that donor-derived oligodendrocytes should be functional and, hence, form healthier myelin throughout the brain. Indeed, as early as 2 weeks posttransplant, a subpopulation of donor-derived oligodendrocytes extended processes that enwrapped host axons and dendrites and began laying down myelin around neuronal processes (Fig. 5A). Over a period of 3–4 weeks, the myelin produced by these oligodendrocytes appeared healthier, thicker, and better compacted (Fig. 5B). By 6 weeks posttransplant, a mean of  $\approx 40\%$  of host neuronal processes (Table 1) (up to 52% in some representative specimens examined) were ensheathed by donor-

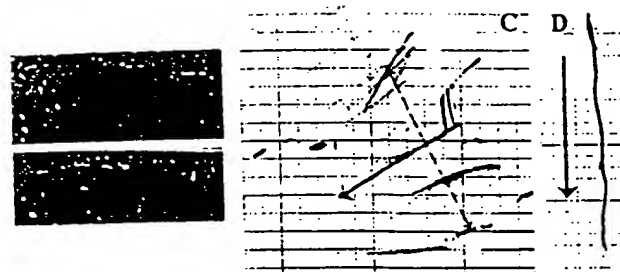


FIG. 6. Functional and behavioral assessment of transplanted *shi* mutants and controls. The *shi* mutation is characterized by the onset of tremor and a "shivering gait" by the second to third postnatal week. The degree of motor dysfunction in animals was gauged in two ways: (i) by blindly scoring periods of standardized videotaped cage behavior of experimental and control animals and (ii) by measuring the amplitude of tail displacement from the body's rostral-caudal axis (an objective, quantifiable index of tremor) (see *Materials and Methods*). Video freeze-frames of representative unengrafted and successfully engrafted *shi* mice are seen in A and B, respectively. The whole-body tremor and ataxic movement observed in the unengrafted symptomatic animal (A) causes the frame to blur, a contrast to the well focused frame of the asymptomatic transplanted *shi* mouse (B). The neurologic scoring of such mice is detailed in *Materials and Methods* and Table 1: 60% of transplanted mutants evinced nearly normal-appearing behavior as in B and attained scores that were not significantly different from normal controls. C and D depict the manner in which whole-body tremor was mirrored by the amplitude of tail displacement (hatched, gray arrow in C), measured perpendicularly from a line drawn in the direction of the animal's movement (solid, gray arrow, which represents the body's long axis) (see *Materials and Methods*). Measurements were made by permitting a mouse, whose tail had been dipped in India ink, to move freely in a straight line on a sheet of graph paper as shown. Large degrees of tremor cause the tail to make widely divergent ink marks away from the midline, representing the body's axis (C). Absence of tremor allows the tail to make long, straight, uninterrupted ink lines on the paper congruent with the body's axis (D). The distance between points of maximal tail displacement from the axis was measured and averaged for transplanted and untransplanted *shi* mutants and for unaffected controls (hatched, gray arrow). C shows data from a poorly engrafted mutant that did not improve with respect to tremor whereas D reveals lack of tail displacement in a successfully engrafted, now asymptomatic *shi* mutant. Overall, 64% of transplanted *shi* mice examined displayed at least a 50% decrement in the degree of tremor or "shiver." Several showed zero displacement (see Table 1).

derived myelin (Fig. 5C) that contrasted dramatically with that observed in untransplanted control mutants or even with that in unengrafted areas of successfully transplanted *shi* animals (Fig. 5D) (an internal control for the efficacy of engraftment) and that compared quite favorably with wild-type myelin. Morphometric analysis of myelinated neuronal processes in engrafted mutants confirmed that the periodicity of myelin was significantly closer to and the mean thickness of myelin virtually equaled ( $P > 0.1$ ) that of normal controls (Table 1).

The success of NSC transplantation in *shi* ultimately is determined by its ability to achieve functional improvement. To this end, transplanted mutants as well as unaffected (positive control) and untransplanted *shi* (negative control) mice were analyzed (as detailed in *Materials and Methods*) for functional improvement by (i) scored neurologic assessment during free-cage behavior and (ii) quantifying the degree of "shiver" as reflected in the amplitude of tail tremor. Behaviorally relevant tremors were decreased significantly in a significant number of representative recipient mutants (Fig. 6 and Table 1): 60% of tested transplanted mutants evinced behavior that approximated normal (Fig. 6B), i.e., attained neurologic scores that both individually and as a group mean were statistically indistinguishable from normal controls ( $P > 0.1$ ) on the behavioral scale detailed in *Materials and Methods* (Table 1); 64% of transplanted animals showed at least a 50% decrement in measured tremor, and some engrafted animals evinced virtually no "shiver" (and, hence, essentially no



tail displacement) (Fig. 6D). This suggests that the "replacement cells" (in this case, oligodendrocytes) were integrated into host CNS in a functionally relevant manner.

The variability in behavioral improvement after engraftment does not have a simple explanation: there did not appear to be a simple correlation between functional improvement and the degree of NSC engraftment or MBP expression. Etiology of the "shivering" phenotype, however, is complex and not well understood. Symptomatic improvement may not be simply a measure of the overall amount of successful myelination. Instead, it may be more reflective of successful remyelination in specific CNS regions. Indeed, one hypothesis holds that there is a shivering "center" affected in *shi* mice. If this hypothesis holds, variations in experimental animals may represent the degree to which such a center was myelinated successfully. It is also important to note that we did not focus on addressing spinal cord defects in *shi*; these lesions likely mediate expression of symptoms as well. Despite the fact that we obtained significant NSC engraftment, MBP expression, oligodendrocyte differentiation, and myelination, it is likely that these could be optimized further: given that NSCs are so readily manipulated (5–8), future studies could use NSCs genetically engineered or pretreated (3, 6) *ex vivo* to enhance these capacities. It is also unclear which role donor-derived nonoligodendroglial cells might have played in effecting repair of the dysmyelinated *shi* brain. Neurons and astrocytes have been implicated in oligodendrocyte migration and differentiation and may influence myelination. The extent to which such other neural cell types, derived from the same clone of NSCs, may have had "helper" roles in improvement might constitute an additional argument for the use of multipotent cells rather than those with a more restricted fate. Indeed, many diseases—even those classically characterized as purely disorders of white or gray matter—actually affect a mixed population of cell types and would benefit from the concurrent replacement of both neuronal and glial elements.

### Conclusions

Transplanted NSCs can differentiate into MBP-expressing oligodendrocytes throughout the *shi* brain, in turn promoting improved widespread remyelination with extensive amelioration of neuropathology and symptoms. These results suggest that NSCs may be useful for a variety of diseases characterized by profuse white matter degeneration that might benefit from the replacement of oligodendroglia. Disordered myelination plays an important role in many other genetic and acquired neurodegenerative processes. In a broader sense, with oligodendroglia serving as a model for neural cells in general and *shi* serving as a prototype for a broad range of maladies characterized by extensive neural cell dysfunction, these results suggest that therapeutic cell replacement in a widely disseminated, even "global," manner is feasible when cells with stem-like qualities are used as graft material, a recognition that broadens the paradigmatic scope of neural transplantation. Furthermore, an NSC-based approach, whether with exogenous NSCs or with appropriately mobilized endogenous NSCs, may address therapeutic challenges that previously have been inaccessible. Many promising gene therapy vehicles and biochemical treatment modalities depend on relaying "new" genetic information through "old" neural substrates that may, in fact, have been lost, become dysfunctional, or failed to develop. Reconstitution of aspects of this anatomy may enable more significant recovery. Furthermore, although the ability of NSCs to engraft diffusely has been exploited for widespread distribution of enzymes (1, 2) and, now, cells, it seems apparent that a similar strategy can be used for dissemination of a variety of diffusible (e.g., neurotrophins, viral vectors) (33) and nondiffusible (e.g., extracellular matrix) factors for a wide range of therapeutic and research demands. Combined therapies may forestall damage while restoring lost neural elements. NSCs with similar properties recently have been generated from human

tissue, laying the groundwork for potential treatments of heretofore refractory human diseases (27, 34). The persistence of a periventricular zone in the human for prolonged periods postnatally suggests that implantation strategies similar to those described may be feasible.

We thank D. Kirschner, J. Karthegasen, R. Mozell, and R. M. Taylor for advice and D. Colman for his generous gift of MBP antibody. This work was supported in part by grants from the National Institute of Neurological Disorders and Stroke, the Hood Foundation, the American Paralysis Association, the Paralyzed Veterans of America, the Canavan's Research Fund, and a Mental Retardation Research Center grant to Children's Hospital. L.L.B. was funded in part by the Society for Pediatric Research.

1. Snyder, E. Y., Taylor, R. M., & Wolfe, J. H. (1995) *Nature (London)* 374, 367–370.
2. Lacorazza, H. D., Flax, J. D., Snyder, E. Y., & Jendoubi, M. (1996) *Nat. Med.* 4, 424–429.
3. McKay, R. (1997) *Science* 276, 66–71.
4. Gage, F. H., Ray, J., & Fisher, L. J. (1995) *Annu. Rev. Neurosci.* 18, 159–192.
5. Gage, F. H., & Christen, Y., eds. (1997) *Isolation, Characterization, and Utilization of CNS Stem Cells—Research and Perspectives in Neuroscience* (Springer, Berlin).
6. Snyder, E. Y. (1998) *Neuroscientist* 4, 408–425.
7. Martinez-Serrano, A., & Bjorklund, A. (1997) *Trends Neurosci.* 20, 530–538.
8. Whittemore, S. R., & Snyder, E. Y. (1996) *Mol. Neurobiol.* 12, 13–36.
9. Pincus, D. W., Goodman, R. R., Fraser, R. A. R., Nedergaard, M., & Goldman, S. A. (1998) *Neurosurgery* 42, 858–868.
10. Morrison, S. J., Shah, N. M., & Anderson, D. J. (1997) *Cell* 88, 287–298.
11. Weiss, S., Reynolds, B. A., Vescovi, A. L., Morshead, C., Craig, C., & van der Kooy, D. (1996) *Trends Neurosci.* 19, 387–393.
12. Alvarez-Buylla, A., & Lois, C. (1995) *Stem Cells* 13, 263–272.
13. Qian, X., Davis, A. A., Goderie, S. K., & Temple, S. (1997) *Neuron* 18, 81–93.
14. Kilpatrick, T., & Bartlett, P. F. (1993) *Neuron* 10, 255–265.
15. Gritti, A., Parati, E. A., Cova, L., Frolichsthal, P., Galli, R., Wanke, E., Faravelli, L., Morassutti, D. J., Roisen, F., Nickel, D. D., et al. (1996) *J. Neurosci.* 16, 1091–1100.
16. Molineaux, S. M., Engh, H., de Ferra, F., Hudson, L., & Lazzarini, R. A. (1986) *Proc. Natl. Acad. Sci. USA* 83, 7542–7546.
17. Readhead, C., Popko, B., Takahashi, N., Shine, H. D., Saavedra, R. A., Sidman, R. L., & Hood, L. (1987) *Cell* 48, 703–712.
18. Popko, B., Puckett, C., Lai, E., Shine, H. D., Readhead, C., Takahashi, N., Hunt, S. W., Sidman, R. L., & Hood, L. (1987) *Cell* 48, 713–721.
19. Gout, O., Gansmuller, A., Baumann, N., & Gumpel, M. (1988) *Neurosci. Lett.* 87, 195–199.
20. Katsuki, M., Sato, M., Kimura, M., Yokoyama, M., Kobayashi, K., & Nomura, T. (1988) *Science* 241, 593–595.
21. Duncan, I. D., Grever, W. E., & Zhang, S.-C. (1997) *Mol. Med. Today* 3, 554–561.
22. Franklin, R. J. M., & Blakemore, W. F. (1995) *Trends Neurosci.* 18, 151–156.
23. Foster, L. M., Landry, C., Phan, T., & Campagnoni, A. T. (1995) *Dev. Neurosci.* 17, 160–170.
24. Snyder, E. Y., Deitcher, D. L., Walsh, C., Arnold-Aldea, S., Hartwig, E. A., & Cepko, C. L. (1992) *Cell* 68, 33–51.
25. Snyder, E. Y., Yoon, C., Flax, J. D., & Macklis, J. D. (1997) *Proc. Natl. Acad. Sci. USA* 94, 11663–11668.
26. Rosaño, C. M., Yandava, B. D., Kosar, B., Zurakowski, D., Sidman, R. L., & Snyder, E. Y. (1997) *Development* 124, 4213–4224.
27. Flax, J. D., Aurora, S., Yang, C., Simonin, C., Wills, A. M., Billingham, L., Jendoubi, M., Sidman, R. L., Wolfe, J. H., Kim, S. U., & Snyder, E. Y. (1998) *Nat. Biotech.* 16, 1033–1039.
28. Peters, A., Palay, S. L., & Webster, H. D. (1991) *The Fine Structure of the Nervous System. Neurons and Their Supporting Cells* (Oxford Univ. Press, Oxford).
29. Jones, E. G. (1981) *The Structural Basis of Neurobiology* (Elsevier, New York).
30. Palay, S. L., & Chan-Palay, V. (1973) *J. Microsc. (Oxford)* 97, 41–47.
31. Gumpel, M., Bauman, N., Raoul, M., & Jacque, C. (1983) *Neurosci. Lett.* 37, 307–311.
32. Knapp, P. E., Bartlett, W. P., & Skoff, R. P. (1987) *Dev. Biol.* 120, 356–365.
33. Lynch, W. P., Sharpe, A. H., & Snyder, E. Y. (1999) *J. Virol.*, in press.
34. Vescovi, A. L., Parati, E. A., Gritti, A., Poulin, P., Ferrario, M., Wante, E., Frolichsthal-Schoeller, P., Cova, L., Arcellana-Panlilio, M., Colombo, A., & Galli, R. (1999) *Exp. Neurol.* 156, 71–83.

# Engraftable human neural stem cells respond to developmental cues, replace neurons, and express foreign genes

Jonathan D. Flax<sup>1</sup>, Sanjay Aurora<sup>1</sup>, Chunhua Yang, Clemence Simonin, Ann Marie Wills, Lori L. Billingham, Moncef Jendoubi<sup>1</sup>, Richard L. Sidman<sup>2</sup>, John H. Wolfe<sup>3</sup>, Seung U. Kim<sup>4</sup>, and Evan Y. Snyder<sup>\*</sup>

<sup>1</sup>Departments of Neurology, Pediatrics, and Neurosurgery, Children's Hospital, Harvard Medical School, Boston, MA. <sup>2</sup>National Eye Institute, National Institute of Health, Bethesda, MD. <sup>3</sup>New England Regional Primate Center, Harvard Medical School, Southborough, MA. <sup>4</sup>Department of Pathobiology and Center for Comparative Medical Genetics, School of Veterinary Medicine, University of Pennsylvania, Philadelphia, PA. <sup>\*</sup>Division of Neurology, Department of Medicine, University Hospital, University of British Columbia, Vancouver, BC, Canada. <sup>\*</sup>These authors contributed equally to this work. <sup>\*</sup>Corresponding author (e-mail: Snyder@A1.TCH.Harvard.edu).

Received 10 July 1998; accepted 23 September 1998

Repayment has been made to the Copyright Clearance Center for this article.

Stable clones of neural stem cells (NSCs) have been isolated from the human fetal telencephalon. These self-renewing clones give rise to all fundamental neural lineages *in vitro*. Following transplantation into germinal zones of the newborn mouse brain they participate in aspects of normal development, including migration along established migratory pathways to disseminated central nervous system regions, differentiation into multiple developmentally and regionally appropriate cell types, and nondisruptive interspersions with host progenitors and their progeny. These human NSCs can be genetically engineered and are capable of expressing foreign transgenes *in vivo*. Supporting their gene therapy potential, secretory products from NSCs can correct a prototypical genetic metabolic defect in neurons and glia *in vitro*. The human NSCs can also replace specific deficient neuronal populations. Cryopreservable human NSCs may be propagated by both epigenetic and genetic means that are comparably safe and effective. By analogy to rodent NSCs, these observations may allow the development of NSC transplantation for a range of disorders.

**Keywords:** cell therapy, progenitor cell, gene therapy, Tay-Sachs disease, transplantation, differentiation

Neural stem cells (NSCs) are primordial, uncommitted cells postulated to give rise to the array of more specialized cells of the central nervous system (CNS)<sup>1-3</sup>. They are operationally defined by their ability (1) to differentiate into cells of all neural lineages (i.e., neurons—ideally of multiple subtypes, oligodendroglia, astroglia) in multiple regional and developmental contexts; (2) to self-renew (to give rise to new NSCs with similar potential); and (3) to populate developing and/or degenerating CNS regions. The demonstration of a monoclonal derivation of progeny is obligatory to the definition (i.e., a single cell must possess these attributes). With the earliest recognition that rodent neural cells with stem cell properties, propagated in culture, could be reimplanted into mammalian brain where they could reintegrate appropriately and stably express foreign genes<sup>4-7</sup>, gene therapists and neurobiologists began to speculate how such a phenomenon might be harnessed for therapeutic advantage as well as for understanding developmental mechanisms. These, and the studies they spawned (reviewed in refs. 14–16), provided hope that the use of NSCs might circumvent some limitations of presently available graft material<sup>8</sup> and gene transfer vehicles<sup>9</sup> and make feasible a variety of therapeutic strategies.

Neural cells with stem cell properties have been isolated from the embryonic, neonatal, and adult rodent CNS and propagated *in vitro* by a variety of equally effective and safe means—both epigenetic (with mitogens such as epidermal growth factor [EGF]<sup>10</sup> or basic fibroblast growth factor [bFGF]<sup>11,12</sup>) or with membrane substrates<sup>13</sup>) and genetic (with propagating genes<sup>14</sup> such as *v-myc*<sup>15,16</sup> or large T-antigen [*T-Ag*]<sup>17</sup>). Maintaining NSCs in a proliferative state in culture does not subvert their ability to respond to normal

developmental cues *in vivo* following transplantation (such as the ability to withdraw from the cell cycle, interact with host cells, and differentiate<sup>18</sup>). These extremely plastic cells migrate and differentiate in a temporally and regionally appropriate manner particularly following implantation into germinal zones. Intermingling nondisruptively with endogenous progenitors, responding similarly to local cues for their phenotypic determination, and appropriately differentiating into diverse neuronal and glial types, they participate in normal development along the rodent neuraxis. In addition, they can express foreign genes *in vivo*<sup>19,20</sup>, often in widely disseminated CNS regions<sup>21,22</sup>, and are capable of neural cell replacement<sup>23</sup>.

The presumption has been that the biology that endows such rodent cells with their therapeutic potential is conserved in the human CNS. If true, then progress toward human applications may be accelerated. We demonstrate the potential of clones of human NSCs to perform these critical functions *in vitro* and *in vivo* in a manner analogous to their rodent counterparts.

## Results and discussion

Isolation, propagation, and cloning of human NSCs. The isolation, propagation, characterization, cloning, and transplantation of NSCs from the human CNS mirrored strategies used for the murine NSC clone C17.2 (propagated following transduction of a constitutively downregulated *v-myc*<sup>24</sup>) and for growth factor-expanded murine NSC clones<sup>25</sup>. NSCs—even genetically propagated clones<sup>26</sup>—require molecules like bFGF and/or EGF in serum-free medium to divide<sup>27</sup>. Therefore, this dual responsiveness was



## RESEARCH

chosen for both screening and enriching a starting population of stable, dissociated, cultured primary human neural tissue for cells. Cells dissociated from human fetal telencephalon—particularly the ventricular zone, which has been postulated to harbor (in lower mammals) a rich NSC population—were initially grown as a polyclonal population first in serum-supplemented and then in serum-free medium containing bFGF and/or EGF. Cells were transferred between media containing one or the other of the mitogens to select for dual responsiveness. Some populations were then maintained in bFGF alone for subsequent manipulation and cloning; others were used for retrovirally mediated transduction of *v-myc* and subsequent cloning.

To provide an unambiguous molecular tag for assessing the clonal relationships of the cells, as well as to facilitate identification of some cells following transplantation and to assess their capacity to express exogenous genes *in vivo*, some bFGF-propagated subpopulations were infected with an amphotropic replication-incompetent retroviral vector encoding *lacZ* (and *neo* for selection). Single resistant colonies were initially isolated by limiting dilution. Monoclonality of the cells in a given colony was then confirmed by demonstrating the presence of only one copy of the *lacZ/neo*-encoding retrovirus, with a unique chromosomal insertion site. In clone H1, for example, all *lacZ/neo*-positive cells, had a single, common retroviral integration site indicating that they were derived from a single infected "parent" cell (Fig. 1A).

In rodents, genes (such as *v-myc* and *T-Ag*) that interact with cell cycle regulatory proteins have been used to propagate NSCs<sup>10</sup>, neural progenitors<sup>11</sup>, and neuroblasts<sup>12</sup>, resulting in engraftable rodent NSC clones that can be manipulated and have therapeutic potential<sup>13</sup>. Therefore, some of the bFGF-maintained human cell populations, enriched for NSCs, were infected with an amphotropic, replication-incompetent retroviral vector encoding *v-myc* and *neo*<sup>14</sup> yielding multiple colonies. All of the putative clones had only one unique retroviral insertion site, demonstrating their monoclonality (Fig. 1B). Five clones (H6, H9, D10, C2, and E11) were generated and maintained in serum-free medium containing bFGF.

Multipotency and self-renewal *in vitro*. In uncoated dishes and in serum-free medium supplemented with bFGF, all clones grew in culture as clusters that could be passaged weekly for at least 1 year (Fig. 2A). The cells within these clusters expressed vimentin, a neural progenitor marker<sup>15</sup>. By dissociating these clusters and plat-

ing them in serum-containing medium, these clones differentiated spontaneously into neurons and oligodendrocytes (Figs. 2B and C). After 5 days under these differentiating conditions, 90% of the cells in all clones became immunoreactive for the neuronal marker neurofilament (NF; Fig. 2B); 10% expressed CNPase, a marker for oligodendroglia (Fig. 2C). Mature astroglia containing glial fibrillary acidic protein (GFAP) were not initially observed, even after 1 month under these culture conditions. However, GFAP production could be induced by coculture with primary dissociated embryonic murine CNS tissue (Fig. 2D). In addition to cells expressing the variety of differentiated lineage-specific markers (establishing "multipotency"), each clone gave rise to new immature vimentin-positive cells (Fig. 2E), which could, upon subsequent passage, give rise to new cells expressing multiple differentiated neural markers as well as to new vimentin-positive passageable cells (i.e., "self-renewability"). All the clones, whether genetically modified or epigenetically maintained, were similar *in vitro*.

Ability to cross-correct a genetic defect. To assess their potential as vehicles for molecular therapies, we compared the ability of human NSCs to complement a prototypical genetic defect to murine NSCs<sup>16</sup>. The neurogenetic defect chosen was in the  $\alpha$ -subunit of  $\beta$ -hexosaminidase, a mutation that leads to hexosaminidase-A deficiency and a failure to metabolize GM<sub>1</sub> ganglioside to GM<sub>2</sub> (Tay-Sachs disease [TSD]). Pathologic GM<sub>1</sub> accumulation in the brain leads to progressive neurodegeneration. The ability of human NSCs to cross-correct was compared with that of two established murine NSC clones: C17.2 and a subclone of C17.2 (C17.2H) engineered via retroviral transduction of the human  $\alpha$ -subunit gene to overexpress hexosaminidase<sup>17</sup>. These murine NSC clones secrete functional hexosaminidase-A<sup>18</sup>. A transgenic mouse with an  $\alpha$ -subunit deletion<sup>19</sup> permitted examination of the ability of human NSCs to secrete a gene product capable of rescuing TSD neural cells. NSCs (murine and human) were cocultured with dissociated TSD mouse brain cells from which they were separated by a porous membrane that allowed passage of hexosaminidase but not cells. After 10 days, the mutant neural cells were examined: (1) for the presence of hexosaminidase activity (Fig. 3A–C, and M); (2) with antibodies to the  $\alpha$ -subunit and to CNS cell type markers to determine which TSD neural cells internalized corrective gene product (Fig. 3D–L); and (3) for reduction in GM<sub>1</sub> storage (Fig. 3N). While there was minimal intrinsic hexosaminidase activity in TSD cells cultured alone (Fig. 3A), hexosaminidase activity increased to normal intensity when the cells were cocultured with murine or human NSCs (Fig. 3B and C). The extent of human NSC-mediated cross-correction matched the success of murine NSCs, yielding percentages of hexosaminidase-positive TSD cells significantly greater than in untreated controls ( $p < 0.01$ ) (Fig. 3M). All neural cell types from the TSD mouse brain were corrected (Figs. 3D–L). The percentage of TSD CNS cells without abnormal GM<sub>1</sub> accumulation was significantly lower in those exposed to secretory products from human NSCs than in untreated TSD cultures ( $p < 0.01$ ), approaching those from wild-type mouse brain (Fig. 3N).

Multipotency and plasticity *in vivo*. We next determined whether human NSC clones (whether epigenetically or genetically propagated) could respond appropriately to normal developmental cues *in vivo*, which include migrating appropriately; integrating into host parenchyma; and differentiating into neural cell types appropriate to a given region's stage of development, even if that stage is not the one in which the NSCs were obtained. Although there are many approaches for testing these qualities<sup>20–22</sup>, we used paradigms similar to those we have used with murine NSCs to assess their developmental ability<sup>10</sup>. When murine NSC clones are implanted into the cerebral ventricles of newborn mice, the cells engraft in the subventricular germinal zone (SVZ)<sup>23</sup> and follow the

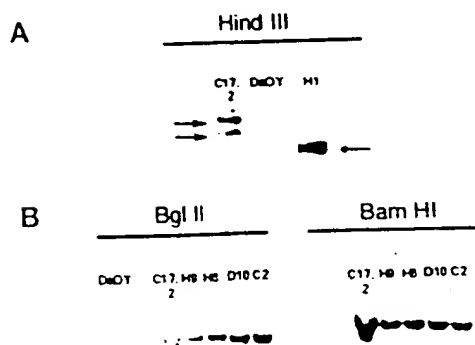
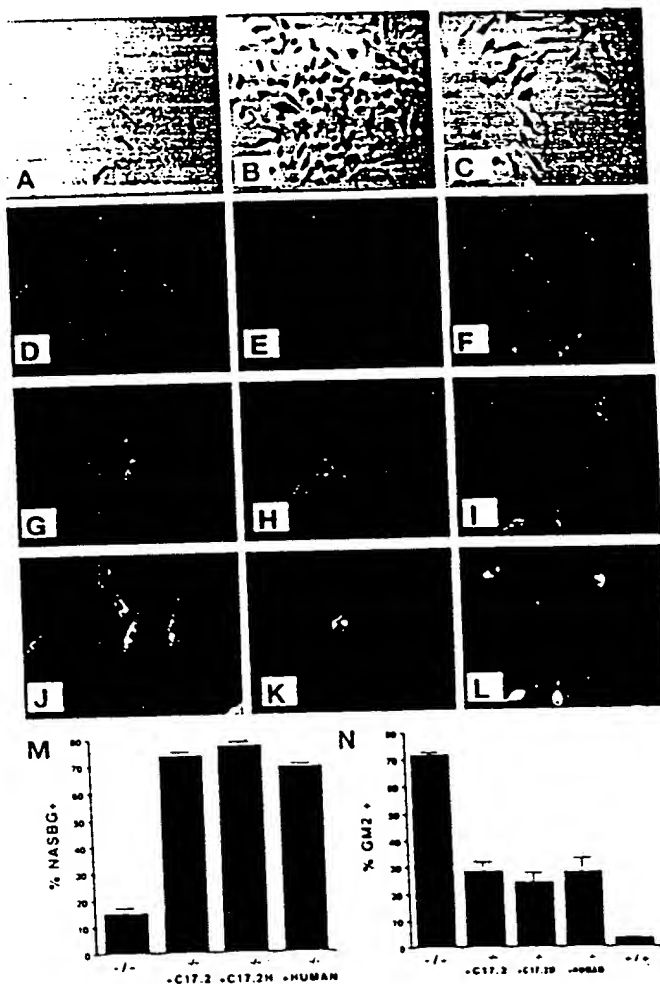
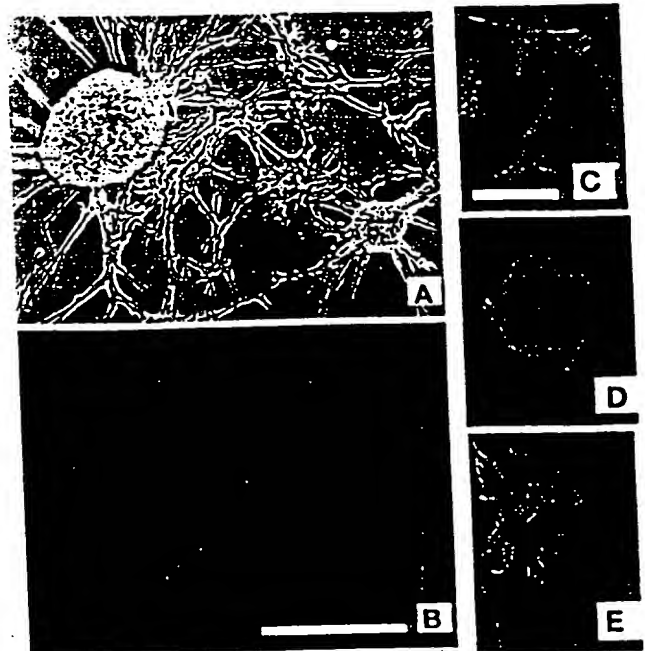


Figure 1. Southern blot analysis of retroviral insertion into human NSC clones. (A) Genomic DNA from clone H1 (propagated in bFGF and transduced with a retrovirus encoding *lacZ* and *neo*) digested with Hind III (cuts once within the provirus) and incubated with a radiolabeled *neo* probe. The murine NSC clone C17.2 contains two integrated proviruses encoding *neo*<sup>14</sup>. DaOY is an uninfected human medulloblastoma cell line. (B) Genomic DNA from clones H9, H6, D10, and C2 (propagated in bFGF and/or EGF and infected with a retrovirus encoding *v-myc*) were digested with BglII or BamHI (cuts once within the provirus) and probed for *v-myc*. C17.2 contains one *v-myc*-encoding provirus.

established pathways used by endogenous progenitors, either migrating along the rostral migratory stream (RMS) to the olfactory bulb (OB), becoming neurons, or migrating into subcortical and cortical regions (where gliogenesis predominates and neurogenesis has ceased) becoming oligodendroglia and astroglia. When transplanted into the germinal zone of the neonatal mouse cerebellum (the external germinal layer [EGL]), these same NSCs migrate inward and differentiate into granule neurons in the emerging internal granule cell layer (IGL). Following intraventricular implantation, human NSC clones emulated the developmentally appropriate behavior of their murine counterparts (Fig. 4 and 5). The engraftment, migration, and differentiation of epigenetically perpetuated clones were identical to that of *v-myc* perpetuated clones. Three of the five *v-myc* clones engrafted well (Table 1).



**Figure 3.** Dissociated brain cells from mice with mutated  $\alpha$ -subunit of  $\beta$ -hexosaminidase (Tay-Sachs disease) cocultured with human NSCs. (A-C) Hexosaminidase activity determined by NASBG histochemistry. (A) TSD neural cells (arrows) not exposed to NSCs. TSD cells exposed to secretory products from (B) murine NSC clone C17.2H or from (C) human NSCs. (D-L) TSD cells cocultured with human NSCs immunostained with a (D-F) fluorescein-labeled antibody to the human  $\alpha$ -subunit of  $\beta$ -hexosaminidase and (G-I) with antibodies to neural cell type-specific antigens. (G) Neuronal-specific NeuN marker; (H) glial specific GFAP marker; and (I) precursor marker, nestin. (J-L) Dual filter microscopy of the  $\alpha$ -subunit and cell-type markers. (M) Percentage of  $\beta$ -hexosaminidase positive TSD cells; -/-: TSD  $\alpha$ -subunit-null cells; TSD cells exposed to secretory products from C17.2+ murine NSCs; C17.2H+: murine NSC engineered to overexpress murine hexosaminidase; +human: human NSCs. (N) GM, accumulation in TSD cells; labels as in (M); +/-: wild-type mouse brain.



**Figure 2.** Characterization of human NSCs in vitro. (A) NSCs grown in serum-free medium. Immunostaining for (B) the neuronal marker neurofilament or (C) the oligodendroglia marker CNPase in serum-containing medium. (D) Immunostaining for the astrocyte marker human GFAP upon coculture with primary murine CNS cultures. (E) Immunostaining for the immature neural marker vimentin at transfer to serum-containing medium.

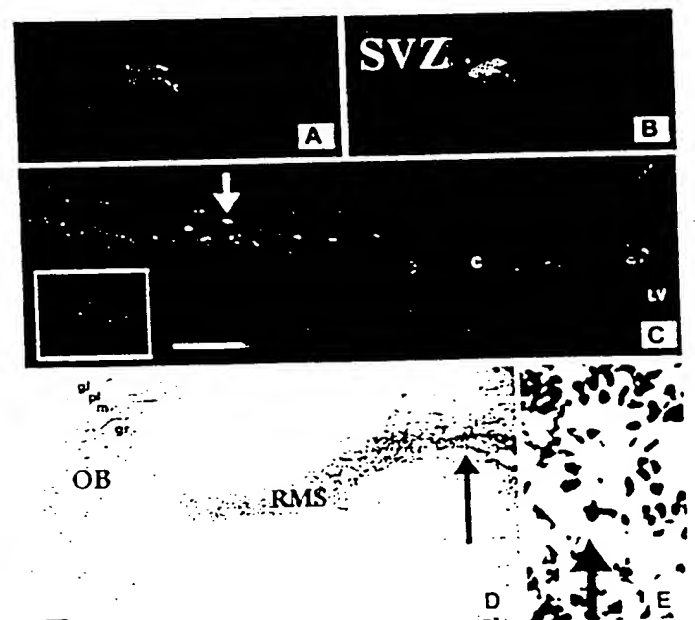


**Figure 4.** Migration of human NSCs following engraftment into the SVZ of newborn mice. (A,B) Human NSCs 24 h after transplantation. (A) Donor-derived cell (red) interspersed with (B) densely packed endogenous SVZ cells, visualized by DAPI (blue) in the merged image. (C) Donor-derived cells (red) within the subcortical white matter (arrow) and corpus callosum (c) and their site of implantation in the lateral ventricle (LV). Arrow indicates the cell shown at higher magnification within the inset. (D) Donor-derived cell migration from the SVZ into the rostral migratory stream (RMS) leading to the olfactory bulb (OB), in a cresyl-violet counterstained parasagittal section; gl: glomerular layer; pl: plexiform layer; m: mitral layer; gr: granular layer. Scale bars: 100  $\mu$ m. (E) Higher magnification of area indicated by the arrow in (D). Brown staining indicates BrdU-immunoperoxidase-positive donor-derived cells.

## RESEARCH

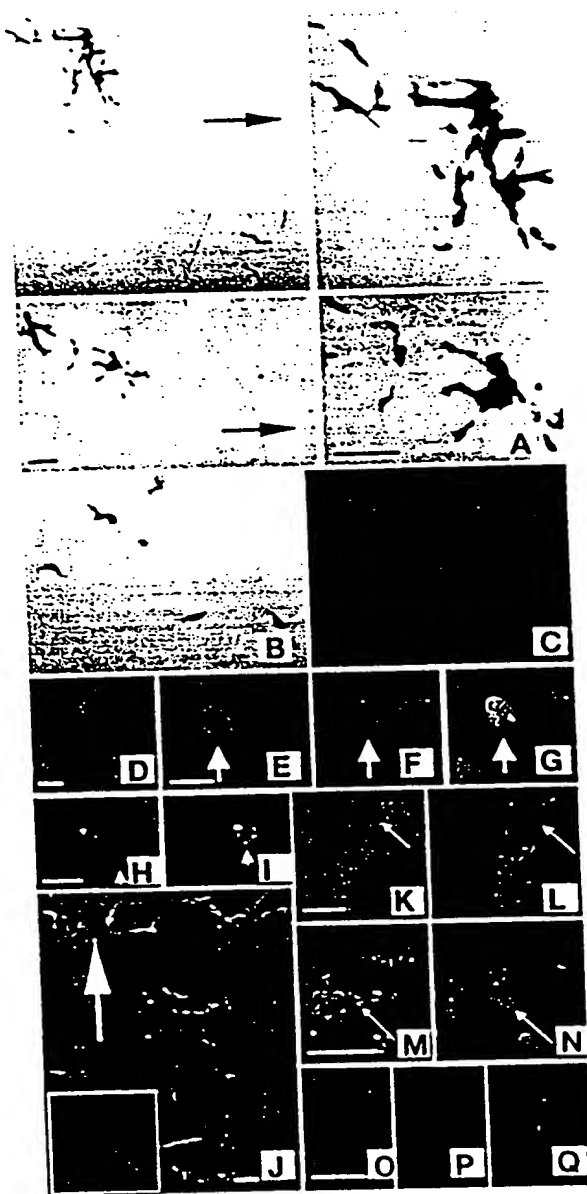


**Figure 5.** Characterization of human NSC clones in vivo following engraftment into SVZ of neonatal mice. (A–C) *LacZ*-expressing donor-derived cells from human NSC clone H1 detected with (A,B) Xgal and with (C) anti- $\beta$ -galactosidase within (A) the periventricular and subcortical white matter regions and (B,C) OB granule layer. The arrows in (A) indicate the lateral ventricles. (D–G) BrdU-labeled NSCs (clone H6) implanted into the SVZ at birth identified in the OB with a (D) human-specific NF antibody and by (E–G) BrdU ICC via confocal microscopy. (E) BrdU-positive cell visualized by fluorescein; (F) anti-NeuN+ antibody visualized by Texas Red; (G) same cell visualized by dual filter. Donor-derived clone H6 in the adult subcortical white matter double-labeled with (H) an oligodendrocyte-specific antibody to CNPase and (I) BrdU. The arrowhead in (H) indicates a cytoplasmic process extending from the soma. (J) Donor-derived astrocytes (clone H6) in the adult subcortical white matter (indicated by the arrow) and striatum following neonatal intraventricular implantation, immunostained with a human astrocyte-specific anti-GFAP antibody. Inset is higher magnification. (K–Q) Expression of *v-myc* by human NSC clone H6 (K–N) 24 hours and (O–Q) 3 weeks following engraftment in the SVZ. (K,M,O) DAPI nuclear stains of the adjacent panels (L,N,P), immunostained for *v-myc* and (Q) immunostained for BrdU-positive donor-derived cells. (Q) is same as (P). Scale bars: (A and K): 100  $\mu$ m; (D and E): 10  $\mu$ m; (O): 50  $\mu$ m.

Human NSCs integrated into the SVZ within 48 h following implantation (Figs. 4A and B, 5K–N). As with endogenous SVZ progenitors, engrafted human NSCs migrated out along the subcortical white matter by 2 weeks following engraftment (Fig. 4C), and, by 3–5 weeks had appropriately differentiated into oligodendrocytes and astrocytes (Fig. 5A and H–J). The ready detection of donor-derived astrocytes in vivo (Fig. 5J) contrasts with the initial absence of mature astrocytes when human NSC clones were maintained in vitro in isolation from the in vivo environment (Fig. 2D). Signals emanating from other components of the murine CNS appear necessary for promoting astrocyte differentiation and/or maturation from multipotent cells.

Endogenous SVZ progenitors also migrate anteriorly along the RMS and differentiate into OB interneurons. By 1 week following transplantation, a subpopulation of donor-derived human cells from the SVZ migrated along the RMS (Fig. 4D and E). In some cases, these cells migrated together in small groups (Fig. 4E), a

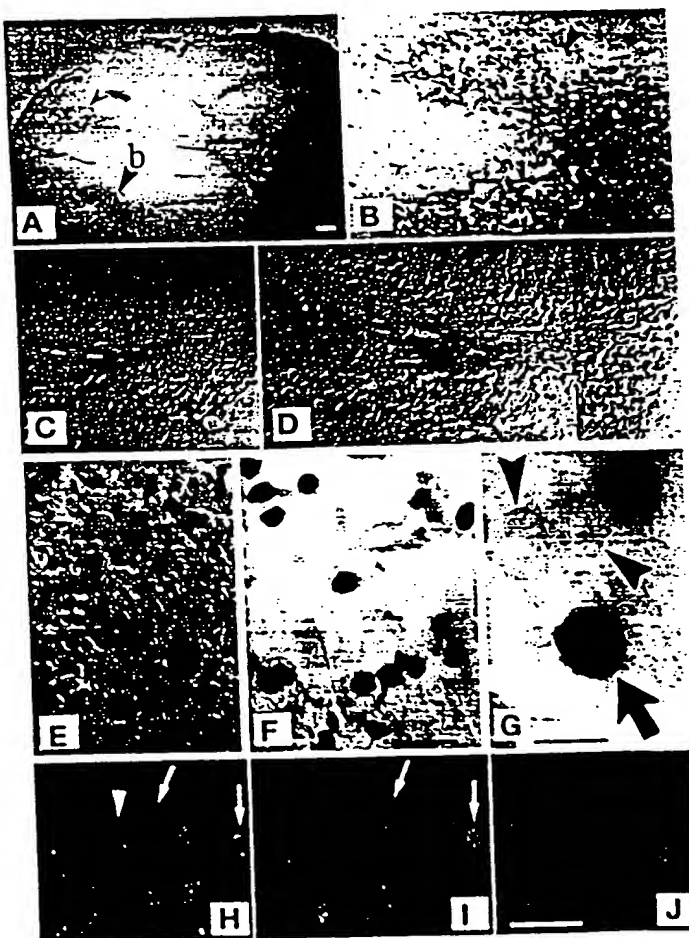


**Figure 6.** Transplantation of human NSCs into granule neuron-deficient cerebellum. (A–G) Donor-derived cells (clone H6) identified in the mature cerebellum by anti-BrdU immunoperoxidase cytochemistry (brown nuclei) following implantation into and migration from the neonatal *mea* EGL. (A) The internal granule cell layer (IGL and arrowheads) within the parasagittal section of the cerebellum. (B) Higher magnification of the posterior lobe indicated by "b" in (A). (C–G) Increasing magnifications of donor-derived cells within the IGL of a *mea* anterior lobe (different animal from [A,B]). (G) Normarski optics: residual host granule neurons indicated by arrowheads, representative BrdU positive donor-derived neuron indicated by the arrow. (H) Colabeling with anti-BrdU (green) and (I) NeuN (red) indicated with arrows. Arrowhead indicates BrdU+/NeuN+ cell. (J) Fluorescent in situ hybridization of cells within the IGL using a human-specific probe (red). Scale bars: (A and B): 100  $\mu$ m; (F, G, and J): 10  $\mu$ m.

Table 1. Human neural stem cell clones.

Clone	Propagation technique	Engraftable
H1	bFGF	+
H6	v-myc	+
H9	v-myc	+
E11	v-myc	+
D10	v-myc	-
C2	v-myc	-

behavior typical of endogenous murine SVZ precursors<sup>11</sup>. Three weeks following transplantation, a subpopulation of donor-derived neurons (human-specific NF-positive cells) were present within the parenchyma of the OB, intermingled with host neurons (Fig. 5B–G). Not only were these donor-derived cells human NF-positive (Fig. 5D), but, when sections through the OB were reacted with both an antibody against BrDU (to identify prelabeled donor-derived human cells) and with an antibody to the mature neuronal marker NeuN, a large number of double-labeled BrDU+/NeuN+ donor-derived cells were integrated within the granule layer (Fig. 5E–G), mimicking the NeuN expression pattern of endogenous host, murine interneurons (Fig. 5F and G).

Identical clones were implanted into a different germinal zone at the opposite end of the neuraxis to determine their plasticity. Transplants of the same human NSCs into the EGLs of newborn mouse cerebella appropriately yielded different neuronal cell types in this different location, primarily cerebellar granule cells in the IGL (Fig. 6A–I), detailed below.

Therefore, *in vivo*—as *in vitro* (Fig. 2)—all engraftable human NSC clones gave rise to cells in all three fundamental neural lineages: neurons (Figs. 5D–G and 6), oligodendrocytes (Fig. 5H and I), and astrocytes (Fig. 5J). Not only did transplanted brains look histologically normal (donor cells migrated and integrated seamlessly into host parenchyma yielding no discernible graft margins), but engrafted animals exhibited no indications of neurologic dysfunction. Thus, structures that received contributions from donor human NSCs appeared to have developed normally.

Although most clones engrafted well, two appeared to engraft poorly (Table 1). Nevertheless, *in vitro* these clones displayed characteristics seemingly identical to those of the more robustly engrafting clones. Thus, ostensibly equivalent multipotency *in vitro* does not necessarily translate into equivalent potential *in vivo*, suggesting that each clone should be individually tested. This observation also suggests that transplantation of mixed polyclonal populations, because of their shifting representations of various clones, may be a problematic strategy.

Foreign transgene expression *in vivo*. Many CNS gene therapy needs require that donor cells express foreign genes in widely disseminated locations<sup>12</sup> (in addition to being able to do so in anatomically restricted regions<sup>13</sup>). Murine NSC clones have this capacity<sup>14,15</sup>. Human NSCs appear similarly capable. A representative retrovirally transduced, lacZ-expressing clone (Fig. 5A–C) continued to produce  $\beta$ -galactosidase after migration to, and stable integration and maturation within, host parenchyma at distant sites in the mature animal.

Spontaneous constitutive downregulation of v-myc expression. In the case of genetically manipulated human NSC clones, the propagating gene product v-myc is undetectable in donor human cells beyond 24–48 h following engraftment (Fig. 5K–Q) despite the fact that the brains of transplant recipients contain numerous stably engrafted, healthy, well-differentiated, nondisruptive, donor-derived cells (Figs. 4, 5A–I and Q, and 6). Identical findings have been observed with v-myc-propagated murine NSC clones<sup>16</sup> in which v-myc downregulation occurs constitutively and spontaneously and correlates with the typical quiescence of engrafted cells

within 24–48 h posttransplantation. These observations suggest that v-myc is regulated by the normal developmental mechanisms that downregulate endogenous cellular myc in CNS precursors during mitotic arrest and/or differentiation. The loss of v-myc expression from stably engrafted NSCs following transplantation is consistent with the invariant absence of brain tumors derived from implanted v-myc-propagated NSCs, even after several years in mice<sup>10</sup>. As with mouse NSCs, neoplasms are never seen using human NSCs.

Neural cell replacement *in vivo*. Neurologic mouse mutants have provided ideal models for testing specific neural cell replacement strategies. The *meander tail* (*mea*) mutant is one such model of neurodegeneration and impaired development. *Mea* is characterized by a cell-autonomous failure of granule neurons to develop and/or survive in the cerebellum, especially in the anterior lobe<sup>17</sup>. Murine NSCs are capable of reconstituting the granule neuron-deficient IGL<sup>18</sup>. To assess whether human cells may be comparably effective in replacing neurons in CNS disorders, human NSC clones were engrafted into EGLs of newborn *mea* cerebella. When analyzed at the completion of cerebellar organogenesis, donor-derived human cells were present throughout the IGL (Fig. 6). They possessed the definitive size, morphology, and location of cerebellar granule neurons (Fig. 6E–G), identical to the few residual endogenous murine host granule neurons with which they were intermixed (Fig. 6G). That these replacement neurons were of human origin was confirmed by fluorescence *in situ* hybridization (FISH), using a human-specific chromosomal probe (Fig. 6I). The neuronal phenotype was confirmed by demonstrating that most engrafted cells in the *mea* IGL were immunoreactive for NeuN (Fig. 6H and I); as in the OB, endogenous interneurons in the IGL similarly express NeuN. Thus, engrafted NSCs of human origin appear sufficiently plastic to respond appropriately to varying local cues for lineage determination; recall that the donor human cells were not initially derived from a postnatal brain or from a cerebellum. Furthermore, human NSCs may be capable of appropriate neural cell replacement, much as murine NSCs are<sup>19</sup>. While many gene therapy vehicles depend on relaying new genetic information through established neural circuits—that may, in fact, have degenerated—NSCs may participate in the reconstitution of these pathways.

We have presented evidence that neural cells with stem cell features may be isolated from human brains and emulate NSCs in lower mammals<sup>20</sup>, vouchsafing conservation of neurodevelopmental principles and suggesting that this cell type may be applied to a range of research and clinical problems in humans. NSCs may serve as adjuncts to other cellular<sup>21</sup>, viral<sup>22</sup>, and nonviral<sup>23</sup> vectors, including other human-derived neural cells<sup>24</sup>. Not only might the clones described here serve these functions, but our data suggest that investigators may readily utilize NSCs from other human material via a variety of equally safe and effective epigenetic and genetic means. That the methods used here yielded comparable cells suggests that investigators may choose the technique that best serves their needs. Insights from studies of NSCs perpetuated by one strategy may be legitimately joined to those derived from studies using others, providing a more complete picture of NSC biology and its applications.

### Experimental protocol

Maintenance and propagation of human NSCs in culture. A suspension of primary dissociated neural cells ( $5 \times 10^5$  cells/ml), initially prepared and stably cultured from the periventricular region of the telencephalon of a 15-week human fetus<sup>25</sup> was plated on uncoated tissue culture dishes (Corning, Cambridge, MA) in the following growth medium: Dulbecco's Modified Eagles Medium (DMEM) + F12 medium (1:1) supplemented with N2 medium (Gibco, Grand Island, NY) to which was added bFGF (10–20  $\mu$ g/ml) + heparin (8  $\mu$ g/ml) and/or EGF (10–20  $\mu$ g/ml). Medium was changed every 5

## RESEARCH

days. Cell aggregates were dissociated in trypsin-EDTA (0.05%) when >10 cell diameters in size and replated in growth medium at  $5 \times 10^4$  cells/ml.

Differentiating culture conditions. Dissociated NSCs were plated on poly-L-lysine (PLL)-coated slides (Nunc, Naperville, IL) in DMEM + 10% fetal bovine serum (FBS) and processed weekly for immunocytochemistry (ICC). In most cases, differentiation occurred spontaneously. For astrocytic maturation, clones were cocultured with primary dissociated embryonic CD-1 mouse brain<sup>24</sup>.

Retrovirus-mediated gene transfer. Two xenotropic, replication-incompetent retroviral vectors were used to infect human NSCs. A vector encoding *lacZ* was similar to BAG<sup>25</sup> except for the PG13 xenotropic envelope. An amphotropic vector encoding *v-myc* was generated using the ecotropic vector described for generating murine NSC clone C17.2 (ref. 20) to infect the GP + envAM12 amphotropic packaging line<sup>26</sup>. No helper virus was produced. Infection of bFGF- and/or EGF-maintained human neural cells with either vector ( $4 \times 10^6$  colony-forming units) was as described<sup>26</sup>.

Cloning of human NSCs. Cells were dissociated, diluted to 1 cell/15  $\mu$ l and plated at 15  $\mu$ l/well of a Terasaki or 96-well dish. Wells with single cells were immediately identified. Single-cell clones were expanded and maintained in bFGF-containing growth medium. Monoclonality was confirmed by identifying a single and identical genomic insertion site by Southern blot analysis for either the *lacZ*- or the *v-myc*-encoding provirus in all progeny as described<sup>26</sup>. The *v-myc* probe was generated by nick translation labeling with <sup>32</sup>P dCTP; a probe to the *neo* sequence of the *lacZ*-encoding vector was generated by PCR using <sup>32</sup>P dCTP.

Cryopreservation. Trypsinized human cells were resuspended in a freezing solution comprising 10% dimethyl sulfoxide, 50% FBS, and 40% bFGF-containing growth medium and brought slowly to -140°C.

Cross-correction of mutation-induced  $\beta$ -hexosaminidase deficiency. The murine NSC clones C17.2 and C17.2H (ref. 22) were maintained in similar serum-free conditions as the human cells. NSCs were cocultured in a transwell system with primary dissociated neural cultures<sup>27</sup> from the brains of either wild-type or  $\alpha$ -subunit null (TSD) neonatal mice<sup>28</sup>. These cultures were prepared under serum-free conditions, plated onto PLL-coated glass coverslips, and maintained in the medium described for NSCs. To assess production of a secreted gene product capable of rescuing the mutant phenotype, NSCs (murine and human) were cultured on one side of a membrane with 0.4  $\mu$ m pores (sufficient to allow passage of hexosaminidase but not cells). The membrane was immersed in a well at the bottom of which rested the coverslip. After 10 days, coverslips were examined for hexosaminidase activity; for expression of the  $\alpha$ -subunit in cells of various CNS lineages; for reduction in GM<sub>1</sub> storage. Hexosaminidase activity was assayed by standard histochemical techniques using the substrate naphthol-AS-BI-N-acetyl- $\beta$ -D-glucuronide (NASBG)<sup>29</sup>; cells stain increasingly pink-red in direct proportion to their enzyme activity. NASBG staining of dissociated wild-type mouse brain cells served as a positive control for both intensity of normal staining and percentage of NASBG-positive cells (~100%). Neural cell types were identified by ICC with antibodies to standard markers: for neurons, NeuN (1:100; gift of R. Mullen, Chemicorp, Temecula, CA); for astrocytes, GFAP (1:500; Sigma, St. Louis, MO); for oligodendrocytes, CNPase (1:500; Sternberger Monoclonals, Baltimore, MD); and for immature undifferentiated progenitors, nestin (1:1000; Pharmingen, San Diego, CA). The  $\alpha$ -subunit of human  $\beta$ -hexosaminidase was detected with a specific antibody<sup>30</sup>. Cells were assessed for dual immunoreactivity to that antibody and to the cell type-specific antibodies to assess which TSD CNS cell types had internalized enzyme from human NSCs. Intracytoplasmic GM<sub>1</sub> was recognized by a specific antibody<sup>31</sup>.

Transplantation. For some models, each lateral ventricle of cryoanesthetized postnatal day 0 (P0) mice was injected as described<sup>32</sup> with 2  $\mu$ l of NSCs suspended in phosphate buffered saline (PBS) ( $4 \times 10^4$  cells/ $\mu$ l). For other models, 2  $\mu$ l of the NSC suspension were implanted into the EGL of each cerebellar hemisphere and the vermis as described<sup>33</sup>. All transplant recipients and untransplanted controls received daily cyclosporin 10 mg/kg given intraperitoneally (Sandoz, East Hanover, NJ) beginning on day of transplant. CD1 and *mea* mouse colonies are maintained in our lab.

Detection and characterization of donor human NSCs in vivo. Brains of transplanted mice were fixed and cryosectioned as described<sup>34</sup> at serial time points: P1, P2, and weekly through 5 weeks of age. Prior to transplantation, some human cells were transduced with *lacZ*. To control for and circumvent the risk of transgene downregulation, cells were also prelabeled either by in vitro exposure to BrdU (20  $\mu$ M; 48 h prior to transplantation) and/or with the nondiffusible vital fluorescent membrane dye PKH-26 (immediately

prior to transplantation as per Sigma protocol). Engrafted cells were then detected, as appropriate, by Xgal histochemistry<sup>35</sup>; by ICC with antibodies against  $\beta$ -galactosidase<sup>36</sup> (1:1000, XXX, Durham, NC), BrdU (1:10; Boehringer, Indianapolis, IN), human-specific NF (1:150; Boehringer), and/or human-specific GFAP (1:200; Sternberger Monoclonals); by FISH using a digoxigenin-labeled probe complementary to regions of the centromere present uniquely and specifically on all human chromosomes (Oncor, Gaithersburg, MD); and/or by PKH-26 fluorescence (through a Texas Red [TR] filter), with nondiffusibility having been verified for NSCs. Cell type identity of donor-derived cells was also established as necessary by dual staining with antibodies to neural cell type-specific markers: anti-NF (1:250; Sternberger) and anti-NeuN (1:20) to identify neurons; anti-CNPase (1:200–1:500) to identify oligodendrocytes; and anti-GFAP (1:150) to identify astrocytes. Immunostaining used standard procedures<sup>37</sup> and a TR-conjugated secondary antibody (1:200; Vector, Burlingame, CA). Immunoreactivity to human-specific antibodies also used standard procedures and a fluorescein-conjugated antimouse IgG secondary antibody (1:200; Vector). To reveal BrdU-intercalated cells, tissue sections were first incubated in 2N HCl (37°C for 30 min), washed twice in 0.1 M sodium borate buffer (pH 8.3), washed thrice in PBS, and permeabilized before exposure to anti-BrdU. Immunoreactivity was revealed with either a fluorescein-conjugated (1:250; Jackson, West Grove, PA) or a biotinylated (1:200; Vector) secondary antibody. *V-myc* expression (unique to donor-derived cells) was assessed with an antibody to the protein (1:1000; UBI, Lake Placid, NY). To visualize cellular nuclei, sections were incubated in the blue fluorescent nuclear label DAPI (10 min at 20°C). FISH for the human-specific centromere probe was performed on cryosections from 4% paraformaldehyde/2% glutaraldehyde-fixed brains that were permeabilized, incubated in 0.2 N HCl, exposed to proteinase K (100  $\mu$ g/ml in 0.1M Tris, 0.005 M EDTA [pH 8.0]), washed (0.1% glycine), and rinsed (50% formamide/2x SSC). Probe was then added to the sections, which were coverslipped, denatured (100°C for 10 min), hybridized (15 h at 37°C), and washed (per manufacturer's protocol). Probe was detected by an antidigoxigenin TR-conjugated antibody (Boehringer) diluted 1:5 in 0.5% bovine serum albumin + 5% normal human serum in PBS. For some donor cells, multiple detection techniques were performed.

## Acknowledgments

We thank Angelo Vescovi, Ron McKay, and Jeff Macklis for advice and critique, and Baolin Chang for technical assistance. This work was supported in part by grants to E.Y.S. from NINDS (NS33852), the Paralyzed Veterans of America, the American Paralysis Association, Late Onset Tay-Sachs Foundation, and Hood Foundation; to J.H.W. from NIDDK (DK42707; DK46637); to S.U.K. from the Myelin Project of Canada; and to R.L.S. from NINDS (NS20820). J.D.F. and S.A. were partially supported by NIH training grants.

- McKay, R.D.G. 1997. Stem cells in the central nervous system. *Science* 276:66–71.
- Gage, F.H. and Chnsten, Y. (eds.). 1997. *Isolation, characterization, and utilization of CNS stem cells—research & perspectives in neuroscience*. Springer-Verlag, Heidelberg, Berlin.
- Momson, S.J., Shah, N.M., and Anderson, D.J. 1997. Regulatory mechanisms in stem cell biology. *Cell* 88:287–298.
- Stemple, D.L. and Mahanthappa, N.K. 1997. Neural stem cells are blasting off. *Neuron* 18:1–4.
- Weiss, S., Reynolds, B.A., Vescovi, A.L., Morshead, C., Craig, C., and van der Kooy, D. 1996. Is there a neural stem cell in the mammalian forebrain. *Trends Neurosci.* 19:387–393.
- Alvarez-Buylla, A. and Lois, C. 1995. Neuronal stem cells in the brain of adult vertebrates. *Stem Cells (Dayton OH)* 13:263–272.
- Qian, X., Davis, A.A., Goderie, S.K., and Temple, S. 1997. FGF2 concentration regulated the generation of neurons and glia from multipotent cortical stem cells. *Neuron* 18:81–93.
- Snyder, E.Y. 1998. Neural stem-like cells: Developmental lessons with therapeutic potential. *The Neuroscientist*. In press.
- Martinez-Serrano, A. and Bjorklund, A. 1997. Immortalized neural progenitor cells for CNS gene transfer and repair. *Trends Neurosci.* 20:530–538.
- Snyder, E.Y., Deitcher, D.L., Walsh, C., Arnold-Aldea, S., Hartweg, E.A., and Cepko, C.L. 1992. Multipotent cell lines can engraft and participate in the development of mouse cerebellum. *Cell* 68:1–20.
- Reinfranz, P.J., Cunningham, M.G., and McKay, R.D.G. 1991. Region-specific differentiation of the hippocampal stem cell line H19.5 upon implantation into the developing mammalian brain. *Cell* 66:713–729.
- Shinabuddin, L.S., Hertz, J.A., Holets, V.R., and Whittemore, S.R. 1995. The adult CNS retains the potential to direct region-specific differentiation of a transplanted neuronal precursor cell line. *J. Neurosci.* 15:6666–6678.
- Gage, F.H., Coates, P.W., and Palmer, T.D. 1995. Survival and differentiation of

- adult neuronal progenitor cells transplanted to the adult brain. *Proc. Natl. Acad. Sci. USA* 92:11879-11883.
14. Fisher, L.J. 1997. Neural precursor cells: application for the study and repair of the central nervous system. *Neurobiol. Dis.* 4:1-22.
  15. Whittemore, S.R. and Snyder, E.Y. 1996. The physiologic relevance and functional potential of central nervous system-derived cell lines. *Mol. Neurobiol.* 12:13-38.
  16. Gage, F.H. 1998. Cell therapy. *Nature* (suppl.) 392:18-24.
  17. Verma, I.M. and Somia, N. 1997. Gene therapy: promises, problems, and prospect. *Nature* 389:239-242.
  18. Kilpatrick, T. and Bartlett, P.F. 1993. Cloning and growth of multipotential neural precursors: requirements for proliferation and differentiation. *Neuron* 10:255-265.
  19. Gritti, A., Parati, E.A., Cova, L., Frolichsthal, P., Galli, R., Wanke, E. et al. 1996. Multipotential stem cells from the adult mouse brain proliferate and self-renew in response to basic fibroblast growth factor. *J. Neurosci.* 16:1091-1100.
  20. Ryder, E.F., Snyder, E.Y., and Cepko, C.L. 1990. Establishment and characterization of multipotent neural cell lines using retrovirus vector mediated oncogene transfer. *J. Neurobiol.* 21:356-375.
  21. Snyder, E.Y., Taylor, R.M., and Wolfe, J.H. 1995. Neural progenitor cell engraftment corrects lysosomal storage throughout the MPS VII mouse brain. *Nature* 374:367-370.
  22. Lacorazza, H.D., Flax, J.D., Snyder, E.Y., and Jendoubi, M. 1996. Expression of human  $\beta$ -hexosaminidase  $\alpha$ -subunit gene (the gene defect of Tay-Sachs disease) in mouse brains upon engraftment of transduced progenitor cells. *Nat. Med.* 4:424-429.
  23. Kitchens, D.L., Snyder, E.Y., and Gottlieb, D.I. 1994. bFGF and EGF are mitogens for immortalized neural progenitors. *J. Neurobiol.* 25:797-807.
  24. Kornblum, H.I., Raymon, H.K., Momson, R.S., Cavanaugh, K.P., Bradshaw, R.A., and Leslie, F.M. 1990. Epidermal growth factor and basic fibroblast growth factor: effects on an overlapping population of neocortical neurons in vitro. *Brain Res.* 535:255-263.
  25. Birren, S.J., Verdi, J.M., and Anderson, D.J. 1992. Membrane depolarization induces p140trk and NGF responsiveness, but not p75LNGFR, in MAH cells. *Science* 257:395-397.
  26. Snyder, E.Y. and Wolfe, J.H. 1996. CNS cell transplantation: a novel therapy for storage diseases? *Current Opin. Neurol.* 9:126-136.
  27. Yamanaka, S., Johnson, M.D., Grinberg, A., Westphal, H., Crawley, J.N., Taniike, M. et al. 1994. Targeted disruption of the HexA gene results in mice with biochemical and pathologic features of Tay-Sachs disease. *Proc. Natl. Acad. Sci. USA* 91:9975-9979.
  28. Suhonen, J.O., Peterson, D.A., Ray, J., and Gage, F.H. 1996. Differentiation of adult hippocampus-derived progenitors into olfactory neurons in vivo. *Nature* 383:624-627.
  29. Fishell, G. 1995. Striatal precursors adopt cortical identities in response to local cues. *Development* 121:803-812.
  30. Campbell, K., Olsson, M., and Bjorklund, A. 1995. Regional incorporation and site-specific differentiation of striatal precursors transplanted to the embryonic forebrain ventricle. *Neuron* 15:1259-1273.
  31. Sidman, R.L., Miale, I.L., and Feder, N. 1959. Cell proliferation and migration in the primitive ependymal zone: an autoradiographic study of histogenesis in the nervous system. *Exp. Neurol.* 1:322-333.
  32. Lois, C., Garcia-Verdugo, J.-M., and Alvarez-Buylla, A. 1996. Chain migration of neuronal precursors. *Science* 271:978-981.
  33. Goldman, S.A. and Luskin, M.B. 1998. Strategies utilized by migrating neurons of the postnatal vertebrate forebrain. *Trends Neurosci.* 21:107-114.
  34. Rosano, C.M., Yandava, B.D., Kosaras, B., Zurakowski, D., Sidman, R.L., and Snyder, E.Y. 1997. Differentiation of engrafted multipotent neural progenitors towards replacement of missing granule neurons in meander tail cerebellum may help determine the locus of mutant gene action. *Development* 124:4213-4224.
  35. Snyder, E.Y., Yoon, C.H., Flax, J.D., and Macklis, J.D. 1997. Multipotent neural progenitors can differentiate toward replacement of neurons undergoing targeted apoptotic degeneration in adult mouse neocortex. *Proc. Natl. Acad. Sci. USA* 94:11645-11650.
  36. Svendsen, C.N., Caldwell, M.A., Shen, J., ter Borg, M.G., Rosser, A.E., Tyers, P. et al. 1997. Long-term survival of human central nervous system progenitor cells transplanted into a rat model of Parkinson's disease. *Exp. Neurol.* 148:135-146.
  37. Sabaate, O., Horellou, P., Vigne, E., Colin, P., Pemcaudat, M., Buc-Caron, M.-H. et al. 1995. Transplantation to the rat brain of human neural progenitors that were genetically modified using adenovirus. *Nat. Genet.* 9:256-260.
  38. Borlongan, C.V., Tajima, Y., Trojanowski, J.Q., Lee, V.M., and Sanberg, P.R. 1998. Transplantation of cryopreserved human embryonal carcinoma-derived neurons (NT2N cells) promotes functional recovery in ischemic rats. *Exp. Neurol.* 149:310-321.
  39. Sah, D.W.Y., Ray, J., and Gage, F.H. 1997. Bipotent progenitor cell lines from the human CNS. *Nat. Biotechnol.* 15:574-580.
  40. Moretto, G., Xu, R.Y., Walker, D.G., and Kim, S.U. 1994. Co-expression of mRNA for neurotrophic factors in human neurons and glial cells in culture. *J. Neuropathol. Exp. Neurol.* 53:78-85.
  41. Markowitz, D., Goff, S., and Bank, A. 1988. Construction and use of a safe and efficient amphotropic packaging cell line. *Virology* 167:400-406.



# Site-Specific Migration and Neuronal Differentiation of Human Neural Progenitor Cells after Transplantation in the Adult Rat Brain

Rosemary A. Fricker,<sup>1,2</sup> Melissa K. Carpenter,<sup>2,4</sup> Christian Winkler,<sup>1</sup> Corinne Greco,<sup>3</sup> Monte A. Gatos,<sup>1,2</sup> and Anders Björklund<sup>1</sup>

<sup>1</sup>Wallenberg Neuroscience Center, Division of Neurobiology, Lund University, S-223 Lund, Sweden, <sup>2</sup>Department of Neurology, Harvard Medical School, Children's Hospital, Boston, Massachusetts 02115, <sup>3</sup>CytoTherapeutics, Lincoln, Rhode Island 02865, and <sup>4</sup>Geron Corporation, Menlo Park, California 94025

Neural progenitor cells obtained from the embryonic human forebrain were expanded up to 10<sup>7</sup>-fold in culture in the presence of epidermal growth factor, basic fibroblast growth factor, and leukemia inhibitory growth factor. When transplanted into neurogenic regions in the adult rat brain, the subventricular zone, and hippocampus, the *in vitro* propagated cells migrated specifically along the routes normally taken by the endogenous neuronal precursors: along the rostral migratory stream to the olfactory bulb and within the subgranular zone in the dentate gyrus, and exhibited site-specific neuronal differentiation in the granular and periglomerular layers of the bulb and in the dentate granular cell layer. The cells exhibited substantial migration also within the non-neurogenic region, the striatum, in a seem-

ingly nondirected manner up to ~1–1.5 mm from the graft core, and showed differentiation into both neuronal and glial phenotypes. Only cells with glial-like features migrated over longer distances within the mature striatum, whereas the cells expressing neuronal phenotypes remained close to the implantation site. The ability of the human neural progenitors to respond *in vivo* to guidance cues and signals that can direct their differentiation along multiple phenotypic pathways suggests that they can provide a powerful and virtually unlimited source of cells for experimental and clinical transplantation.

**Key words:** progenitor cells; human; transplantation; neuron; subventricular zone; dentate gyrus; striatum

The limited capacity for structural repair in the mammalian brain is in part explained by the inability of the mature CNS to generate new cellular elements in response to damage. Cell transplantation offers a possibility to circumvent this limitation. Both rodent and primate experiments show that neuroblasts and young postmitotic neurons obtained from defined parts of the neuraxis during development can survive, mature, and grow extensive functional axonal connections after transplantation to brain-damaged recipients, and both structurally and functionally replace lost neurons in the mature brain (for review, see Dunnett and Björklund, 1994). Because of the limited migratory capacity of the differentiated cells, however, these types of implants are unable to integrate into the cellular architecture of the host.

Previous studies have shown that less differentiated precursor cells, taken at premigratory stages of neuronal development, can make use of available substrates or pathways for migration, mix with endogenous pools of precursors, and participate in ongoing neurogenesis, both during development (McConnell, 1988; Gao and Hatten, 1994; Zigova et al., 1996) and in areas of the mature brain, the anterior subventricular zone (SVZ), and the hip-

popampal dentate gyrus, where neurogenesis continues into adulthood (Lois and Alvarez-Buylla, 1993; Vilaro-Abejon et al., 1995). Similarly, mixed precursor cell populations, injected *in utero* into the developing forebrain, integrate across the ventricular wall and undergo site-specific migration and neuronal differentiation in widespread brain regions (Brösle et al., 1995; Campbell et al., 1995; Fishell, 1995), suggesting that undifferentiated progenitors may be an interesting source of cells for intracerebral transplantation.

Recently, neural progenitors with the capacity to give rise to all major cell types of the mature CNS have been isolated from the developing or adult CNS (Weiss et al., 1996b; Alvarez-Buylla, 1997; Lusk et al., 1997; Ray et al., 1997). They become more restricted in number during development and remain as a small, relatively quiescent population of dividing cells in the subventricular regions of the adult CNS. These neural progenitors can be grown *in vitro* in the presence of either epidermal growth factor (EGF) or basic fibroblast growth factor (bFGF, FGF-2), as a population of continuously dividing progenitors capable of differentiating into both neurons and glia (Murphy et al., 1990; Reynolds and Weiss, 1992a,b, 1996; Richards et al., 1992; Ray et al., 1993; Vescovi et al., 1993; Sosenbrenner et al., 1994; Palmer et al., 1995). Cells isolated from the rat hippocampus in the presence of bFGF have been shown to express region-specific migration and neuronal differentiation after transplantation to the adult rat brain (Gage et al., 1995; Suhonen et al., 1996). Embryonic mouse or rat forebrain progenitors expanded in the presence of EGF, by contrast, develop into predominantly glial phenotypes *in vivo*, as observed after transplantation to the adult rat spinal cord (Hummel et al., 1997) or the developing rat forebrain (Winkler et al., 1998).

Received Dec. 7, 1998; revised April 13, 1999; accepted April 27, 1999.

This study was supported by the Wellcome Trust, the Swedish Medical Research Council, the Wenner-Gren Foundation, and CytoTherapeutics Inc. We thank Åke Seliger and Lars Wahlberg for the supply of human embryonic tissue; Tamas Kirik, Olov Lindvall, Olov Lindvall, Alice Plesch, Birgit Hvalby, Jørgen Jensen, Ulla Jørgensen, Karin Oden, Sandy Sherman, and Olov Lindvall for excellent technical assistance; and Joe Hwang for useful discussions and comments on this manuscript. The illustrations were a generous gift from Dr. Steven A. Goldman, and the DARPP-32 antibody was a generous gift from Dr. Paul Greengard.

Correspondence should be addressed to Dr. Rosemary Fricker, Department of Neurology, Division of Neurobiology, Harvard Medical School, 330 Longwood Avenue, Boston, MA 02115.

Copyright © 1999 Society for Neuroscience 0270-6474/99/195990-14\$05.00/0



Here, we have examined the question of whether progenitors isolated from the developing human CNS can exhibit *in vivo* neurogenic properties after implantation into the brain of adult recipients. Cells obtained from the forebrain of 6.5- to 9-week-old human fetuses were maintained as continuously dividing cultures in the presence of EGF, bFGF, and leukemia inhibitory growth factor (LIF). Cells expanded  $10^3$ - $10^5$ -fold in culture (over 9–21 passages) survived well after transplantation to both neurogenic and non-neurogenic sites; cells contained within these grafts showed migration, integration, and site-specific differentiation into both neurons and glia.

## MATERIALS AND METHODS

**Generation and *in vitro* culture of human progenitor cells.** Generation of the human progenitor cell lines has been described previously (Carpenter et al., 1994). Embryonic brain tissue was obtained from one 6.5 week and one 9 week embryo (post-conception) under compliance with National Institutes of Health guidelines, Swedish government guidelines, and the local ethics committee, and appropriate consent forms were used. Tissue from the forebrain was dissected in sterile saline and transferred to N2 medium, a defined DMEM/F12-based medium (Life Technologies, Grand Island, NY) containing 0.6% glucose, 25  $\mu$ M human insulin, 100  $\mu$ M human transferrin, 20 nM progesterone, 60  $\mu$ M putrescine, 30 nM selenium chloride, 2 mM glutamine, 3 mM sodium butyrate, 3 mM LIF, and 2  $\mu$ M heparin (Sigma, St. Louis, MO). The tissue was dissociated using a standard glass homogenizer, and the dissociated cells were grown on uncoated plastic T75 flasks in N2 medium containing human EGF (hEGF, 20 ng/ml; Life Technologies), human basic FGF (bbFGF, 20 ng/ml; Life Technologies), and human LIF (hLIF) (10 ng/ml, R+D Systems, UK), at a density of  $\sim 100,000$  cells/ml.

The cells grew as free-floating clusters ("neurospheres"), and were prevented from attachment by gently knocking the flasks each day. Any cells that adhered to the plastic and began to extend processes were not removed by this procedure and therefore were not carried through to the next passage. The spheres were passaged by mechanical dissociation every 7–10 d and reseeded as single cells at a density of  $\sim 100,000$  cells/ml. The cells used for transplantation (the 6.5FBr and 9FBr cultures) had been expanded over 9–21 passages, which corresponds to a total increase in cell numbers of  $\sim 10^5$  at 9 passages to at least  $10^7$  at 21 passages (Carpenter et al., 1994).

**Labeling methods and preparation of cells for transplantation.** To enable the detection of the cells *in vivo*, cultures were labeled with 1  $\mu$ M bromodeoxyuridine (BrdU), which was added to the culture medium 48 hr before the preparation of the cells for transplantation. This resulted in  $\sim 80\%$  labeling efficiency, with no apparent changes in growth rate of the spheres.

Cells were taken for transplantation 4–5 d after the last passage as small spheres of 3–30 cells. The spheres were collected by centrifugation at 1000 rpm for 3 min and resuspended in 1 ml DMEM/F12 medium. To check the cell viability, an aliquot of the sphere suspension was removed and mixed with trypan blue. After this was ascertained, a second cell count was performed by triturating the trypan blue aliquot to give single cells. The sphere suspension was centrifuged a second time and resuspended in a smaller volume to give the equivalent of  $\sim 100,000$  cells/ $\mu$ l.

**Transplantation.** Adult female Sprague Dawley rats (B&K Universal, Stockholm, Sweden), weighing  $\sim 250$  g at the beginning of the study, were used. They were caged in groups of two and maintained on a 12 hr light/dark cycle with constant temperature and humidity, with ad libitum food and water. The animals were immunosuppressed throughout the experiment by daily injections of 10 mg/kg cyclosporin, beginning 1 d before transplantation.

Stereotaxic surgery was performed under deep equithesin anesthesia (3 ml/kg body weight, i.p.). Rats received 1  $\mu$ l cell suspension bilaterally in either the SVZ, rostral migratory stream (RMS), or hippocampus, or 2  $\mu$ l in the striatum, according to the following coordinates: SVZ, anterior (A) = +1.6, lateral (L) = +1.5, ventral (V) = -4.2; RMS, A = -3.7, L = +1.5, V = -3.0; hippocampus, A = -3.6, L = +2.0, V = -3.0; -2.6; striatum, A = 0.6, L = +2.6, V = -4.8, -4.2. The tooth bar was set at -2.3, and all ventral coordinates were taken from dura. Cells were implanted via a glass capillary (inner diameter  $\sim 70$   $\mu$ m) attached to a 2  $\mu$ l Hamilton syringe. For the SVZ transplants, 100,000 cells from the 6.5FBr cell line were transplanted, and the brains were analyzed after 6

weeks ( $n = 10$ ). For the RMS transplants, 100,000 cells were transplanted, and the brains were analyzed at either 2 weeks (6.5FBr,  $n = 10$ ; 9FBr,  $n = 4$ ) or 6 weeks (6.5FBr,  $n = 10$ ). Both cell lines were transplanted to either the striatum (200,000 cells) or hippocampus (100,000 cells), and the brains were analyzed at either 2 or 6 weeks ( $n = 10$  per group).

**Tissue processing.** At either 2 or 6 weeks after transplantation, rats were terminally anesthetized with 5% chloral hydrate and transcardially perfused with 0.1 M PBS followed by 5 min rapid fixation with ice-cold 4% paraformaldehyde (PFA) in 0.1 M phosphate buffer. Brains were removed and placed in PFA overnight, before being transferred to 25% sucrose in PBS. Coronal or sagittal sections were cut on a freezing microtome at a thickness of 30  $\mu$ m. In each case, eight series were collected for further processing.

**Immunocytochemistry.** For BrdU labeling, all sections were pretreated with 1 M HCl for 30 min at 65°C. Sections were incubated in primary antibodies for 36 hr at 4°C. All primary antibodies were diluted in 0.02 M potassium PBS (KPBS) containing 5% normal serum of the species in which the secondary antibody was raised and 0.25% Triton X-100, except for 32 kDa dopamine- and  $\alpha$ -MIF-regulated phosphoprotein (DARPP-32) and  $\gamma$ -aminobutyrate decarboxylase (GAD67) in which Triton X-100 was omitted. Antibodies used in this study were BrdU rat monoclonal (1:100, Chemicon, Temecula, CA), mouse monoclonal 125, Becton Dickinson, Franklin Lakes, NJ),  $\beta$ -tubulin-N1 (1:400, Sigma), calbindin (1:1000, Sigma), DARPP-32 (1:20,000; Dr. P. Greengard, Rockefeller), GAD67 (1:1000, Chemicon), glial fibrillary acidic protein (GFAP, 1:500, Dako-patts), RNA binding protein (Hrb, 1:1000; Dr. S. Goldman, Coriell), neuronal nuclei (NucN, 1:100, Chemicon), tyrosine hydroxylase (TH, 1:500, Polysciences, Rogers, AR), Vimentin (VIM, 1:25, Dako-patts), and human-specific tau (hTau, 1:100, Calbiochem, La Jolla, CA). For all immunohistochemical procedures, adjacent sections served as negative controls and were processed using identical procedures, except for incubation without the primary antibody in each case.

For fluorescent double-labeling (immunocytochemistry, after rinses in KPBS containing 2% of the normal serum, sections were incubated in the secondary antibodies (1:200). For rat anti-BrdU this was donkey anti-rat conjugated to FITC or Cy2 (Jackson); for mouse anti-BrdU, donkey anti-mouse conjugated to FITC or Cy2 (Jackson); for all other primary antibodies raised in mouse, rat-absorbed biotinylated horse anti-mouse (Vector); and for all primary antibodies raised in rabbit, biotinylated swine anti-rabbit (Dako-patts). All secondaries were diluted in KPBS containing 2% normal serum, and sections were reacted for 2 hr at room temperature in the dark. After three rinses in KPBS, sections were reacted with streptavidin conjugated to Cy3 (Jackson) for a further 2 hr at room temperature in the dark.

For immunohistochemistry with hTau, sections were pretreated with 3% H<sub>2</sub>O<sub>2</sub> in 10% methanol to quench endogenous peroxidase activity. Incubation in the primary antibody was performed in KPBS containing 5% normal horse serum and 0.25% Triton X-100 for 36 hr at 4°C. After three rinses in KPBS, sections were incubated in the secondary antibody: rat-absorbed biotinylated horse anti-mouse (Vector) in KPBS containing 2% normal horse serum for 2 hr at room temperature. Further washing in KPBS was followed by incubation with avidin-biotin-peroxidase complex (Vectastain, Vector), for 1.5 hr at room temperature. 3,3'-Diaminobenzidine (Sigma) in 0.03% H<sub>2</sub>O<sub>2</sub> in KPBS was used as the chromogen.

The sections were mounted on chrome-alum-coated slides, and the fluorescent sections were coverslipped using polyvinyl alcohol-1,4-diazabicyclo[2.2.2]octane mounting medium. The hTau slides were dehydrated in ascending alcohols and coverslipped using DAPI mountant.

**Confocal microscopy.** Colocalization of BrdU with neuronal and glial markers was conducted by confocal microscopy to enable exact definition of each of the antibodies, using a Bio-Rad MRC1024UV confocal scanning light microscope. Double-labeled cells were always verified, both by collecting serial sections of 1–2  $\mu$ m throughout the specimen, and by eye, using an Olympus binocular microscope. In all figures, all double-labeled cells that are denoted were identified in this way.

## RESULTS

### *In vitro* characteristics of the transplanted cells

Two different human progenitor cell cultures obtained post mortem from the forebrain of one 6.5 week (6.5FBr) and one 9 week (9FBr) embryo were analyzed. The cells were cultured in the presence of EGF, bFGF and LIF and passaged every 7–10 d. In

these cultures bFGF was necessary to maintain continuous cell proliferation over extended time periods, and this effect was further enhanced by the addition of LIF. Parallel *in vitro* experiments (Carpenter et al., 1999) indicate that LIF promotes the sustained proliferation of the human progenitors in the neurosphere cultures. Moreover, in agreement with previous findings (Sato and Yoshida, 1997), the proportion of cells that differentiated into neurons appeared to be increased in the presence of LIF.

The *in vitro* characteristics of the 6SFB and 9FB progenitor cell cultures have been presented in detail elsewhere (Carpenter et al., 1999). Briefly, both cultures showed a growth rate that was similar to each other and to other human progenitor cell cultures derived from different gestational ages. Cells within undifferentiated spheres were immunopositive for the immature cell marker nestin and were shown to incorporate BrdU, indicative of cell division. To assess the differentiation capacity of these cells, dissociated single cells were plated onto poly-orbitine-coated glass coverslips and cultured for 12–14 d in N2 medium containing 1% FBS. On differentiation, both cell cultures demonstrated the capacity to form neurons, astrocytes, and oligodendrocytes. Immunohistochemistry using an antibody to GFAP revealed a range of 15–55% astrocytes present in both the 6SFB and 9FB cultures between passage 5 (P5) and P35. An antibody to  $\beta$ -tubulin isotype III was used to detect neurons. At P5 the 6SFB cultures generated more  $\beta$ -tubulin-III-positive cells than the 9FB cells (37 vs 20%, respectively). At P20–P30 (150–300 d *in vitro*), the percentage of neurons had decreased to ~15% in both cultures.

#### Survival and differentiation after transplantation to the adult rat brain

Cells from the 6SFB and 9FB cultures were transplanted, under immunosuppression, into two neurogenic sites: the dentate gyrus of the hippocampus and the SVZ and its associated RMS, as well as to a non-neurogenic site, the striatum. Transplantation was performed using cells that had been passaged 9–21 times. The cells were labeled with BrdU during the last 48 hr before transplantation. This resulted in ~80% labeling efficiency and enabled analysis of the grafts by fluorescent immunohistochemistry using a double-labeling technique for BrdU in combination with specific neuronal and glial markers. In addition, hTau was used to identify the grafted cells.

In all animals, BrdU-positive transplanted cells were identified in all graft sites, at both 2 and 6 weeks after transplantation. Similarly, staining with the human-specific tau antibody revealed cellular and axonal profiles at all transplant sites, indicating graft survival in all cases. Extensive migration of BrdU-labeled cells, as described below, were seen in all animals where the graft deposits had been correctly placed in the RMS, SVZ, or hippocampus, respectively. No evidence of tumor formation was observed.

The transplants from both cell cultures (6SFB and 9FB), regardless of the number of passages, were indistinguishable in terms of graft survival, migrational patterns, and phenotypic differentiation of the transplanted cells. Control transplants of cells that had been killed by freeze-thawing before transplantation showed no transfer of the BrdU marker to the host cells, which is in agreement with previous reports (Cogo et al., 1995; Sullivan et al., 1996).

#### The subventricular zone and rostral migratory stream

Single deposits of 100,000 cells were deposited in or close to the SVZ, just ventral to the corpus callosum, or just above the RMS

midway between the SVZ and the olfactory bulb. In the SVZ a core of BrdU-positive cells was located close to the ventricular ependyma, extending in some cases into the white matter of the overlying corpus callosum (Fig. 1A) (6 weeks survival). Cells were seen to leave the transplantation site in a stream of rostral migration (Fig. 1B) after the RMS, i.e., along the path of endogenous progenitors toward the olfactory bulb. Once they reached the bulb, BrdU-positive cells left the migratory stream, becoming dispersed throughout the subependymal, granular (Fig. 1C,D), and glomerular cell layers. The cells within the olfactory bulb were more weakly BrdU-labeled than the cells in the SVZ (which were uniformly highly labeled), suggesting that the labeled cells had undergone further cell division on their route to the bulb, similar to the endogenous progenitors from the SVZ (Menczer et al., 1995).

In the RMS transplants the deposits of BrdU-labeled cells were localized just above, and occasionally within, the RMS itself (see Fig. 4A). At 2 weeks after transplantation the cells remained clustered at the graft site, and there was very little migration from the graft core. Thus only few cells were observed rostral and caudal to the graft placement at this time point. Six weeks after grafting, cells were seen to have migrated rostrally toward the olfactory bulb (see Fig. 4B) and into the granular and periglomerular layers (see Fig. 4C–F).

The immature cell marker VIM was used to delineate the SVZ and RMS along which BrdU-positive cells were seen in their migratory stream (Fig. 2A). BrdU-positive cells were not VIM positive. The vast majority of the BrdU-labeled nuclei did not diverge from the RMS; however, in the region adjacent to the transplant core, occasional cells could be seen migrating dorsally toward the overlying cortex (data not shown). Some of the cells migrating within the RMS were double-labeled with the early neuronal marker Hu (Fig. 2B) and  $\beta$ -tubulin-III (see Fig. 4B). Both of these markers, which identify both early differentiated neuronal precursors and mature neurons, are known to be expressed by the endogenous progenitors from the SVZ as they migrate along the RMS (Barami et al., 1995; Menczer et al., 1995). The presence of these markers thus indicates their early commitment to a neuronal phenotype. None of the BrdU-positive cells within the SVZ or RMS stained positively for the NeuN marker. Within the olfactory bulb, the majority of BrdU-labeled cells, both in the deeper layers and in the periglomerular layer, were Hu positive (Figs. 2C, 4C), and approximately half of the BrdU-positive cells were also double-labeled with the more mature neuronal marker NeuN (Fig. 2D,E), indicating a progressive maturation of the cells toward a neuronal phenotype as they entered the bulb. Many of the BrdU-labeled cells, within both the granule cell layer and periglomerular layer, also expressed the GABA-synthesizing enzyme GAD67 (see Fig. 4D,E). TH, which is a characteristic feature of the dopaminergic periglomerular neurons, was clearly expressed in some of the BrdU-labeled cells within the periglomerular layer (Fig. 4F, arrowheads and inset). None of the BrdU-labeled cells stained positively for the glial marker GFAP, neither within the astrocyte-rich RMS (see Fig. 2A) nor within the olfactory bulb (see Fig. 2B). In addition, no cells were double-labeled with BrdU and the receptor phosphoprotein DARPP-32, which is present in the medium spiny neurons of the striatum but not normally expressed in neurons of the olfactory bulb. Table 1 gives a semiquantitative summary of neuronal and glial differentiation of the transplanted cells within the RMS and the olfactory bulb.

Using a human-specific antibody to the cytoskeletal protein

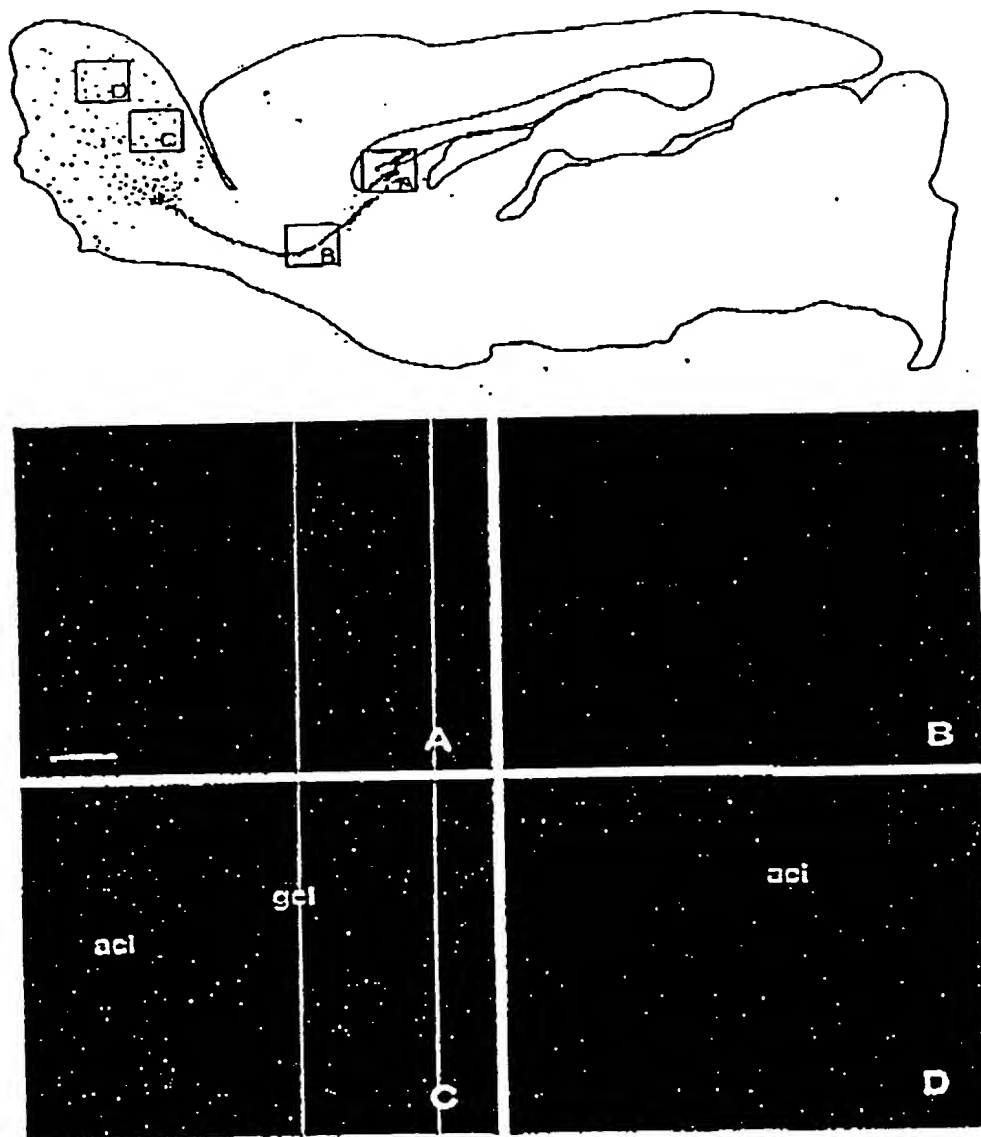


**Figure 3.** Low-power illustration of a transplant in the SVZa in a sagittal section, analyzed at 6 weeks after transplantation, shows an overview of the injection site of BrdU-labeled cells (green) and their distribution throughout the RMS. In the olfactory bulb, the cells were found dispersed through all layers. *A–D*, Grafted cells at different sites (indicated in the top panel), with BrdU-labeled cells shown in green and the NcuN shown in red. Double-labeled cells present in the bulb display a yellow color (*C, D*). *A*, Transplant core; *B*, cells migrating along the RMS; *C, D*, cells in the granule cell layer of the olfactory bulb. Scale bar, 250  $\mu$ m. *acf*, intrabulbar portion of the anterior commissure; *gcl*, granule cell layer.

tau, positive staining was observed at the injection site in both cellular and axonal profiles (Fig. 3A). Typically, cells that remained at the graft core or migrated only a short distance from the implantation site had developed axons that projected laterally into either the corpus callosum or striatum adjacent to the transplant (Fig. 3A,B). Tau-positive cells were distributed along the RMS, several millimeters from the graft site (Fig. 3C,D). Those

cells often showed a short leading process, oriented in the direction of the RMS (Fig. 4). Small tau-positive profiles were observed in the deeper layers of the olfactory bulb, and occasionally mature cells with axonal processes were found in this region (Fig. 3E,F). High background from the immunohistochemical procedure precluded the identification of tau-positive profiles in the periglomerular layer.

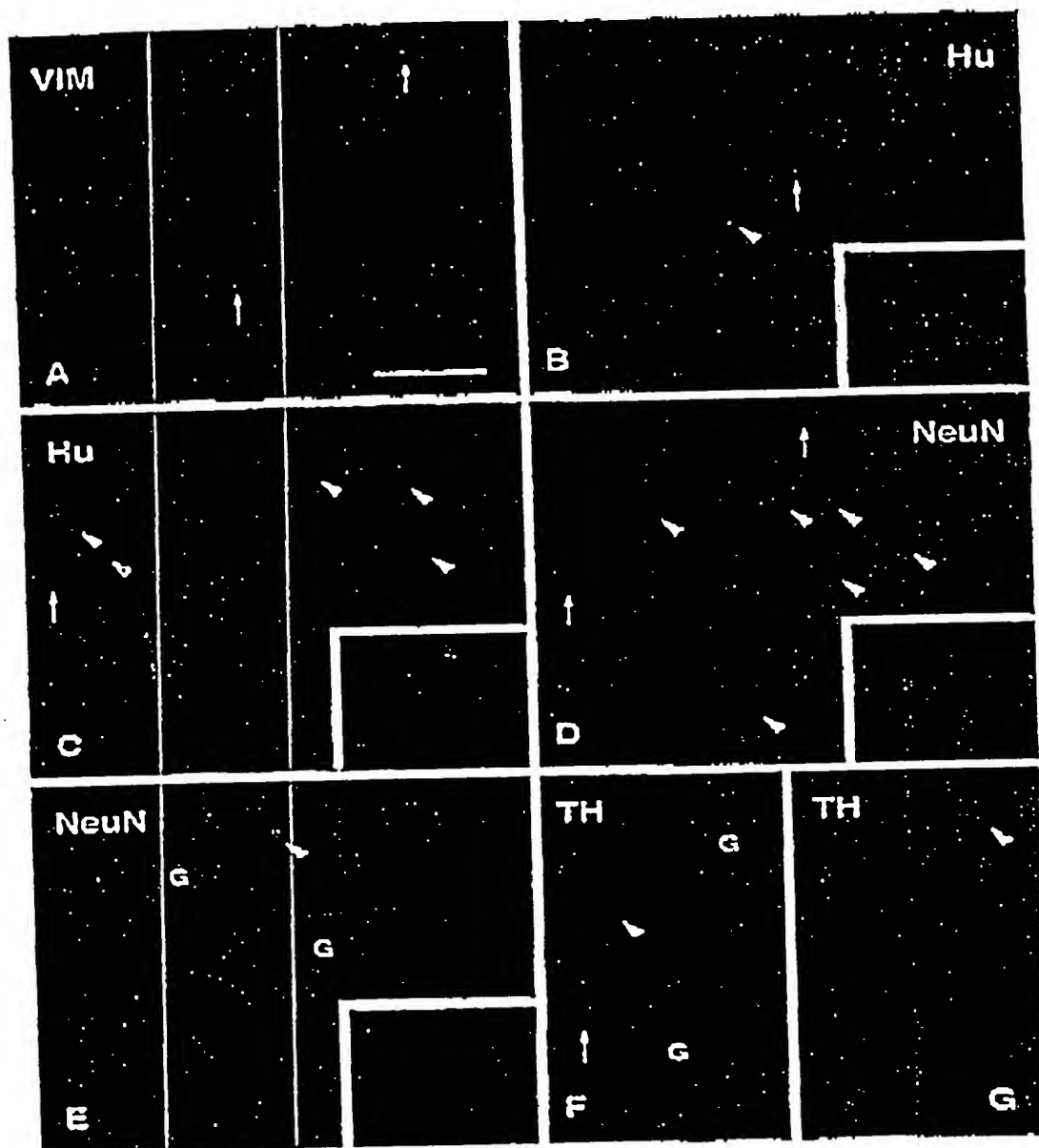


**Figure 2.** Confocal images of BrdU-labeled (green) and double-labeled cells (yellow) transplanted in the SVZa at 6 weeks after transplantation. *A*, Vimocin (VIM) staining delineates the RMS. BrdU-positive cells (arrow) were observed along the RMS but were not VIM positive. *B*, Many host cells present within the RMS were positively stained with an antibody to Hu, a neuronal phenotypic marker, and some transplanted cells were also Hu positive (arrowhead, enlarged in the inset). *C*, Many Hu-positive transplanted cells (arrowheads) were located within the granule cell layer of the olfactory bulb. The inset shows two Hu-positive, BrdU-labeled cells (one strongly and one weakly BrdU labeled). *D*, Approximately half of the transplanted cells (arrowheads) were double-labeled with NeuN in both the granule cell layer (*D*) and the periglomerular layer (*E*). *E*, Oligomerulus. Insets to *D* and *E* show double-labeled cells in higher magnification. *F*, *G*, A small proportion of the BrdU-positive cells found in the periglomerular layer were also TH positive (arrowheads). Scale bar (shown in *A*): *A–F*, 100  $\mu$ m; *G*, 50  $\mu$ m.

Table 2. The proportion of BrdU-labeled cells, which also express other markers of mature CNS phenotypes, at 6 weeks after transplantation to different regions of the adult rat brain

	SVZ and RMS transplants			
	Graft core	RMS	Granular layer	Periglomerular layer
Hu	0	+	++++	+++
$\beta$ -tubulin-III	0	+	-	-
NeuN	0	0	+++	++
GAD <sub>67</sub>	0	0	+++	++
TH	0	0	-	+
DARPP-32	0	0	0	0
GFAP	0	0	0	0
Vimentin	0	0	0	0

	Hippocampal transplants				
	Graft core	Subgranular layer	Granule cell layer	Hilus	CA3
Hu	++	+++++	++++	+	0
$\beta$ -tubulin-III	++	+++++	++++	-	0
NeuN	+	+++++	++++	0	0
GAD <sub>67</sub>	-	0	0	-	-
TH	0	0	0	0	0
DARPP-32	0	0	0	0	0
Calbindin	+	+++++	++++	0	0
GFAP	++	0	0	++	++

	Striatal transplants		
	Graft core	<0.4 mm from core	0.4-1.5 mm from core
Hu	+++++	++++	0
NeuN	0	0	0
GAD <sub>67</sub>	+++	++	+
TH	0	0	0
DARPP-32	0	+	0
Calbindin	0	+	0
GFAP	++	+++	+++

The frequency of double-labeled cells was quite variable for the different phenotypic markers among the animals used for this analysis: olfactory bulb,  $n = 8$ ; hippocampus,  $n = 10$ ; striatum,  $n = 10$ . Double-labeling was assessed by confocal microscopy of randomly selected areas in sections stained with a combination of FITC-, Cy2-, and Cy3-labeled antibodies (see Materials and Methods). The data are based on observations from three representative animals in each group. 0, Cells not found; +, 1-10%; ++, 11-40%; +++, 41-60%; ++++, 61-80%; +++++, >80%.

### The hippocampus

Transplants of 100,000 cells were placed within the hilar region of the dentate gyrus. At both 2 and 6 weeks after grafting, many of the injected BrdU-positive cells remained as a cluster just below the granule cell layer (Fig. 5A). This position of the cell deposit is characteristic for cells that are implanted by passive injection into the dentate gyrus, because of the presence of a cleavage plane underneath the granule cell layer (Wells et al., 1988). A significant proportion of the BrdU-positive cells, however, had migrated within the subgranular layer of the dentate gyrus and into the granule cell layer itself (Fig. 5D-F). In addition, some cells were found scattered in the hilus and the molecular layer of the dentate gyrus, as well as in the overlying CA3 region. The extent of cell migration was similar at 2 and 6 weeks. Typically, cells that had migrated longer distances from the transplant core were more weakly labeled with BrdU, suggesting that the migrated cells had undergone further cell divisions.

The BrdU-labeled cells that had integrated into the granular and subgranular layers had the same size and shape as the intrinsic host granule cells, and a large number of them expressed

the neuronal markers Hu (Fig. 5B), NeuN (Fig. 5C), and  $\beta$ -tubulin-III (Fig. 5D) at both time points. The calbindin marker that is characteristic for the intrinsic granule cells was clearly present in many of the transplanted cells at 6 weeks but not at 2 weeks after transplantation. Occasional BrdU/Hu double-labeled cells, but no BrdU/NeuN or BrdU/calbindin double-labeled cells, were found outside these layers. A large proportion of the transplanted cells within the granule cell layer were calbindin positive (Fig. 5E). No BrdU/GAD<sub>67</sub> double-labeled cells were observed in these transplants (Fig. 5F). Similarly, no cells that coexpressed BrdU and DARPP-32 were observed within any region of the hippocampus. BrdU-labeled cells expressing the glial marker GFAP were found in areas outside the dentate gyrus, both in the CA3 area and in areas close to ventricle as well as within or close to the graft core (see Fig. 9C). The extent of neuronal and glial differentiation of the transplanted cells within each region of the hippocampus is given in Table 1.

Staining with the hTau antibody revealed scattered axonal and cellular profiles, both within the graft core and in individual cells that had migrated away from the initial transplant site within the

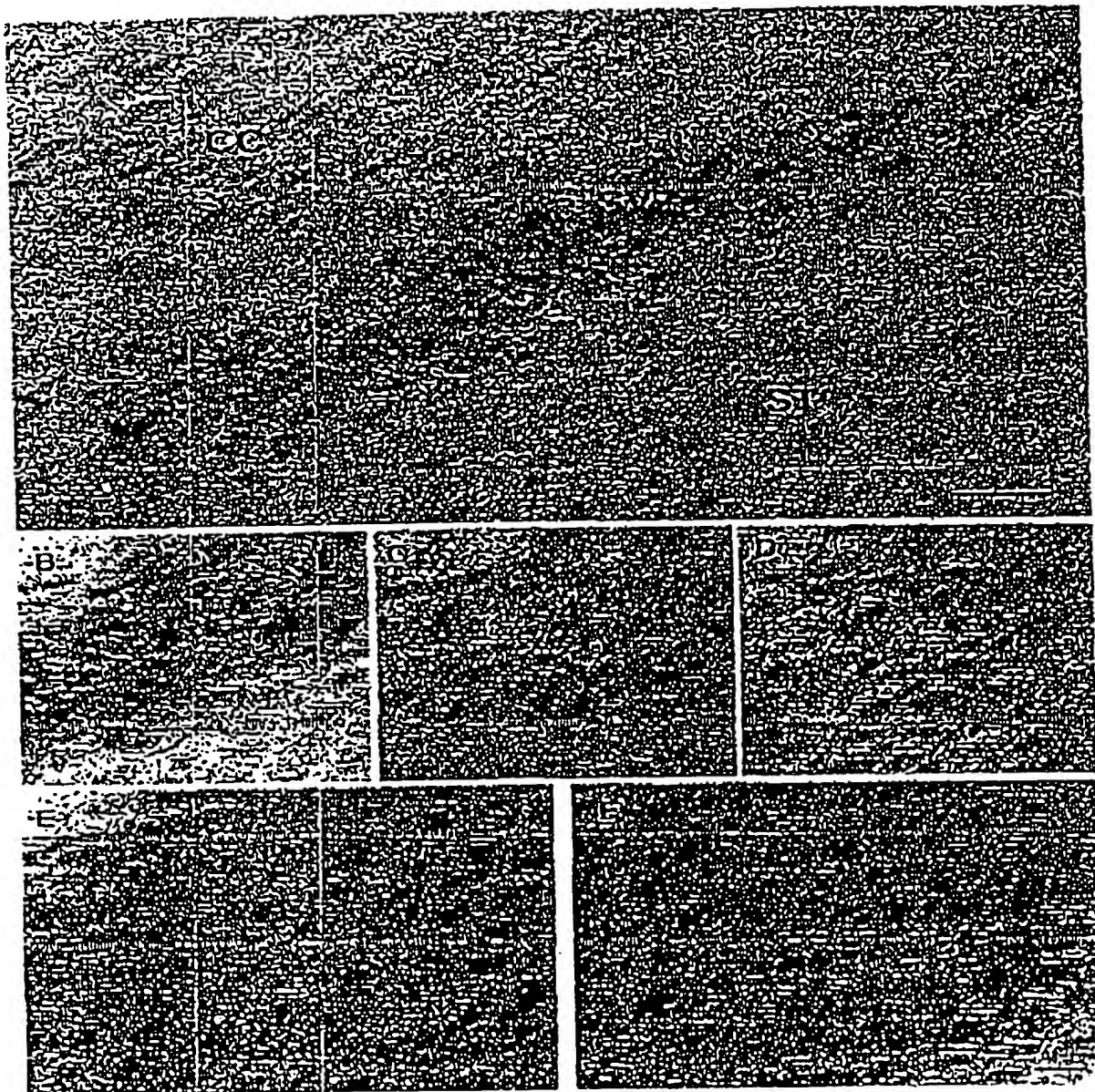


**Figure 3.** Grafts to the SVZ stained with a human-specific antibody to tau, at 6 weeks after transplantation. *A*, Sagittal section showing neuronal cell bodies and axons located within the SVZs, between the striatum (ST) and the overlying corpus callosum (CC). *B–D*, Higher magnification of individual neuronal profiles at the periphery of the transplant (*B*) and migrating in the RMS (*C*, *D*). *E*, *F*, Individual cells located deep within the olfactory bulb, showing morphological features of mature neurons. Scale bars: *A*, 100  $\mu$ m; (shown in *F*) *B–F*, 10  $\mu$ m.



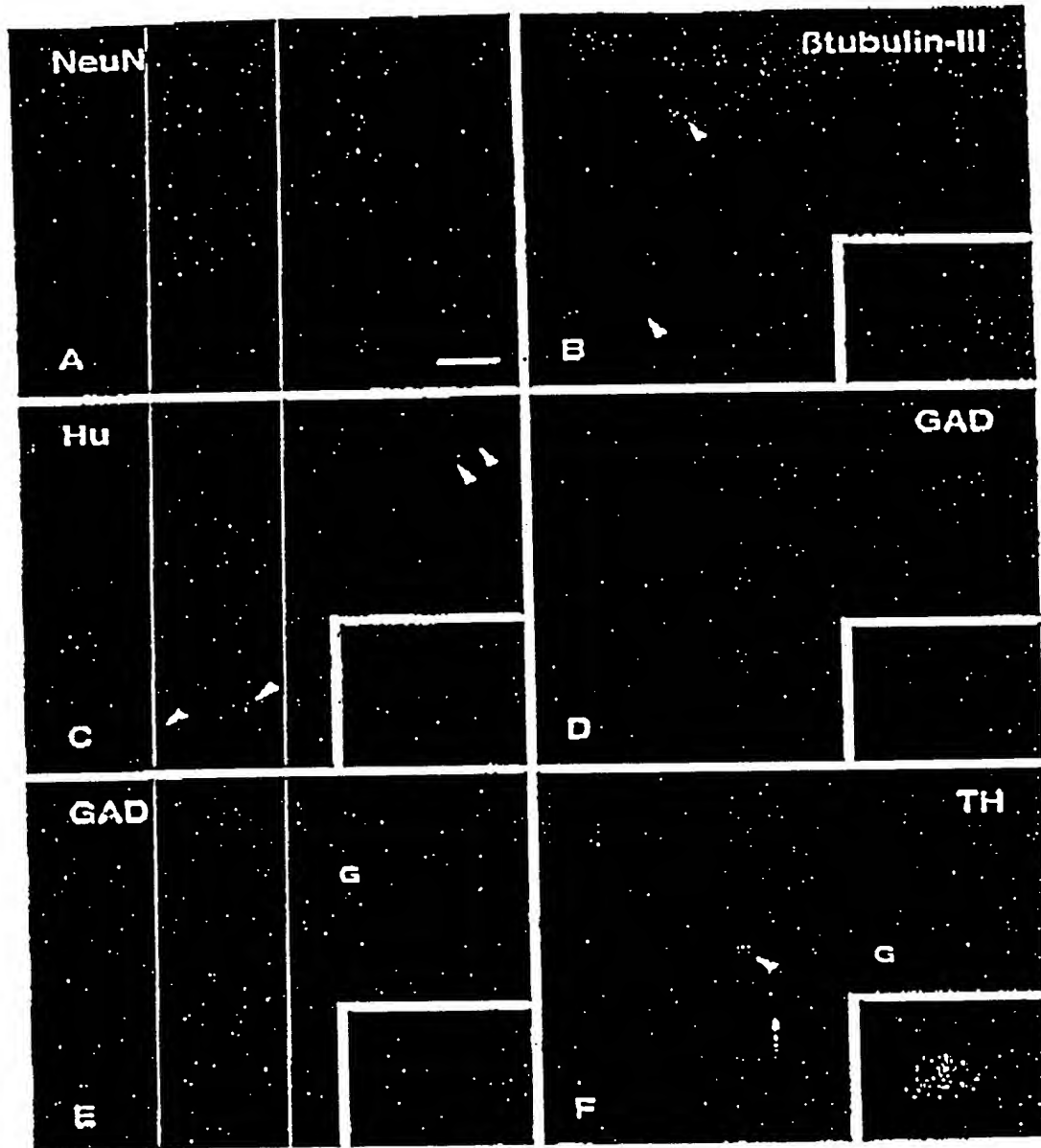


**Figure 4.** Confocal images of BrdU-labeled (green) and double-labeled cells (yellow) transplanted in the RMS. *A*, A typical graft at 2 weeks after transplantation, situated in the RMS with only moderate migration of grafted cells in either rostral and caudal direction from the graft core. *B*, At 6 weeks after transplantation cells were seen migrating along the RMS. A small proportion of the transplanted cells were labeled with the early neuronal marker  $\beta$ -tubulin III (arrowheads). This marker was also present in many of the host cells within this pathway. *C*, Transplanted cells were found scattered throughout the olfactory bulb. Many of them were Hu positive (arrowheads), indicating their differentiation to a neuronal phenotype. *D*, Within the granule cell layer many of the BrdU-labeled cells were GAD<sub>65</sub> positive. Within the periglomerular layer, BrdU-positive cells stained positively for either GAD<sub>65</sub> (*E*) or TH (*F*). Insets show individual double-labeled cells in higher magnification. Arrow in *F* marks a TH-negative transplanted cell. Scale bar (shown in *A*): *A*, 150  $\mu$ m; *B*, *C*, 50  $\mu$ m; *D*–*F*, 25  $\mu$ m.

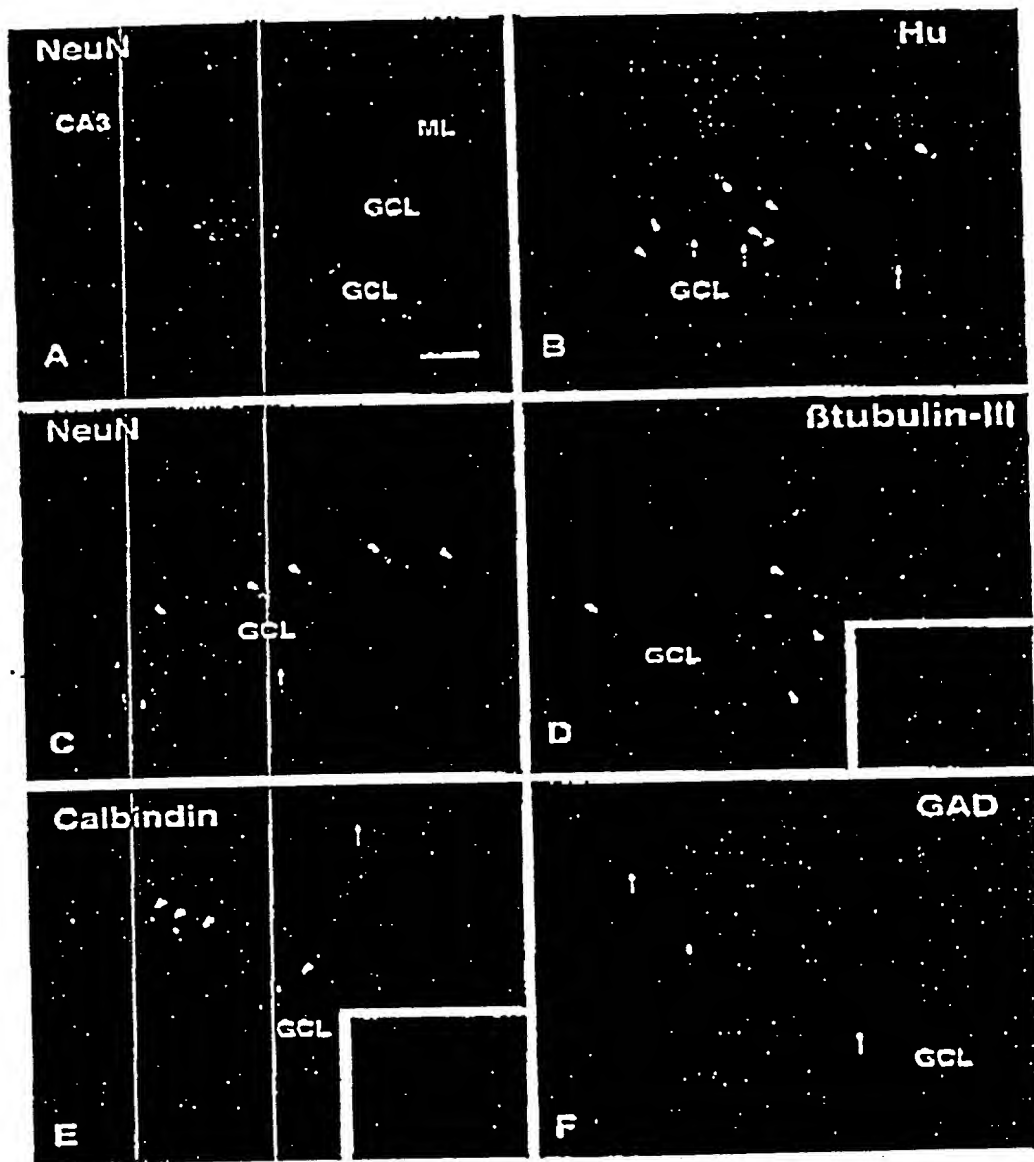


**Figure 3.** Confocal images of BrdU-labeled (green) and double-labeled cells (yellow) transplanted in the hippocampus. *A*, The core of transplanted cells was located within either the dorsal or ventral blades of the granule cell layer (GCL) in the dentate gyrus. *B*, *C*, By 2 weeks after transplantation, Hu- and NeuN-positive BrdU-labeled cells were observed at some distance from the graft core, mainly in the subgranular layer and also within the granule cell layer (arrowheads). *D*, BrdU-labeled transplanted cells positive for the neuronal marker  $\beta$ -tubulin-III (arrowheads) were found both within the graft core and in cells that had migrated along the subgranular layer. *E*, At 6 weeks (but not at 2 weeks) after transplantation, calbindin-positive cells were observed in the granule cell layer (arrowheads). *F*, No GAD-positive interneurons were observed. *Arrows* show an individual  $\beta$ -tubulin-III/BrdU-labeled cell in the cluster of grafted cells in the subgranular layer in *D*, and two calbindin/BrdU-labeled cells within the deep part of the granule cell layer. *Arrows* indicate single-labeled BrdU-positive cells. Scale bar (shown in *A*): *A*, 150  $\mu$ m; *B*, *C*, 75  $\mu$ m; *D*–*F*, 50  $\mu$ m. CA3, CA3 region of hippocampus; ML, molecular layer; GCL, granule cell layer.

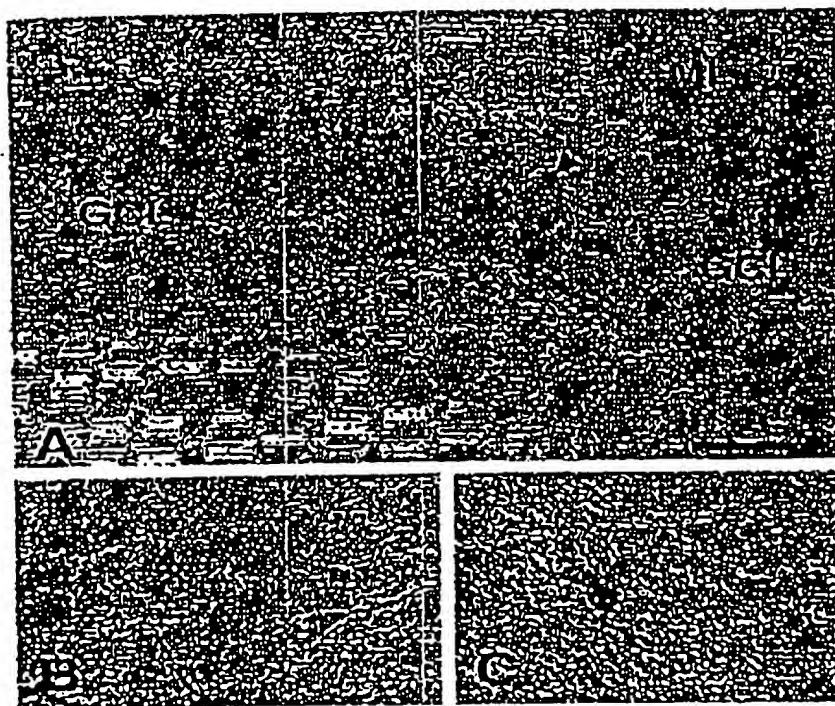


**Figure 6.** Hippocampal transplants stained with the bTau antibody. *A*, A transplant in the dentate gyrus at 6 weeks after transplantation. *B*, A tau-positive cell with a typically immature dendritic profile with one primary process. *C*, A more differentiated tau-positive neuron with more complex processes, situated within the subgranular layer (arrowhead in *A*). Scale bar (shown in *A*): *A*, 150  $\mu$ m; *B*, *C*, 30  $\mu$ m. *ML*, Molecular layer; *GCL*, granule cell layer; *H*, hilus.

granular and subgranular cell layers (Fig. 6*A*). At 2 weeks the cells appeared fairly immature, with a few short Tau-positive processes. At 6 weeks, cells with morphological features of neurons with processes were observed (Fig. 6*B,C*). Tau-positive cells were also seen in the hilus and molecular layer and along the needle tract.

#### The striatum

The transplants were placed centrally within the head of the caudate-putamen. At both 2 and 6 weeks after grafting, the grafted cells were found as a BrdU-labeled cell cluster at the site of implantation. Many of the BrdU-labeled cells, however, were observed to have migrated into the surrounding host striatum, without any preferential direction, to a distance of  $\sim 1$ – $1.5$  mm from the graft core (Fig. 7*A*). The size of individual BrdU nuclei varied considerably, both within the graft core and in cells that were located in the adjacent host striatum ( $<0.4$  mm from the graft core). All of the cells that had migrated over longer distances were of small size and more faintly labeled, suggesting a dilution of the BrdU label caused by cell division. In sagittal sections the BrdU-positive cells could be seen to be aligned with the gray matter, interspersed with the fibers of the internal capsule.

Double-staining revealed that the majority of the BrdU-positive cells in the graft core and in the adjacent host striatum were double-labeled for the early neuronal marker Hu (Fig. 7*B*) but negative for NeuN (Fig. 7*C*). Many BrdU/Hu double-labeled cells occurred also at the graft-host border and within the adja-

cent host striatum, up to a distance of  $\sim 0.3$ – $0.4$  mm from the graft core. Although the majority of the Hu-positive cells within the graft core were small in size and round or oval in shape, similar to the Hu-positive cells within the SVZ of the host brain, a substantial proportion of the BrdU/Hu-positive cells at the graft-host border and in the host striatum were larger in size (10–15  $\mu$ m), i.e., in the range of the Hu-positive neurons within the host striatum. None of the cells expressed NeuN, which is also the case, however, for most of the host striatal neurons. All BrdU-labeled cells located farther away from the graft core were Hu negative. Those cells were all of small size and often found in satellite positions, closely apposed to host striatal neurons (Fig. 7*C*, arrows) or close to blood vessels. The location and staining properties of these small-sized cells suggest that they had differentiated, at least in part, into glia. Colocalization of BrdU and the astrocyte marker GFAP was unequivocally demonstrated at the graft-host border, i.e., within the area of GFAP-positive reactive astrocytes surrounding the graft core (see Fig. 9*D*, inset).

The neuronal phenotype of the transplanted cells was further investigated using antibodies against the GABA-synthesizing enzyme GAD<sub>67</sub>, which is present in the vast majority ( $>90\%$ ) of the neurons within the striatum; DARPP-32, which is a marker for the medium-sized spiny striatal projection neurons; and calbindin, which is normally present in the medium spiny projection neurons in the matrix component of the striatum (for review, see Goffinet, 1992). BrdU/GAD<sub>67</sub> double-labeled cells were observed both in the transplant core and within the host striatum at the

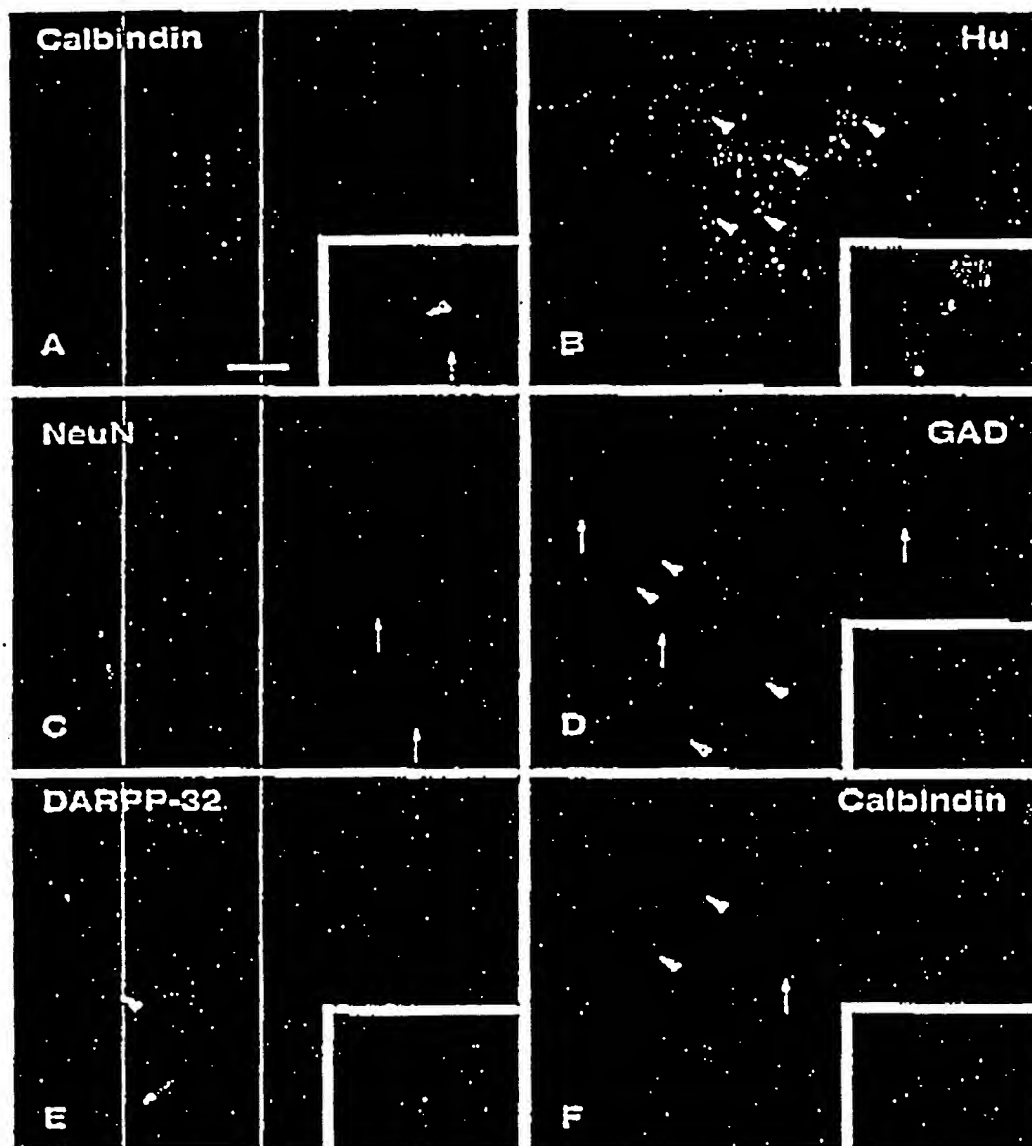


**Figure 2.** Confocal images of BrdU-labeled (green) and double-labeled cells (yellow) transplanted in the striatum. *A*, Coronal section through the graft core at 6 weeks after transplantation, showing a dense cluster of cells at the injection site and migration of BrdU-labeled cells away from the graft core. In both gray and white matter, *Inset* shows region in box at higher magnification, also illustrated in *F*. *B*, Many of the transplanted cells were positively stained with Hu (red), even within the graft core (arrowheads, enlarged in the *Inset*). *C*, No BrdU/NeuN double-labeled cells were found in the graft core or among those cells that had migrated into the host striatum. Arrows indicate transplanted cells that were found in close association with NeuN-positive host neurons (red). *D*, A number of transplanted cells were positive for the enzyme GAD<sub>65</sub> in the periphery of the graft core (arrowheads). One of the double-labeled cells is shown at higher magnification in the *Inset*. *E*, BrdU/DARPP-32 double-labeled cells were occasionally observed (arrowhead and *Inset* at higher magnification). These were generally sparsely labeled and found only in the immediate vicinity of the transplant core. *F*, Similarly, BrdU/Calbindin double-labeled cells were found both in the periphery of the graft and in adjacent regions of the host striatum. Scale bar (shown in *A*): *A*, 200  $\mu$ m; *B*, 150  $\mu$ m; *D*–*F*, 25  $\mu$ m.

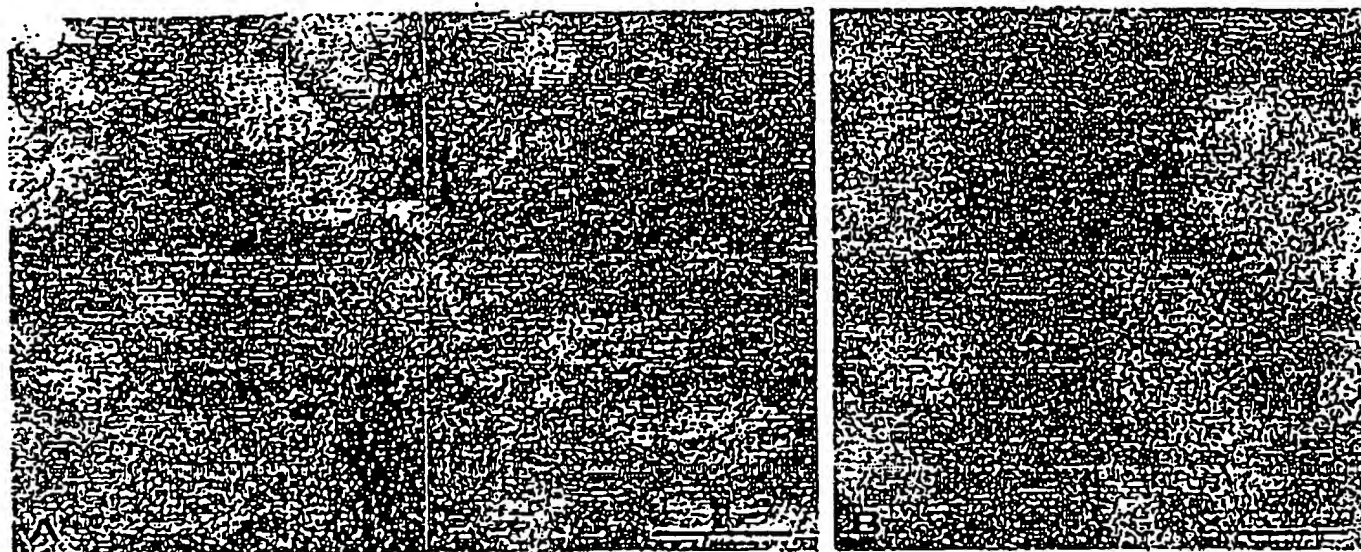


**Figure 8.** Striatal transplants stained with the hTau antibody. Six weeks after transplantation, coronal sections revealed tau-positive neuronal profiles densely packed within the graft core (*A*). Individual cells with neuronal profiles were observed also in the host striatum adjacent to the graft (arrowheads in *A* and *B*). Axonal processes were seen to extend caudally within the white matter bundles of the internal capsule (arrows in *A* and *B*). Scale bars: *A*, 500  $\mu$ m; *B*, 100  $\mu$ m.

periphery of the transplants (Fig. 7*D*). In addition, some BrdU-labeled cells expressed calbindin (Fig. 7*A,F*, *inset*) and occasionally also DARPP-32. These cells were located at the periphery of the transplants and in the adjacent host striatum up to a distance of  $\sim 0.3$ – $0.4$  mm from the graft–host border and were similar in size and shape to those present within the host striatum. The BrdU/DARPP-32 double-labeled cells were only weakly DARPP-32 positive but were comparable in size to the host DARPP-32-positive neurons (Fig. 7*E*). None of the transplanted cells expressed TH, either within the graft core or within the host striatum. Table 1 outlines the extent of expression of neuronal and glial markers at different distances from the graft core.

Staining with the hTau antibody revealed a graft core of clustered tau-positive cells and fibers (Fig. 8*A*). In sagittal sections, loose bundles of tau-positive fibers were seen to leave the graft core in both the rostral and caudal direction, along the white matter bundles of the internal capsule. In cross section, these fibers were found primarily within the white matter bundles (Fig. 8*B*, arrows). Individual cells were also observed at some distance from the graft core (Fig. 8*A,B*, arrowheads). In these cases, the cell bodies were often located within the gray matter, with their processes projecting into the white matter tracts. At 6 weeks, tau-positive axons could be traced caudally from the graft core within the internal capsule bundles for a distance of  $\sim 1$ – $2$  mm; some of these fibers were seen to enter the globus pallidus, and in some cases scattered tau-positive fibers could be traced as far as the entopeduncular nucleus.

#### DISCUSSION

These present results show that the long-term propagated human neurosphere cultures contained progenitors that can respond *in*

*vivo* to cues present in both neurogenic and non-neurogenic regions of the adult rat brain. The expression of phenotypic markers provided evidence for site-specific neural differentiation within each of the three grafted regions. In the olfactory bulb the cells that integrated into the granular and periglomerular layers expressed NeuN, TH, and GAD<sub>67</sub>, similar to the dopaminergic and GABAergic cells normally present in these regions. In the dentate gyrus some of the cells assumed a position, morphology, and phenotype similar to the NeuN/calbindin-positive granule cells within the granule cell layer. And in the striatum, cells located in the periphery of the transplants expressed GAD<sub>67</sub> and calbindin as well as low levels of the striatum-specific marker DARPP-32.

A combination of EGF, bFGF, and LIF was used to expand the human progenitors. It has been shown previously that EGF and bFGF act cooperatively in promoting the proliferation of rat and human neural progenitors (Vescovi et al., 1993; Welles et al., 1996a; Svendsen et al., 1997). bFGF appears to be a mitogen for both unipotent and multipotent neuronal and glial progenitors (Murphy et al., 1990; Vescovi et al., 1993; Ray and O'Leary, 1994; Kippatrick and Bartlett, 1995; Palmer et al., 1995) and may act broadly to maintain neural progenitor cells as a constitutively proliferating population *in vitro* (Palmer et al., 1995). It seems likely, therefore, that the combination of growth factors used here served to maintain both multipotent and lineage-restricted progenitors in continuous cell cycle and that the ability to migrate and integrate into the adult host brain was expressed by specific subsets of cells. Previous studies suggest that the *in vivo* properties of *in vitro* expanded neural progenitors may differ depending on the growth factors used. Rat or mouse neurosphere cells ex-

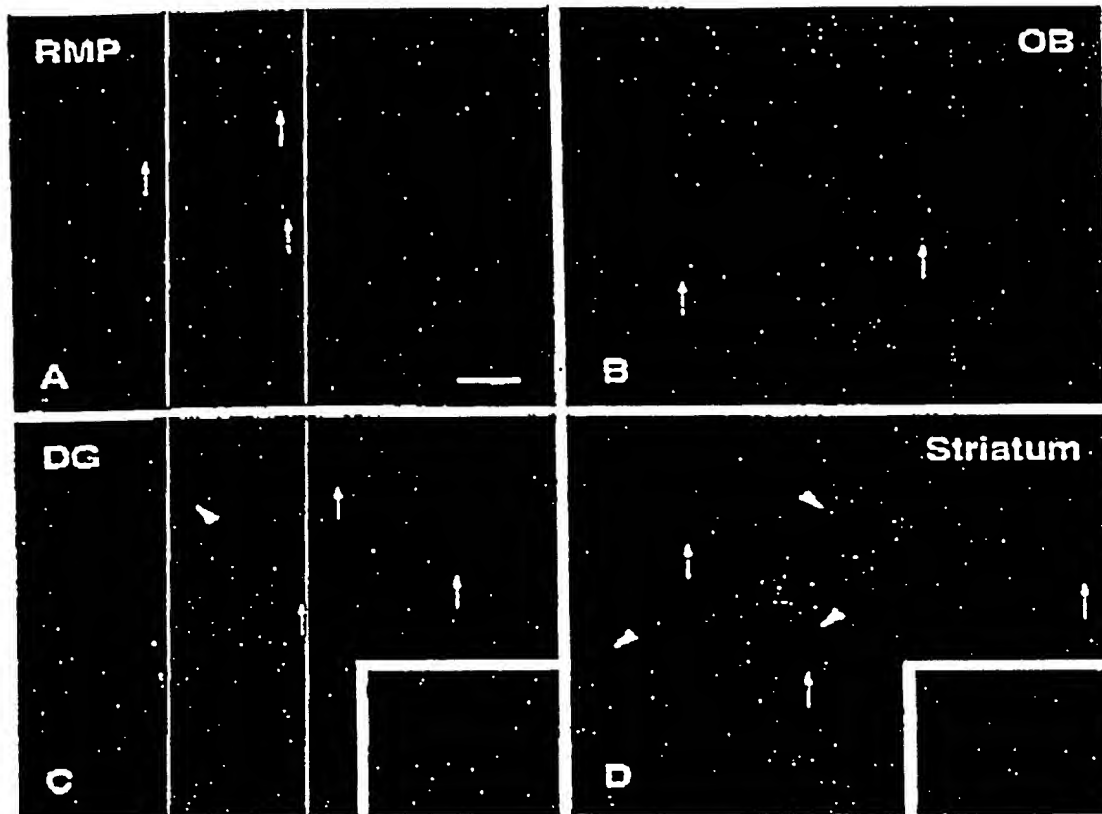


**Figure 9.** GFAP was used to label astrocytes within the graft areas (red) to assess the extent of colocalization with BrdU-labeled transplanted cells (green). *A*, Cells within the RMS at 6 weeks after transplantation were often closely associated with GFAP profiles, although no double-labeled cells were observed (arrows). *B*, Within the granule cell layer of the olfactory bulb, BrdU-positive cells were interspersed with, but not colocalized with, GFAP (arrows). *C*, In the dentate gyrus, cells within the transplant core were occasionally closely associated with GFAP-positive cytoplasmic staining, possibly indicating a double-labeled cell. *D*, Staining within the striatum revealed a dense network of GFAP-positive processes (red) intermingled with the BrdU-positive cells (green). Many clear examples of double-labeled cells were observed (arrowheads), although examples of BrdU single-labeled cells were also frequently observed (arrows). Insets show BrdU/GFAP double-labeled cells at higher magnification. Scale bar (shown in *A*): *A*, *C*, 50  $\mu$ m; *B*, 25  $\mu$ m; *D*, 150  $\mu$ m.

posed in the presence of EGF alone have generated only glial cells and no neurons after transplantation to the developing rat forebrain (Winkler et al., 1998) or adult rat spinal cord (Hammang et al., 1997), and they exhibit poor survival and integration after transplantation to the striatum (Svendsen et al., 1996; C. Winkler, R. A. Fricker, A. Björklund, unpublished observations). By contrast, adult rat hippocampal progenitors cultured in the presence of bFGF exhibit both migration and neurogenesis after transplantation in the adult rat brain (Gago et al., 1995; Suhonen et al., 1996).

#### Site-specific differentiation of the grafted cells

In the SVZa, which is one of the two sites where neurogenesis continues into adulthood in the mammalian CNS, the endogenous neuronal progenitors have been shown to migrate along the

RMS and reach the bulb within 2–15 d after their generation in the SVZa (Lois and Alvarez-Buylla, 1994). The cells are already committed to a neuronal phenotype while in the migratory path, although they continue to divide during migration (Monczos et al., 1993). The cells generated by SVZa postnatally are interneurons, above all GABAergic and dopaminergic interneurons in the granular and periglomerular layers of the olfactory bulb (Luskin, 1993; Lois and Alvarez-Buylla, 1994; Betarbet et al., 1996).

The transplanted human neural progenitor cells expressed the early neuronal markers Hu and  $\beta$ -tubulin-III during migration to the olfactory bulb, indicating that some of the transplanted progenitors were committed to a neuronal fate already in the SVZ, similar to the endogenous neuronal progenitors generated in the SVZa (Lois and Alvarez-Buylla, 1994; Monczos et al., 1993). On



reaching the bulb, BrdU-positive cells distributed in the granular and periglomerular layers and coexpressed neuronal markers such as Hu and NeuN, as well as hTau. This is in agreement with previous results obtained with rat or mouse SVZa progenitors (Luskin, 1993; Lois and Alvarez-Buylla, 1994) and a recent study using transplantation of human neural stem cells (Flax et al., 1998). One interesting difference between the transplanted human cells in the current study and endogenous SVZa progenitors is the time course of migration: few of the transplanted human progenitors had entered the RMS at 2 weeks, and many still remained dispersed along the RMS by 6 weeks. One reason for this may be a species difference. Transplants of human primary cells show a more protracted development than rat-to-rat grafts, which suggests that the human cells retain some type of internal developmental clock for their differentiation and maturation (Grabson-Frodil et al., 1996, 1997). Indeed, Suhonen et al. (1996) reported that adult rat neural progenitors transplanted to the SVZa in adult rats are distributed along the entire length of the RMS by 1 week, and by 8 weeks ~90% of the cells had reached the bulb. Similarly, Lois and Alvarez-Buylla (1994) observed that SVZa progenitors, implanted into the adult SVZa, reach the bulb within 30 d after transplantation. These observations indicate that the slow onset and protracted time course of migration of the human cells reflect intrinsic developmental constraints.

In hippocampus the transplanted cells distributed along the subgranular and granular layers of the dentate gyrus. Although cells were observed also in other layers of the dentate and the CA3 region, cells expressing neuronal markers occurred only within the subgranular or granular layers, suggesting that the human progenitors, similar to rat hippocampal and cerebellar progenitors (Gage et al., 1995; Vicario-Abejón et al., 1995), are able to respond to local cues specifically localized in these layers. The transition zone between the hilus and the granule cell layer is the site where endogenous neuronal progenitors are normally generated (Altman and Das, 1966; Altman and Bayer, 1990), providing a source of new granule cells throughout life (Kaplan and Hinds, 1977; Cameron et al., 1993; Kuhn et al., 1996). As judged by morphological criteria, i.e., size, shape, and distribution of the cells, and expression of characteristic neuronal markers, the grafted progenitors are induced by local signals to express neuronal features similar to the resident granule cells. It remains to be demonstrated, however, to what extent these newly formed neurons can undergo complete maturation and establish appropriate axonal and dendritic connectivity.

#### Cells grafted to the striatum generate both neurons and glia

Expression of neuronal markers in the striatal transplants indicate that a substantial fraction of the grafted human progenitors had developed toward a neuronal phenotype. Many of the Hu-positive cells within the transplant core were small and round or oval in shape, similar to the neuronal precursors normally present in the proliferative subependyma in the adult brain. These cells did not express any of the more mature neuronal markers and therefore may be classified as poorly differentiated neuronal precursors. The GAD<sub>67</sub>, calbindin-, and DARPP-32-positive cells were exclusively located at the graft-host border and within the adjacent host striatum, up to a distance of ~0.3–0.4 mm. The size and shape of these cells were similar to the medium-sized neurons of the host striatum. Many of these are GABAergic and stain positively for GAD<sub>67</sub>; one subclass, the striatal projection neu-

rons, is further characterized by the expression of calbindin and/or DARPP-32.

These data indicate that the human neural progenitors can undergo neurogenesis also in the normally non-neurogenic environment of the adult striatum and assume neuronal phenotype(s) similar to those normally present here but that in the absence of suitable substrates for migration they remain close to the implantation site. Interestingly, in sections stained with the hTau antibody some of these newly formed neurons were seen to extend long axon-like processes that could be traced along the fascicles of the internal capsule to the globus pallidus and in some cases also the entopeduncular nucleus, a distance of ~2 mm.

The cells that migrated over longer distances within the adult striatum were all Hu negative and of small size. Many of them were found in satellite position to the medium-sized host striatal neurons or close to blood vessels, suggesting that they had assumed a glial-like phenotype (Fig. 9). A migratory capacity of immature glia (or glial precursors) within the adult CNS has been reported for both astrocytes and oligodendrocytes by several investigators (Blakemore and Franklin, 1991). Extensive astrocytic migration within the adult striatum, similar in extent to the one observed here, has previously been described in transplants of human neuronal progenitors (Svendsen et al., 1997) and freshly dissociated human embryonic striatal and diencephalic tissue (Pundt et al., 1995). In these cases the migratory cells appear to be glial precursors in a proliferative, migratory stage of their development. Consistent with this, we observed that cells located at progressively greater distances from the transplant core had lower levels of BrdU labeling than the cells that remained at the implantation site, suggesting that the migrating cells continued to divide as they dispersed within the host striatal parenchyma.

#### Implications for brain repair

The human neurosphere cultures are particularly suitable for transplantation in that they can be harvested and implanted without dissociation and detachment from a culture substrate. The cultures used here had been expanded up to 10 million-fold, which means that each transplant of 100,000–200,000 cells in theory could be derived from a single cell in the original cell preparation. Because the *in vivo* properties of the cells were indistinguishable over a wide range of passages (from 9 to 21), the present culture system could provide an almost unlimited source of human neural progenitor cells for transplantation.

The present results show that subpopulations of cells contained within the human neurosphere cultures can respond appropriately to specific extracellular cues present in each of the four target regions in the adult rat brain. Because the human neurosphere cultures are likely to contain a mixture of multipotent and lineage-restricted progenitors, the specific migratory patterns seen in the different locations may be explained either by the ability of an undifferentiated stem cell-like cell to differentiate along alternative neuronal or glial pathways in response to diverse local cues, or alternatively, by the presence of different subpopulations of lineage-restricted neuronal or glial precursors that were already committed to specific neuronal or glial fates. The present data seem compatible with both alternatives.

In conclusion, the long-term propagated human neural progenitors described here demonstrate a remarkable capacity for migration, integration, and site-specific differentiation in the adult brain. The growth factor combination used here acted to maintain the progenitors as a constitutively proliferating cell popula-

tion without losing their capacity to respond to those extracellular cues normally present in the adult CNS. With further refinement of the procedure, e.g., by application of cell enrichment and cell sorting techniques, this culture system may provide an almost unlimited source of human neural progenitors at different stages of differentiation and lineage restriction. Such cells will be of great interest both as an experimental tool and as an alternative to primary embryonic brain tissue for intracerebral transplantation.

# REFERENCES

- Altman J, Bayer SA (1990) Migration and distribution of two populations of hippocampal granule cell precursors during the perinatal and postnatal periods. *J Comp Neurol* 304:319-335.
- Altman J, Das GD (1966) Autoradiographic and histological studies of postnatal rat neurogenesis. I. A longitudinal investigation of the kinetics, migration and transformation of cells incorporating tritiated thymidine in rats, with special reference to postnatal neurogenesis in some brain regions. *J Comp Neurol* 136:337-389.
- Alvarez-Buylla A (1977) Neurogenesis in the adult brain: prospects for brain repair. In: *Isolated, characterization and utilization of CNS stem cells* (Gage FH, Christen Y, eds), pp 87-100. New York: Springer.
- Barami K, Iversen K, Fumey H, Goldman SA (1993) Hu protein as an early marker of neuronal phenotypic differentiation by subependymal zone cells of the adult songbird forebrain. *J Neurobiol* 28:82-101.
- Betarbat R, Zigova T, Bakay RA, Lusk MB (1996) Dopamine and GABAergic interneurons of the olfactory bulb are derived from the neonatal subependymal zone. *Dev Neurosci* 14:921-930.
- Blackmore WF, Franklin RJM (1991) Transplantation of glial cells into the CNS. *Trends Neurosci* 14:323-327.
- Bröske O, Messing U, McKay RDG (1993) Host-guided migration allows targeted introduction of neurons into the embryonic brain. *Neuron* 15:1275-1285.
- Cameron HA, Woolsey CS, McEwen BS, Gould E (1993) Differentiation of newly born neurons and glia in the dentate gyrus of the adult rat. *Neuroscience* 56:337-344.
- Campbell K, Olson M, Björklund A (1993) Regional incorporation and site-specific differentiation of striatal precursors transplanted to the embryonic forebrain ventricle. *Neuron* 15:1259-1273.
- Carpenter MK, Cui X, Hu Z, Jackson J, Sherman S, Seliger A, Wahlborg L (1999) In vitro expansion of a multipotent population of human neural progenitor cells. *Exp Neurol*, in press.
- Dunnett SB, Björklund A (1994) Functional neural transplantation. New York: Raven.
- Fishell O (1993) (1995) Striatal precursors adopt cortical identities in response to local cues. *Development* 121:803-812.
- Fitz JD, Aurora S, Yang C, Simonin C, Willis AM, Billingham LL, Jendryak M, Sidman RL, Wolfe JH, Kim SU, Snyder EY (1998) Engraftable human neural stem cells respond to developmental cues, replace neurons and express foreign genes. *Nat Biotechnol* 16:1033-1039.
- Gage FH, Coates FW, Palmer TD, Kuhn HO, Fisher LJ, Suhonen JO, Peterson DA, Suhr ST, Ray J (1995) Survival and differentiation of adult neural progenitor cells transplanted to the adult brain. *Proc Natl Acad Sci USA* 92:11879-11883.
- Gao W-Q, Hatten MB (1994) Immunizing oncogenes robust the establishment of granule cell identity in developing cerebellum. *Development* 120:1059-1070.
- Gierken CR (1992) The neocortical mosaic: multiple levels of compartmental organization. *Trends Neurosci* 15:133-139.
- Graebner-Frull KM, Nakao N, Lachy O, Brundin P (1996) Phenotypic development of the human embryonic striatal primordium: a study of cultured and grafted neurons from the lateral and medial ganglionic eminences. *Neuroscience* 73:171-183.
- Graebner-Frull KM, Nakao N, Lachy O, Brundin P (1997) Developmental features of human striatal tissue transplanted in a rat model of Huntington's Disease. *Neurobiol Dis* 3:299-311.
- Hammar JP, Archer DR, Duncan ID (1997) Myelination following transplantation of EGF-responsive neural stem cells in a myelin deficient environment. *Exp Neurol* 147:84-95.
- Kaplan MS, Hinds JW (1977) Neurogenesis in the adult rat: electron microscopic analysis of light radioautographs. *Science* 197:1092-1094.
- Kippatrick TJ, Bartlett PF (1995) Cloned multipotential precursors from the mouse cerebellum require FGF-2, whereas glial restricted precursors are stimulated with either FGF-2 or EGF. *J Neurosci* 15:3653-3661.
- Kuhn HO, Dickerson-Anson H, Gage FH (1996) Neurogenesis in the dentate gyrus of the adult rat: age-related decrease of neuronal progenitor proliferation. *J Neurosci* 16:3027-3033.
- Lis C, Alvarez-Buylla A (1993) Proliferating subventricular zone cells in the adult mammalian forebrain can differentiate into neurons and glia. *Proc Natl Acad Sci USA* 90:2074-2077.
- Lis C, Alvarez-Buylla A (1994) Long-distance neuronal migration in the adult mammalian brain. *Science* 264:1145-1148.
- Luskin MB (1993) Restricted proliferation and migration of postnatally generated neurons derived from the forebrain subventricular zone. *Neuron* 11:173-182.
- Luskin MB, Zigova T, Betarbat R, Sommer BJ (1997) Characterization of neuronal progenitor cells of the neonatal forebrain: Isolation, characterization and utilization of CNS stem cells (Gage FH, Christen Y, eds), pp 67-86. New York: Springer.
- McConnell S (1988) Development and decision making in the mammalian cerebral cortex. *Brain Res* 472:1-23.
- McNeer JR, Smith CM, Nelson KC, Luskin MB (1995) The division of neuronal progenitors during migration in the neonatal mammalian forebrain. *Mol Cell Neurosci* 6:496-508.
- Murphy M, Drago J, Bartlett PF (1990) Fibroblast growth factor stimulates the proliferation of neural precursor cells in vitro. *J Neurosci* 10:473-477.
- Palmer TD, Ray J, Gage FH (1995) FGF-2-responsive progenitors reside in proliferative and quiescent regions of the adult rodent brain. *Mol Cell Neurosci* 6:474-486.
- Fundt LL, Kondoh T, Low WC (1995) The fate of human glial cells following transplantation in normal rodents and rodent models of neurodegenerative disease. *Brain Res* 693:23-36.
- Ray J, Gage FH (1994) Spinal cord neuroblasts proliferate in response to basic fibroblast growth factor. *J Neurosci* 14:3548-3564.
- Ray J, Peterson DA, Schladt M, Gage FH (1993) Proliferation, differentiation and long-term culture of primary hippocampal neurons. *Proc Natl Acad Sci USA* 90:3602-3606.
- Ray J, Palmer TD, Suhonen J, Takahashi J, Gage FH (1997) Neurogenesis in the adult brain: lessons learned from the studies of progenitor cells from the embryonic and adult central nervous system. In: *Isolation, characterization and utilization of CNS stem cells* (Gage FH, Christen Y, eds), pp 129-149. New York: Springer.
- Reynolds BA, Weiss S (1992a) Generation of neurons and astrocytes from isolated cells of the adult mammalian central nervous system. *Science* 255:1707-1710.
- Reynolds BA, Weiss S (1992b) A multipotent EGF-responsive striatal embryonic progenitor cell produces neurons and astrocytes. *J Neurosci* 12:4563-4574.
- Reynolds BA, Weiss S (1996) Clonal and population analyses demonstrate that an EGF-responsive mammalian embryonic precursor is a stem cell. *Dev Biol* 175:1-13.
- Richards J, Kippatrick TJ, Bartlett PF (1992) Do novo generation of neuronal cells from the adult mouse brain. *Proc Natl Acad Sci USA* 89:8591-8595.
- Sato M, Yoshida T (1997) Promotion of neurogenesis in mouse olfactory neuronal progenitor cells by leukemia inhibitory factor in vitro. *Neurosci Lett* 225:165-168.
- Somjen-Brenner M, Deloume JC, Gensburger C (1994) Proliferation of neuronal precursor cells from the central nervous system in culture. *Rev Neurosci* 5:43-53.
- Suhonen JO, Peterson DA, Ray J, Gage FH (1996) Differentiation of adult hippocampus-derived progenitors into olfactory neurons in vivo. *Nature* 383:624-627.
- Svensson CN, Clarke DJ, Rowse AE, Dunnett SB (1996) Survival and differentiation of rat and human epidermal growth factor-responsive precursor cells following grafting into the lesioned adult central nervous system. *Exp Neurol* 137:376-388.
- Svensson CN, Caldwell MA, Shen J, von Borg MO, Rowse A, Tyers P, Karlsson J, Dunnett SB (1997) Long-term survival of human central nervous system progenitor cells transplanted into a rat model of Parkinson's disease. *Exp Neurol* 148:133-146.
- Vaccaro A, Reynolds BA, Fraser DD, Weiss S (1993) Basic fibroblast growth factor regulates the proliferative fate of both unipotent (neu-

- rocal) and bipotent (neuronal/astroglial) epithelial growth factor-generated progenitor cells. *Neuron* 11:951-956.
- Vicario-Abejon C, Cunningham MO, McKay RJ (1995) Cerebellar precursors transplanted to the neonatal dentate gyrus express features characteristic of hippocampal neurons. *Neuron* 15:105-114.
- Wells S, Dunne C, Hewson J, Wohl C, Wheatley M, Peterson AC, Reynolds BA (1996a) Multipotential CNS stem cells are present in the adult mammalian spinal cord and ventricular neuroaxis. *J Neurosci* 16:7349-7359.
- Wells S, Reynolds BA, Vescovi AL, Monahan C, Craig CO, van der Kooy D (1996b) Is there a neural stem cell in the mammalian forebrain? *Trends Neurosci* 19:387-393.
- Wells J, Vintje BP, Wells DG, Dunn ME (1988) Cell-sized microspheres in the hippocampus show cleavage planes and passive displacement. *Brain Res Bull* 21:601-603.
- Winkler C, Fricker RA, Gates MA, Olsson M, Hammarang JP, Carpenter MK, Björklund A (1998) Incorporation and glial differentiation of mouse EGF-responsive neural progenitor cells after transplantation into the embryonic rat brain. *Mol Cell Neurosci* 11:99-116.
- Zigova T, Betarbet R, Soteres MJ, Brock S, Bakay RA, Luskus MD (1996) A comparison of the patterns of migration and the distribution of homotopically transplanted neonatal subventricular zone cells and heterotopically transplanted ventricular zone cells. *Dev Biol* 173:459-474.

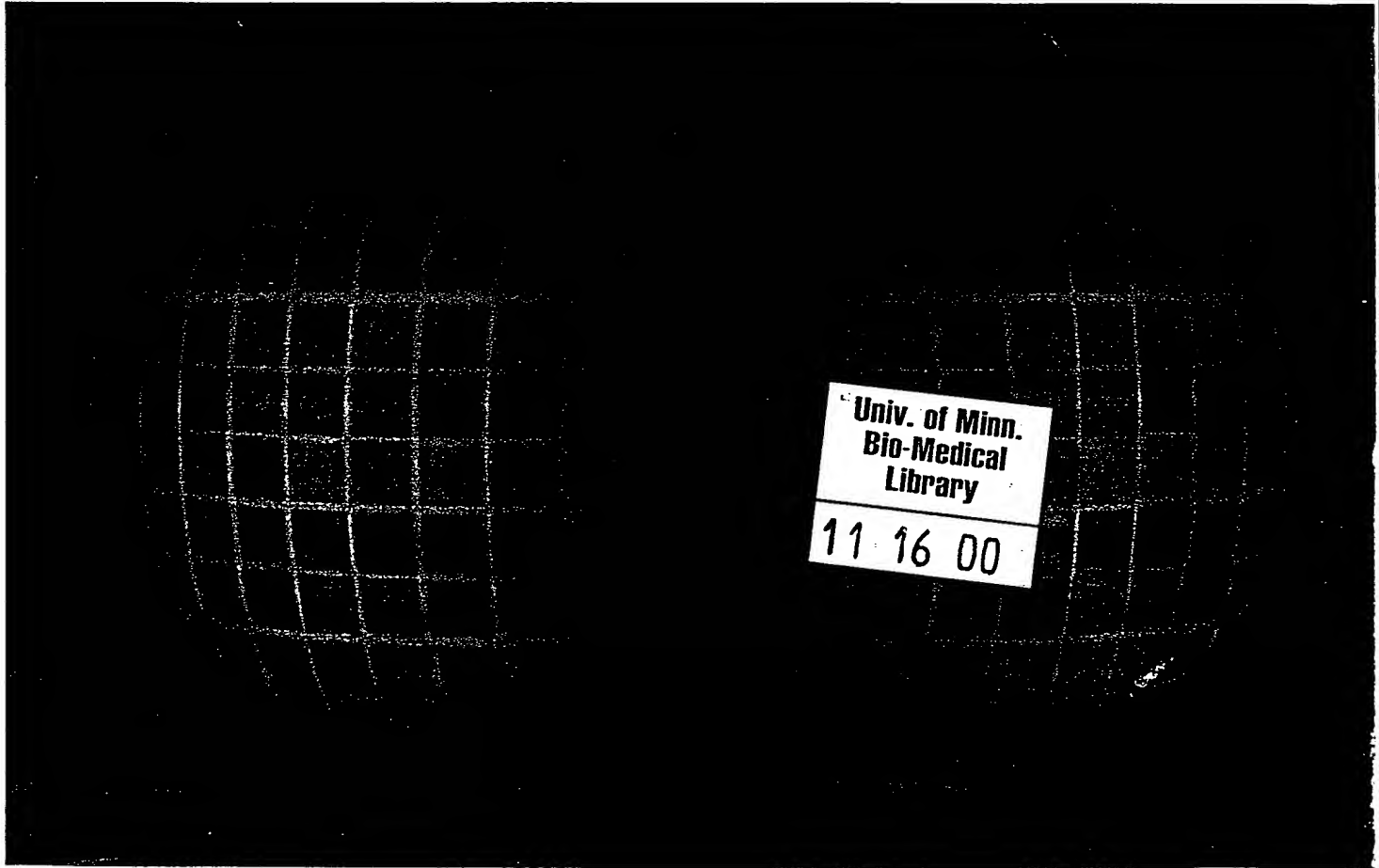
~~CONTENTS~~  
~~REVIEWS~~  
~~ISSUE~~

# PNAS

Proceedings of the National Academy of Sciences  
of the United States of America

**DOES NOT  
LEAVE LIBRARY**

N vember 7, 2000 | vol. 97 | no. 23 | pp. 12389–12932 | [www.pnas.org](http://www.pnas.org)



Univ. of Minn.  
Bio-Medical  
Library  
11 16 00

An empirical explanation of color contrast  
Are denatured proteins ever random coils?  
Natural selection and speciation  
Fine mapping of quantitative trait loci  
Neural stem cells and tumor damage repair  
Japanese–American Frontiers of Science

# Neural stem cells display extensive tropism for pathology in adult brain: Evidence from intracranial gliomas

Karen S. Aboody<sup>\*†‡</sup>, Alice Brown<sup>†</sup>, Nikolai G. Rainov<sup>†</sup>, Kate A. Bower<sup>\*</sup>, Shaoxiong Liu<sup>\*</sup>, Wendy Yang<sup>\*</sup>, Juan E. Small<sup>†</sup>, Ulrich Herrlinger<sup>†</sup>, Vaclav Ourednik<sup>\*</sup>, Peter McL. Black<sup>§</sup>, Xandra O. Breakefield<sup>†</sup>, and Evan Y. Snyder<sup>\*†§</sup>

<sup>\*</sup>Departments of Neurology, Pediatrics, and Neurosurgery, Children's Hospital; <sup>†</sup>Molecular Neurogenetics Unit, Department of Neurology, Massachusetts General Hospital; and <sup>§</sup>Brain Tumor Service, Department of Neurosurgery, Brigham and Women's Hospital, Harvard Medical School, Boston, MA 02115; and <sup>‡</sup>Layton Bioscience, Sunnyvale, CA 94086

Communicated by Richard L. Sidman, Harvard Medical School, Southborough, MA, July 24, 2000 (received for review May 19, 2000)

One of the impediments to the treatment of brain tumors (e.g., gliomas) has been the degree to which they expand, infiltrate surrounding tissue, and migrate widely into normal brain, usually rendering them "elusive" to effective resection, irradiation, chemotherapy, or gene therapy. We demonstrate that neural stem cells (NSCs), when implanted into experimental intracranial gliomas *in vivo* in adult rodents, distribute themselves quickly and extensively throughout the tumor bed and migrate uniquely in juxtaposition to widely expanding and aggressively advancing tumor cells, while continuing to stably express a foreign gene. The NSCs "surround" the invading tumor border while "chasing down" infiltrating tumor cells. When implanted intracranially at distant sites from the tumor (e.g., into normal tissue, into the contralateral hemisphere, or into the cerebral ventricles), the donor cells migrate through normal tissue targeting the tumor cells (including human glioblastomas). When implanted outside the CNS intravascularly, NSCs will target an intracranial tumor. NSCs can deliver a therapeutically relevant molecule—cytosine deaminase—such that quantifiable reduction in tumor burden results. These data suggest the adjunctive use of inherently migratory NSCs as a delivery vehicle for targeting therapeutic genes and vectors to refractory, migratory, invasive brain tumors. More broadly, they suggest that NSC migration can be extensive, even in the adult brain and along nonstereotypical routes, if pathology (as modeled here by tumor) is present.

gene therapy | transplantation | migration | brain tumors | vascular

**M**alignant brain tumors, e.g., glioblastoma multiforme, remain virtually untreatable and inevitably lethal despite extensive surgical excision and adjuvant radio- and chemotherapy (1). Their treatment resistance is related to their exceptional migratory nature and ability to insinuate themselves seamlessly and extensively into normal neural tissue, often migrating great distances from the main tumor mass. These cells are responsible for the recurrent tumor growth near the borders of the resection cavity (1). It is this behavior that has also limited their accessibility to otherwise promising gene therapeutic vectors and interventions (2). Intriguingly, one of the cardinal features of neural stem cells (NSCs) is their exceptional migratory ability (3–10). Indeed, it is their migratory capacity that has made them so useful in therapeutic paradigms demanding brainwide gene and cell replacement in various animal models of neurodegeneration, albeit usually in the newborn (8–10). We hypothesized that pathology promotes NSC migration to an extent not assumed possible based on knowledge drawn from the normal adult brain and that, therefore, an approach for targeting gene therapy to the most migratory tumor cells in the adult central nervous system (CNS) might be the use of inherently migratory NSCs to deliver therapeutic genes and/or their products.

## Experimental Methods

**In Vitro Migration Studies.** CNS-1 is a virulent, invasive rat-derived glioblastoma cell line. Cells engineered to express green fluorescent

protein (GFP) as previously described (11, 12) were plated to 60–70% confluence onto 100-mm culture dishes around a central 5-mm metal cylinder that was sealed and, therefore, remained cell-free. The plate was incubated overnight, by which time the glioma cells had attached. A suspension of  $4 \times 10^4$  dissociated fibroblasts (in control dishes) or murine NSCs (in experimental dishes) were seeded into the central cylinder (i.e., no direct contact with CNS-1 cells) (Fig. 1, arrowheads). A similar number of fibroblasts or NSCs, respectively, were placed into a 5-mm cylinder placed directly on top of the adherent CNS-1 monolayer and cultured as before (at extreme right edge of plates) (Fig. 1, arrows). The fibroblasts (clone TR-10) were derived from 3T3 cells infected with a retroviral vector encoding *lacZ*. The murine NSCs were derived from the prototypical constitutively *lacZ*-expressing helper virus-free murine NSC clonal line C17.2 (8–10, 13), which, because of its well-documented ability to integrate into most CNS structures and in a number of normal and abnormal animal models, has been useful for delineating the range of therapeutic possibilities for NSCs (8–10, 13). (Although self-renewing, NSCs become contact inhibited; never grow in soft agar; are nontumorigenic in nude mice; fail to incorporate BrdUrd after 48 h *in vivo*; and respond to normal cues for cell cycle withdrawal, differentiation, and interaction with host cells.) The day after plating of fibroblasts and NSCs, the cylinders were removed, and the dishes were rinsed and incubated for an additional 5 days. Dishes were stained for the *lacZ* gene product *Escherichia coli*  $\beta$ -galactosidase ( $\beta$ -gal) by 5-bromo-4-chloro-3-indolyl  $\beta$ -D-galactoside (X-Gal) histochemistry (8).

**Animal Studies *in Vivo*.** For some studies, not only were murine NSCs (C17.2) used but also some of human derivation were used (5). To establish intracranial tumors, either the CNS-1 rat glioblastoma line (11, 12) or the HGL21 human glioblastoma line (14) was implanted into the brains of adult female nude mice, or the D74 glioma line was implanted into the brains of adult female Fisher rats by using procedures previously described (15). Briefly, animals received stereotactically guided injections over 3–5 min into the forebrain (2 mm lateral and 1 mm anterior to bregma; depth 2–4 mm from dura) of tumor cells (of a number specified below) suspended in 1  $\mu$ l of PBS. Animals receiving a second implant at a later date of NSCs or fibroblasts [suspended in PBS at  $2\text{--}4 \times 10^4$  cells per  $\mu$ l as detailed elsewhere (8–10, 13)] were injected stereotactically with cells in a quantity and location to yield the various paradigms described below. On

Abbreviations: NSC, neural stem cell; CNS, central nervous system; GFP, green fluorescent protein;  $\beta$ -gal,  $\beta$ -galactosidase; X-Gal, 5-bromo-4-chloro-3-indolyl  $\beta$ -D-galactoside; CD, cytosine deaminase; 5-FC, 5-fluorocytosine; CD-NSC, CD-transduced NSC.

See commentary on page 12393.

<sup>†</sup>To whom reprint requests should be addressed. E-mail: Snyder@A1.TCH.harvard.edu.

The publication costs of this article were defrayed in part by page charge payment. This article must therefore be hereby marked "advertisement" in accordance with 16 U.S.C. §1734 solely to indicate this fact.

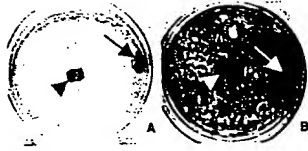


**Fig. 1.** Migratory capacity of NSCs in culture. CNS-1 glioblastoma cells were plated around a central cylinder (i.e., free of CNS-1 cells). Fibroblasts (A) or NSCs (B) were seeded into the center cylinder (i.e., no direct contact with CNS-1 cells) (arrowheads) or into cylinders placed directly on top of adherent tumor cells (at the extreme right edge of plates; arrows). After removal of the cylinders and 5 additional days of incubation, there was wide distribution of blue X-Gal<sup>+</sup> NSCs (B), compared with fibroblasts (A), which remained localized to their area of initial seeding.

the days specified below, the brains were processed as detailed below (e.g., for  $\beta$ -gal, GFP, BrdUrd, human markers, and/or cell type-specific antigen expression). CD-1 mice, when used, received daily cyclosporin injections (10  $\mu$ g/g).

**Specific Protocols for *in Vivo* Experiments.** *NSC implantation directly into tumor bed* (Fig. 2, Paradigm 1). On day 0, recipients received injections of tumor cells ( $3\text{--}4 \times 10^4$  in 1  $\mu$ l of PBS) into the right frontal lobe. On day 4–6, NSCs or fibroblasts ( $4\text{--}10 \times 10^4$  in 1.5  $\mu$ l of PBS) were injected directly into the tumor bed, using identical coordinates. Recipients were killed on days 6–9, 10–12, 14–16, and 21 after tumor implantation.

*NSC implantation at distant intracranial site from tumor bed: In same hemisphere* (Fig. 3, Paradigm 2). On day 0, recipients received injections of glioblastoma cells ( $3 \times 10^4$  in 1  $\mu$ l of PBS) into the right frontal lobe. On day 6, NSCs ( $4 \times 10^4$  in 1.5  $\mu$ l of PBS) were injected also into the right frontoparietal lobe at the following coordinates: 3 mm lateral and 4 mm caudal to bregma; depth 3 mm from dura—i.e., 1 mm lateral and 4 mm behind the tumor. Animals were killed on days 12 and 21.

*In contralateral hemisphere* (Fig. 3, Paradigm 3). On day 0, recipients received injections of glioblastoma cells ( $3\text{--}5 \times 10^4$  in 1  $\mu$ l of PBS) into the right frontal lobe (2.5 mm lateral and 2 mm caudal to bregma; depth 3 mm from dura). On day 6, NSCs ( $8 \times 10^4$  in 2  $\mu$ l of PBS) were injected into the left frontal lobe at the following coordinates: 2 mm lateral and 2 mm caudal to bregma; depth 3 mm from dura. Animals were killed on days 12 and 21.

*Into ventricles* (Fig. 3, Paradigm 4). On day 0, recipients received injections of glioblastoma cells ( $5\text{--}8 \times 10^4$  in 1  $\mu$ l of PBS) into the right frontal lobe (2 mm lateral to bregma on the coronal suture; depth 3 mm from dura). On day 6, NSCs ( $8 \times 10^4$  in 2  $\mu$ l of PBS) were injected into the contralateral or ipsilateral cerebral ventricle at the following coordinates on the respective side: 1 mm lateral and 3 mm caudal to bregma; depth 2 mm from dura. Animals were killed on days 8, 12, and/or 21.

*NSC implantation into a peripheral, intravascular site* (Fig. 4, Paradigm 5). On day 0, adult nude mice received injections of CNS-1 glioblastoma cells ( $1 \times 10^5$  in 2  $\mu$ l of PBS) into the right frontal lobe. On day 7, murine NSCs ( $2 \times 10^6$  in 200  $\mu$ l of PBS) were injected into the tail vein. Animals were killed on day 12.

**Retroviral Transduction of NSCs with Cytosine Deaminase (CD).** A plasmid using the retroviral pBabePuro backbone (16) was constructed to include the *E. coli* CD cDNA (1.5-kb fragment) transcribed from the long terminal repeat. Vectors were packaged by cotransduction of the CDpuro plasmid with the MV12 envelope coding plasmid cDNA (17) into 293T/17 cells (18). CDpuro retroviral supernatant was used for multiple infections of the murine NSCs. Transduced NSCs (“CD-NSCs”) were placed under puromycin selection for  $\approx 2$  wk.

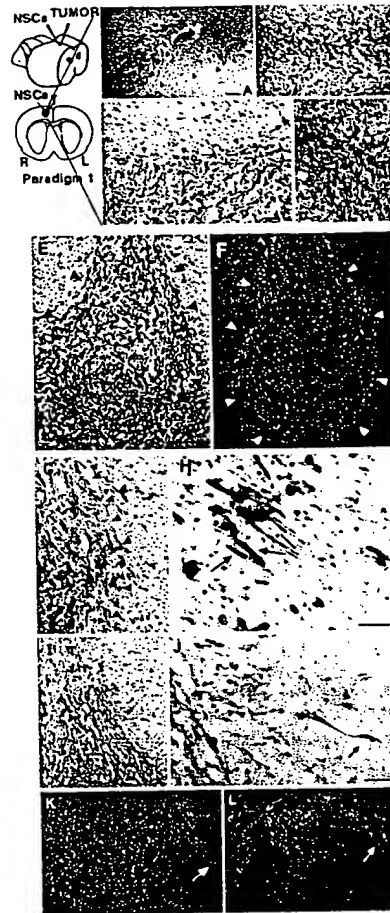


**Fig. 2.** NSCs migrate extensively throughout a brain tumor mass *in vivo* and “trail” advancing tumor cells. Paradigm 1 is illustrated schematically. Section of brain under low (A) and high (B) power from an adult rat killed 48 h after NSC injection into an established D74 glioma, processed with X-Gal to detect blue-staining  $\beta$ -gal-producing NSCs and counterstained with neutral red to show dark red tumor cells; arrowheads demarcate approximate edges of the tumor mass where it interfaces with normal tissue. Donor X-Gal<sup>+</sup> blue NSCs (arrows) can be seen extensively distributed throughout the mass, interspersed among the red tumor cells. (C) Tumor, 10 days after NSC injection, illustrating that, although NSCs (arrows) have infiltrated the mass, they largely stop at the junction between tumor and normal tissue (arrowheads) except where a tumor cell (dark red, elongated) is entering normal tissue; then NSCs appear to “follow” the invading tumor cell into surrounding tissue (upper right arrow). This phenomenon becomes more dramatic when examining NSC behavior in a more virulent and aggressively invasive tumor, the CNS-1 glioblastoma in the adult nude mouse, pictured in D. This section illustrates extensive migration and distribution of blue NSCs (arrows) throughout the infiltrating glioblastoma up to and along the infiltrating tumor edge (red arrowheads) and into surrounding tissue in juxtaposition to many dark red<sup>+</sup> tumor cells invading normal tissue. The “tracking” of individual glioblastoma cells is examined in greater detail in E–L, where CNS-1 cells have been labeled *ex vivo* by transduction with GFP cDNA. (E and F) Sister sections showing a low power view of transgene-expressing NSCs distributed throughout the main tumor mass to the tumor edge (outlined by arrowheads). Sections were either costained with X-Gal (NSCs, blue) and neutral red (tumor cells, dark red and elongated) (E) or processed for double immunofluorescence using an anti- $\beta$ -gal antibody (NSCs, red) and an FITC-conjugated anti-GFP antibody (glioblastoma cells, green) (F). Low (G) and high (H) power views of tumor edge (arrowheads) with blue NSCs (blue arrow) in immediate proximity to and intermixed with an invading tumor “island” (dark red spindle-shaped cells) (red arrow). (I and J) Low and high power views, respectively (boxed area in I is magnified in J), of a blue NSC in direct juxtaposition to a single migrating neutral red<sup>+</sup>, spindle-shaped tumor cell (arrow), the NSC “riding” the glioma cell in “piggy-back” fashion. (K and L) Low and high power views, respectively, under fluorescence microscopy, of single migrating GFP<sup>+</sup> tumor cells (green) in juxtaposition to  $\beta$ -gal<sup>+</sup> NSCs (red). Region indicated by white arrow in K and magnified in L illustrates NSCs apposed to tumor cells migrating away from the main tumor bed. (Scale bars: A, 40  $\mu$ m, 30  $\mu$ m in B; C, 30  $\mu$ m, 25  $\mu$ m in D; E, 90  $\mu$ m in F; H, 15  $\mu$ m, 60  $\mu$ m in G; J, 30  $\mu$ m, 60  $\mu$ m in I, 70  $\mu$ m in K, 35  $\mu$ m in L.)

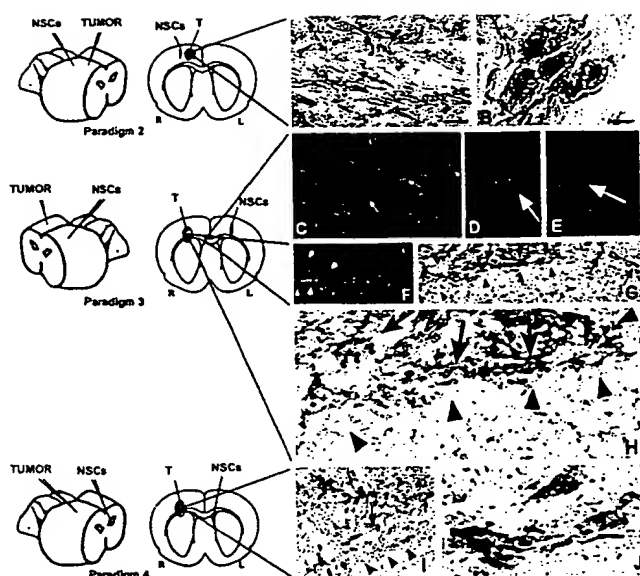


**Fig. 3.** NSCs implanted at various intracranial sites distant from main tumor bed migrate through normal adult tissue toward glioma cells. (A and B) Same hemisphere but *behind* tumor (Paradigm 2). Shown here is a section through the tumor from an adult nude mouse 6 days after NSC implantation caudal to tumor. In A (as per the schematic, a coned down view of a tumor populated as pictured under low power in Figs. 2A and 3A and B), note X-Gal<sup>+</sup> blue NSCs interspersed among dark neutral red<sup>+</sup> tumor cells. (B) High power view of NSCs in juxtaposition to islands of tumor cells. (C–H) Contralateral hemisphere (Paradigm 3). (C–E) As indicated on the schematic, these panels are views through the corpus callosum ("c") where  $\beta$ -gal<sup>+</sup> NSCs (red cells, arrows) are seen migrating from their site of implantation on one side of the brain toward tumor on the other. Two representative NSCs indicated by arrows in C are viewed at higher magnification in D and E, respectively, to visualize the classic elongated morphology and leading process of a migrating neural progenitor oriented toward its target. In F,  $\beta$ -gal<sup>+</sup> NSCs (red) are "homing in" on the GFP<sup>+</sup> tumor (green) having migrated from the other hemisphere. In G, and magnified further in H, the X-Gal<sup>+</sup> blue NSCs (arrows) have now actually entered the neutral red<sup>+</sup> tumor (arrowheads) from the opposite hemisphere. (I and J) Intraventricular (Paradigm 4). Shown here is a section through the brain tumor of an adult nude mouse 6 days following NSC injection into the contralateral cerebral ventricle. In I, as per the schematic, blue X-Gal<sup>+</sup> NSCs are distributed within the neutral red<sup>+</sup> main tumor bed (edge delineated by arrowheads). At higher power in J, the NSCs are in juxtaposition to migrating islands of red glioblastoma cells. Fibroblast control cells never migrated from their injection site in any paradigm. All X-Gal-positivity was corroborated by anti- $\beta$ -gal immunoreactivity. (Scale bar: A, 20  $\mu$ m, and applies to C; B, 8  $\mu$ m, 14  $\mu$ m in D and E, 30  $\mu$ m in F and G, 15  $\mu$ m in H, 20  $\mu$ m in I, and 15  $\mu$ m in J.)

**Oncolysis Assays of CD Bioactivity.** For *in vitro* assays, CNS-1 cells ( $2 \times 10^5$ ) were plated onto 10-cm dishes (day 1). On day 2, murine or human CD-NSCs ( $5$ – $10 \times 10^4$ ) were added. On day 3, 5-fluorocytosine (5-FC, 500  $\mu$ g/ml) was added. Control dishes included (i) cocultures with no 5-FC and (ii) tumor cells alone with 5-FC. On day 6, plates were stained by means of X-Gal histochemistry to visualize NSCs and with neutral red to visualize tumor cells (Fig. 6A and B). The number of tumor cells was extrapolated from the average of 20 random high power fields per plate. For *in vivo* assays, animals bearing CNS-1 cells ( $7 \times 10^4$ ) alone or CNS-1 cells interspersed with CD-NSCs ( $3.5 \times 10^4$ ) received 10 i.p. injections of 5-FC (900 mg/kg) over 10 days. Control tumor-bearing animals received no 5-FC, 5-FC without NSCs, or NSCs without 5-FC. One day after the last 5-FC dose, the brains were cryosectioned and stained with X-Gal and neutral red, and measurements of the tumor were made from camera lucida drawings of the mass from interval sections through the tumor from which relative surface areas were then calculated by image analysis (Fig. 7).



**Fig. 4.** NSCs injected into tail vein "target" intracerebral gliomas. Paradigm 5 is illustrated. (A–C) Progressively higher power views of representative 10- $\mu$ m sections through the brain 4 days after NSC injection, processed with X-Gal histochemistry (A) and anti- $\beta$ -gal immunocytochemistry (B and C) to identify donor NSCs and counterstained with neutral red to delineate the tumor border. (The  $\beta$ -gal immunoprecipitate, in addition to providing independent identity confirmation, typically fills cells and processes much better than X-Gal.) At low power (A), X-Gal<sup>+</sup> NSCs (representative X-Gal precipitate enlarged in *Inset*) are distributed throughout the tumor but not in surrounding normal tissue. Sister sections, reacted with an anti- $\beta$ -gal antibody and visualized at higher power in B and further magnified in C confirm the presence of donor-derived cells (arrow) within the tumor. (Scale bar: A, 25  $\mu$ m, 20  $\mu$ m in B, and 12  $\mu$ m in C.)

**BrdUrd Uptake by Engrafted NSCs.** Selected animals received three i.p. injections of BrdUrd (1 ml/100 g body weight of a 20  $\mu$ M stock solution) over 24 h before sacrifice.

**Histopathological and Immunocytochemical Analysis.** On the days specified in the paradigms above, animals were killed, and 10- to 15- $\mu$ m serial coronal cryosections from 4% paraformaldehyde-fixed brains were processed for light microscopy with X-Gal histochemistry to identify *lacZ*-expressing blue donor cells (8–10, 13) and counterstained with neutral red to detect distinctively dark red, elongated tumor cells (2). Sister sections were prepared for dual-filter immunofluorescence where an anti- $\beta$ -gal antibody was revealed with a Texas Red-conjugated secondary antibody (1:1,000; Vectastain) (to identify donor cells as red) (8–10, 13), and an anti-GFP antibody (1:500; CLONTECH) was revealed with an FITC-conjugated secondary antibody (1:1,000; Vectastain) (to recognize CNS-1 tumor cells as green). BrdUrd<sup>+</sup>-intercalated cells were identified by an anti-BrdUrd antibody (5). Sections containing human NSCs were additionally stained with multiple human-specific antibodies, including against to ribonuclear protein (Chemicon, 1:20), against NuMA (Chemicon, 1:40 and Calbiochem, 1:400), and against the human EGF receptor (Upstate Biotechnology, 1:100), revealed by a biotinylated goat anti-mouse IgM (1:250; Vectastain) followed by the standard ABC and diaminobenzidine (DAB) reaction (Vectastain).

## Results

This study's focus was documenting the migratory behavior of NSCs [specifically those reported to be effective delivery vehicles for genes (5, 8) and viral vectors (10)] in relation to aggressively invasive experimental intracranial tumors in adult brain and then to arm some of these cells with a bioactive, therapeutic gene requiring relative proximity to tumor cells (allowing oncolysis to be a measure of the efficiency and specificity of gene expression).

**Migratory Capacity of NSCs in Culture.** To visualize the migratory properties of NSCs when confronted with a tumor, *in vitro* studies first assessed the relative migratory capacity of NSCs compared with fibroblasts cocultured with glioma cells. In contrast to fibroblasts, which remained localized to the area of initial seeding (Fig. 1A), NSCs migrated rapidly and interspersed throughout the glioma monolayer, far from their initial site of seeding, robustly expressing *lacZ* (Fig. 1B). These patterns were observed whether the cells were plated directly on top of (i.e., in direct contact with) the glioma cells (arrows) or merely within the same culture medium and environment without direct contact (arrowheads). The migratory



ing NSCs then became contact-inhibited and quiescent (do not incorporate BrdUrd; ref. 5).

**NSCs Migrate Throughout and "Surround" Tumor *in Vivo*.** To determine the behavior of NSCs introduced to brain tumors *in vivo*, adult rats first received an implant of syngeneic D74 rat glioma cells (19) into the right frontal lobe. Four days later, *lacZ*-expressing murine NSCs were injected directly into the tumor bed (Paradigm 1, Fig. 2). Animals were killed at 2- to 4-day intervals after intratumoral injection and brain sections processed to detect  $\beta$ -gal-producing NSCs. As early as 2 days after injection, X-Gal<sup>+</sup> blue donor NSCs were found distributed extensively throughout the darkly neutral red-stained tumor mass (Fig. 2A). Although the transgene-expressing NSCs remained stably intermixed throughout the tumor (Fig. 2B, arrows), up to and along the infiltrating tumor edge, they largely stopped at the border of the tumor where it interfaced with normal tissue (Fig. 2C, arrowheads) as if "surrounding" the advancing neoplasm. Normal adult parenchyma presented a less permissive migratory environment to NSCs, except under one circumstance: where tumor cells began to infiltrate normal brain. In those instances, the NSCs migrated slightly beyond the tumor edge in conjunction with—as if following or "trailing"—individual infiltrating tumor cells (Fig. 2C, arrow). This phenomenon was most dramatic when examined in the context of the more virulent and aggressively infiltrative CNS-1 glioblastoma cell line (11) (Fig. 2D), which, in adult nude mice, demonstrates single cell invasive characteristics analogous to those of human glioblastomas. After implantation as per Paradigm 1, extensive migration and distribution of  $\beta$ -gal<sup>+</sup> donor cells was again noted throughout the darkly red-stained infiltrating tumor mass, up to, and along the encroaching tumor edge (red arrowheads), with further migration into the surrounding tissue in concert with and in virtual juxtaposition to aggressively invading tumor cells (Fig. 2D, black arrows).

**NSCs "Track" Infiltrating Tumor Cells.** To better distinguish single tumor cells migrating away from the main tumor mass, CNS-1 glioblastoma cells were labeled *ex vivo* by retroviral transduction of GFP cDNA before implantation (12). After implantation (as per Paradigm 1) of *lacZ*-expressing NSCs into the GFP-expressing CNS-1 tumor bed (Fig. 2 E–L), NSCs could not only be seen to distribute themselves throughout the tumor to its invading edge (Fig. 2 E and F), but could even more clearly be seen to "trail" islands of tumor cells migrating away from the main tumor mass (Fig. 2 G and H) as well as individual aggressive, dark red, or GFP<sup>+</sup>, elongated infiltrating tumor cells (Fig. 2 I–L). Of note is the frequently observed apposition of transgene-expressing NSCs to invasive tumor cells (Fig. 2 J–L, arrows). The NSCs themselves never became tumorigenic. BrdUrd pulsing of animals before sacrifice confirmed prior observations that donor NSCs were quiescent in normal tissue (5), nonmitotic (i.e., BrdUrd<sup>−</sup>) in the heart of the tumor, and with an occasional NSC that could still incorporate BrdUrd at the advancing edge, a situation optimal for targeting therapy toward invading tumors. The vast majority of NSCs remained not only quiescent but undifferentiated, expressing only nestin.

**NSCs Implanted Intracranially at Distant Sites Migrate Toward Tumor.** To determine whether NSCs have the capacity to migrate specifically toward the tumor, NSCs were injected into uninvolved intracranial sites distant from the main tumor mass in three separate paradigms (Fig. 3). In each case, donor NSCs migrating through normal adult tissue "targeted" the tumor. In Paradigm 2, NSCs were injected behind the glioblastoma. NSCs were always found distributed within the main tumor bed, as well as in apposition to migrating tumor cells in surrounding tissue (Fig. 3 A and B), with very few NSCs in other locations. In Paradigm 3, murine NSCs were injected into the contralateral hemisphere. NSCs (fluorescent red or X-Gal<sup>+</sup> blue) were seen migrating across the corpus

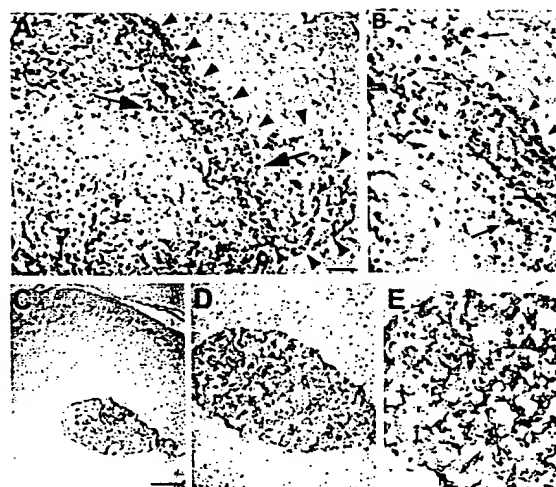


**Fig. 5.** Human NSCs (hNSCs) possess tumor tracking characteristics. (A and B) Rodent CNS-1 glioblastoma cells and human NSCs were implanted as per Paradigm 3 into opposite hemispheres of an adult mouse. Pictured 7 days later at low power (A) and high power (B) is a section through the neutral red-stained tumor (outlined by arrowheads) intermixed with human NSCs (identified by their brown nuclei following reaction with an anti-human nuclear antibody) (arrows) that migrated from the contralateral side. (C–E) Human HGL21 glioblastoma cells and hNSCs were similarly implanted into opposite hemispheres. Pictured at progressively higher power are sections through that neutral red-stained tumor intermixed with human NSCs (X-Gal<sup>+</sup> blue) that migrated from the contralateral side. (Scale bars: A, 20  $\mu$ m, 15  $\mu$ m in B; C, 60  $\mu$ m, 30  $\mu$ m in D, and 15  $\mu$ m in E.)

callosum and central commissures (Fig. 3 C–E, arrows) toward the tumor (fluorescent green or dark neutral red<sup>+</sup> masses delineated by arrowheads in Fig. 3F), ultimately entering and populating (Fig. 3 G and H, arrows) the tumor on the opposite side of the brain. In Paradigm 4, NSCs were injected into the ipsilateral or contralateral cerebral ventricle. NSCs (blue) again were seen within the main tumor bed (Fig. 3I), as well as in juxtaposition to migrating "islands" of tumor cells (dark red) (Fig. 3J). The only source of blue cells in these paradigms was the "distant" NSC implant. Very few NSC-derived cells were found in normal brain tissue beyond the injection site, except when tracking toward the main tumor mass or near infiltrating tumor cells, suggesting that, whereas NSCs migrated freely within the tumor, the normal adult brain parenchyma presented a less permissive environment for migration. The NSCs themselves never became tumorigenic. The tumors in transplant recipients were never larger than those in non-transplant recipients. NSC-derived cells continued to express their *lacZ* transgene exuberantly, often in direct contact with tumor cells. These NSC behaviors appeared to be independent of the size or location of the tumor; findings were similar for large tumors, small tumor foci, and even single scattered tumor cells surrounding the main tumor mass. Fibroblasts grafted as controls never showed this dispersion or tropism, consistent with previous reports (15).

**NSCs Injected into Systemic Circulation "Target" Intracerebral Gliomas.** Murine NSCs were injected into the tail vein of adult nude mice in which a CNS-1 glioblastoma had been established 1 wk before in the frontal lobe. Four days after i.v. NSC injection, albeit with low efficiency, anti- $\beta$ -gal<sup>+</sup> NSCs were distributed throughout the intracerebral tumor mass, but were not found in surrounding normal-appearing brain tissue, elsewhere in the brain, or in the brains of control animals (NSC-injected mice without intracerebral gliomas or tumor-bearing mice in the absence of NSC-injection).

**Human NSCs and NSCs Expressing a Therapeutic Gene Migrate to Tumors.** Because of the clinical implications of these migratory phenomena, we asked two further questions: (i) did these migratory



**Fig. 6.** Bioactive transgene (CD) remains functional (as assayed by *in vitro* oncolysis) when expressed within NSCs. CNS-1 glioblastoma cells (red) were cocultured with CD-transduced murine NSCs (A and B) (blue). Cocultures unexposed to 5-FC grew healthily and confluent (A), whereas plates exposed to 5-FC showed dramatic loss of tumor cells (B), represented quantitatively by the histograms (\*,  $P < 0.001$ ). The oncolytic effect was identical whether  $1 \times 10^5$  CD-NSCs or half that number were cocultured with a constant number of tumor cells. (In this paradigm, subconfluent NSCs were still mitotic at the time of 5-FC exposure and thus also subject to self-elimination by the generated 5-fluorouracil and its toxic metabolites.)

properties extend to human NSCs? and (ii) could relevant bioactive genes be expressed?

In answer to the first, human NSCs (brown nuclei, arrows in Fig. 5A and B) transplanted into the hemisphere *contralateral* to a CNS-1 glioma (Paradigm 3) indeed migrated across the corpus callosum and infiltrated and distributed themselves throughout the targeted tumor (arrowheads) as previously observed. That human NSCs could similarly target a true human glioblastoma is suggested in Fig. 5C–E in which Paradigm 3 was repeated employing human NSCs implanted contralateral to an HGL-21-derived tumor established in the nude mouse cerebrum; again, human NSCs migrated from one hemisphere to the other to infiltrate the glioblastoma.

To address the second question, NSCs were stably transduced with a transgene encoding the enzyme CD. CD can convert the nontoxic “prodrug” 5-FC to the oncolytic drug 5-fluorouracil, a chemotherapeutic agent that readily diffuses into tumor cells and has selective toxicity to rapidly dividing cells (18, 19). The CD gene provided an opportunity to examine a prototypical bioactive gene with a relevant, specific, quantifiable read-out of functionality (oncolysis) that might be enhanced by tumor proximity. CD-bearing NSCs retained their extensive migratory, tumor-tracking properties. To determine quantitatively whether a gene such as CD within an NSC retains its bioactivity—as assayed in this case by its anti-tumor effect—CD-bearing NSCs were first cocultured with glioma cells and then, when nearly confluent (Fig. 6A), exposed to 5-FC. Death of surrounding tumor cells was induced (Fig. 6B), even when the ratio of NSCs-to-tumor cells was as low as 1:4. NSCs that were mitotic at the time of 5-FC exposure self-eliminated. Control plates of tumor alone were not significantly killed by the same dose of 5-FC. To determine whether this bioactivity was retained *in vivo*, we used CD-transduced NSCs to express this gene within an intracranial glioma established in an adult nude mouse ( $3.5 \times 10^4$  NSCs to  $7 \times 10^4$  CNS-1 tumor cells in a 1:2 ratio). After systemic treatment with 5-FC, there was dramatic ( $\approx 80\%$ ) reduction in the resultant tumor mass at 2 wk postimplantation as compared with that in untreated animals (Fig. 7), indicative of CD bioactivity.

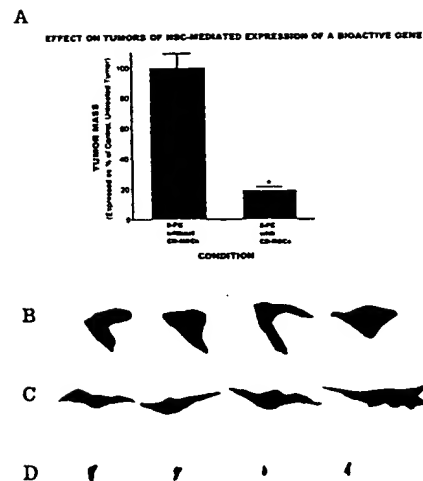


**Fig. 7.** Expression of a bioactive transgene (CD) delivered by NSCs is retained *in vivo* as assayed by reduction in tumor mass. The size of an intracranial glioblastoma populated with CD-NSCs in an adult nude mouse treated with 5-FC was compared with that of tumor treated with 5-FC but lacking CD-NSCs. These data, standardized against and expressed as a percentage of a control tumor populated with CD-NSCs receiving no treatment, are presented in the histograms in A. These measurements were derived from measuring the surface area of tumors (like those in Figs. 2–5), representative camera lucidas of which are presented in B–D. Note the large areas of a control non-5-FC-treated tumor containing CD-NSCs (B) and a control 5-FC-treated tumor lacking CD-NSCs (C) as compared with the dramatically smaller tumor areas of the 5-FC-treated animal who also received CD-NSCs (D) ( $\approx 80\%$  reduction as per the histogram in A; \*,  $P < 0.001$ ), suggesting both activity and specificity of the transgene. The lack of effect of 5-FC on tumor mass when no CD-bearing NSCs were within the tumor (C) was identical to the effect of CD-NSCs in the tumor without the gene being used (B).

## Discussion

Transplanted NSCs have recently been recognized for their remarkable ability to migrate throughout the CNS, become normal constituents of the host cytoarchitecture, and disseminate bioactive molecules and retroviral vectors (3–10). Intriguingly, this migratory ability emulates the invasive spread of some brain tumors, e.g., gliomas. Here, we show that an unanticipated benefit of the directed, migratory capacity of transgene-expressing NSCs, including of human origin, may be to target invasive primary brain tumors (also including of human origin) that have proven refractory to current treatments (1, 2). Most gene therapy strategies employ viral vectors to deliver genes directly to tumor cells *in vivo*; however, the distribution of genes to the extensive regions and large numbers of cells in need of attack has been limited. The present study demonstrates the ability of NSCs to migrate expeditiously throughout a tumor mass and, presumably drawn by the degenerative or inflammatory environment created at the infiltrating tumor edge, to “surround” the invading tumor border, all while continuing to express a bioactively relevant transgene. Moreover, the foreign gene-expressing NSCs seem to follow or “track”—virtually ride “piggy-back” upon—those aggressively infiltrating tumor cells escaping into normal tissue. Although the NSCs migrate freely through the tumor, the normal adult brain parenchyma seems to present a less permissive environment for their migration, except when NSCs (even at sites distant from the tumor) travel in a directed fashion through normal adult CNS tissue to target the main tumor mass as well as individual infiltrating, tumor cells. The practical implication is that NSCs might actually “seek out” tumor foci that may have migrated undetected far away from the main tumor mass, not an uncommon occurrence with glioblastoma. Such behaviors are not displayed by cells of nonneural origin (15). Indeed, targeting may be so powerful that even NSCs injected into

the systemic circulation may preferentially populate intracerebral gliomas.

Hence, NSCs evince extensive tropism for the tumor itself or for the degenerating CNS it engenders. That the tumor itself elaborates at least some of the tropic cues is suggested by our *in vitro* studies in which glioma cells in culture, isolated from surrounding brain, prompted NSCs to migrate, by both contact and non-contact-mediated factors. Alternatively, or in addition, tropic cytokines may be released by extensively damaged normal tissue. That minor CNS destruction alone could not prompt the dramatic migration seen *in vivo* was suggested by NSC transplants into "mock" tumor bearing animals, i.e., animals in which a needle was inserted to emulate the tissue damage of establishing an experimental tumor bed but without the actual implantation of glioblastoma cells; NSCs did not migrate toward the site in this circumstance. Nevertheless, in other previously reported experimental situations in which significant neuronal death was rendered (13), NSC differentiation was altered by apparent trophic influences. Therefore, the signals to which the NSCs are responding are most likely complex, from multiple sources, and representing a "mixture" of attractants, adhesion and substrate molecules, chemokines, etc. Of broader biological significance, these findings suggest that migration can be unexpectedly extensive, even in adult brain and along nonstereotypical routes, if pathology (as modeled here by tumor) is present.

Having documented this powerful tropic interaction between NSCs and intracranial pathology, we believe that exogenous NSCs, genetically engineered *ex vivo* and strategically implanted, may provide a "platform" for the dissemination of therapeutic genes and/or gene products to previously inaccessible infiltrating tumor cells. As suggested in our CD/5-FC prodrug paradigm, NSCs were able to express a bioactive transgene *in vivo* to effect a significant biologically relevant read-out (dramatic reduction in tumor burden). Cytotoxic 5-fluorouracil and its toxic metabolites can readily diffuse into surrounding tumor cells giving CD an impressive

"bystander" effect; as little as 2% of the tumor mass containing CD-expressing cells may generate significant oncolysis (22). Indeed, NSCs engineered to express CD are attractive as molecular pumps because they can generate agents that kill tumor cells yet undergo self-elimination should the NSCs themselves become mitotic. This prototypical genetic strategy represents one of many potential approaches to treating brain tumors with migratory genetically engineered NSCs. Other candidates include genes encoding: proteins that induce differentiation of neoplastic cells and/or their signal-transduction mediators; cell cycle modulators; apoptosis-promoting agents; anti-angiogenesis factors; immune-enhancing agents (23); fusion agents; and oncolytic factors (24). That these same engraftable migratory NSCs have been demonstrated to serve as intracerebral viral vector producer cells (10) may allow "extended" delivery of lethal viral-mediated genes to larger numbers of tumor cells in broader regions of brain. Instilled into the resection or biopsy cavity, or applied intermittently into or near the tumor mass or suspicious tissue or into cerebral ventricles, engineered NSCs could be used in conjunction with other interventions. An NSC-based strategy—responding to the altered biology of the abnormal adult brain and by virtue of their unique inherent biology—may both optimize present approaches and make feasible new ones for more effectively, selectively, and safely targeting genes and vectors to refractory, migratory, invasive brain tumors.

We thank M. Sena-Esteves for help with generating retrovirus vectors. This work is supported by National Institutes of Health Grants HD07466 and CA86768 (to K.S.A.) and CA69246 (to X.O.B.), the Toennies Stiftung (to N.G.R.), the Deutsche Forschungsgemeinschaft (to U.H.), National Institutes of Health Grants NS33852 and NS34247, and the Brain Tumor Society (to E.Y.S.). Portions of this work were presented at the Second Conference on Cellular and Molecular Treatments of Neurological Diseases, Cambridge, MA, October 10, 1998. This work is dedicated to the memory of Dr. James A. Galambos.

- Black, P. M. & Loeffler, J., eds. (1997) *Cancer of the Nervous System* (Blackwell, Oxford).
- Kramm, C. M., Sena-Esteves M., Barnett F. H., Rainov, N. G., Schuback, D. E., Yu, J. S., Pechan, P. A., Paulus, W., Chiocca, E. A. & Breakefield, X. O. (1995) *Brain Pathol.* 5, 345–381.
- Gage, F. H. (2000) *Science* 287, 1433–1438.
- McKay, R. (1997) *Science* 276, 66–71.
- Flax, J. D., Aurora, S., Yang, C., Simonin, C., Wills, A. M., Billingham, M. J., Sidman, R. L., Wolfe, J. H., Kim, S. U. & Snyder, E. Y. (1998) *Nat. Biotech.* 16, 1033–1039.
- Weiss, S., Reynolds, B. A., Vescovi, A. L., Morshead, C. & Van der Kooy, D. (1996) *Trends Neurosci.* 19, 387–393.
- Alvarez-Buylla, A. & Temple, S. (1998) *J. Neurobiol.* 36, 105–314.
- Snyder, E. Y., Taylor, R. M. & Wolfe, J. H. (1995) *Nature (London)* 374, 367–370.
- Yandava, B. D., Billingham, L. L. & Snyder, E. Y. (1999) *Proc. Natl. Acad. Sci. USA* 96, 7029–7034.
- Lynch, W. P., Sharpe, A. H. & Snyder, E. Y. (1999) *J. Virol.* 73, 6841–6851.
- Kruse, C. A., Molleston, M., Parks, E. P., Schiltz, P. M., Kleinschmidt-DeMasters, B. K. & Hickey, W. F. (1994) *J. Neurooncol.* 22, 191–200.
- Aboudy-Guterman, K. S., Pechan, P. A., Rainov, N. G., Sena-Esteves, M., Snyder, E. Y., Wild, P., Schraner, E., Tobler, K., Breakefield, X. O. & Fraefel, C. (1997) *NeuroReport* 8, 3801–3808.
- Snyder, E. Y., Yoon, C. H., Flax, J. D. & Macklis, J. D. (1997) *Proc. Natl. Acad. Sci. USA* 94, 11663–11668.
- Yuan, F., Salehi H. A., Boucher Y., Vasthary U. S., Tuma R. F. & Jain R. K. (1994) *Cancer Res.* 54, 4564–4568.
- Tamiya, T., Wei, M. X., Chase, M., Ono, Y., Lee, F., Breakefield, X. O. & Chiocca, E. A. (1995) *Gene Ther.* 2, 531–538.
- Morgenstern, J. P. & Land, H. (1990) *Nucleic Acids Res.* 18, 3587–3596.
- Sena-Esteves, M., Saeki, Y., Camp, S., Chiocca, E. A. & Breakefield, X. O. (1999) *J. Virol.* 73, 10426–10439.
- Pear, W. S., Nolan, G. P., Scott, M. L. & Baltimore, D. (1993) *Proc. Natl. Acad. Sci. USA* 90, 8392–8396.
- Ko, L., Koestner, A. & Wechsler, W. (1980) *Acta Neuropathol.* 51, 23–34.
- Topf, N., Worgall, S., Hackett, N. R. & Crystal, R. G. (1998) *Gene Ther.* 5, 507–513.
- Mullen, C., Kilstrup, M. & Blaese, R. M. (1992) *Proc. Natl. Acad. Sci. USA* 89, 33–37.
- Huber, B. E., Austin, E. A., Richards, C. A., Davis, S. T. & Good, S. (1994) *Proc. Natl. Acad. Sci. USA* 91, 8302–8306.
- Benedetti, S., Pirola B., Pollo, B., Gagrassi, L., Briuzzone, M. G., Rigamonti, D., Galli, R., Sella, S., DiMeco, R., DeFraja, C., et al. (2000) *Nat. Med.* 6, 447–450.
- Herrlinger, U., Woiciechowski, C., Aboudy, K. S., Jacobs, A. H., Rainov, N. G., Snyder, E. Y. & Breakefield, X. O. (2000) *Mol. Ther.* 1, 347–357.

16' 03 16:09/ST. 16:00/NO. 4862209877 P. 1  
International weekly journal of science

**\$10.00**

**Stem cells**  
Nature Insight

\*\*\*\*\*5-DIGIT 55455  
02000

AUTO \*\*\*\*\*  
55455UNIVERSITY OF MINNESOTA  
UNIVERSITY OF MINNESOTA  
BIO MED B 325A DIEHL HALL  
505 EXESSEX ST  
MINNEAPOLIS MN 55455-0350 00/002/0128

Univ. of Minn.  
Bio-Medical  
Library

11 19 01

spotlight on Cambridge, UK

# The development of neural stem cells

Sally Temple

© NOTICE: THIS MATERIAL MAY BE PROTECTED BY COPYRIGHT LAW (TITLE 17 U.S. CODE)

Center for Neuropharmacology and Neuroscience, Albany Medical College, 47 New Scotland Avenue, Albany, New York 12208, USA  
(e-mail: temples@mail.amc.edu)

The discovery of stem cells that can generate neural tissue has raised new possibilities for repairing the nervous system. A rush of papers proclaiming adult stem cell plasticity has fostered the notion that there is essentially one stem cell type that, with the right impetus, can create whatever progeny our heart, liver or other vital organ desires. But studies aimed at understanding the role of stem cells during development have led to a different view — that stem cells are restricted regionally and temporally, and thus not all stem cells are equivalent. Can these views be reconciled?

**T**he discovery of neural stem cells was rooted in classic studies of haematopoiesis and of invertebrate neural development, which inspired examination of single neural progenitor cells. (In this review, I will use the term 'progenitor cell' to refer to all classes of immature, proliferating cells. Neural stem cells are a subtype of progenitor cells in the nervous system that can self-renew and generate both neurons and glia.) The early studies led to the isolation of stem-like cells from the embryonic mammalian central nervous system (CNS)<sup>1-4</sup> and the peripheral nervous system (PNS)<sup>5</sup>. Since then, stem cells have been isolated from many regions of the embryonic nervous system, indicating their ubiquity (Fig. 1a). After the discovery of neural stem cells in the embryo, the first isolation of stem-like cells from adult brain<sup>6,7</sup> began yet another chapter of neuroscience. Adult neural stem cells have now been found in the two principal adult neurogenic regions, the hippocampus and the subventricular zone (SVZ), and in some non-neurogenic

regions, including spinal cord<sup>8-10</sup> (Fig. 1a). These pioneering studies provided a cellular mechanism for adult neurogenesis, which was well-established in birds and becoming accepted in mammals, and raised the possibility that the most intractable of tissues — the CNS — might have regenerative powers.

Markers that define CNS stem cells are only now being developed<sup>11-14</sup>. Hence, they are usually identified retrospectively on the basis of their behaviour after isolation. In adherent cultures, CNS stem cells produce large clones containing neurons, glia and more stem cells; they can also be cultured as floating, multicellular neurospheres<sup>8-10</sup>. PNS neural crest stem cells express the low-affinity neurotrophin receptor p75 (ref. 5), and grow as adherent clones containing peripheral neurons and glia, smooth muscle cells and more stem cells<sup>15</sup>.

This review summarizes what we currently know about stem cells in the developing nervous system, and evaluates the idea that embryonic neural stem cells are heterogeneous and restricted. Studies that indicate broad plasticity of adult

**Figure 1** The location of neural stem cells.

**a**, The principal regions of the embryonic and adult nervous system from which neural stem cells have been isolated<sup>6,10,63-65</sup>. **b**, Three models describing stem cells in the vertebrate neural plate. All neural plate cells are stem cells (left), or stem cells are a minor population that is evenly distributed (middle) or located in particular regions such as the midline and lateral edges (right). Factors such as bone morphogenetic proteins (BMPs), Noggin, retinoids, Sonic hedgehog and fibroblast growth factors (FGFs), which provide anterior-posterior (A-P) and dorsal-ventral (D-V) patterning information, may regionalize stem cells<sup>24</sup>.

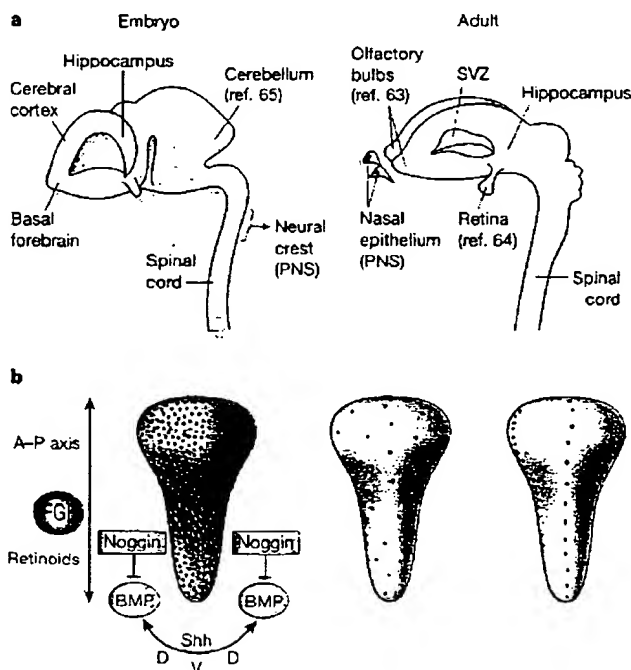
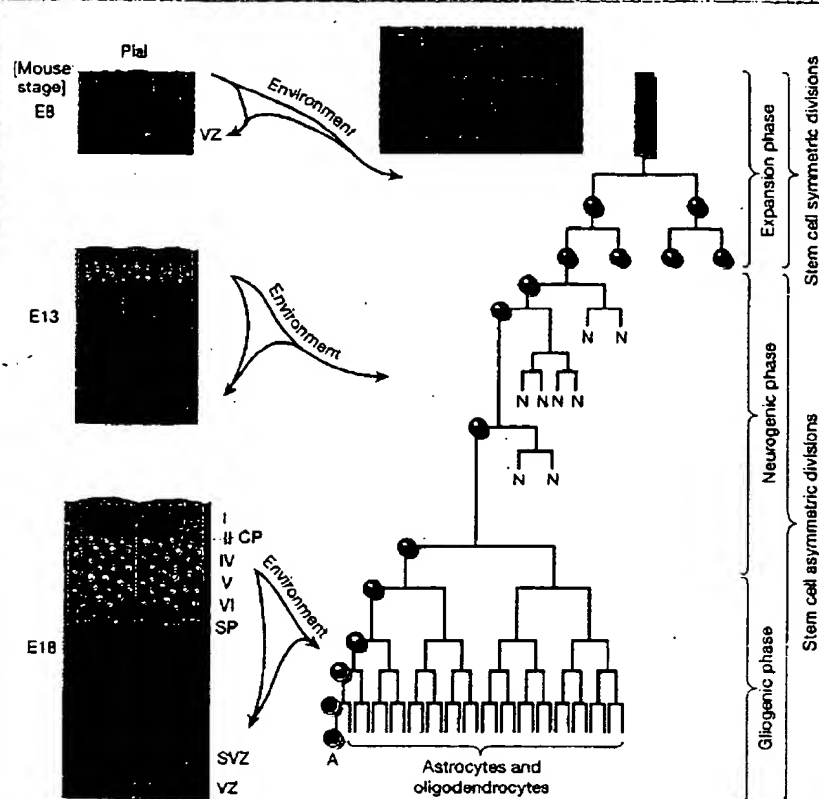




**Figure 2** The development of stem cells in the mammalian CNS. Alignment of the developmental axes, showing the behavior of stem cells derived from multipotent neural stem cells in the following period of time. Stem cells change even into fully differentiated cells and colonize the brain. The radial glial cells are columnar cells that line the ventricular surfaces during the early cell division. In the young animals have migrated above the germinal ventricular zone (VZ) radial glia continue to contact both ventricle and pia guiding neuronal migration and a second germinal zone arises, the subventricular zone (SVZ). By postnatal ages, radial glia have transformed into astrocytes and the VZ also disappears, but the SVZ remains in adulthood in some areas. Stem cells present in the early cerebral cortical neuroepithelium divide symmetrically first, and then asymmetrically to generate differentiated progeny. Neurons are produced first, and migrate along radial glia up towards the pia surface where they settle in the subplate (SP) and the cortical plate (CP). After the neurogenic period, the stem cell makes glial progenitor cells that proliferate largely in the SVZ. By birth, the stem cell has developed and has different characteristics, such as responses to growth factors, to those of the original embryonic stem cell. Stem cell development might be driven by a combination of intrinsic temporal programmes and extracellular signals from the changing environment of the developing brain.



stem cells are also discussed. By examining these two different aspects of stem cell research, future directions of exploration are highlighted that might help explain this apparent dichotomy.

### Stem cells at the beginning of the nervous system

Many fundamental questions regarding specification of early neural stem cells remain unanswered. When the neural plate first emerges, does it consist solely of stem cells or does it include both stem cells and restricted progenitor types (Fig. 1)? Analysis of adherent clone production suggests stem cells are prevalent at early stages. In spinal neural tube from embryonic day 8 (E8) rat, over 50% of the viable cells at 24 hours are stem cells<sup>16,17</sup>. In telencephalon from E10 mouse, estimates of stem cells range from 5 to 20% (refs 4, 18, 19). Most of the premigratory neural crest consists of stem cells<sup>20</sup>.

But the frequency of stem cells declines rapidly, diluted by the production of restricted progenitors and differentiated cells; for example, in spinal cord it drops to 10% at E12 and 1% at postnatal day 1 (P1)<sup>16,17</sup>. Notably, stem cells seem to be much rarer when neurosphere production is used as the assay: only 0.3% of E8.5 mouse anterior neural plate cells make neurospheres<sup>21</sup>. Perhaps neurosphere-generating cells are a subpopulation of early stem cells, or perhaps stem cells are more prevalent in spinal cord than anterior regions at this age.

How are neural stem cells initially specified? The stem cell could be the default state or, alternatively, stem cells might be induced. Pluripotent embryonic stem cells can produce a primitive type of neural stem cell when grown in isolation, but only 0.2% of embryonic stem cells generate neurospheres<sup>22</sup>. Although this study suggests that there is a default pathway for acquiring the stem cell state, the low frequency indicates that it may be normally enhanced by inductive mechanisms.

If stem cells are, or rapidly become, a subset of early neural progenitor cells *in vivo*, how are they distributed (Fig. 1)? Without

specific markers, important questions regarding stem cell frequency and location *in vivo* remain open.

The early, widespread presence of stem cells in the embryonic nervous system raises another important issue of their role in development. Given their prolific, multipotent nature *in vitro*, they are likely to be principal progenitors *in vivo*, but this remains to be shown directly. For example, it is possible that early restricted neuroblasts rather than stem cells might generate the preponderance of neurons. Clonal studies suggest that most glia, both astrocytes and oligodendrocytes, originate from stem cells<sup>9,18,19</sup>, signifying their importance for gliogenesis. In fact, as described below, there may be an intimate association between glia and the neural stem cell state.

### Neural stem cells acquire positional information

Patterning of the body axis occurs through signalling systems that impart positional information. For example, gradients of signalling molecules can regionally specify a population of progenitor cells if the cells respond differently to different concentrations of the signal<sup>23</sup>. In the nervous system, the salient patterning in anterior-posterior and dorsal-ventral axes occurs early, concomitantly with neural induction (Fig. 1)<sup>24</sup>.

Do both stem cells and restricted progenitor cells exhibit regionalization, or do stem cells remain unspecified, maintaining their plasticity? In *Drosophila* and grasshopper, each stem cell-like neuroblast has a unique identity based on its position in the neuroectoderm<sup>25</sup>. In vertebrates, this question is just beginning to be explored. Neurospheres generated from different CNS regions express region-appropriate markers, indicating that the original stem cells were indeed regionally specified<sup>26</sup>. Regulatory sequences control region-specific expression of the transcription factor Sox2, so that expression is seen in telencephalic but not spinal cord stem cells<sup>27</sup>.

## insight review articles

**Table 1 Summary of transplantation studies assessing stem and progenitor cell behaviour**

Donor	Host site	CNS incorporation	Differentiation	References
<b>Embryonic stem cells</b>				
Mouse ES cells or ES cell-derived neurospheres	Blastocyst	Incorporation into all embryonic tissues	Both glutamate- and GABA-mediated neurons in cortex	50,51
Mouse ES cell-derived neural precursors	E16–18 rat LV	Widespread incorporation	Neurons, oligodendrocytes and astrocytes	52
<b>Embryonic neural cells</b>				
E9.5 and E14.5 forebrain-derived neurospheres	Blastocyst or morula	No aggregation		22
EGF-generated neurosphere cells from E14 mouse fore- and midbrain	E15 rat LV	Fore- and midbrain structures	Astrocytes	53
Fetal human brain-derived neurospheres or primary cells	E17–18 rat or P0 mouse LV	Widespread incorporation in the brain	Neurons (projection), oligodendrocytes and astrocytes	54,55
E10.5 mid/hindbrain	E13.5 MGE	Dispersed into forebrain	Site-specific neuronal differentiation	31
E12–14 mouse forebrain	E15 to P1 rat LV	Into forebrain and midbrain; incorporation and migration reduced as host age increases	Site-specific neuronal differentiation	56,57
E13.5 mid/hindbrain	E13.5 LGE or MGE	No integration into forebrain		31
E36 ferret cortex (making layer 4)	E30 ferret (making layer 6)	Neocortex and hippocampus	Layers 2–5; no transplanted cells in layer 6	29
	P2 (making 2/3)	Neocortex and hippocampus	Layer 2/3 neurons	
<b>Early postnatal</b>				
Postnatal mouse SVZ cells	E15 mouse LV	Septum, thalamus, hypothalamus and inferior colliculus; not cortex or hippocampus	No principal projection neurons	32
Neonatal mouse SVZ neurospheres	Chick embryo	Migrate in isolation	Neural crest derivatives	46
Neonatal mouse SVZ cells	Chick embryo	Chain migration in the neural crest pathway	Progenitors and neurons; not neural crest phenotypes	46
	Neonatal striatum	Migration	Neuronal precursors and olfactory bulb neurons	58
P0–5 mouse SVZ cells	Adult striatum	Some migration	Olfactory bulb interneurons	59
<b>Adult</b>				
Mouse forebrain neurospheres	Blastocyst or morula	No aggregation		22
	Mouse morula or chick embryo	Rare neural chimeras	Cell types not reported	60
Mouse SVZ neurospheres	Chick embryo	Migrate as isolated cells	Phenotypes of neural crest derivatives	46
Mouse SVZ cells	Chick embryo	Cells die		46
	Adult mouse striatum	Minimum migration	Some neurons, mostly astrocytes in striatum	61
	Adult olfactory bulb	Extensive migration	Olfactory bulb neurons	61
Cultured rat hippocampal progenitors	Adult rat hippocampus	Migrate	Neurons in granule cell layer of dentate gyrus	42, 62
	Adult rat rostral migratory stream	Migrate to olfactory bulb	Neuroblasts and olfactory neurons	42
	Adult rat cerebellum	Incorporation	No neurons	42
FGF-responsive rat spinal cord progenitors	Adult hippocampus	Broad dispersion	Hippocampal granule neurons	41
	Adult spinal cord	Broad dispersion	No neurons	41

These studies indicate stage-dependent restrictions in the potential of donor progenitor populations (which include some neural stem cells). They also emphasize the impact of interaction between implanted cells and the host environment. Different treatments of stem and progenitor cells *in vitro* can significantly alter their behaviour after implantation. EGF, epidermal growth factor; ES, embryonic stem; FGF, fibroblast growth factor; LGE/MGE, lateral/medial ganglionic eminence; LV, lateral ventricle.

In addition, stem cells isolated from different neural regions generate region-appropriate progeny. Spinal cord stem cells generate spinal cord progeny<sup>17</sup>. Basal forebrain stem cells cultured at clonal density generate significantly more GABA ( $\gamma$ -amino butyric acid)-containing neurons, which are characteristic of basal regions, than dorsal stem cells cultured under identical conditions<sup>19</sup>. PNS neural crest stem cells, which arise at the lateral edges of the neural plate, express distinct genes and generate progeny distinct from those of CNS stem cells<sup>15,28</sup>. Hence, vertebrate stem cells seem to be positionally specified.

### Neural stem cells acquire temporal information

Different neural cell types arise in a precise temporal order that is characteristic for a particular region and species. In general, CNS and PNS neurons arise before glia, and specific types of each cell have specific birthdates. Timing seems to be encoded in progenitor cells, so that besides positional information they have 'temporal information', which is seen as stage-dependent changes in progenitor cells (Table 1). Thus, late-embryonic ferret cortical progenitor cells

cannot make cells appropriate for younger stages when transplanted into early cerebral cortex<sup>29</sup>. Rat cortical progenitors become restricted in their ability to generate limbic system-associated membrane protein (LAMP)-positive limbic cortical progeny after E14 (ref. 30). Mid/hindbrain progenitor cells are unable to generate telencephalic phenotypes after E13.5 in mouse<sup>31</sup>. SVZ cells can no longer make projection neurons by birth<sup>32,33</sup>, and retinal progenitor cells seem to be similarly restricted temporally<sup>34,35</sup>.

Stem cells are a minor component of the progenitor population in these studies, but experiments indicate that they also exhibit stage-dependent changes in potential. Some early neural tube cells produce both CNS and PNS stem cells, suggesting that there is a common progenitor for two separate stem cell lineages with more restricted potentials<sup>28</sup>. Each of these lineages also changes over time. CNS stem cells undergo repeated asymmetric cell divisions, first producing neurons then glia<sup>14</sup>, thus reproducing the normal neuron–glia order (Fig. 2). Moreover, they have an active role in this process by altering their intrinsic properties. Thus, stem cells from earlier stage cortices



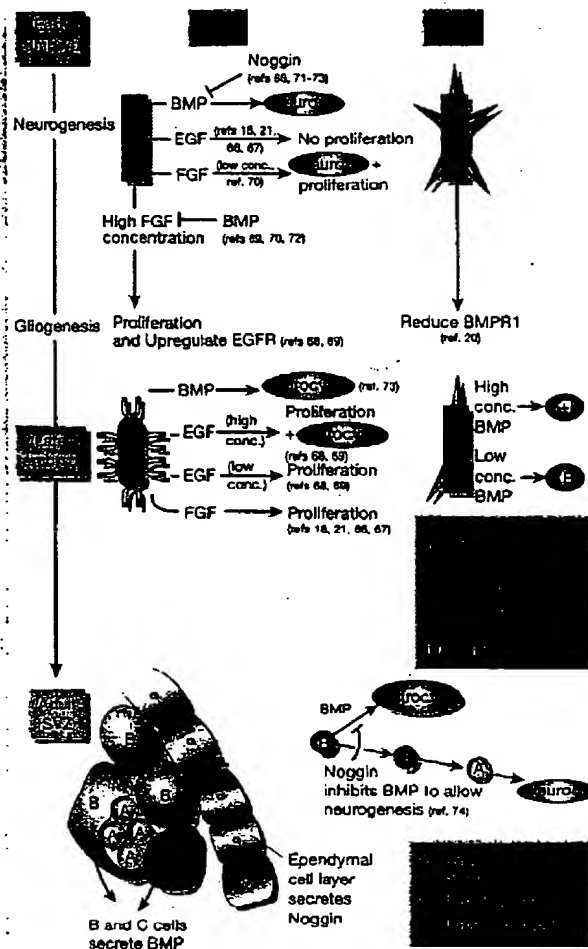


**Figure 3** Stem cells after their responses to growth factors over time. Central and peripheral nervous system (neural crest) stem cells extracted from different ages show differing responses to application of the same growth factor. Changes in levels of growth factor receptors have been observed. In addition, stem cells exhibit different responses to growth factors applied at different concentrations. BMP, bone morphogenetic protein; EGF, epidermal growth factor; EGFR, EGF receptor; FGF, fibroblast growth factor.

produce more neurons and have a lower tendency to produce glia than those from later stages.

Temporal specification of stem cell populations also occurs in the PNS. Mouse neural crest stem cells isolated from the rat neural tube have been compared with later stem cells isolated prospectively from E14 sciatic nerve after transplantation into different sites of the chick embryo<sup>20</sup>. Early neural crest stem cells generate significantly more neurons than later stage cells: like CNS stem cells, their neurogenic capacity declines with stage. Furthermore, the range of neurons generated by late neural crest stem cells is more restricted. Early transplants that are highly enriched for neural crest stem cells but contain some restricted sensory progenitor cells can generate dorsal root ganglion (DRG) sensory neurons, and adrenergic and cholinergic autonomic neurons. By contrast, older-stage neural crest stem cells made no DRG neurons, only rare adrenergic sympathetic neurons, but they could generate cholinergic autonomic neurons.

Stem cells also undergo phenotypic changes as germinal zones develop (Fig. 2). It has been suggested recently that some radial glia

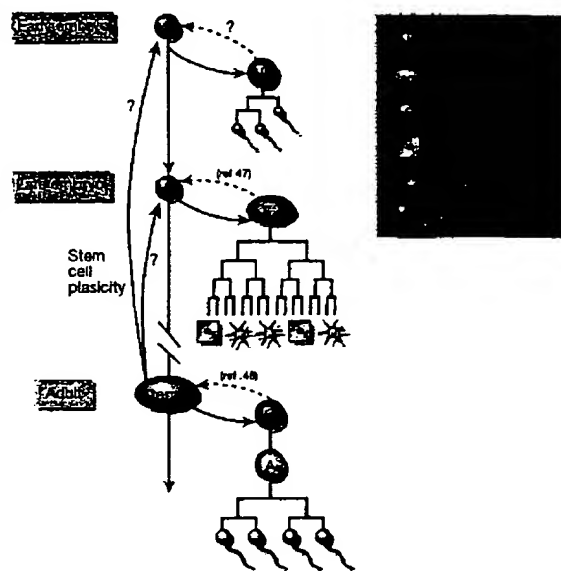


**Figure 4** Can the stem cell lineage be reversed? Evidence indicates that neural stem cell progeny can reacquire stem cell properties. An important issue is whether adult stem cells can revert to an earlier embryonic state, with a wider potential.

present at mid-gestation might be stem cells (reviewed in ref. 36). This idea is appealing, given that radial glia are thought to be neurogenic precursors in adult canary brains, and that astrocytes, the lineal descendants of radial glia, have stem cell properties in the adult mammalian SVZ<sup>37</sup>.

Developmental changes in stem cells — for example, in their potential and phenotype — are accomplished by, and perhaps driven by, changes in their growth factor responsiveness (Fig. 3; and see accompanying reviews by Spradling and colleagues, pages 98–104, and Weissman and colleagues, pages 105–111). Thus signalling molecules, such as fibroblast growth factors, bone morphogenetic proteins and Noggin, can influence neural stem cells from neural induction through adulthood, but their responses to these factors vary with stage.

The mechanisms underlying temporal changes in neural stem cells are not understood. The lineage trees of mouse CNS stem cells are remarkably similar to those of invertebrates<sup>38</sup>. *Drosophila* CNS neuroblasts express sequentially the transcription factors Hunchback, Krüppel, POU-domain genes 1 and 2, Castor and grainyhead, which specify the production of different neurons at different times<sup>39,40</sup>. The expression sequence may be driven by a cell-intrinsic clock<sup>40</sup>. Perhaps similar intrinsic timing mechanisms, combined with environmental input, temporally specify mammalian CNS stem cells. Growth factor concentrations vary during development and neural stem cells respond differently to different concentrations of the same molecule (Fig. 3). Hence, it is tempting to speculate that, just as positional information can be imparted by spatial gradients of signals<sup>23</sup>, temporal information might be imparted by temporal gradients of signalling molecules.

#### Examining the plasticity of adult stem cells

If stem cells undergo developmental changes, adult stem cells are likely to differ from those in the embryo and to be regionally and temporally restricted.

One way to examine the plasticity of adult neural stem cells is to transplant them directly into the developing embryo and examine

# insight review articles

Box 1

## Potential therapeutic uses of stem cells to repair the nervous system

Stem cells are under active consideration as a source of donor tissues for neuronal cell therapy<sup>75</sup>.

**Parkinson's disease.** The requirement is to generate cells that synthesize and release dopamine for implantation into the dopamine-depleted striatum. For this therapy to be effective, it is unknown whether these cells must also mature into projection neurons with synaptic host connections — a process that is required for optimal effects of embryonic nigral grafts.

**Huntington's disease.** If we can control differentiation into mature neuronal phenotypes then many other diseases that involve loss of specific neuronal types, such as the striatal medium spiny projection neurons lost in Huntington's disease, might be suitable for transplantation of neurons expanded from stem cell sources.

**Spinal cord injury.** Stem cells may be able to repopulate the site of injury, provide a substrate for axon growth across the transection, and block syrinx progression. Each of these effects has been found with primary embryonic cells; however, studies using stem or immortalized precursors are still preliminary.

**Stroke.** Stem cells and immortalized precursors may be able to migrate through the central nervous system and repopulate sites of ischaemia. In spite of rather limited evidence from animal studies, clinical trials of this strategy are already underway.

**Multiple sclerosis.** Oligodendrocyte lineages are better characterized than neuron lineages, and oligodendrocyte precursors can differentiate and provide a functional remyelination of axons after focal experimental demyelination. For application in multiple sclerosis, the main problem is how to stimulate the migration of such cells to diverse sites of demyelination that occur sporadically in the human disease. Notwithstanding the potential applications of oligodendrocyte lineages in several diseases, many key technical problems remain to be resolved.

**Sources.** If we select early embryonic stem cells, then the number of transformations and the complexity of signals required to achieve a specific differentiated phenotype may prove prohibitive; instead, it may be easier to control the phenotypic differentiation of developing neuronal precursors, but that might in turn limit their capacity for expansion. Adult-derived cells may circumvent both ethical and immunological constraints, but their plasticity for expansion and differentiation remains to be established. Cross-lineage transformation offers a new prospect for a more flexible source, in particular to derive autografts from patients themselves. A further advance is that precursor cells are less immunogenic than primary embryonic neurons in xenografts, highlighting a way to overcome one of the main difficulties of transplantation from non-human donors.

**Expansion.** Neuronal stem cells from species other than mice seem to senesce on repeated passage, with only limited potential for expansion. Conversely, if not fully differentiated at the time of implantation, there is always the possibility of tumour formation — a problem that is still not resolved for either embryonic stem cells or immortalized precursors.

**Differentiation.** The biggest single problem still to be solved is how to direct and control the differentiation of specific target phenotypes required for replacement and repair in each disease. Selection of appropriate starting cells by embryonic regional dissection and stage of development, as well as diverse parameters of *in vitro* manipulation, are likely to be crucial factors in directing appropriate phenotypic differentiation. Failure can lead not only to a lack of benefit but also to significant side-effects from proliferation of non-neuronal phenotypes.

All these problems can be solved, but it will require more than a single breakthrough to transform the potential attributed to stem cells into a realistic clinical strategy for cellular repair.

what neural cell types they produce; this still remains to be done. Emerging methods for the prospective isolation of adult CNS stem cells<sup>11–14</sup> should facilitate this important experiment. Experiments using culture-expanded adult CNS stem cells indicate that there is some plasticity in adult environments (Table 1). For example, adult spinal-cord-derived stem cells, which do not normally make neurons, can make interneurons if injected into the adult hippocampus<sup>41</sup>, and adult hippocampal-derived stem cells can make olfactory interneurons after transplantation to the SVZ<sup>42</sup>. As yet, however, there is no direct evidence that adult-derived stem cells can make the types of projection neuron that are normally generated in the embryo.

Given the vital gaps in our understanding of adult neural stem cells, we cannot yet conclude that they are highly plastic. Evidence that they can generate different somatic cell types is limited, and may be restricted to rare events or rare cells<sup>43–45</sup>. In considering the two different ideas raised at the beginning of this review, there may be in fact no dichotomy. Most neural stem cells might be regionally and temporally specified. There may also be rare stem cells present in the nervous system, perhaps not even of neural origin, that have greater plasticity, at least in terms of producing diverse somatic cell types<sup>43</sup>.

### Reversing the stem cell lineage

If stem cells are restricted, can these restrictions be reversed (Fig. 4)? For example, can an adult stem cell re-acquire the ability to generate cell types normally made in the embryo? A study has indicated that culturing SVZ stem cells as neurospheres expands their potential and allows them to generate PNS progeny after injection into chick neural crest pathways<sup>46</sup>. Furthermore, descendants of neural stem cells may

be able to revert. Optic nerve O2A progenitor cells, which normally produce solely glia, can be converted *in vitro* into multipotent, neurosphere-generating stem cells<sup>47</sup>. In the adult SVZ, both type B stem cells and their progeny, type C progenitor cells, can make neurospheres *in vitro*. Moreover, type C cells are stimulated to convert to stem cells by epidermal growth factor<sup>48</sup>. In the postnatal chick retina after damage, Muller radial glia, which are maintained throughout life, can re-enter the cell cycle, re-express retinal progenitor cell markers and generate new neurons and glia<sup>49</sup>.

If environmental factors can enhance the acquisition of neural stem cell fates, or increase the plasticity of stem cells, this may be of enormous benefit therapeutically, as indicated in Box 1.

### Future studies

As regions of the embryo are patterned and development unfolds, neural stem cells may be an essential mediator of developmental signals, acquiring a changing repertoire of gene expression, morphology and behaviour. Despite differences in the properties of stem cells isolated from different regions and at different times, they still self-renew. Self-renewal can therefore be considered as the propagation of stem cells, rather than the production of exactly the same type of cell.

It will be important to examine how developmental signals, both spatial and temporal, specify changes in neural stem cells. Markers for neural stem cells will allow their selection from different stages and regions to examine their potential after transplantation into the embryo or adult, and a comparison of their gene expression. Such explorations will help identify essential mediators of stem cell self-renewal, and genes that determine production of different types of progeny. Markers will also help solve the tantalizing issue of which cells *in vivo* are stem cells.

Although research to identify adult sources of highly plastic stem cells for therapeutic use will continue, it seems likely that most neural-generating stem cells might be specified during development. In that case, we must explore this diversity to understand how different neural cells are, and can be, made.

1. Temple, S. Division and differentiation of isolated CNS blast cells in microculture. *Nature* 340, 471-473 (1989).
2. Cattaneo, E. & McKay, R. Proliferation and differentiation of neuronal stem cells regulated by nerve growth factor. *Nature* 347, 762-765 (1990).
3. Reynolds, B. A., Tetzlaff, W. & Weiss, S. A multipotent EGF-responsive striatal embryonic progenitor cell produces neurons and astrocytes. *J. Neurosci.* 12, 4365-4374 (1992).
4. Kilpatrick, T. J. & Bartlett, P. F. Cloning and growth of multipotential neural precursors: requirements for proliferation and differentiation. *Neuron* 10, 255-263 (1993).
5. Stemple, D. L. & Anderson, D. J. Isolation of a stem cell for neurons and glia from the mammalian neural crest. *Cell* 71, 973-985 (1992).
6. Reynolds, B. A. & Weiss, S. Generation of neurons and astrocytes from isolated cells of the adult mammalian central nervous system. *Science* 255, 1707-1710 (1992).
7. Lois, C. & Alvarez-Buylla, A. Proliferating subventricular zone cells in the adult mammalian forebrain can differentiate into neurons and glia. *Proc. Natl Acad. Sci. USA* 90, 2074-2077 (1993).
8. McKay, R. Stem cells in the central nervous system. *Science* 276, 66-71 (1997).
9. Rao, M. S. Multipotent and restricted precursors in the central nervous system. *Anat. Rec.* 257, 137-148 (1999).
10. Gage, F. H. Mammalian neural stem cells. *Science* 287, 1433-1438 (2000).
11. Capela, A. & Temple, S. A putative surface marker for adult mouse neural stem cells. *Soc. Neurosci. Abstr.* 24.19 <<http://sfn.scholarone.com/itin2000/>> (2000).
12. Kawaguchi, A. et al. Nestin-EGFP transgenic mice: visualization of the self-renewal and multipotency of CNS stem cells. *Mol. Cell. Neurosci.* 17, 259-273 (2001).
13. Uchida, N. et al. Direct isolation of human central nervous system stem cells. *Proc. Natl Acad. Sci. USA* 97, 14720-14725 (2000).
14. Nietze, R. L. et al. Purification of a pluripotent neural stem cell from the adult mouse brain. *Nature* 412, 736-739 (2001).
15. Anderson, D. J. et al. Cell lineage determination and the control of neuronal identity in the neural crest. *Cold Spring Harb. Symp. Quant. Biol.* 62, 493-504 (1997).
16. Kalyani, A., Hobson, K. & Rao, M. S. Neuroepithelial stem cells from the embryonic spinal cord: isolation, characterization, and clonal analysis. *Dev. Biol.* 186, 202-223 (1997).
17. Kalyani, A., Piper, D., Mujtaba, T., Lucero, M. T. & Rao, M. S. Spinal cord neuronal precursors generate multiple neuronal phenotypes in culture. *J. Neurosci.* 18, 7856-7868 (1998).
18. Qian, X. et al. Timing of CNS cell generation: a programmed sequence of neuron and glial cell production from isolated murine cortical stem cells. *Neuron* 28, 69-80 (2000).
19. He, W., Ingraham, C., Rising, L., Goderie, S. & Temple, S. Multipotent stem cells from the mouse basal forebrain contribute GABAergic neurons and oligodendrocytes to the cerebral cortex during embryogenesis. *J. Neurosci.* (in press).
20. White, P. M. et al. Neural crest stem cells undergo cell-intrinsic developmental changes in sensitivity to instructive differentiation signals. *Neuron* 29, 57-71 (2001).
21. Tropepe, V. et al. Distinct neural stem cells proliferate in response to EGF and FGF in the developing mouse telencephalon. *Dev. Biol.* 208, 166-188 (1999).
22. Tropepe, V. et al. Neural stem cell fate specification from embryonic stem cells. A primitive mammalian neural stem cell stage acquired through a default mechanism. *Neuron* 30, 65-78 (2001).
23. Wolpert, L. Positional information and pattern formation in development. *Dev. Genet.* 15, 485-490 (1994).
24. Altman, C. R. & Brivanlou, A. H. Neural patterning in the vertebrate embryo. *Int. Rev. Cytol.* 203, 447-482 (2001).
25. Skerch, J. B. At the nexus between pattern formation and cell-type specification: the generation of individual neuroblast fates in the *Drosophila* embryonic central nervous system. *BioEssays* 21, 922-931 (1999).
26. Tropepe, V., Hinojosa, S., Ekker, M. & van der Kooy, D. Neural stem cells and their progeny express region-specific genes in the developing CNS, but this expression is not irreversible and can be altered by local inductive cues. *Soc. Neurosci. Abstr.* 23.1 <<http://sfn.scholarone.com/itin2000/>> (2000).
27. Zappone, M. V. et al. Sox2 regulatory sequences direct expression of a  $\beta$ -geo transgene to telencephalic neural stem cells and precursors of the mouse embryo, revealing regionalization of gene expression in CNS stem cells. *Development* 127, 2367-2382 (2000).
28. Mujtaba, T., Mayer-Proschel, M. & Rao, M. S. A common neural progenitor for the CNS and PNS. *Dev. Biol.* 200, 1-15 (1998).
29. Desai, A. R. & McConnell, S. K. Progressive restriction in fate potential by neural progenitors during cerebral cortical development. *Development* 127, 2863-2872 (2000).
30. Barbe, M. F. & Levitt, P. The early commitment of fetal neurons to the limbic cortex. *J. Neurosci.* 11, 519-533 (1991).
31. Olsson, M., Campbell, K. & Turnbull, D. H. Specification of mouse telencephalic and mid-hindbrain progenitors following heterotopic ultrasound-guided embryonic transplantation. *Neuron* 19, 761-772 (1997).
32. Lim, D. A., Fishell, G. J. & Alvarez-Buylla, A. Postnatal mouse subventricular zone neuronal precursors can migrate and differentiate within multiple levels of the developing neuraxis. *Proc. Natl Acad. Sci. USA* 94, 14832-14836 (1997).
33. Alvarez-Buylla, A., Herrera, D. G. & Wichterle, H. The subventricular zone: source of neuronal precursors for brain repair. *Prog. Brain Res.* 127, 1-11 (2000).
34. Reh, T. A. & Levine, E. M. Multipotential stem cells and progenitors in the vertebrate retina. *J. Neurobiol.* 36, 206-220 (1998).
35. Livesey, F. J. & Cepko, C. L. Vertebrate neural cell-fate determination: lessons from the retina. *Nature Rev. Neurosci.* 2, 109-118 (2001).
36. Alvarez-Buylla, A., Garcia-Verdugo, J. M. & Tramontin, A. D. A unified hypothesis on the lineage of neural stem cells. *Nature Rev. Neurosci.* 2, 287-293 (2001).
37. Doetsch, F., Caille, L., Lim, D. A., Garcia-Verdugo, J. M. & Alvarez-Buylla, A. Subventricular zone astrocytes are neural stem cells in the adult mammalian brain. *Cell* 97, 703-716 (1999).
38. Shen, Q., Qian, X., Capela, A. & Temple, S. Stem cells in the embryonic cerebral cortex: their role in histogenesis and patterning. *J. Neurobiol.* 36, 162-174 (1998).
39. Brody, T. & Odenwald, W. F. Programmed transformations in neuroblast gene expression during *Drosophila* CNS lineage development. *Dev. Biol.* 226, 34-44 (2000).
40. Ishida, T., Pearson, B., Holbrook, S. & Doe, C. Q. *Drosophila* neuroblasts sequentially express transcription factors which specify the temporal identity of their neuronal progeny. *Cell* 106, 511-521 (2001).
41. Shihabuddin, L. S., Hoerner, P. J., Ray, J. & Gage, F. H. Adult spinal cord stem cells generate neurons after transplantation in the adult dentate gyrus. *J. Neurosci.* 20, 8727-8735 (2000).
42. Subonen, J. O., Peterson, D. A., Ray, J. & Gage, F. H. Differentiation of adult hippocampus-derived progenitors into olfactory neurons in vivo. *Nature* 383, 624-627 (1996).
43. Weissman, L. L. Stem cells: units of development, units of regeneration, and units in evolution. *Cell* 100, 157-168 (2000).
44. Anderson, D. J. Stem cells and pattern formation in the nervous system. The possible versus the actual. *Neuron* 30, 19-35 (2001).
45. Temple, S. Stem cell plasticity—building the brain of our dreams. *Nature Neurosci. Rev.* 2, 513-520 (2001).
46. Durbec, P. & Rougon, G. Transplantation of mammalian olfactory progenitors into chick hosts reveals migration and differentiation potentials dependent on cell commitment. *Mol. Cell. Neurosci.* 17, 561-576 (2001).
47. Kondo, T. & Raff, M. Oligodendrocyte precursor cells reprogrammed to become multipotential CNS stem cells. *Science* 289, 1754-1757 (2000).
48. Doetsch, F. K., Caille, L., Garcia-Verdugo, J. M. & Alvarez-Buylla, A. EGF induces conversion of transit amplifying neurogenic precursors into multipotential invasive cells in the adult brain. *Soc. Neurosci. Abstr.* 24.4 <<http://sfn.scholarone.com/itin2001/>> (2001).
49. Fischer, A. J. & Reh, T. A. Muller glia are a potential source of neural regeneration in the postnatal chicken retina. *Nature Neurosci.* 4, 247-252 (2001).
50. Goldowitz, D. Cell allocation in mammalian CNS formation: evidence from murine interspecies aggregation chimeras. *Neuron* 3, 705-713 (1989).
51. Tan, S. S. et al. Separate progenitors for radial and tangential cell dispersion during development of the cerebral neocortex. *Neuron* 21, 295-304 (1998).
52. Brustle, O. et al. In vitro-generated neural precursors participate in mammalian brain development. *Proc. Natl Acad. Sci. USA* 94, 14809-14814 (1997).
53. Winkler, C. et al. Incorporation and glial differentiation of mouse EGF-responsive neural progenitor cells after transplantation into the embryonic rat brain. *Mol. Cell. Neurosci.* 11, 99-116 (1998).
54. Brustle, O. et al. Chimeric brains generated by intraventricular transplantation of fetal human brain cells into embryonic rats. *Nature Biotechnol.* 16, 1040-1044 (1998).
55. Flax, J. D. et al. Engraftable human neural stem cells respond to developmental cues, replace neurons, and express foreign genes. *Nature Biotechnol.* 16, 1035-1039 (1998).
56. Brustle, O., Maskos, U. & McKay, R. D. Host-guided migration allows targeted introduction of neurons into the embryonic brain. *Neuron* 15, 1275-1285 (1995).
57. Campbell, K., Olsson, M. & Bjorklund, A. Regional incorporation and site-specific differentiation of striatal precursors transplanted to the embryonic forebrain ventricle. *Neuron* 15, 1259-1273 (1995).
58. Betarbet, R., Zigova, T., Bakay, R. A. & Luskin, M. B. Migration patterns of neonatal subventricular zone progenitor cells transplanted into the neonatal striatum. *Cell Transplant.* 5, 165-170 (1996).
59. Lois, C. & Alvarez-Buylla, A. Long-distance neuronal migration in the adult mammalian brain. *Science* 264, 1145-1148 (1994).
60. Clarke, D. L. et al. Generalized potential of adult neural stem cells. *Science* 288, 1660-1663 (2000).
61. Herrera, D. G., Garcia-Verdugo, J. M. & Alvarez-Buylla, A. Adult-derived neural precursors transplanted into multiple regions in the adult brain. *Ann. Neurol.* 46, 867-877 (1999).
62. Gage, F. H. et al. Survival and differentiation of adult neuronal progenitor cells transplanted to the adult brain. *Proc. Natl Acad. Sci. USA* 92, 11879-11883 (1995).
63. Pignino, S. E. et al. Isolation and characterization of neural stem cells from the adult human olfactory bulb. *Stem Cells* 18, 295-300 (2000).
64. Tropepe, V. et al. Retinal stem cells in the adult mammalian eye. *Science* 287, 2032-2036 (2000).
65. Laywell, E. D., Rakic, P., Kukekov, V. G., Holland, E. C. & Steinleider, D. A. Identification of a multipotent astrocytic stem cell in the immature and adult mouse brain. *Proc. Natl Acad. Sci. USA* 97, 13683-13688 (2000).
66. Zhu, G., Mehler, M. F., Mabie, P. C. & Kessler, J. A. Developmental changes in progenitor cell responsiveness to cytokines. *J. Neurosci. Res.* 56, 131-145 (1999).
67. Gritti, A. et al. Epidermal and fibroblast growth factors behave as mitogenic regulators for a single multipotent stem cell-like population from the subventricular region of the adult mouse forebrain. *J. Neurosci.* 19, 3287-3297 (1999).
68. Burrows, R. C., Wancio, D., Levitt, P. & Lillien, L. Response diversity and the timing of progenitor cell maturation are regulated by developmental changes in EGFR expression in the cortex. *Neuron* 19, 251-267 (1997).
69. Lillien, L. & Raphael, H. BMP and FGF regulate the development of EGF-responsive neural progenitor cells. *Development* 127, 4993-5005 (2000).
70. Qian, X., Davis, A. A., Goderie, S. K. & Temple, S. FGF2 concentration regulates the generation of neurons and glia from multipotent cortical stem cells. *Neuron* 18, 81-93 (1997).
71. Li, W., Cogswell, C. A. & LoTurco, J. J. Neuronal differentiation of precursors in the neocortical ventricular zone is triggered by BMP. *J. Neurosci.* 18, 8853-8862 (1998).
72. Li, W. & LoTurco, J. J. Noggin is a negative regulator of neuronal differentiation in developing neocortex. *Dev. Neurosci.* 22, 68-73 (2000).
73. Mehler, M. F., Mabie, P. C., Zhu, G., Gokhan, S. & Kessler, J. A. Developmental changes in progenitor cell responsiveness to bone morphogenetic proteins differentially modulate progressive CNS lineage fate. *Dev. Neurosci.* 22, 74-85 (2000).
74. Lim, D. A. et al. Noggin antagonizes BMP signaling to create a niche for adult neurogenesis. *Neuron* 28, 713-726 (2000).
75. Kirschstein, R. & Skirbell, L. R. *Stem Cells: Scientific Progress and Future Research Directions* (NIH, Bethesda, 2001).

#### Acknowledgements

I thank Q. Shen for her help with Table 1 and for invaluable discussions; K. Kirchofer for preparing the manuscript; and S. Dunnett for summarizing the potential therapeutic applications of stem cells in Box 1.